Master of Science Thesis

Comparison of on-board vs stationary energy storage systems for PV-powered multifunctional trolleybus grids

Konstantinos Giitsidis

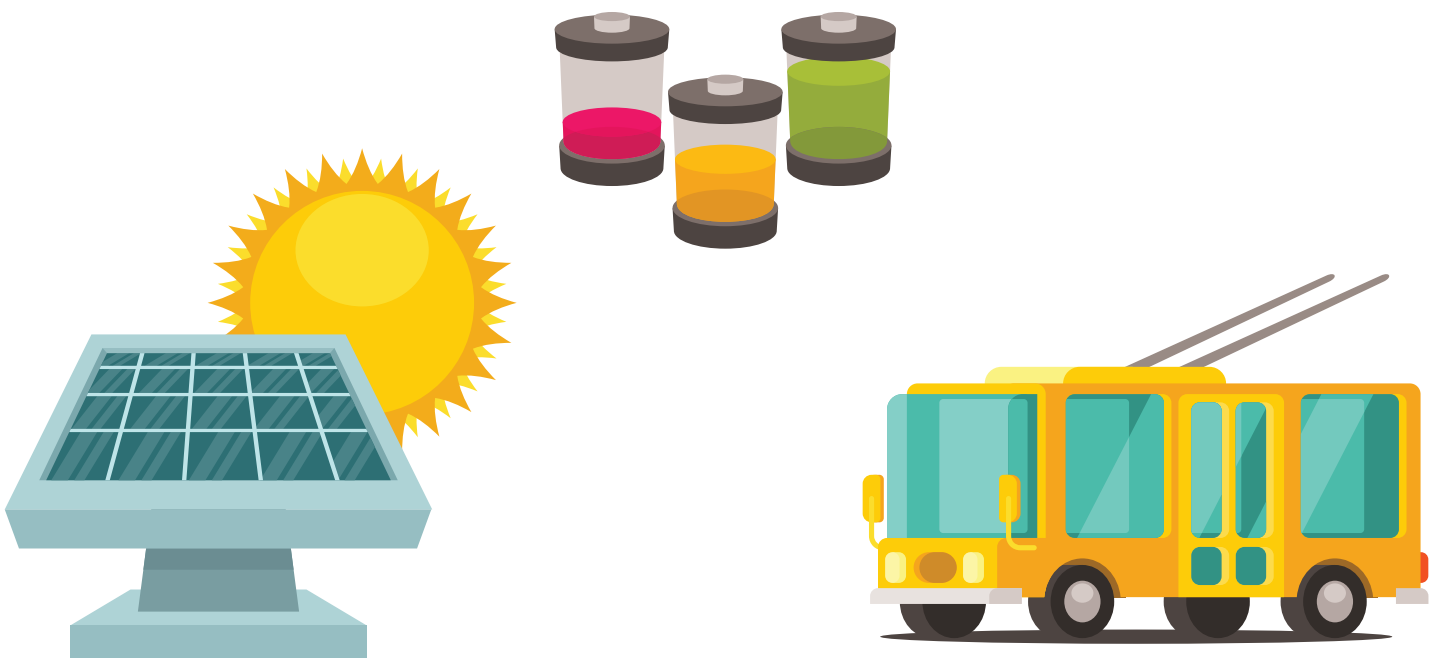

TU Delft

DC Systems, Energy Conversion, and Storage (DCE&S)

COMPARISON OF ON-BOARD VS STATIONARY ENERGY STORAGE SYSTEMS FOR PV-POWERED MULTIFUNCTIONAL TROLLEYBUS GRIDS

A thesis submitted to the Delft University of Technology in partial fulfillment of the requirements for the degree of

Master of Science in Sustainable Energy Technology
Profile Cluster: Electric Mobility & Economics

by

Konstantinos Giitsidis
5376785

26 August 2022

Delft University of Technology
Faculty of Electrical Engineering, Mathematics & Computer Science
Department of Electrical Sustainable Energy
DC Systems, Energy Conversion, and Storage (DCE&S) group

The work in this thesis was made in:

Delft University of Technology.

Faculty of Electrical Engineering, Mathematics & Computer Science.

Department of Electrical Sustainable Energy.

DC Systems, Energy Conversion, and Storage (DCE&S) group.

Promoter/reader:	Prof.dr.ir. Pavol Bauer
Supervisor/reader:	Dr.ir. G.R (Gautham Ram) Chandra Mouli
Co-supervisor:	Ir. Ibrahim Diab
Reader:	Dr.ir. Robin Vismara

To all the people that devote their time selflessly
contributing in finding solutions to problems,
beneficial for the greater good.

PREFACE

This report has been written as a result of a mandatory thesis project, necessary for the completion of the *Sustainable Energy Technology* master program offered by *Technical University of Delft (TU Delft)*, following the *Electric Mobility & Economics* Profile Cluster. The thesis work and the writing of this report have been conducted and executed by me, Konstantinos Giitsidis, an electrical and computer engineer (BSc & integrated MSc) from Greece.

Interested in anything that has to do with electricity, I was intrigued by the nature of this topic. Trolleybuses is a public transportation mean that, even today, some people are not familiar with. It is very interesting to see how this sector of public transit can be expanded with functionalities which are in favour of the environment, and as an extension, of the human kind.

I would like to extend my gratitude to the DCE&S group for providing me the opportunity to contribute with my own way to the research done in this sector, as well as to anyone that may have helped with the completion of this thesis work. Finally, I pay my respects to anyone in the scientific community who devotes their time selflessly contributing in finding solutions to problems, beneficial for the greater good.

Konstantinos Giitsidis
The Hague, the Netherlands, 2022

ABSTRACT

Trolleybuses are electric buses than run on electric power from overhead electric power lines (catenary) like trams do. Although is a service that dates all the way back to 1882, it has managed to regain interest in the recent years due to the constant electrification of various aspects of the world. This comes as a response towards environmental challenges as, even today, the majority of the energy necessary to cover our need comes from fossil fuels, making the transition to renewable energy sources more vital. One promising form of renewable energy source is solar energy and its use with photovoltaic (PV) systems. An interesting implementation of such systems is in catenary grids like trolleybus grids. Nevertheless, their integration has a low potential as the gaps in the trolleybus schedule and the intermittent behavior of the PV electric power leave a lot of excess PV electric energy unused. Possible solutions to this problem could be either the storage of this excess energy in *on-board* energy storage systems (OESS) or *stationary* energy storage systems (SESS). Besides that, in preparation for the future, more attention is given every day to the *multifunctionality* of trolleybus grids. This is related to parameters such as voltage drops, that have important role in rendering the trolleybus grid capable of being expanded with components other than trolleybuses, such as electric vehicle chargers.

The objective of this thesis work is to find out which energy storage systems (*on-board* or *stationary*) are most favorable for a PV-powered multifunctional trolleybus grid for increasing the PV system utilization and improving its multifunctionality. Parameters related to the *multifunctionality* of trolleybus grids can be the yearly electric energy consumption and the voltage drops.

For the conduction of this work is used an existing, verified trolleybus grid model of Arnhem in MATLAB® that has realistic trolleybus electric power profiles as an input. By using the backward-forward sweep method are determined precise values such as the total electric power needed, voltage drops, ohmic losses and more. Also, is used as an existing, verified PV system model that provides the PV electric power as an output based on measured data. Then is developed a model for the *on-board* energy storage system which with the help of a constraint checking algorithm, that simulates the energy storage technologies, it provides new, adjusted trolleybus electric power profiles that are used as input to the trolleybus grid model. Finally, for the *stationary* energy storage system, the main trolleybus grid model is expanded with storage capabilities based on voltage control and a similar constraint checking algorithm for the storage technologies.

The results show that the impact of *stationary* energy storage systems on the PV system utilization and on parameters of the trolleybus grid in general is heavily correlated to the control strategy used. The technology, the PV system size, the trolleybus grid section, and the targeted outcome (improve the PV system utilization or reduce the voltage drops) have key role to the selection of the control strategy. The comparison of *stationary* energy storage systems to other energy storage systems cannot be straightforward. Besides that, *on-board* energy storage systems can perform better on parameters regarding the *multifunctionality* of the trolleybus grid such as the total yearly electric energy consumption and the mitigation of the severity of the voltage drops. On the other hand, *stationary* energy storage systems can perform well on a wide range of parameters according to their control strategy. For the one used in this work, they perform better on parameters regarding the PV system utilization, managing to have a positive impact.

CONTENTS

LIST OF FIGURES

LIST OF TABLES

1 INTRODUCTION

In this chapter is given an introductory presentation of information important for this work. Firstly, the operational principles of a trolleybus grid and the concept of its multifunctionality are presented. Afterwards, the statement of the problem that led to the creation of this work is outlined. Finally, the research objectives and the methodology of this work, as well as the structure of this report are listed.

1.1 THE TROLLEYBUS GRID

Trolleybuses are electric buses than run on electric power from overhead electric power lines (catenary) like trams do. Although is a service that dates all the way back to 1882, it has managed to regain interest in the recent years due to the constant electrification of various aspects of the world, including means of transportation, as a response towards environmental challenges [9, 10].

1.1.1 Operational principles of a trolleybus grid

Those unique buses can operate in specific routes equipped with a grid of overhead electric power lines and can be found in places all over the world [10]. To get a better idea of the topology of a such grid, in figure 1.1 is presented a representation of a part of a typical trolleybus grid layout along with its components.

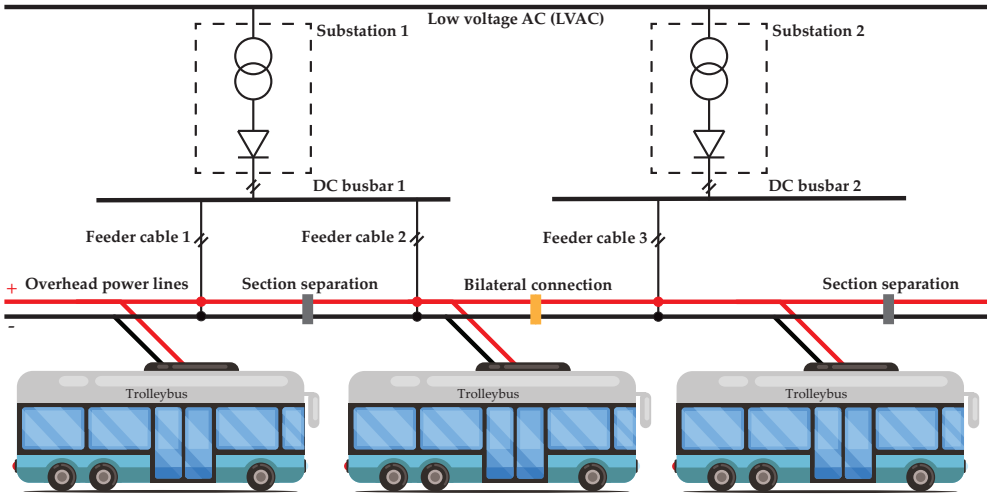

Figure 1.1: A representation of a part of trolleybus grid and its components.

As observed, the grid is divided into sections which are fed with electric power by substations. The substations are AC to DC meaning that they are equipped with a step-down transformer, connected to low voltage AC (LVAC), and an AC-DC converter. The nominal voltage of a section is usually around 600 V_{dc} to 700 V_{dc} depending of the trolleybus grid topology. Also, is important to note that one substation may feed multiple sections at the same time via different feeder cables. This is done for reasons such as minimizing the transmission losses as well as containing possible faults to smaller areas. Those sections can have a length of a few hundred

meters up to a couple kilometers depending on the layout of the grid and the city that the trolleybus grid is implemented to [2].

Substations in trolleybus grids are usually unilateral, meaning that they can only provide electric power to the trolleybus grid and not vice versa. This is due to the diodes of the AC-DC converters in the substations [2]. An example of an occasion that there may be electric power available that could be provided to the AC grid is when the trolleybuses are operating in "braking mode". In other words, like trams, when the trolleybuses are producing recuperating energy via regenerative braking [11]. Usually this electric power is provided to the trolleybus grid section that the trolleybus is operating on, or the other connected sections to the same busbar, for the other trolleybuses to use. Nevertheless, in occasions where other trolleybuses are not present, or the voltage gets too high, this recuperated energy has to be wasted on resistors located inside the trolleybuses, as thermal energy. The amount of energy to be wasted is controlled by DC-DC converter (chopper). Interesting to note is that there can be bilateral connections too between sections that belong to different substations. A bilateral connection is basically a controlled connection that can be either open (isolated) or closed (connected). This kind of connection provides the opportunity for the recuperated energy to be used to even more sections or provides a redundancy feed-in electric power route in case of an emergency [2].

Considering the overhead electric power lines, those must always be at least two. In tram grids this is not the case as the electric path closes via the metal rails. This is not possible for trolleybuses as their rubber tyres are very bad conductors of electricity. Thus, there are used two distinct electric power lines, one for the positive DC pole (+) and one for the negative DC pole (-). Furthermore, catenary grids, such as trolleybus and tram grids, may also have dual, parallel lines for each conductor for increasing the current capacity and also for reducing the resistance to almost half [2]. For trolleybus grids specifically this is achieved by connecting the same pole electric power lines in a section every few hundred meters, of the going and the returning routes.

Figure 1.2: Trolleybus and the overhead electric power lines in the city of Arnhem, the Netherlands [© OVPro].

In figure 1.2 is presented an example of a trolleybus and the overhead electric power lines in the city of Arnhem, the Netherlands. There, is observed how the vehicle has to follow a specific route on the street, only where there are overhead electric power lines available.

1.1.2 Multifunctionality of a trolleybus grid

The *multifunctionality* of a trolleybus grid is a term that slowly but steadily gains more attention. This means that the grid could be expanded with various components besides trolleybuses. This can even go as far as giving to it microgrid characteristics.

Some of the components that the trolleybus grid can be expanded with are:

1. *On-board* energy storage systems (OESS).
2. *Stationary* energy storage systems (SESS).
3. *In-motion charging* (IMC).
4. Electrical vehicles (EV) chargers.
5. Photovoltaic (PV) systems.
6. Other direct current (DC) components.

All these together can transform the trolleybus grid to a bigger, more advance grid that will be able to cope with the energy necessities and the environmental challenges of the future. Thus, they can create the so-called "*trolleybus grid of the future*". In this work are investigated only the first two components in conjunction with the PV-systems but with the latter placed in the AC side of the grid. Analytical information about them and the reason behind the choices taken is presented in chapter 2. In figure 1.3 is presented an illustration of how the *trolleybus grid of the future* may look like.

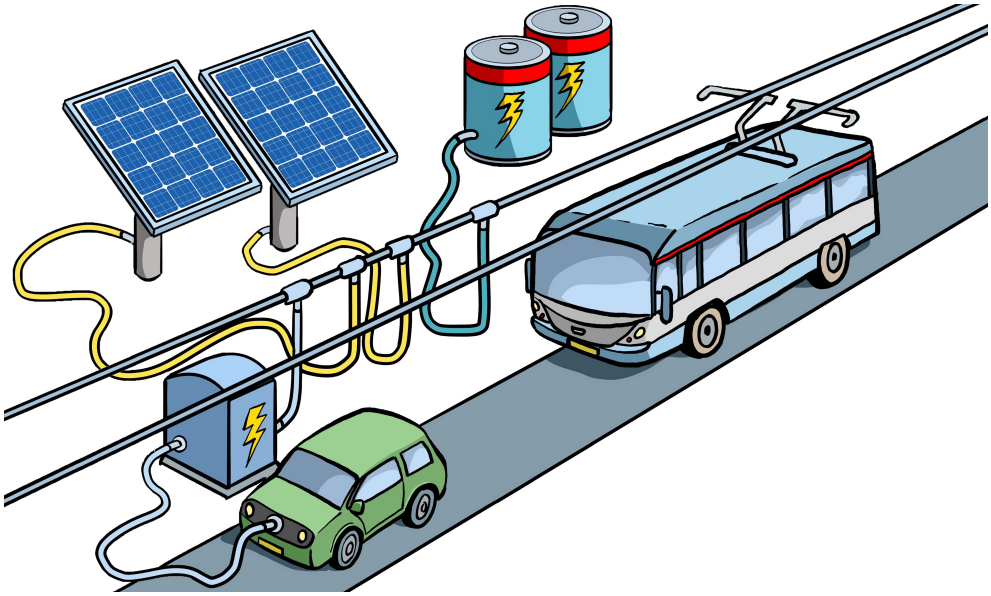

Figure 1.3: Visualization of the *trolleybus grid of the future* [© Suvaal 2021].

1.2 THE STATEMENT OF THE PROBLEM

To understand better the importance of multifunctional trolleybus grids, is important first to take a look at the motive behind it as well as its challenges. Global greenhouse gas emissions follow an increasing trajectory in planet earth during the last years. This comes mainly as a result to our increasing needs for energy day by day as a society [12].

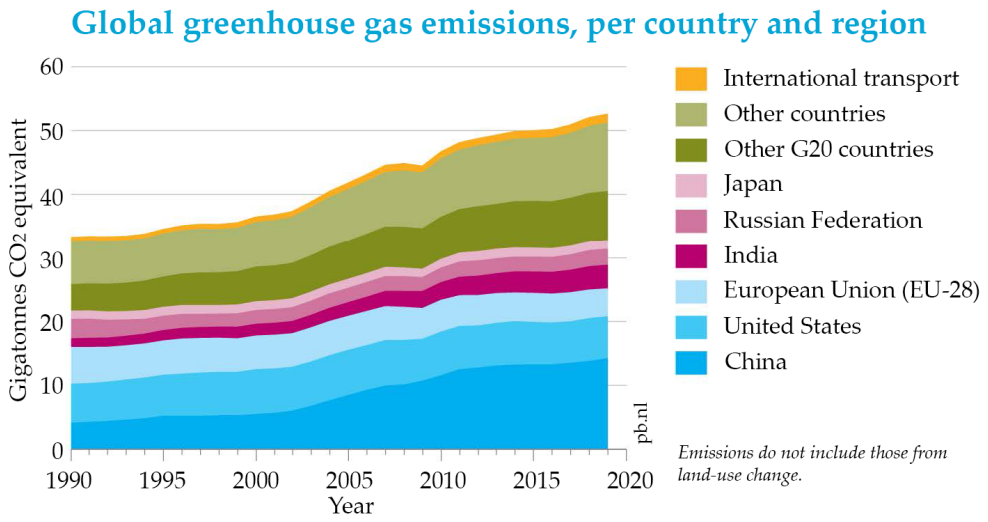

Figure 1.4: Global greenhouse gas emissions, per country and region [1].

In figure 1.4 are presented the global greenhouse gas emissions per country and region. As observed, the last 30 years the CO_2 emissions have increased over 17 Gigatonnes. Even today, the majority of the energy necessary to cover our need comes from fossil fuels, responsible of producing big amounts of greenhouse gas emissions. It has already been proven that CO_2 emissions do have a severe impact on the climate change, thus degrading our standard of living [12]. Two ways to solve this issue is either by lowering the energy used for our needs, or transitioning to more sustainable energy sources, such as renewable energy sources [13]. The first solution, although may be applicable for some occasions, it may not be viable in the long run as is necessary for the human kind to use increasingly more energy to transition to a higher level of civilization. The amount of energy extracted by environment by a species can be used as measurable metric for the progress of it. In other words, the abilities of a civilization are connected to the energy extraction abilities of it according to the Kardashev scale [14]. Thus, a viable, future-proof solution, would be to focus on renewable energy sources and energy sources with low greenhouse gas emissions to cover our needs, while at the same time increasing the efficiency of doing it so.

One promising form of renewable energy source is solar energy, and more precisely its use with photovoltaic (PV) systems. Currently there are some areas that this technology is being utilized and others that still require investigation. One of them is the implementation of such PV systems in catenary grids like trolleybus grids [15]. Nevertheless, currently, the integration of PV systems in trolleybus grids has a low potential as the gaps in the trolleybus schedule and the intermittent behavior of the PV electric power leave a lot of excess PV electric energy unused [3]. This makes it a rather poor choice to include PV systems in such grids as their utilization will be low.

In figure 1.5 is illustrated the issue of PV system electric power production intermittency compared to the total electric power demand of substation No 12 during day No 268 of the year in Arnhem. As can be seen, there are periods that no electric power is demanded by the trolleybus grid while there is electric power generated from the PV system. This leads to poor PV system utilization as the electric power generated from it can not be all utilized. For this reason, possible solutions to this problem should be investigated. Some of those may be either the storage of this excess energy in *on-board* energy storage systems (OESS) or *stationary* energy storage systems (SESS). Those systems are investigated as solutions in this work. More particularly, is conducted a comparison of *on-board* vs *stationary* energy storage sys-

tems for PV-powered multifunctional trolleybus grids. The work is a simulation case study of the trolleybus grid of Arnhem, the Netherlands.

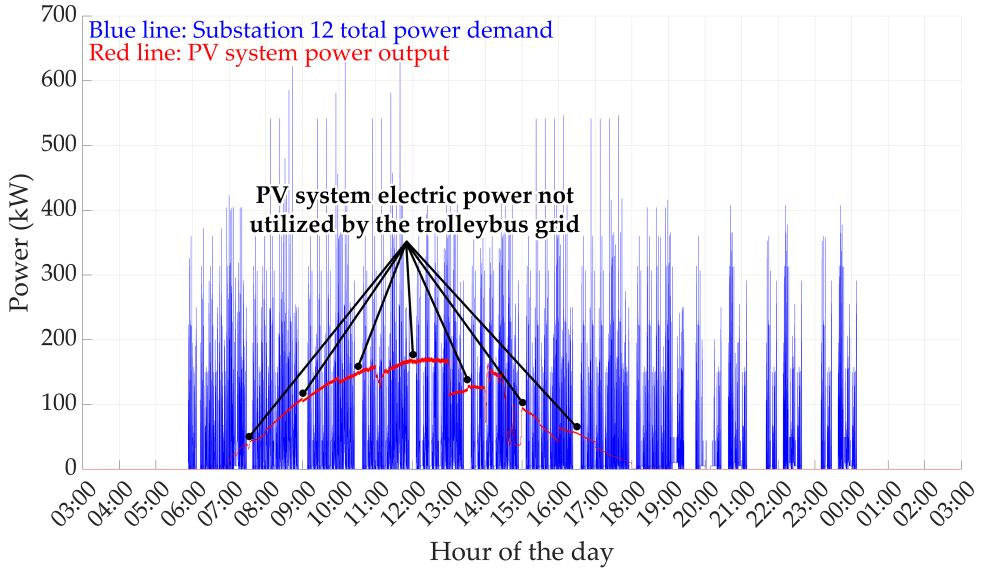

Figure 1.5: PV system (195 kWp) electric power production compared to the electric power demand of substation No 12 during day No 268 of the year in Arnhem.

1.3 RESEARCH OBJECTIVES AND METHODOLOGY

Having said all the above, the main goal of this thesis can be summarized in the following sentence:

Investigating which energy storage systems (on-board or stationary) are most favorable for a PV-powered multifunctional trolleybus grid for increasing the PV system utilization and improving its multifunctionality.

1.3.1 Research questions

To better specify the problem analyzed in this work, is important to form research questions. The main goal, that is stated previously, is actually the first, main, general research question. All the rest research questions can be summarized in table 1.1.

Table 1.1: Research questions.

No	Question
1	Which energy storage systems (*on-board* or *stationary*) are most favorable for a PV-powered multifunctional trolleybus grid for increasing the PV system utilization and improving its multifunctionality?
2	Which energy storage systems technology in terms of their characteristics (capacity, self-discharge etc.) is preferable for a PV-powered multifunctional trolleybus grid?
3	What effect do these energy storage systems have on the PV system utilization, the yearly electric energy consumption, and the voltage drops on the trolleybus grid?
4	Which of energy storage systems' variables (capacity, placement position etc.) have a greater effect on each trolleybus grid parameter (PV system utilization, yearly electric energy consumption, voltage drops)?

1.3.2 Methodology

For the conduction of this work, an existing verified trolleybus grid model of Arnhem in MATLAB® that has realistic trolleybus electric power profiles as an input is used. By using the backward-forward sweep method are determined precise values like the total electric power needed, voltage drops, ohmic losses and more. Also, is used as an existing, verified PV system model that provides the PV electric power as an output based on measured data. Then, a model for the *on-board* energy storage system is developed, which with the help of a constraint checking algorithm, that simulates the energy storage technologies, it provides new, adjusted trolleybus electric power profiles that are used as input to the trolleybus grid model. Finally, for the *stationary* energy storage system, the main trolleybus grid model is expanded with storage capabilities based on voltage control and a similar constraint checking algorithm for the storage technologies.

1.4 REPORT STRUCTURE

In figure 1.6 is presented in an illustrative way the structure of the report of this work.

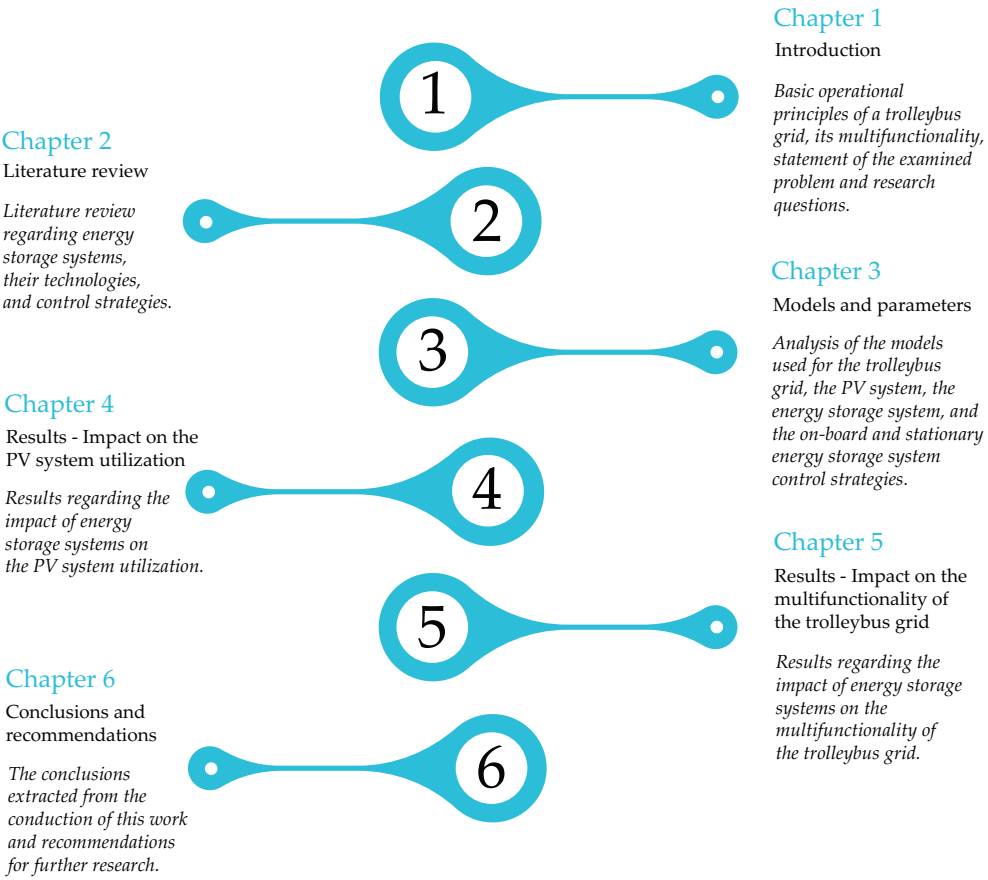

Figure 1.6: The structure of the report of this thesis work.

2 LITERATURE REVIEW

In this chapter is presented a survey on the functionalities of energy storage systems used in electric transport grids, their technologies, and their control strategies. The basic decisions considering the scenarios and control strategies used for the simulations of this work are presented in the end.

2.1 FUNCTIONALITIES OF ENERGY STORAGE IN ELECTRIC TRANSPORT GRIDS

Energy storage can have a significant role in reducing the overall CO_2 emissions and energy costs in electric transport grids [16]. This is an outcome of acting as energy buffers for the intermittent nature of energy demanded in electric transport grids [17]. Additionally, the integration of renewable energy sources (RES), such as PV systems, to the electric transport grids, makes their role even more important [15]. Thus, in an effort to transit the word to a more sustainable future, energy storage becomes increasingly more significant day by day [13].

From analyzing the literature, the functionalities of the energy storage systems in electric transport grids may be sorted into two main categories [18]. In one are included those who are mainly correlated with *electric power quality assurance*, and in the other are those primarily focusing on *energy cost reduction*. Nevertheless, the borderline of these two categories can be vague as they are deeply interconnected as some of the functionalities of the one category can also be assigned to the other. It is important to go into these functionalities as they can have a significant role on the criteria for choosing the most suitable energy storage systems for the implementation of PV systems in a multifunctional trolleybus.

2.1.1 Electric power quality assurance functionalities

These are functionalities that have as a primal role a high electric power quality delivery. By the term *electric power quality*, it is defined the extend to which the voltage, the frequency, and the waveform delivered by an electric power supply unit comply with its predefined specifications [19]. In the case of electric transport grids, this term is limited only to the voltage, as in those it is used *Direct Current* (DC) [20, 21].

The functionalities related to electric power quality assurance are:

1. Line voltage drop reduction.
2. Transmission losses reduction.
3. Electric power peak shaving.

LINE VOLTAGE DROP REDUCTION *Line voltage drop reduction* is related to voltage drops along the DC lines of the electric transport grid, causing vehicle cut off at very low values and increased current drawn for the same electric power. According to Ohm's law, the current flow through a conductor between two points is proportional with the voltage drop across those points [22]. This is described by equation 2.1.

$$I = \frac{V}{R} \tag{2.1}$$

Thus, by rearranging equation 2.1, it can be derived that the voltage between two points of a conductor equals with the product of the current flow through the conductor and the resistance between those points. This is described by equation 2.2.

$$V = I * R \tag{2.2}$$

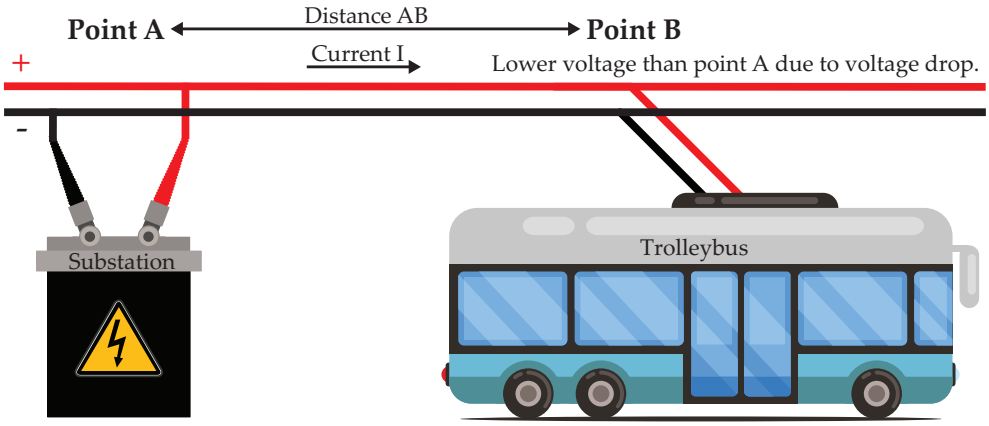

Figure 2.1: The effect of voltage drop between the electric power feeding point of a section and a trolleybus in traction mode, in a simplified trolleybus grid.

In figure 2.1 is illustrated the effect of voltage drop between the electric power feeding point of a section (point A) and a trolleybus (point B) in traction mode, in a simplified trolleybus grid. According to Ohm's law, there is a voltage drop between point A and point B which is proportional to the current flowing through that section and the total resistance of that section [22]. The magnitude of the current is solely depended by the load, which in this case it is the trolleybus. Thus, depending if the trolleybus needs more electric power (e.g. electric power for HVAC or electric power for a hard acceleration), the voltage drop may get increased. Furthermore, the resistance of the overhead electric power lines also contributes to the voltage drop. As an electrical resistance of an object is considered its opposition to the flow of electric current through it [22]. It is dependent on two factors which are its geometric and material characteristics. This is described by equation 2.3.

$$R = \rho * \frac{l}{A} \tag{2.3}$$

Where l is the length of the conductor, A is the cross-section area of the conductor, and ρ is the electrical resistivity (or specific electrical resistance) of the material [22]. As a result, the resistance increases as the trolleybus (point B) gets further from the electric power feeding point of the section (point A). In other words, the further point B is from point A, the bigger the voltage drop is. The presented illustration is simplified, as catenary grids such as trolleybus and tram grids, may also have dual, parallel lines for each conductor (trams can have only one positive overhead set of lines as the negative polarity return is done via the metal tracks), as already mentioned. This is done for reducing the resistance to almost half.

Another solution to this problem is to increase the number of electric power feeding points in a section. Nevertheless, this might not be a cost effective solution, as the costs of additional electric power feeding cables and/or substations may overpass the possible benefits. Thus, the integration of energy storage systems in electric transport grids can provide a viable middle ground solution. Those can be either placed in various points of the grid (*stationary* or *SESS - Stationary Energy Storage*

Systems or *off-board energy storage*) or inside each catenary vehicle (*on-board* or *OESS - On-board Energy Storage Systems*). A more analytical comparison between those two types of storage is conducted in section 2.2.2.

figure 2.2 illustrates the effect of voltage drop between the electric power feeding point of a section (point A) and a trolleybus (point B) in traction mode, in a simplified trolleybus grid, with the integration of a *stationary* energy storage system (point C). Also, in figure 2.3 is illustrated the same concept with the integration of an *on-board* energy storage, inside the trolleybus (point B). For simplicity, the use of power electronic converters is not illustrated in the figures.

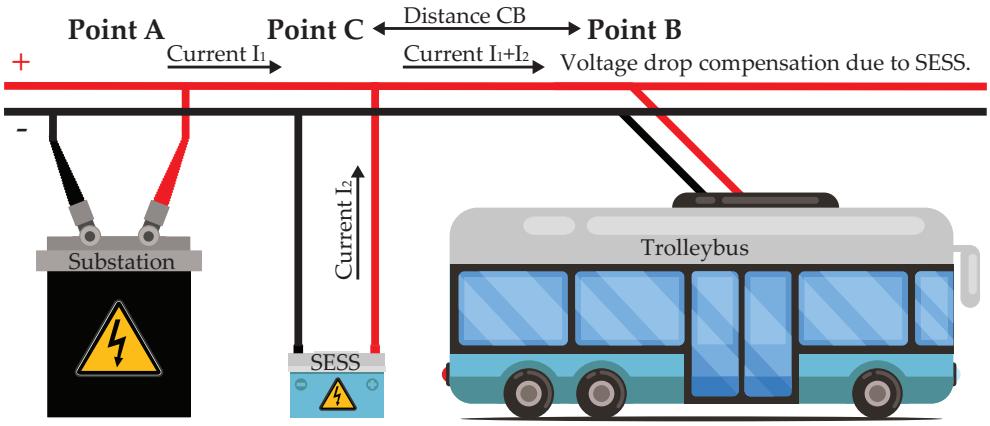

Figure 2.2: The effect of voltage drop between the electric power feeding point of a section and a trolleybus in traction mode, in a simplified trolleybus grid, equipped with a *stationary* energy storage.

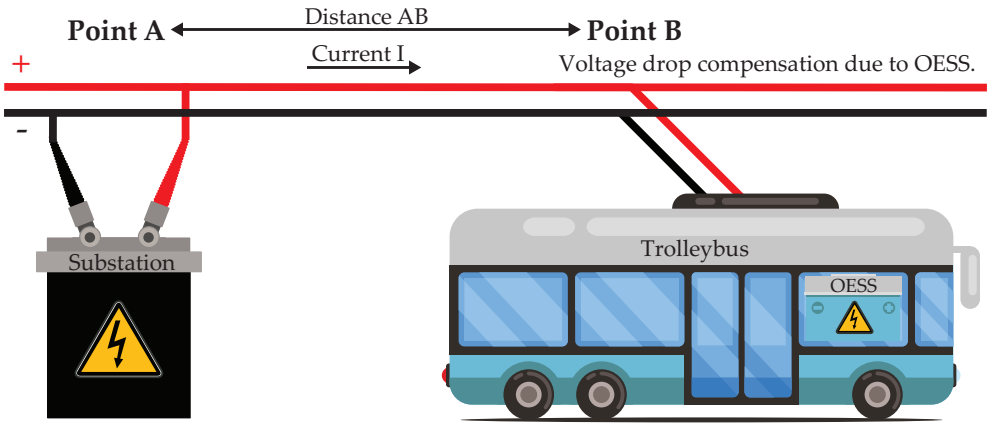

Figure 2.3: The effect of voltage drop between the electric power feeding point of a section and a trolleybus in traction mode, in a simplified trolleybus grid, equipped with an *on-board* energy storage.

As can be understood by figure 2.2, the *stationary* energy storage system can act as a new electric power feeding point of the section (point C), reducing the distance between the main electric power feeding point from the substation to the section (point A) and the trolleybus (point B). On the other hand, in figure 2.3 the energy source now is inside the trolleybus, which theoretically limits the distance of the trolleybus (point B) with the electric power feeding point of the section (point A) theoretically to zero. The main downside of both of these solutions is that the maximum energy that can be provided is limited by the capacity the energy storage systems. Also, charging the energy storage system could potentially increase the current flow and voltage drops in the electric power lines. The advantages and disadvantages of each type, from reviewing the literature, are presented in section 2.2.2.

Thus, when modeling the implementation of an energy storage system in a trolleybus grid, is important to take into consideration of the voltage drop on the lines as this could have a considerable impact on the results. Depending on the distance of the trolleybus from the energy source, it may render it less or more suitable solution for the implementation of PV systems in the a multifunctional trolleybus grid. This is something that is taken into consideration for this work.

TRANSMISSION LOSSES REDUCTION *Transmission losses reduction* is a functionality correlated with the *line voltage drop reduction* as is based on the same principle. More specifically, it is based on Joule's first law which states that the power that causes energy to be lost in the form of heat on a conductor in which there is a flow of direct current, is proportional to the product of its electrical resistance and the square of the current flowing through it [22]. This is described by equation 2.4.

$$P \propto I^2 * R \tag{2.4}$$

More practically, this translates to higher ohmic losses and voltage drops the further the trolleybus is from the electric power feeding point of the section. As the current is depending on the trolleybus, the variable available for reducing the losses is the resistance of the overhead electric power lines. By implementing an electric power feeding source closer to the trolleybus, this distance is reduced, resulting in reduced energy losses. Thus, it can be concluded that it may also have a rather important impact in cost savings, as it renders the system more efficient [18].

ELECTRIC POWER PEAK SHAVING *Electric power peak shaving* is the reduction of the abrupt, usually short bursts of electric power demanded by the trolleybuses [18, 23]. These may occur due to a high electric power demand during an abrupt phenomenon, such as a hard acceleration. They can become rather dangerous for the trolleybus grid system as they can overwhelm the substations, leading to possible breaker trips or even permanent damage to the components of the grid, causing disturbances [23]. Also, electric power peaks may be accompanied with higher electricity costs, especially depending on the energy measuring technique applied at the substations [24]. The use of energy storage systems can solve this problem adequately by providing part of the abrupt electric power demanded by the load, thus relieving the strain from the main electric power feeding substation [24].

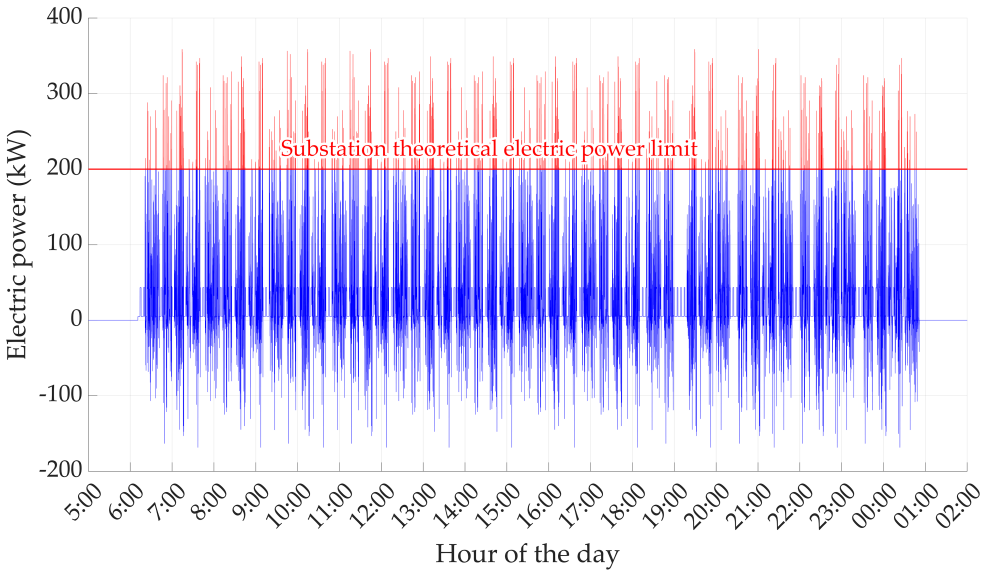

Figure 2.4: Electric power profile of trolleybus No 1 during the first day of the year in Arnhem, with a substation with a theoretical electric power limit of 200 kW.

In figure 2.4 is presented the electric power profile of trolleybus No 1 during the first day of the year in Arnhem. The trolleybus is being supplied the demanded electric power from a substation without the integration of any energy storage system. For the purposes of this example, an hypothetical substation electric power limit of 200 kW is assumed, indicated by the red straight line. In the graph, is observed how the peak electric power demands (red parts of the electric power profile) during its operation can overwhelm the capabilities of the substation and its components. If an energy storage system was used, (i.e. *on-board* energy storage systems), the demanded electric power above the capabilities of the substation could be provided by the energy storage system. This illustrates how energy storage systems could mitigate the issue overwhelming the substation and its components due to electric power peak demands.

2.1.2 Energy cost reduction functionalities

These are functionalities that focus primarily on *energy cost reduction*. In other words, using energy storage systems in the electric transport grid to reduce the costs of electricity consumption from the main grid.

The functionalities related to energy cost reduction are:

1. Catenary free trolleybus.
2. Energy recuperation.
3. Integration of RES.

CATENARY FREE TROLLEYBUS This functionality implies that the trolleybuses are able to move freely on their own, by using an energy source different than the grid. This can only be achieved by implementing energy storage systems inside the vehicle, that need to be big enough and able to be charged in a decent rate. A common way that this can be achieved is via *in-motion charging* (IMC).

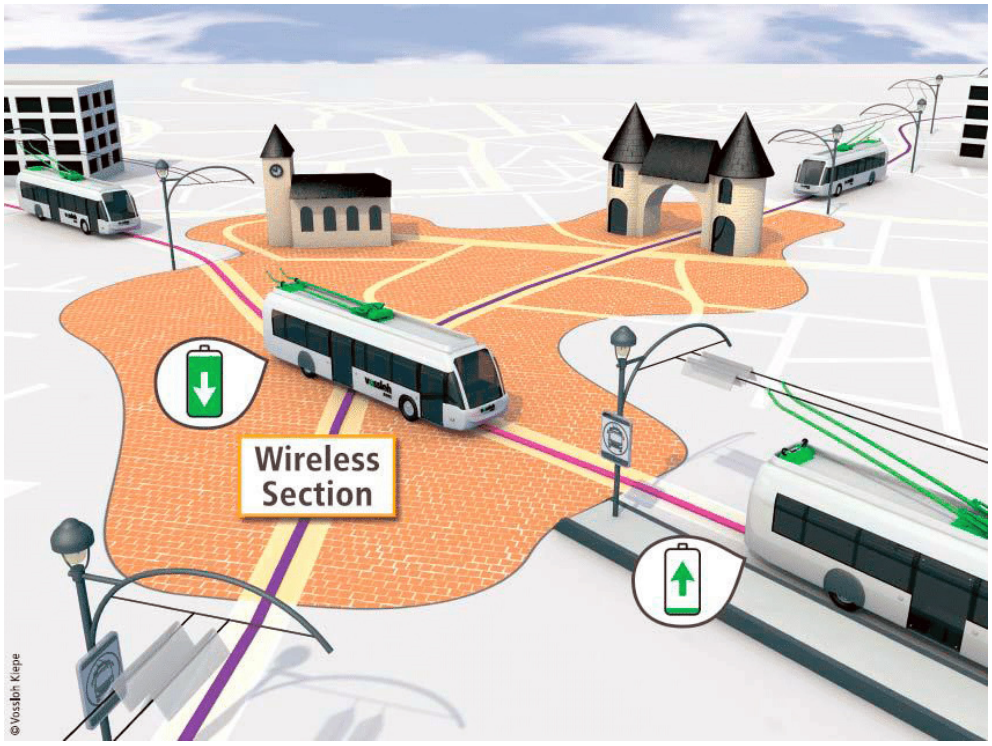

Figure 2.5: The idea of *in-motion charging* system (IMC) [© Vossloh Kiepe].

In figure 2.5 is presented an illustration of the idea of *in-motion charging* (IMC), applied on the trolleybus grid.

In-motion charging (IMC) implies that trolleybuses are equipped with an energy storage system of a considerable capacity (e.g. a battery) that charges while the trolleybus is roaming through the catenary grid. In other words, it acts as an extra load, storing energy from the grid in order to be used in a later stage in areas where there is no catenary infrastructure. In those areas, the trolleybus disconnects from the catenary grid and can operate like an autonomous electric bus. This can be financially beneficial as it can greatly extend the area that the trolleybuses are serving without the need of expensive and time-consuming construction of the necessary grid infrastructure. Also, it is rather usable for areas where there is no possibility of catenary build, such as dense city centers and historical areas. Finally, it provides to trolleybuses the possibility to move out of their predefined route, in case for example there are unplanned disruptions on the road [25, 26].

Today, most trolleybuses are already equipped with an internal combustion engine (usually diesel cycle) in order to cope with the aforementioned scenarios [26]. Switching from diesel internal combustion engines to electric ones, can reduce greatly the energy cost for the trolleybuses. Also, diesel contributes greatly to the creation of hydrocarbons in the atmosphere, which has a severe impact on the environment, thus making the transition to alternative energy storage systems vital [13]. It is interesting to mention that *in-motion charging* (IMC) is also implemented to tram grids. There, the main scope is the reduction of the need for big substations, and the reduction of costs for overhead lines. Thus, in this case the cost reduction is also the main functionality for this application [27, 25, 17, 28, 29].

ENERGY RECUPERATION By *energy recuperation* is meant the storage of electric energy from excess kinetic energy provided by the electrical machine of the vehicle when it is braking. This is also known in the electric vehicle sector as *regenerative braking*. This technique uses the inertia of the vehicle to generate electricity by using the electric machine of the vehicle in generating mode, and it is used when the vehicle needs to slow down. Instead of using convectional mechanical means of dissipating the excess kinetic energy to, it recoups some of the otherwise unused energy to an energy storage system in order to be used in a later stage (i.e. above a certain electric power demand threshold). Thus, it provides a sort of *power load-shifting* solution to the electric transport catenary grid. This can be integrated either with *stationary* or *on-board* energy storage systems, with the latter having the advantage of reduced transmission losses of the recuperated energy [30, 31, 11].

In figure 2.6 is presented the electric power profile of trolleybus No 1 during the first day of the year in Arnhem, with two electric power thresholds of 0 kW and 200 kW for charging and discharging a possible energy storage system respectively. The trolleybus is being supplied the demanded electric power from a substation without the integration of energy storage systems. In the graph, they are presented two threshold limits indicated by the red lines - the upper electric power threshold limit, and the lower electric power threshold limit. For the purposes of this example, a theoretical upper and lower electric power threshold limit of 200 kW and 0 kW respectively is assumed. The upper threshold limit indicates the electric power that above of which could be provided by an energy storage system - in more particular by an *on-board* energy storage system. On the other hand, the lower threshold limit indicates the electric power that below of which could be stored to the the energy storage system - in this case too an *on-board* energy storage system. As a result, this causes a *power load-shifting* phenomenon of the demanded electric power by storing excess energy via recuperation to the energy storage system and using it in a later stage for electric power demands higher than a set electric power threshold value.

Currently, most catenary electric vehicles, waste the recuperated energy to resistors in the vehicle, if they are not able to send it to other electric power consuming vehicles in the same section, such as other trolleybuses and trams. This only helps in preserving the braking system as it does not need to provide all the braking force necessary for the vehicle to stop. It is interesting to mention also that the higher the speed of the vehicle, the stronger the breaking force is from the *energy recuperation* [30, 31, 11].

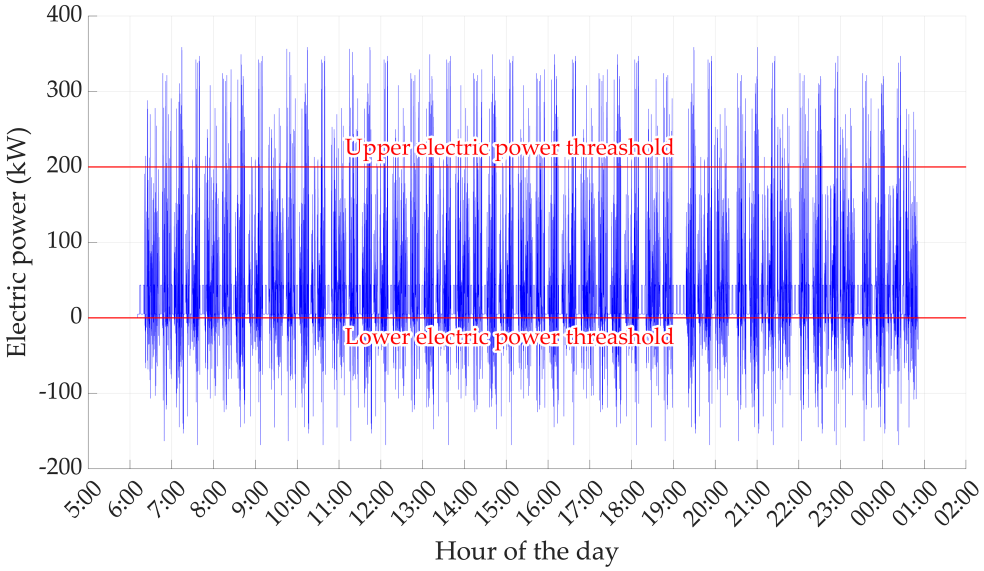

Figure 2.6: Electric power profile of trolleybus No 1 during the first day of the year in Arnhem, with two electric power thresholds of 0 kW and 200 kW for charging and discharging a possible energy storage system respectively.

INTEGRATION OF RES Finally, another functionality of energy storage systems that gets increasingly more attention is the *integration of RES* to the electric transport grids [32, 33]. More particularly, this is mainly referred to the integration of PV systems, because electricity production from photovoltaic panels is also DC, making their integration to the catenary grid an interesting sector for research [34, 35].

Currently, the integration of PV systems in trolleybus grids has a low potential as the gaps in the trolleybus schedule and the intermittent behavior of the electric power provided by the PV systems leave a lot of excess produced energy unused [15, 16]. In other words, the timetables of the trolleybuses (or trams) do not match the electricity production schedule of the PV systems. This results in leaving a lot of energy provided from PV systems unused [36, 37]. Thus, the implementation of energy storage systems to confront this issue is important. By using either *stationary* or *on-board* energy storage systems, the energy produced by PV systems can be stored and used in the electric transport grid when needed [38]. This can greatly increase the utilization percentage of the PV systems, making them a more effective solution of providing electric power from green energy sources as well as more financially viable to be implemented to trolleybus grids [35, 39, 40].

The implementation of PV systems (or any RES) in any electrical grid has already become a necessity in order to adequately reduce the amount of CO_2 emissions on the planet [13]. Thus, all possible ways that this can be achieved should be evaluated, and the integration of energy storage systems in electric transport grids is one of them.

2.2 TECHNOLOGIES OF ENERGY STORAGE SYSTEMS IN ELECTRIC TRANSPORT GRIDS

Energy storage systems used in electric transport grids can vary depending on their technology [17]. More specifically, this can be due to targets and goals set hierarchically by the designers of the system. For example, when the main goal is to achieve *electric power peak shaving*, then is usually preferred an energy storage system with small capacity but with high discharge capabilities. Similarly, when the goal focuses on other functionalities such as the the *integration of RES*, then should be utilized an energy storage system with high capacity but not necessarily high discharge capabilities [41]. Thus, each functionality of the energy storage implementation in the electric transport grid can be best satisfied by a specific energy storage system technology. This is something worth noting for the completion of this work.

Besides the technology of the energy storage systems, key role to their implementation in the electric transport grid has their placement position. As briefly explained in section 2.1, their position can be either somewhere in the grid (*stationary*), or inside the vehicle itself (*on-board*). These are two different approaches, each one with its advantages and disadvantages [17]. Those are analyzed below.

2.2.1 Characteristics of various energy storage systems

The technologies of energy storage systems have been developing with a fast pace during the last years [42]. As the necessity to lower CO_2 emissions gets more significant day by day, production of electricity from RES acquires an increasingly more important role [13]. Thus, in order to confront the intermittency issues derived by the nature of the RES, energy storage technologies need to be evolving constantly [43, 44, 45].

Energy storage systems can be categorized into six main categories depending on their technology [42].

1. Chemical batteries.
2. Capacitors.
3. Flywheels.
4. Compressed and liquid air storage.
5. Thermal storage.
6. Superconducting magnetic storage.

Considering the implementation of energy storage systems in trolleybus grids, those are found to usually be chemical batteries, capacitors, and flywheels [30, 46, 47]. This is due to their advantages compared to the rest, in various sectors. Some of them are their *energy density*, *power density*, *cycle efficiency*, *self-discharge*, *response time*, and *power capital cost*, *energy capital cost* [42, 48].

In table 2.1 is presented a comparison of the characteristics of various energy storage systems. With red are highlighted technologies of energy storage systems frequently used in trolleybus grids.

Table 2.1: comparison of the characteristics of various energy storage systems.

Technology	Energy density (Wh/L)	Power density (W/L)	Specific energy (Wh/kg)	Specific power (W/kg)	Discharge efficiency (%)	Cycle efficiency (%)	Self-discharge (%/day)	Life-time (charging cycles)	Life-time (years)	Response time (order of magnitude)	Indicated storage time (order of magnitude)	Power capital cost ($/kW)	Energy capital cost ($/kWh)
Lithium-ion battery (Li-ion)	200-500 [48] 200-400 [49]	1,500-10,000 [49]	75-200 [48] 120-200 [50]	150-315 [48] 300 [51]	85 [52]	~90-97 [48] 75-90 [53]	0.1-0.3 [48]	1,000-10,000 [48] 3,000-10,000 [54]	5-15 [48] 14-16 [55]	milliseconds [44]	minutes-days, short-med term [48]	1,200-4,000 [48] 1,590 [53]	600-2,500 [48]
Lithium-Titanate-oxide battery (LTO)	~84 [56] 128 [57]	~6,000 [56]	45-100 [58] 50-80 [59] 45 [56] 70 [57]	420 [57] 1,000 [60]	90 [57]	81-94.5 [61]	~0.1 [62]	2,000-6,800 [58] >10,000 [60]	10-25 [61]	milliseconds [63]	minutes-days, short-med term [63]	-	1,500-2,000 [58]
Nickel Metal Hydrate battery (NiMH)	<350 [64] 150 [51] 250 [65]	500-3,000 [64]	60-120 [64] 65 [51, 66] 72 [67]	70-756 [64] 200 [51, 66]	-	80 [68] 65-85 [69]	0.4-1.2 [64] 0.6 [66]	300-500 [64] 500 [68]	15 [68]	milliseconds [66]	minutes-days, short-med term [66]	420-1,200 [64]	240-1,200 [64]
Nickel Cadmium battery (NiCd)	60-150 [48] 80 [51]	80-600 [49]	50-75 [48] 45-80 [70]	150-300 [48] 160 [71] 150 [51]	85 [52]	~60-70 [48] 60-83 [44]	0.2-0.6 [48] 0.3 [45]	2,000-2,500 [48]	10-20 [48] 15-20 [45]	milliseconds [44]	minutes-days, short-long term [48]	500-1,500 [48]	800-1,500 [48] 400-2,400 [45]
Lead-acid battery (Pb-acid)	50-80 [48] 50-90 [51]	80-600 [49]	30-50 [48] 25-50 [72]	75-300 [48] 250 [51] 180 [45]	85 [52]	70-80 [48] 75-80 [73]	0.1-0.3 [48] <0.1 [45] 0.2 [74]	500-1,000 [48] 200-1,800 [71]	5-15 [48, 45] 13 [74]	milliseconds [52]	minutes-days, short-med term [48]	300-600 [48] 200-300 [52] 400 [75]	200-400 [48] 330 [75]
Sodium Sulfur battery (NaS)	150-250 [48] 150-300 [49]	~140-180 [49]	150-240 [48] 174 [65]	150-230 [48] 90-230 [76] 115 [71]	85 [52]	~75-90 [48] 75 [75] 75-85 [73]	negligible [71, 77]	2,500 [48] 3,000 [75] 2,500-4,500 [44]	10-15 [48] 15 [74] 12-20 [78]	milliseconds [79]	days, long term [80]	1,000-3,000 [48]	300-500 [48] 350 [75] 450 [81]
Vanadium Redox battery (VRB)	16-33 [48] 25-35 [82]	~<2 [49]	10-30 [48]	166 [83]	~75-82 [84]	75-85 [48] 65-75 [53]	negligible [48, 71]	>12,000 [48] ~13,000 [74]	5-10 [48] 20 [85]	milliseconds [44]	hours-months, long term [48, 86]	600-1,500 [48]	150-1,000 [48] 600 [81]
Zinc Bromine battery (ZnBr)	30-60 [48] ~55-65 [49]	~<25 [49]	30-50 [48] 80 [67]	100 [67]	~60-70 [87]	~65-75 [48] 66-80 [44] 66 [52]	negligible [48, 88]	>2,000 [48] 1,500 [74]	5-10 [48] 10 [74] 8-10 [55]	milliseconds [52]	hours-months, long term [48, 86]	700-2,500 [48]	150-1,000 [48] 500 [70]
Polysulfide Bromine battery (PSB)	~20-30 [42]	~<2 [49]	10-15 [69]	-	-	~60-75 [48, 89] 60-65 [69]	negligible [48, 85]	9,000-10,000 [69]	10-15 [48] 15 [89]	milliseconds [90]	hours-months, long term [48, 86]	700-2,500 [48]	150-1,000 [48] 450 [81]
Capacitor	2-10 [48]	>100,000 [48]	0.05-5 [48] ~0.05 [91]	100,000 [48]	~75-90 [42]	~60-70 [48]	40 [48] ~50 [92]	>50,000 [48]	~5 [48] ~1-10 [92]	milliseconds [44]	seconds-hours, short term [48]	200-400 [48]	500-1,000 [48]
Supercapacitor (SC)	10-30 [48]	>100,000 [48]	2.5-15 [48]	500-5,000 [48]	95 [52] ~98 [42]	~90-97 [48] 84-95 [93]	20-40 [48]	>50,000 [48]	10-30 [48] 10-12 [93]	milliseconds [52]	seconds-hours, short term [48, 86]	100-300 [48]	300-2,000 [48]
Superconducting magnetic energy storage (SMES)	0.2-2.5 [48]	1,000-4,000 [48] ~2,500 [49]	0.5-5 [48]	500-2,000 [48]	95 [52]	~95-97 [48] 95-98 [93]	10-15 [48]	>100,000 [48]	>20 [48] 30 [52]	milliseconds [52]	minutes-hours, short term [48, 86]	200-300 [48] 300 [52]	1,000-10,000 [48]
Compressed air energy storage (CAES)	3-6 [48] 2-6 [49]	0.5-2 [48] ~1 [49]	30-60 [48]	2.2-24 [54]	50-89 [43]	42-54 [48]	negligible [48, 78]	8,000-12,000 [44]	20-40 [48] 30 [51] >20 [74, 42]	minutes [52]	hours-months, long term [48, 86]	400-800 [48]	2-50 [48] 2-120 [94]
Liquid air energy storage (LAES)	80-120 [54] 50-200 [95]	-	214 [42]	-	-	55-80 [96]	negligible [96]	-	20-40 [95] >25 [96]	minutes [97, 95]	hours-months, long term [96]	900-1,000 [96]	260-530 [96]
Flywheel energy storage (FES)	20-80 [48, 49]	1,000-2,000 [48]	10-30 [48] 5-80 [98]	400-1,500 [48]	90-93 [52]	~90-95 [48, 51]	100 [48]	>20,000 [48] >21,000 [74]	~15 [48] >15 [74] 20 [52]	seconds [42]	seconds-minutes, short term [48, 86]	250-350 [48]	1,000-5,000 [48] 1,000-14,000 [94]
Thermal energy storage (TES)	80-500 [48]	-	80-250 [48]	10-30 [48]	30-60 [99]	~30-60 [48]	0.05-1 [48]	2,000-14,600 [99]	10-20 [48] 5-15 [48]	hours [42]	minutes-days, short-long term [48]	200-300 [48] 250 [42]	20-50 [48]

Some important chemical battery types used in trolleybus grids are *lithium-ion* (Li-ion) batteries, and *nickel cadmium* (NiCd) batteries [9]. It is interesting to note that *lithium-titanate-oxide* (LTO) batteries are gaining more attention as they seem to be able to provide much higher charging and discharging currents compared to the other types of batteries, such as *lithium-ion* (Li-ion) [56, 60, 16]. *Capacitors* and *supercapacitors* (SC) are also frequently used in transportation grids. Their ability to provide and receive high currents in a very short time makes them suitable for uses with high electric power peaks, such as the abrupt acceleration of the trolleybuses [30]. Finally, flywheels are also commonly used in trolleybus grids as their main advantage compared to other storage methods is their robustness. Nevertheless, usually they are limited of providing energy only for a short period of time [98, 46]. Deeper analysis for those energy storage systems is presented in section 2.4.

2.2.2 Placement of energy storage systems in electric transport grids

As already mentioned, the placement position of the energy storage systems in the electric transport grid has a significant role in their integration to the system. The two main categories according to placement, *on-board* and *stationary* are accompanied with advantages and disadvantages. Thus, according to the desired goal, either of them or their combination may be suitable to be used [41].

***ON-BOARD* ENERGY STORAGE** By using the term *on-board* energy storage in the electric transport grid, is meant a small energy source system, usually an electric battery or *supercapacitors* (SC), positioned inside the catenary vehicle. This is mainly used to store and supply the recuperating and a part of the accelerating electric power respectively [100]. It is not actively charged with extra electric power from the grid. Thus, it is able to satisfy only some of the functionalities described in section 2.1. Nevertheless, references can be found in the literature for *on-board* energy storage systems which also provide more functionalities, such as catenary free vehicle roaming [30, 47, 27, 25, 17]. This comes down to the definition of the term *on-board*. Technically, an energy storage with a bigger capacity, placed in the vehicle, can still be considered as "*on-board*". Nevertheless, in this work, the term *on-board* is only used following the first definition. In the case that the vehicle is equipped with an energy storage system big enough to provide the opportunity for catenary free roaming and be actively charged with electric power from the grid, this is referred as *in-motion charging* (IMC).

The *on-board* energy storage systems, due to their small capacity size, have the advantage of being more affordable than the *stationary* energy storage systems, which translates to lower capital costs of installation [100, 26]. They are also easier to implement as, usually, they do not require any major modifications to the catenary grid. Existent vehicles, such as trolleybuses or trams, can be modified and retrofitted with those rather easily [101]. Thus, their implementation can provide many benefits with a rather low initial capital cost of installation [100, 26].

Nevertheless, they also do come with disadvantages. One of those is their limited range of functionalities. *On-board* energy storage systems provide a fast and easy implementation of storage to electric transport grids, but with limitations considering their storage capabilities. Due to their small capacity size, they may not be suitable for adequately storing the provided amount of energy from RES and more specifically from PV systems. The limits of their capabilities are easily reachable by most of the aforementioned functionalities such as *line voltage drop reduction*, *electric power peak shaving*, and *energy recuperation*. This means that although they may seem like a promising choice right now, in the long run they will not be able to cope with the increased need for functionalities, such as the integration of RES in the grid [24]. Finally, is interesting to note that the added traction demand from the additional

weight of the vehicle due to the *on-board* energy storage system is insignificant compared to the gain from the functionalities they offer.

In table 2.2 are presented the main advantages and disadvantages of the *on-board* energy storage in electric vehicle transport grids as concluded from the literature.

Table 2.2: Advantages and disadvantages of *on-board* energy storage systems in the electric transport grids.

Advantages	**Disadvantages**
Low installation capital costs.	Limited functionalities.
Easy retrofitting.	Unpromising for future grids (with PV systems).
Easy to be replaced.	Uncontrolled charging scheme.

***STATIONARY* ENERGY STORAGE** *Stationary* energy storage, implies that an energy storage system is connected directly to the electric transport grid and it is not placed on the vehicles [16]. It can can be either placed on the AC side or the DC side, either on the DC busbar or the overhead electric power lines of a section. For this work, is examined only its placement on the DC side.

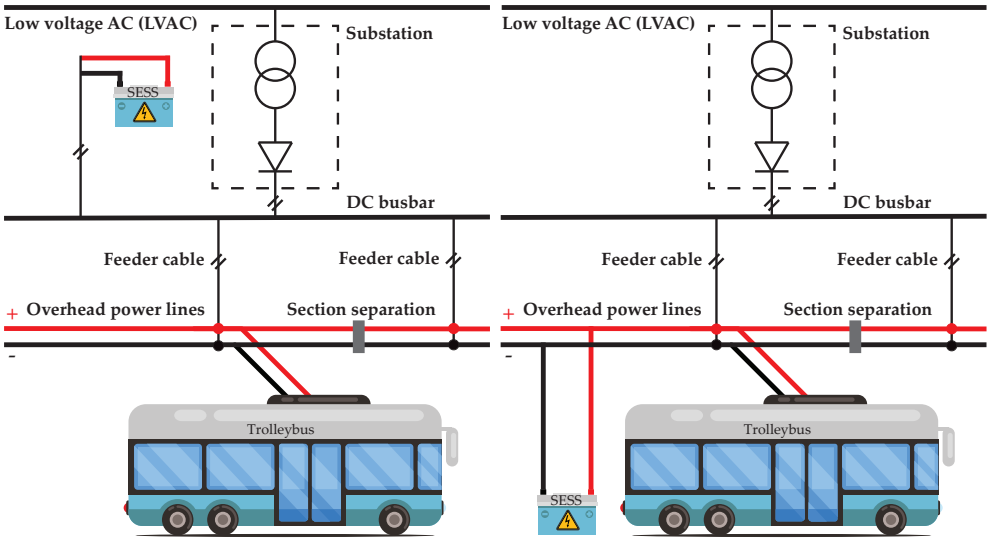

Figure 2.7: *Stationary* energy storage implemented to a substation DC busbar (left) and on the overhead electric power lines of a section (right) of the trolleybus grid, without the illustration of power electronic converters for simplicity.

In figure 2.7 is presented the implementation of a *stationary* energy storage to a substation DC busbar (left) and on the overhead electric power lines of a section (right) of the trolleybus grid. For simplicity, the use of power electronic converters is not illustrated in the figures.

Stationary energy storage offer a wider range of functionalities than *on-board* and are implemented with bigger energy capacities [102]. This is rather important especially for the integration of RES and PV systems in the electric transport grids. They provide the opportunity for the intermittent energy provided by the PV systems to be stored to a great extent, and to be used by the vehicles in the catenary grid when needed [103]. This renders them a future-proof investment, which will be able to cope with the increasing demand of functionalities for the future. Furthermore, since they are stationary, placed to already known location of the electric transport grid, their control strategy is easier to be optimized for a more efficient operation [36]. In this work the *stationary* energy storage is placed on the section and a suitable position is found after simulations that favors primarily the PV sys-

tem utilization while providing a compensation to the voltage drops on the section.

Nevertheless, this storage method is also accompanied by some disadvantages. The most important is the high capital cost for the installation of the energy storage systems. This is something that comes as a result from the big energy capacities usually used in *stationary* storage [104]. The majority of energy storage technologies still suffer from high power and energy capital costs [53, 61]. That is why is important for technological developments in the energy storage sector to continue to progress, in order to be created cheaper energy storage systems. Finally, since they are bigger, heavier, and usually costlier, this makes them more difficult to be replaced in the future. For this reason, surveys should be conducted of which energy storage system technology should be installed and where. This of course increases their cost even further and hides the risk of providing a limited functionalities flexibility for the future, in case the survey is not good enough [104].

In table 2.3 are presented the main advantages and disadvantages of the *stationary* energy storage in electric vehicle transport grids as concluded from the literature.

Table 2.3: Advantages and disadvantages of *stationary* energy storage systems in the electric transport grids.

Advantages	**Disadvantages**
High energy capacities.	High installation capital costs.
Promising for future grids (with PV systems).	Grid modifications necessary.
More flexible and controllable charging scheme.	Expensive to be replaced.

Choosing the most suitable type of energy storage systems regarding their characteristics and placement has a significant role for the scope of this thesis work. Is important to always keep in mind the final goal of the work, which is the finding which energy storage system between *on-board* and *stationary* is most suitable for a multifunctional trolleybus grid. Thus, the technology and placement that best accomplish that should be chosen, simulated and evaluated. In this work, both placements scenarios are simulated, compared, and evaluated.

2.3 CONTROL STRATEGIES OF ENERGY STORAGE SYSTEMS IN ELECTRIC TRANSPORT GRIDS

The implementation of energy storage systems in electric transport grids must be accompanied by the suitable control strategy for their operation. While their technology is important for achieving the desired results, without the proper strategy for their optimal control, they may not be able to provide those results adequately [105]. For this reason, is important to discover the suitable control strategy for the goals of this work. For choosing the most suitable control strategy several factors should be taken into account.

The three most important factors are concluded to be:

1. The technology and characteristics of the storage systems.
2. Their placement in the electric transport grid (*on-board* or *stationary* - section and/or busbar).
3. The final goal - such as increasing PV systems utilization and/or reducing voltage drops.

Depending on the technology of each energy storage system, the proper strategy must be chosen [105]. For example, if a specific type of batteries is used, such as

nickel cadmium (NiCd) or *lead-acid* (Pb-acid), the operation of which is more dependent on their state of charge (SoC) compared to other energy storage systems, then this must be taken into account in the control strategy. This will ensure that they may not to get discharged to a very low level which can cause permanent damage to them [51]. On the other hand, if for example *supercapacitors* (SC) are used, then should be taken into account that they are able to provide a high discharging current but for only a short period of time [48, 52]. Thus, for each energy storage technology, there are specific criteria that must be met for their optimal control.

Furthermore, the placement of the energy storage systems in the electric transport grid has a significant impact on the control strategy that should be used [18]. Depending if the *stationary* energy storage used is placed on the busbar, in the beginning of the section, or at the end, the suitable strategy must be used. For example, *stationary* energy storage systems usually have a larger energy capacity than *on-board*, thus they can store energy provided by PV systems during the day and can be used during the night [103]. In any case, the most important factor behind each control strategy is the desired final goal that needs to be achieved. This is what defines the whole process of creating a suitable control strategy. An interesting example is the work of [106] in which the main goal is the reduction of energy consumption in public transport of the trolleybus system in Gdynia, Poland. The desired goals may vary for each design, as observed in [107] where the main goal is energy conservation and emissions reduction or in [108] where the main goal is to ensure electric power flow and balance in the grid. It is interesting to explore some examples in order to realize how versatile the final goals may be and how deep going into them can benefit this work.

Firstly, [47] proposes an energy management strategy based on dynamic modelling for dual source trolleybus. Their goal is to reduce grid peak electric power in on-line mode and energy consumption in off-line mode, thus improving economy. Also, [109] proposes a rule-based energy management for dual-source electric buses extracted by wavelet transform. In this case, their goal is to ensure durability for the batteries and electric power grid stability, delaying the batteries lifespan and reducing the size of the storage needed. Finally, [110] proposes a strategy for optimal control of reversible substations and wayside storage devices for voltage stabilization and energy savings in metro railway networks. Their goal is the optimal control of reversible substations and wayside storage devices for energy savings and voltage stabilization as well as the maximization of the recovered energy.

As is observed, the control strategies can vary to a great extend depending on the desired goal. The logic behind each control strategy may be more or less complex depending on that and on how accurately this is wanted to to be achieved. That is why it is necessary for simulations to be conducted and each control strategy to be specifically customized for the specific electric transport grid that is applied to. This should always kept in mind while modelling the trolleybus grid in this thesis work. Thus, for this work is preferable for a *rule-based* control strategy based on voltage control to be used. This is done as is found in the literature as the control strategy scheme with the most advantages. More deep analysis regarding the control strategies used for this work is presented in section 2.4.2 and chapter 3. To get a better picture about the control strategies that can be found in the literature and their implementation to electric transport grids, a comparison of literature information is presented in table 2.4. As is observed, when there is a *stationary* energy storage system analyzed, there is also implemented a PV system. This makes more promising the increase of PV utilization with the help of a *stationary* energy storage system rather than an *on-board* energy storage system.

Table 2.4: Comparison of literature information of control strategies of energy storage systems in the electric transport grid.

Title	Area of use	PV System	IMC/ Full EV	On-board (OESS)	Stationary (SESS)	Control strategy basis (variables used)	Logic
Energy management strategy based on dynamic programming for dual source trolleybus. [47]	Trolleybus	No	Yes	Applicable	Not analyzed	• Global optimization energy management strategy. • SoC of SC and SoC of the battery pack.	• Dynamic programming.
A multi-level energy management system for multi-source electric vehicles – An integrated rule-based meta-heuristic approach. [105]	EVs	No	Yes	Applicable	Not analyzed	• SoC. • Power demand.	• Rule-based (strategic decisions). • Meta-heuristic (tactical decisions).
A Planning Method for Partially Grid-Connected Bus Rapid Transit Systems Operating with In-Motion Charging Batteries. [26]	Trolleybus	No	Yes	Applicable	Not analyzed	• In motion charging. • Mixed charging. • Depot (overnight) charging.	• Rule-based.
Reducing of energy consumption in public transport – results of experimental exploitation of super capacitor energy bank in Gdynia trolleybus system. [106]	Trolleybus	No	Not analyzed	Yes	Applicable	• Voltage control.	• Rule-based.
Ensuring sustainable development of urban public transport: A case study of the trolleybus system in Gdynia and Sopot (Poland). [9]	Trolleybus	No	Yes	Applicable	Not analyzed	• Opportunity charging. • Mixed charging. • Depot (overnight) charging.	• Rule-based.
Rule-based energy management for dual-source electric buses extracted by wavelet transform. [109]	Electric bus	No	Yes	Applicable	Not analyzed	• Energy management strategy (wavelet transform). • SoV of SC and SoC of the battery pack.	• Rule-based (wavelet transform).
Multisource Coordination Energy Management Strategy Based on SOC Consensus for a PEMFC–Battery–Supercapacitor Hybrid Tramway. [28]	Tram	No	Yes	Applicable	Not analyzed	• Self-convergence droop control.	• Rule-based.
Stochastic optimization of a stationary energy storage system for a catenary-free tramline. [29]	Tram	No	Not analyzed	Not analyzed	Yes	• Chance-constrained programming for SESS optimization. • Various decision variables (mainly SESS and operating costs).	• Stochastic SESS optimization (Disciplined convex programming).
Power Control Optimization of an Energy Storage System in DC Electric Railways. [20]	Train	No	Not analyzed	Not analyzed	Yes	• Optimal control (voltage based).	• Mixed integer programming.
Optimal control of reversible substations and wayside storage devices for voltage stabilization and energy savings in metro railway networks. [110]	Metro	No	Not analyzed	Not analyzed	Yes	• Optimal control (SoC based).	• Linearization of the DC power flow equations.

Table 2.4 (continued): Comparison of literature information of control strategies of energy storage systems in the electric transport grid.

Title	Area of use	PV System	IMC/ Full EV	On-board (OESS)	Stationary (SESS)	Control strategy basis (variables used)	Logic
Line Voltage Control based on Wayside Energy Storage Systems for Tramway Networks. [18]	Tram	No	Not analyzed	Not analyzed	Yes	• Voltage control.	• Rule-based (heuristic).
Research and analysis of a flexible integrated development model of railway system and photovoltaic in China. [34]	Train	Yes	Not analyzed	Not analyzed	Yes	• SoC. • AC optimal power flow (AC-OPF) problem.	• Rule-based.
Study of trackside photovoltaic power integration into the traction power system of suburban elevated urban rail transit line. [35]	Metro	Yes	Not analyzed	Not analyzed	Yes	• Voltage control.	• Rule-based.
Electric railway smart microgrid system with integration of multiple energy systems and power-quality improvement. [32]	Train	Yes	Not analyzed	Not analyzed	Yes	• Voltage control.	• Rule-based.
Integration of Distributed Energy Resources and EV Fast-Charging Infrastructure in High-Speed Railway Systems. [39]	Train	Yes	Not analyzed	Not analyzed	Yes	• Voltage control. • SoC.	• Rule-based.
Auxiliary power supply system of passenger train based on photovoltaic and energy storage. [107]	Train	Yes	Not analyzed	Not analyzed	Yes	• SoC. • Power demand.	• Rule-based.
Integration of PV and Battery Storage for Catenary Voltage Regulation and Stray Current Mitigation in MVDC Railways. [21]	Train	Yes	Not analyzed	Not analyzed	Yes	• Voltage control. • SoC.	• Rule-based.
Energy Management of A Smart Railway Station Considering Regenerative Braking and Stochastic Behaviour of ESS and PV Generation. [38]	Metro	Yes	Not analyzed	Not analyzed	Yes	• Various decision variables (PV generation, power bought from the grid, power sold to the grid, etc.).	• Mixed integer linear programming (MILP) model - stochastic approach.
Solar PV System for Electric Traction Application with Battery Backup with Battery Backup. [37]	Train	Yes	Not analyzed	Not analyzed	Yes	• Charge during the day and provide the stored energy during the night.	• Rule-based.

2.4 SCENARIOS AND CONTROL STRATEGIES PRINCIPLES

After the literature search considering the functionalities of energy storage in trolleybus grids, the technologies of such systems, and their control strategies, are presented the decisions for the execution of the simulations of this work. First, are presented the scenarios according to the type and the characteristics of the energy storage systems, and then are presented the control strategy principles based on which the simulations will be conducted on, both for *on-board* and *stationary* energy storage systems.

2.4.1 Scenarios

Taking into consideration the information found in the literature, for this work are chosen to be simulated four total scenarios of three different energy storage systems technologies. More specifically, the scenarios are presented in table 2.5.

Table 2.5: Simulation scenarios.

***On-board* energy storage system**	***Stationary* energy storage system**
Supercapacitors (SC)	Flywheels
Lithium-Titanate-oxide batteries (LTO)	Lithium-Titanate-oxide batteries (LTO)

These technologies for energy storage systems have been deemed as the most promising for use in electric transport grids and most interesting for investigation compared to others. This is because is observed that they are been used in that sector increasingly more, as manufactures are transitioning from more traditional energy storage systems (such as *nickel cadmium* (NiCd)) to these. This is especially visible for the case of *lithium-titanate-oxide* (LTO) batteries, which their use has been increasing in the electric transportation sector during the recent years [16]. This comes down to the rapid development of these technologies, which made them a more suitable solution for this kind of applications. Furthermore, hybrid energy storage systems can also be found in transportation grid systems but they are not examined in this work. This is because their modeling is more complex than the modeling of a non hybrid energy storage system. Thus, for the purposes of this work, it has been deemed more important for more time to be put on the comparison of the effects of *on-board* vs *stationary* energy storage systems rather than the effects of single vs hybrid technologies of energy storage systems.

Nevertheless, it should be mentioned that the installation of some of the selected energy storage systems, are more suitable for either to be implemented as an *on-board* energy storage systems or *stationary* energy storage systems. In other words, they may express better results in only one of those two cases. For that reason, it is interesting to observe the characteristics of the energy storage systems selected, from table 2.1 in order to estimate which solution might be more preferable for either *on-board* or *stationary* energy storage methods.

Supercapacitors (SC) have very small energy density but extremely large power density when compared to the other energy storage systems, and especially electrochemical batteries [48]. This translates to having the capability of providing and receiving high currents, making them rather suitable for providing functionalities such as *electric power peak shaving* [25]. Nevertheless, having around the same energy capital costs as *lithium-ion* (Li-ion) batteries, renders them an expensive solution for *stationary* energy storage due to their small energy density [48]. Thus, they seem as a promising choice to be implemented as *on-board* energy storage systems.

Lithium-titanate-oxide (LTO) batteries follow the trend of *supercapacitors* (SC). They express a smaller energy density than *lithium-ion* (Li-ion) batteries but larger power density [57, 56]. More specifically, it is observed to have characteristics similar to a *lithium-ion* (Li-ion) and *supercapacitors* (SC) hybrid system. This means that they are able to provide a middle ground with the best of both of these two worlds. In this case too their rather poor energy density and comparable energy capital costs with *lithium-ion* (Li-ion) batteries, might make them also an expensive solution to be used as a *stationary* energy storage method [58]. Nevertheless, *Lithium-titanate-oxide* (LTO) batteries express a high energy capacity in per cell level [60]. This means that, although they can provide and accept considerable amount of current, when used in small capacities - approximately up to 20 kWh - their string voltage is not high enough to translate to high electric power [111]. Thus, in this case they may be preferable to be used as a *stationary* energy storage system as the larger capacities used in those occasions can enable them to accommodate larger electric powers providing much greater results for the analyzed configurations of energy storage systems investigated in this work. However, it is also interesting to examine the results when used as *on-board* energy storage systems since this technology gains more and more interest everyday to be used for *in-motion charging* (IMC), where bigger capacities are used.

Flywheels have similar behaviour with *lithium-Titanate-oxide* (LTO) batteries but with a bit lower power density than them [48, 49]. Their major disadvantages are their self-discharge and their response time when used in large scale power applications, which can have an order of magnitude of some seconds rather than milliseconds compared to other energy storage systems [42]. For the examined application of this work, the flywheel system sized for the power levels necessary, which are in the order of 200 kW, does not impose a response time larger than a second. Thus, it is not taken into consideration in this work. Also, their indicated storage time can be rather small, having an order of magnitude of some seconds to several minutes, meaning that they usually have a considerable self-discharge rate [48, 86]. That is why it is interesting to observe the results occurred from their implementation as a *stationary* energy storage system. Due to practicality reasons and easiness of acquisition of commercially available flywheel systems for micro-grid applications, it would be preferable to be used as a *stationary* energy storage system. In figure 2.8 is illustrated a 3D render of a flywheel farm and its components.

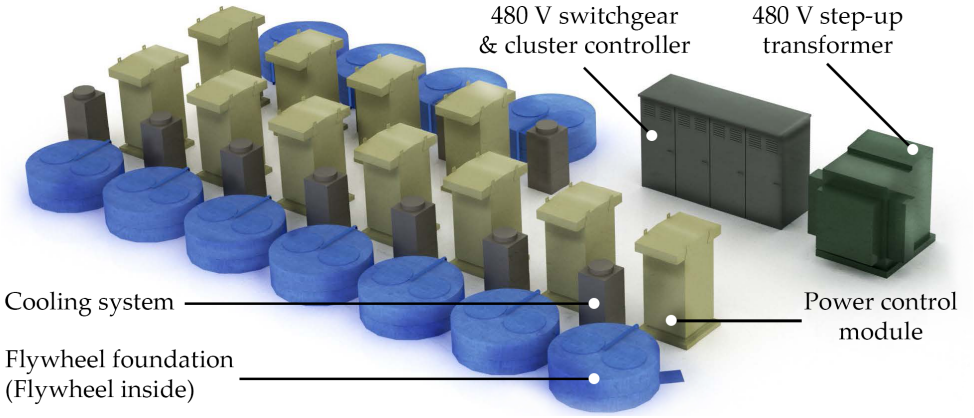

Figure 2.8: 3D render of a flywheel farm and its components [© Beacon Power™].

2.4.2 Control strategies

For the efficient operation of the various types of energy storage systems, a suitable control strategy must be chosen for each one of them. The control strategy is re-

sponsible for respecting the constrains of the energy storage system while trying to accomplish the main goal as accurately as possible. The main goal of this work is the comparison of the utilization of the electric power provided by the PV system implemented in the AC side of the substation supplying the trolleybus grid, by using *on-board* vs *stationary* energy storage systems. Thus, it aims at finding which of those two energy storage systems is more favorable in maximizing the electric power provided by the PV system so is not injected into the AC grid, as well their impact for the rendering the trolleybus grid ready for the future. This may have as a result the need for a smaller PV system size as well as a smaller capacity of energy storage system, which may translate to smaller costs. Nevertheless, constraints for each case should be taken account when trying to achieve this goal.

After research in literature, is observed that the vast majority of the already implemented control strategies in the catenary electric transport grids are mainly *rule-based* [26, 106, 9, 109, 28, 18]. A *rule-based* system is a system that applies human implemented rules, following a pre-decided logic. It is a logical program that uses predefined rules to make choices and deductions for performing automated actions. This assumes that there is an expected behaviour by the system and its components, which makes it predictable to changes. Usually, the more cases of rules there are, the more the system is capable to operate adequately under extreme conditions [112]. The key dilemma and problem when it comes to the implementation of PV systems and *on-board* or *stationary* energy storage systems is the fact that the first are moving along with the trolleybus. Thus, the intermittency problem of PV system electric power generation and trolleybus scheduling always exists. Also, since *on-board* energy storage systems are not able to be charged actively with extra electric power drawn from the grid, their control for charging and discharging is limited and mainly has to do with the electric power profile of the trolleybus. On the other hand, *stationary* energy storage systems seem more promising for increasing the PV system utilization since they are present always at the specific section of the trolleybus grid that they are installed to. Nevertheless, their control strategy should be tuned and developed for the specific part of the grid that they are installed to.

For the completion of this work are used rule-based strategies, both for the control of the *on-board* and the *stationary* energy storage systems. More specifically, for the *on-board* energy storage system is used a technique of *electric power peak shaving* with positive and negative thresholds for determining the electric power for discharging and charging the energy storage system respectively. For the *stationary* energy storage system is used a technique of voltage control and PV electric power generation estimation, which according to specific voltage values measured at the connection point of the energy storage system with the section and an estimation of the electric power generated from the PV system by using a photoresistor at the location of the energy storage system, is determined the electric power either to be charged or to be discharged. More details about their logic of operation and their creation as models are presented in chapter 3.

2.5 CONCLUSIONS

In this chapter has been presented a survey on the functionalities of energy storage systems used in electric transport grids, their technologies, their control strategies, and the basic decisions considering the scenarios simulated in this work. Energy storage systems on trolleybus grids can vary on their provided functionalities, technologies, placement, and control strategies. For each case, a specific type of energy storage system can provide a higher benefit for specific parameters. In the next chapter (chapter 3) are presented and analyzed the various models used for the conduction of the simulations.

3 MODELS AND PARAMETERS

In this chapter are presented the models used for the simulations of this work along with the selected values of their parameters. Firstly, the model of Arnhem's trolleybus grid and the model of the PV system are presented. Afterwards, the model of the energy storage system is presented, while at the end, the control models of the on-board and the stationary energy storage systems are presented. All models are created in MATLAB®.

3.1 ARNHEM TROLLEYBUS GRID MODEL

For this work to have a solid scientific basis, the comparison and analysis of *on-board* vs *stationary* energy storage systems has been made using a real case study using the model of the trolleybus grid of the city of Arnhem, the Netherlands. Therefore, in this section are presented the operational principals of the model used for this work as well as which sections of it are decided to be simulated. It is important to be clarified that the model presented has been created by a third party of people and is analytically described in an article in a published journal [2]. Thus, since this model has already been tested and verified in an other work, no deep and analytical description is given for it here.

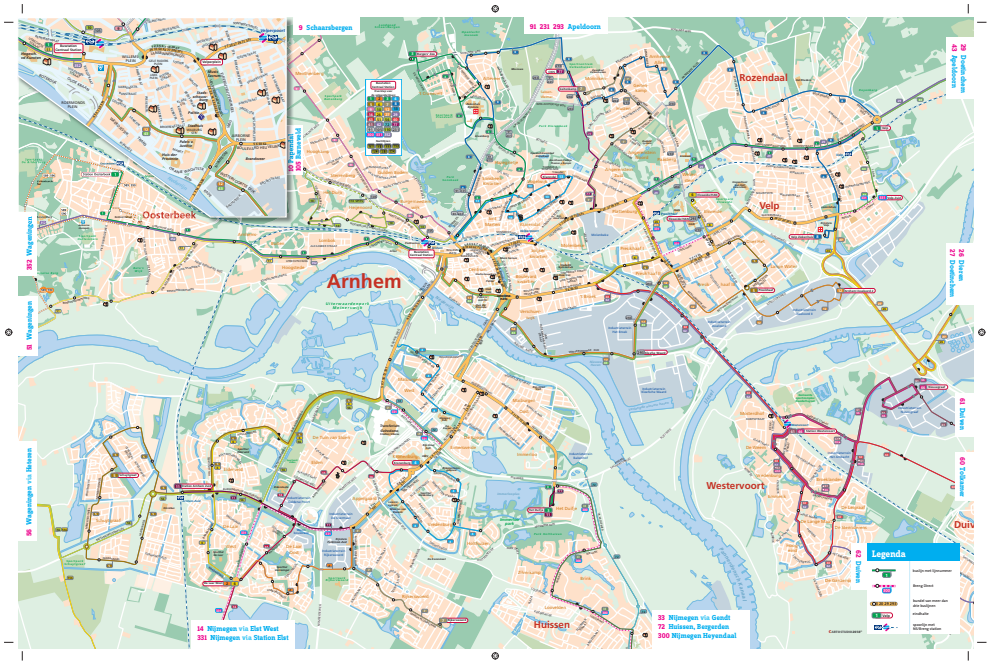

Figure 3.1: Map of Arnhem's trolleybus grid [© Connexxion].

In figure 3.1 is presented a map of Arnhem's trolleybus grid provided by *Connexxion*. The trolleybus grid of Arnhem has been selected as a case study as is considered to be one the biggest trolleybus grids in north-west Europe and the largest one in the Benelux Union. Besides that, Arnhem's trolleybus grid is selected to accommodate the trolley2.0 project which means that it will be enlarged with various components, and mainly *in-motion charging* (IMC) capabilities. This renders it a perfect candidate

for a case study as it can be examined how and to what extend will be able to accommodate other possible components such as EV chargers, as well as *on-board* and *stationary* energy storage systems, transitioning to a multifucntional trolleybus grid.

3.1.1 Operational principles of the model

The trolleybus grid of Arnhem has in total six (6) operating lines (1. De Laar West - Velp, 2. Centraal Station - De Laar West, 3. Burgers Zoo - Het Duifje, 5. Schuytgraaf - Presikhaaf, 6. Centraal Station - Elsweide/HAN, 7. Geitenkamp - Rijkerswoerd). Regarding its construction, it consists of forty-four (44) sections and eighteen (18) substations. One substation can provide electric power to one, two, or more sections at the same time. This is especially profound on sections located close to the city centre. The grid has bilateral connections too. This means that two or more sections that are being fed with electric power by different substations can be connected to each other allowing electric power to flow from one to another. This can improve the efficiency of the system as a whole as now there is more freedom for the electric power to flow between larger parts of the grid, increasing the possibility of the recuperated energy to be utilized rather than to be wasted on the internal resistors of the trolleybuses.

In figure 3.2 is presented the flow chart of the algorithm on which is based the logic of operation of the trolleybus grid model of Arnhem. The model of trolleybus grid of Arnhem is created using MATLAB® and is based on the backward-forward sweep method [113]. It is designed to run in per section level, meaning that it can simulate one section of the grid per simulation run, for a selected period of time; days or a whole year. The user defines the desired section to be simulated, if the simulation should be conducted by taking the possible bilateral connection into consideration, and the period of the simulation. Then the algorithm, based on that inserted data, loads and sorts the already known positions and electric powers of the trolleybuses, as well as all the necessary data for the conduction of the simulation. That data may be the section length, the substation DC nominal voltage at the rectifier output, the resistance of the selected section etc. After that, the operation of the algorithm is basically straight forward as it follows the principle of the backward-forward sweep method. It is important to note that the model is a steady state model and does not take into consideration transient phenomena. In [2] is described why this approach is used and why it does not impose limitations to the results.

For each simulated time instance, which is one second for this case, the algorithm calculates the currents of all the DC components of the trolleybus grid based on their already known, measured, and estimated electric powers of the trolleybuses, using the substation DC voltage as a slack node. Then, based on their calculated currents, it calculates the new voltage of each trolleybus, that occurs due to voltage drop. After that it goes back and recalculates the currents based on the new calculated voltages. This loop, which represents one second of simulation, continues as many times is necessary for the algorithm to converge within a preset margin - i.e. if the the values of the currents between two consecutive loops do not change more than a preset value. In [2] is given a thorough and analytical explanation of the structure of the code and how often neglected characteristics of trolleybus grids in other works, such as recuperated energy, auxiliary loads like HVAC, bilateral connections, and the exact nominal voltage of the substations, can have a significant impact on the results. At the end, the model provides information regarding the total electric power demanded, the voltage, the current, and the transmission losses in the simulated section of the model.

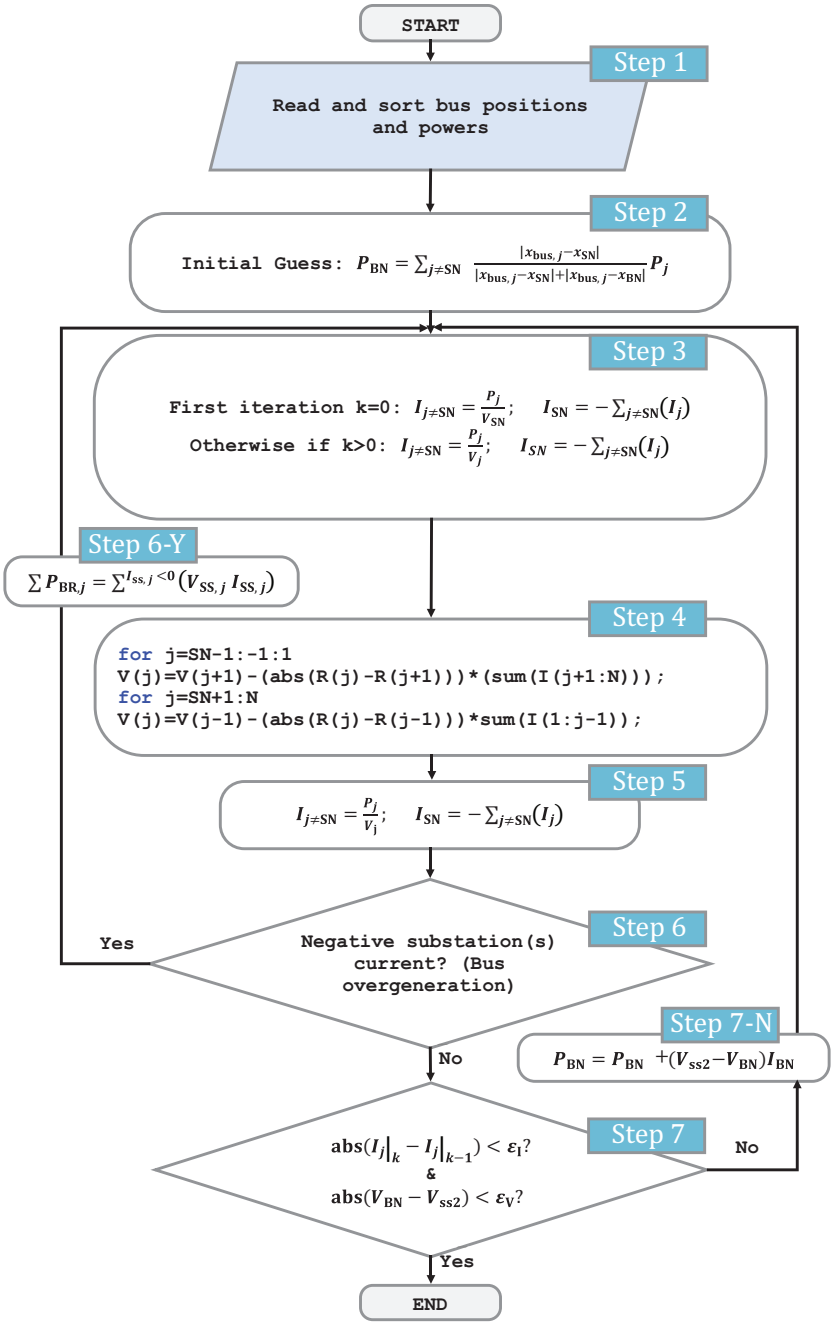

Figure 3.2: Algorithm flow chart of the grid model logic [2].

3.1.2 Simulation parameters

From the above, is clear that the model used is detailed and analytical enough to provide high quality results considering the implementation of various components in it. More particularly, in this work, those components are the trolleybuses with *on-board* energy storage systems or with *stationary* energy storage systems. It should be noted that at every time only one of those two systems will be simulated and not both of them as a combination. Thus, it can be extracted data regarding the impact on the PV system utilization of those two different energy storage systems, on the total electric energy consumption, and the impact on voltage drops.

Regarding the parts of the trolleybus grid to be simulated, are decided three sec-

tions to be simulated, two of which belong to the same substation. More specifically, those are sections 23 and 24 that both belong to substation 12 and section 25 that belongs to substation 9. The substations for both cases do not feed with electric power any other sections. The first two sections are located in the north-west side of the trolleybus grid and are considered to have a normal amount of traffic but far less than the amount of traffic observed in sections located close to the city centre. Section 25 on the other hand is located in the centre of Arherm and is considered to have high traffic compared to to the other two. The reason that those sections are selected is so the intermittencies in electric power demands to be evaluated both for a case with low traffic and with high traffic. Note that when multiple sections are fed with electric power from the same substation, the implementation of the *stationary* energy storage system is made only to one of them. For this work, considering substation 12, is chosen section 23 to be the one having the *stationary* energy storage systems. Considering the *on-board* energy storage system, is chosen for all trolleybuses to be equipped with it at the same time.

Figure 3.3: Sections 23 and 24 on CAD map of Arnhem's trolleybus grid [© Connexxion].

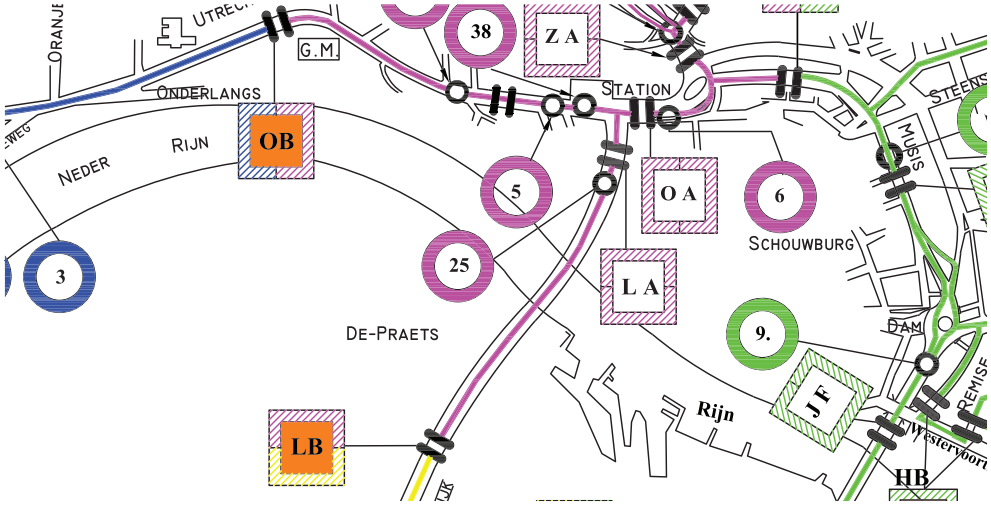

Figure 3.4: Section 25 on CAD map of Arnhem's trolleybus grid [© Connexxion].

In figure 3.3 is presented the part of the map of the trolleybus grid of Arnhem focused on sections 23 and 24 while in figure 3.4 is presented the part of the map of the trolleybus grid of Arnhem focused on section 25. It should be noted that although nearby sections of section 25 are marked with the same colour, section 25 is the only one that is provided with electric power by substation 9.

From the trolleybus grid map is observed that section 23 is bilaterally connected with section 2. Bilateral connections do play a significant role in a DC grid like this as they provide the possibility of electric power exchange between sections [2]. Nevertheless, in this work they are not taken into consideration for one major reason. That is the time limitation considering the simulations duration. In order for one simulation run to be conducted for one section which is not bilaterally connected, for a whole year and without any energy storage systems implemented, is required approximately ten (10) minutes. If the same simulation is to be conducted with a bilateral connection taken into consideration, the simulation time increases to forty-five (45) minutes. Those numbers are then increased enormously with the implementation of energy storage systems and especially with *stationary*, as observed during the conduction of this work. This renders quality assuring the extracted results very time consuming. The results, without bilateral connections, are still accurate as they provide comparable data for the various energy storage systems technologies and placements used in this work. Furthermore, the total simulation time is decided to be a whole year as this is vital for providing accurate results regarding the PV system utilization, which should be evaluated in yearly basis.

Information regarding the selected sections for the conduction of the simulations is presented in table 3.1. The feeder cable resistance and the section resistance are multiplied by the number of two due to the two electric power lines required to complete a DC system; positive and negative. Only the section resistance is then divided by the number of two due to the two parallel electric power lines that exist in those sections. Their existence has as a purpose the reduction of the total resistance as described in section 2.1.1.

Table 3.1: Information of simulated grid sections.

Parameters	**Section 23**	**Section 24**	**Section 25**
Nominal voltage (V):	686	686	677
Length (m):	850	1400	860
Feed-in point, west to east (m):	80	1310	100
Feeder cable length (m):	98	118	180
Section resistance (mΩ/m):	0.172*2/2	0.172*2/2	0.172*2/2
Feeder cable resistance (mΩ/m):	0.0283*2	0.0283*2	0.0283*2

3.2 PV SYSTEM MODEL

Before going through the operational principles of the PV system model, is important first to analyze possible placement positions of such systems in catenary grids. More specifically, the PV systems used for trolleybus grid implementation can be divided into two basic categories depending on the part of the grid that are connected to.

Possible placement positions of PV systems in trolleybus grids:

1. On the DC side, either on the busbar or anywhere on the overhead electric power lines of a section.
2. On the AC side of the substation between the transformer and the AC to DC power electronic converter.

In figure 3.5 is presented the implementation of a PV system to a substation DC busbar (left) and on the AC side (right) of the trolleybus grid. For simplicity, the use of power electronic converters is not illustrated in the figure.

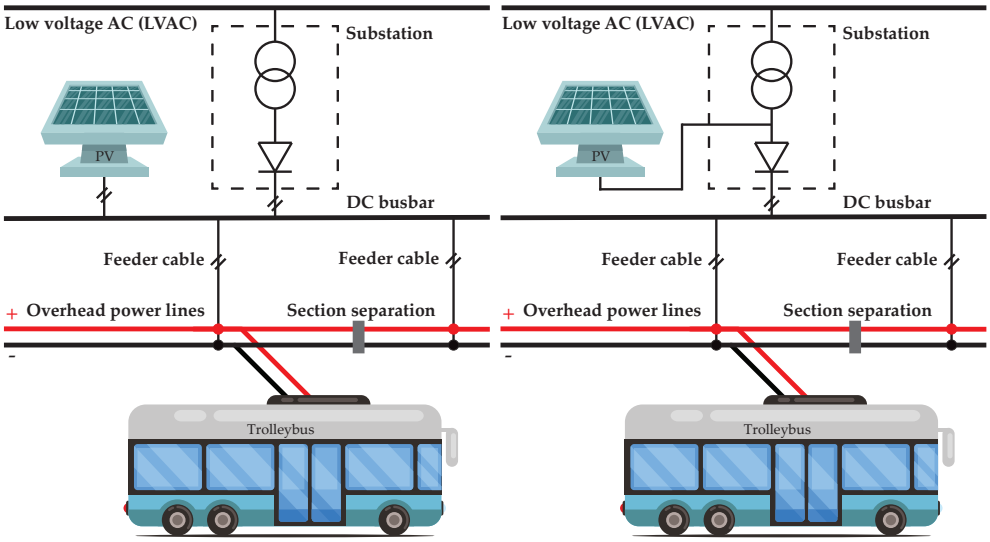

Figure 3.5: PV system implemented to a substation DC busbar (left) and on the overhead electric power lines of a section (right) of the trolleybus grid, without the illustration of power electronic converters for simplicity.

Both of the above possible placements come with advantages and disadvantages. Usually, the first configuration is preferred for such applications as the nature of the electric power provided by PV systems is DC [15]. Thus, by implementing the PV system directly to the DC side, and especially to the overhead electric power lines of the sections, the trolleybuses can directly utilize the provided electric power without the extra losses of a DC to AC and then a AC to DC power electronic converter. This reduces the converter and transmission losses and can increase the efficiency of the system. It can also help compensate for the voltage drops in the sections by acting as another electric power source besides the substation. If the PV system is placed on the DC busbar then it would be able to provide its electric power to all the sections connected to it, again with reduced losses caused by the absence of extra power electronic converters. Nevertheless, in all cases that the PV system is connected to the DC side, is not able to provide electric power to the main AC grid due to the substation's power electronic converter diodes. Thus, when the PV system electric power generation exceeds the load demand in the DC grid, then the electric power available from the PV system cannot be utilized. This requires the electric power to be wasted or to be stored.

On the other hand, if the PV system is placed on the AC side of the substation, this provides the possibility for the excess electric power produced, which may not be able to be utilized by the trolleybus grid, to be injected into the AC grid. This of course has drawbacks compared to placing the PV system to the DC side as now the electric power provided from it has to travel through multiple power electronic converters and longer distances to get to the DC grid loads. Also, now the PV system itself is not able to provide a compensation for the voltage drops in the trolleybus grids when high electric power demands occur. Finally, when the PV system is available to provide electric power to the main AC grid in periods where the trolleybus grid demand is lower than the PV system electric power generated, there may occur phenomena of harmonics that could be injected in the AC grid, causing electric power quality issues [19].

3.2.1 Operational principles of the model

Considering the PV system model, in this case too like the Arnhem trolleybus grid model, has been created by a third party of people and is analytically described in

an article in a published journal [3]. Thus once again, since this model has already been tested and verified in an other work, only the basic principles of operation are presented here.

The model is a simulation of the energy provided from the installed photovoltaic panels as an output and its discretion is one second. As described in [3], the model is advanced enough and takes into consideration multiple parameters such as the solar altitude, the solar azimuth, the global horizontal irradiance (GHI), the diffuse horizontal irradiance (DHI), the ambient temperature, the ground temperature, the wind speed and more. These values are extracted from a global meteorological database using the *Meteonorm* software. Also, although shading due to clouds is implemented in the model, shading from other panels is not taken into consideration as is considered enough spacing between the panels to avoid that. For the model to take shape, is used a commercial mono-crystalline PV panel module from Astroenergy. More specifically is used the AstroSemi 365W PV panel with a rated power of 365 Wp, an efficiency of 19.7%, and a total surface area of 1.85 m^2 [3]. In figure 3.6 is presented the simulated electric power output of the PV system generation in Arnhem per PV panel area in W/m^2 for a whole year.

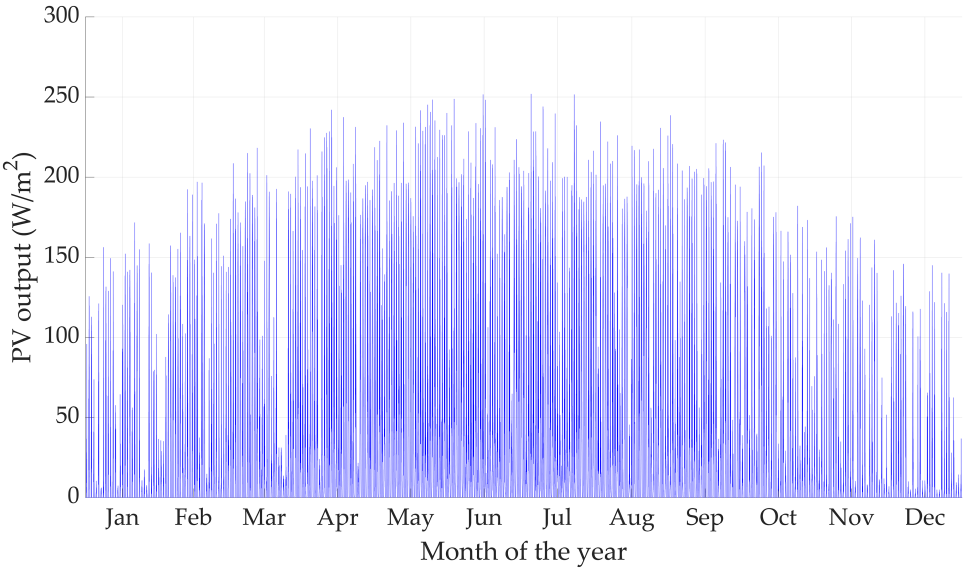

Figure 3.6: Yearly simulated electric power output in W/m^2 of the PV system generation in Arnhem [3].

3.2.2 Simulation parameters

For this work is assumed that the PV system is placed on the AC side of the substation. Is also assumed to be placed very close to the substation so when electric power is being demanded from the trolleybus grid, the majority of is provided by the PV system with minimal transmission losses. So, in this work, after the simulations with the various energy storage systems implemented in the trolleybus grid, is measured the impact in the total demand from the substation, out of which is calculated how much has been supplied by the PV system. This is presented in equation 3.1 with P_{load} the total load electric power demand of the trolleybuses, P_{grid} the electric power delivered from the AC grid, and P_{PV} the PV generated electric power. Placing the PV system to the AC side is chosen because the goal of this work is to compare *on-board* vs *stationary* energy storage systems for a multifunctional trolleybus grid. This includes also increasing the renewable energy share, which in this case is PV system utilization, but without focusing in finding optimal ways to implement a PV system into the DC trolleybus grid. Also, as mentioned

earlier, placing the PV system to the AC side increases the probability that excess generated energy will be used rather than be wasted, something important since it is unlikely that any energy storage system may be sufficient enough to store 100% of the excess generated energy from the PV system.

$$U_{PV} \triangleq \frac{\int_{year}(P_{load} - P_{grid})dt}{\int_{year} P_{PV}dt} \tag{3.1}$$

Considering the sizes of each installed PV system feeding with electric power each substation, those are chosen based on the necessary sizes for achieving an energy-neutrality ratio equal to one (ζ=1) without the implementation of an energy storage system. This is done to be used as a reference for the comparison of the various energy storage systems used for the conduction of this work. As described by equation 3.2, the energy-neutrality ratio is defined as the ratio of the yearly produced energy by the PV system divided by the yearly demanded energy by the load.

$$\zeta \triangleq \frac{\int_{year} P_{PV}dt}{\int_{year} P_{load}dt} \tag{3.2}$$

In addition to those terms, it is important to introduce the term of direct load coverage (Λ), described by equation 3.3. This is the fraction of the load that can be directly supplied by the output of the PV system. It is possible to combine equation 3.1 and equation 3.2 and create equation 3.4, ignoring all power electronic converter losses [3].

$$\Lambda \triangleq \frac{\int_{year}(P_{load} - P_{grid})dt}{\int_{year} P_{load}dt} \tag{3.3}$$

$$\Lambda = \zeta * U_{PV} \tag{3.4}$$

As concluded from [3] and confirmed in this work too, in table 3.2 are presented the sizes of the the PV system implemented in substation 9 (section 25) and the PV system implemented in substation 12 (section 23 and section 24) for an energy-neutrality ratio equal to one (ζ=1) without the implementation of an energy storage system. It is important to note that those values are acquired after taking into consideration the power electronic converter losses. More particularly, since the PV system is placed at the AC side, there will be a portion of energy used directly by the trolleybus grid and another one first sent to the AC grid and re-used later. As described in [3], this efficiency is assumed to be $n^* \approx 0.957$.

Table 3.2: PV system sizes for an energy-neutrality ratio equal to one (ζ=1) without the implementation of an energy storage system.

	Substation 9	**Substation 12**
PV system size (kWp)	129	195

3.3 ENERGY STORAGE SYSTEM MODEL

The energy storage system has a key role for the conduction of this work. For this reason is important that it represents the selected technologies adequately. The model for the various variations of energy storage systems has been developed from the ground up for the purposes of this work and is the same both for the scenarios of the *on-board* and the *stationary* energy storage systems. It is based on a constraint checking algorithm where by using a desired electric power as an input, either for charging or discharging, is determined the amount of energy to be stored or to be

discharged respectively. It has multiple variables as input such as capacity of the energy storage system (Wh), string voltage (V), string resistance when charging (Ω), string resistance when discharging (Ω), string number, power electronic converter efficiency (%), upper state of charge (SoC) limit (%), lower state of charge (SoC) limit (%), self-discharge (% per day), maximum accepted electric power when charging (W), and maximum provided electric power when discharging (W). By using the parameters regarding the characteristics of the strings, the model calculates the dynamic electric power related charging efficiency (%) and the dynamic electric power related discharging efficiency (%). Note that response times (ramp-up and ramp-down times) are not implemented in the model since the technologies selected for this kind of applications, in combination with their capacities, provide a responses times less than a second, which is less than the simulation discretion of the model.

3.3.1 Operational principles of the model

In figure 3.7 is presented the flow chart of the algorithm on which is based the operation of the model. The flow chart represents one simulated second.

First, in **Step 1**, the model reads the desired electric power to be stored or to be utilized. This electric power is the output of the controller of either the *on-board* or the *stationary* energy storage systems. The discretion between those two states is done by using a positive or a negative sign. More specifically, a negatively signed electric power is used for discharging while a positively signed one is used for charging.

Then, in **Step 2**, the model determines if the current simulated second is the first one of the simulated day. If this is true, the model goes to **Step 2-A** where it checks if this is also the first simulated day of the year. If this is also true, then it proceeds to **Step 2-B** where it uses a 60% initial state of charge (SoC). This value has been selected as a random, indicative value. In case this is not the first simulated day of the year, then the model uses as an initial state of charge (SoC) the one from the end of the previous day as can be seen in **Step 2-C**.

Going to **Step 3**, the model then checks if the decided desired electric power by the controller of the *on-board* or the *stationary* energy storage systems, either to be stored or to be utilized, is bigger than what the technology of the specific energy storage system is allowing it to handle. If it is, then it follows **Step 3-A** where it sets the maximum electric power it can handle as a limit and provides or stores energy with an electric power according to its capabilities. If it is not, then the model continues to the next step. In this work, this value is fixed one, and not a dynamic one related to the state of charge (SoC).

In **Step 4** is determined and calculated the charging or the discharging efficiency. Both of those efficiencies are dynamic, meaning that they are dependent on the value of the exchanged electric power. In equation 3.5 and equation 3.6 are presented the formulas for calculating the dynamic charging and the discharging efficiencies of an energy storage system. Those take into consideration the total string resistance (either for charging or discharging), the string voltage, and the string number. Note that is used a 98% efficiency for the power electronic converter at all times as this is concluded as an indicative efficiency for a typical power electronic converter.

$$n_{charging} = \left(\frac{1}{1 + StringResistance * \frac{ElectricPowerDecided}{StringVoltage^2 * StringNumber}}\right) * n_{converter} \tag{3.5}$$

$$n_{discharging} = \left(1 - StringResistance * \frac{ElectricPowerDecided}{StringVoltage^2 * StringNumber}\right) * n_{converter} \tag{3.6}$$

Continuing to **Step 5**, the model is now able to calculate the new state of charge (SoC) of the energy storage system. This is possible by knowing the state of charge (SoC) for the previous simulation instance, which in this case is the previous second, as well as the decided electric power by the controller to be charged or discharged and the capacity of the energy storage system. The equation, based on which is calculated the new state of charge (SoC), is presented in equation 3.7.

$$SoC(t) = SoC(t-1) + \frac{ElectricPowerDecided * n_{charging/discharging}}{Capacity} \tag{3.7}$$

Going to **Step 6**, the model now sees if the new calculated state of charge (SoC) is within the allowed bandwidth given by the user. In other words, if it is lower than the upper limit and higher than the lower limit. In case that this is not true, the model proceeds to **Step 6-A**. In this step, it calculates only the portion of the decided electric power necessary to push the state of charge (SoC) to the accepted limit but without exceeding it. This happens either for charging or discharging. In other words, it uses only part of the electric power provided or demanded so that the state of charge (SoC) remains within the acceptable bandwidth. Also, as described by equation 3.5 and equation 3.6, the charging and discharging efficiencies are related to the electric power provided or demanded respectively. Nevertheless, for this step only (**Step 6-A**), are used charging and discharging efficiencies the ones as if the whole electric power was available for charging or discharging. This is done as the rise in calculation time in MATLAB® is increasing exponentially if the precise charging or discharging efficiencies would to be found. Nevertheless, this does not impose a measurable error to the results as the difference in the efficiency does not alter significantly between those two occasions. If the state of charge (SoC) is already within the selected bandwidth, then the model proceeds to the next and final step.

Finally, in **Step 7**, the model calculates and deducts from the state of charge (SoC) the amount of energy corresponding to the selected self-discharge. By self-discharge is meant the energy lost due to parasitic losses, usually in form of heat. Thus, this is not a usable energy and for this reason the model just lowers the state of charge (SoC) of the energy storage system. Interesting to note is that the model has the possibility to use different self-discharge rates for an active or idling status. Also, if the state of charge (SoC) gets below the lower limit due to self-discharge, the model only charges the energy storage until it reaches the operational bandwidth again.

Besides the aforementioned capabilities of the model, are implemented also some others, some of which are used and some are not. One capability of the model is to use static charging and discharging efficiencies. This means that the user is able to input specific values (%) to be used as charging and discharging efficiencies, rather dynamic ones which depend on the charging/discharging electric power. Also, the model has the possibility to accept or provide different amounts of electric power depending the state of charge (SoC), both for charging and discharging. More specifically, the model provides the opportunity to the user to form three discreet zones in the usable state of charge range, and decide the maximum electric power that can be handled at each one. Those zones can be different for charging and discharging. Although this provides the opportunity for a more complex model to be used for simulations, preliminary results showed that for this kind of applications, this does not affect the results noticeably. Also, is quite difficult for precise values to be determined since the manufactures do not provide this kind of information in their data-sheet. Thus, in this work, this functionality of the model is not utilized.

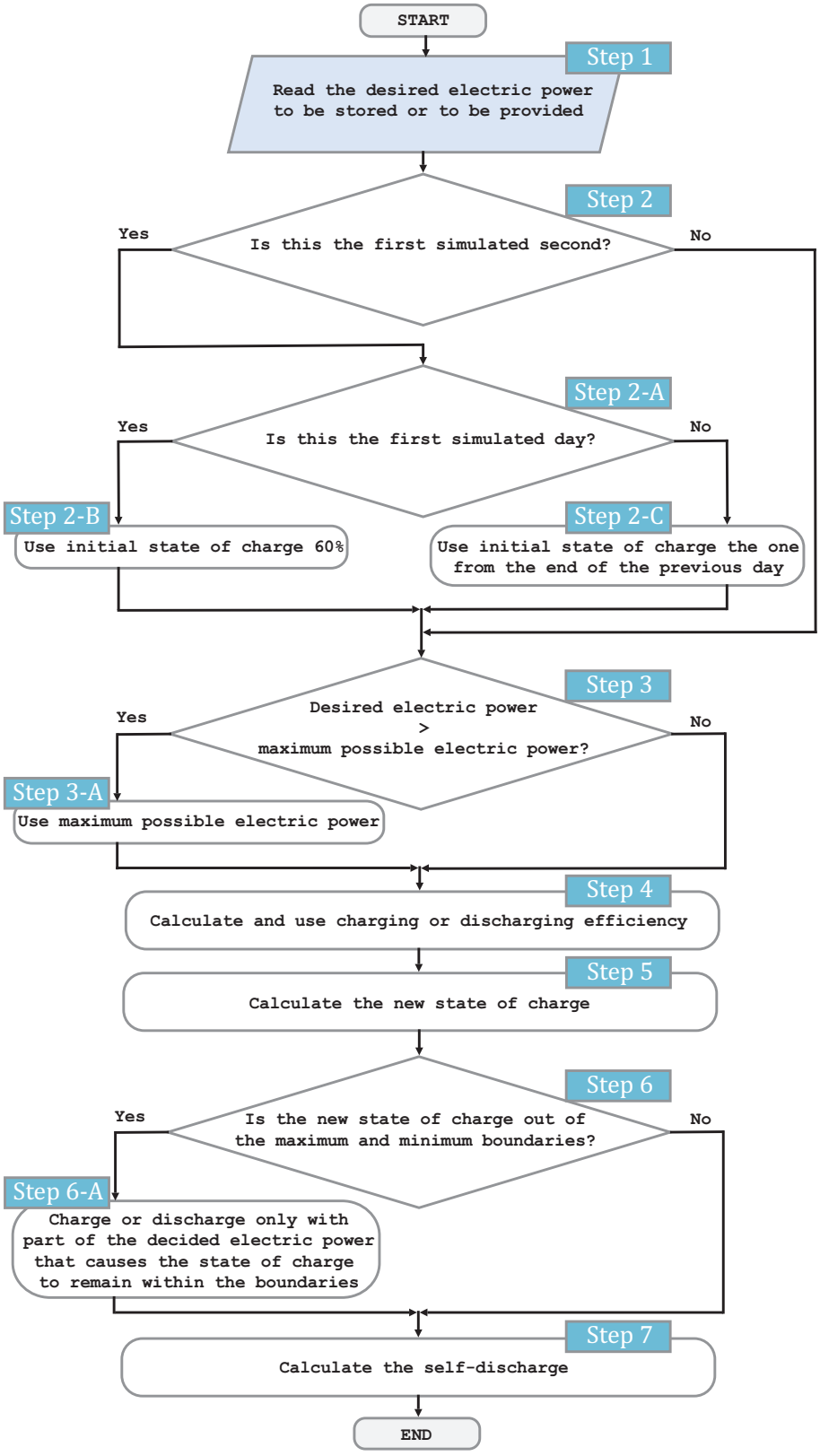

Figure 3.7: Algorithm flow chart of the energy storage system.

3.3.2 Simulation parameters

As already presented in table 2.5 in section 2.4, the technologies to be used for the *on-board* energy storage systems are *supercapacitors* (SC) and *lithium-titanate oxide* (LTO) batteries while for the *stationary* energy storage systems are *flywheels* and

lithium-titanate oxide (LTO) batteries. In that section, are described also the characteristics of each technology.

For the conduction of this work, has been concluded as a best approach to use existing, commercially available energy storage systems. In that way, is possible to use the provided data-sheet from the manufactures and use their data as an input to the energy storage system model. Attention has been made to choose brands which provide products of a technology which are suitable for this kind of application. This is because different brands can provide an energy storage system of the same technology but with different characteristics. Although usually those characteristics are fairly similar between each other as the systems are expressed by the same technology, they may have a significant impact if they fall at opposite ways of their possible spectrum rage.

ON-BOARD ENERGY STORAGE SYSTEM In this work are chosen to be used three different capacities for the *on-board* energy storage system. Those are 1.5 kWh, 3 kWh, and 4.5 kWh. Those capacities are chosen since they are within the spectrum of capacities used for such applications [111, 114, 115, 116].

Considering the *supercapacitors* (SC), is chosen to be created a bank using modules manufactured by Maxwell® Technologies. More specifically is chosen to be used the BMOD0165 P048 CoB module. The characteristics of this module are presented in table 3.3. To create the desired capacities of 1.5 kWh, 3 kWh, and 4.5 kWh, strings of multiple modules must be created. More precisely, are created strings of 14 modules, which have a total capacity 742 Wh each rated at 672 V. In table 3.4 are presented the capacities and strings configurations for the *on-board* energy storage system with *supercapacitors* (SC) used in this work while figure 3.8 is presented a picture of the BMOD0165 P048 CoB module from Maxwell® Technologies.

Table 3.3: Maxwell® Technologies BMOD0165 P048 CoB module characteristics [4, 5, 6].

Variable	Value
Capacity (Wh)	53
Module voltage (V_{DC})	48
Module resistance when charging (Ω)	0.006
Module resistance when discharging (Ω)	0.006
Upper state of charge (SoC) limit (%)	100
Lower state of charge (SoC) limit (%)	0
Self-discharge (% per day)	11.3
Maximum accepted and provided electric power when charging and discharging respectively (W)	3,408

Table 3.4: Capacities and string configurations for *on-board* energy storage system with supercapacitors (SC) [4, 5, 6].

Theoretical capacity (kWh)	Number of modules per string	Number of parallel strings	Actual capacity (kWh)	Maximum accepted and provided power (kW)
1.5	14	2	1.484	95.424
3	14	4	2.968	190.848
4.5	14	6	4.452	286.272

It is interesting to note that the manufacturer claims a 100% depth of discharge (DoD) with a long lifetime for this product. Nevertheless, in this work has been chosen to be used a more sensible range from 95% to 20% [61]. This is done as in this way is extended the life-time of the energy storage system and is accounted

any probability of premature aging of the modules. Regarding the self-discharge, is assumed constant and not to be affected by the state of charge (SoC) levels. Furthermore, in this work is assumed that the power electronic converter, or the arrays of them, are capable of handling all the electric power exchanged by the energy storage system. Thus, they do not impose a limitation to the maximum electric power accepted or provided by the energy storage system. Also, the actual capacities used in the model are slightly lower than the theoretical ones. This comes down to the arrangement of the modules in strings. The configurations used are the ones that best satisfy the desired theoretical capacities.

Figure 3.8: Maxwell® Technologies BMOD0165 P048 CoB module [© Maxwell® Technologies].

Considering the *lithium-titanate oxide* (LTO) batteries, in this case too is chosen to be created a bank using modules manufactured by Altair® Nanotechnologies. More specifically is chosen to be used the 24V 70AH battery module. The characteristics of this module are presented in table 3.5. Similarly to *supercapacitors* (SC), to create the desired capacities of 1.5 kWh, 3 kWh, and 4.5 kWh, strings of multiple modules must be created. Nevertheless, since one module is already 1.5 kWh, while its voltage is considerably lower compared to the voltage levels found in the trolleybus grid, it has been decided for three different string configurations to be used for the different capacities. In other words, the for the case of 1.5 kWh is used one string of one module, for the case of 3 kWh is used one string of two modules, while for the case of 4.5 kWh is used one string of three modules. This is decision has been made since the voltage of as single module is significantly small. Arranging the modules in series helps to increase it, making it easier for the power electronic converter to handle. This is something that has been found as a severe drawback of the *lithium-titanate oxide* (LTO) batteries; in small capacities are simply not able to accept or to provide a considerable amount of electric power, making them a non promising solution to be used as *on-board* energy storage system. In table 3.6 are presented the capacities and strings configurations for the *on-board* energy storage system with *lithium-titanate oxide* (LTO) used in this work while in figure 3.9 is presented a picture of the 24V 70AH battery module from Altair® Nanotechnologies.

In this case too the manufacturer claims a 100% depth of discharge (DoD) with a long lifetime for this product, but again for the same reasons as for *supercapacitors* (SC), has been chosen to be used a more sensible range from 95% to 20%. Once again the self-discharge is assumed to be constant and not to be affected by the state of charge (SoC) as well as is again assumed that the power electronic converter, or

the arrays of them, are capable of handling all the power exchanged by the energy storage system and are not imposing a limitation to it.

Table 3.5: Altair® Nanotechnologies 24V 70AH battery module characteristics [7].

Variable	Value
Capacity (Wh)	1,500
Module voltage (V_{DC})	24
Module resistance when charging (Ω)	0.0045
Module resistance when discharging (Ω)	0.0043
Upper state of charge (SoC) limit (%)	100
Lower state of charge (SoC) limit (%)	0
Self-discharge (% per day)	0.1 [62]
Maximum accepted and provided electric power when charging and discharging respectively (W)	12,000

Table 3.6: Capacities and string configurations for *on-board* energy storage system with lithium-titanate oxide (LTO) batteries [7].

Theoretical capacity (kWh)	Number of modules per string	Number of parallel strings	Actual capacity (kWh)	Maximum accepted and provided power (kW)
1.5	1	1	1.5	12
3	2	1	3	24
4.5	3	1	4.5	36

Figure 3.9: Altair® Nanotechnologies 24V 70AH battery module [© Altair® Nanotechnologies].

STATIONARY ENERGY STORAGE SYSTEM In this work are chosen to be used three different capacities for the *stationary energy storage* system depending from which substation the simulated section is fed with electric power. Those capacities are 129 kWh for section 25, 195 kWh for section 23, and 1 MWh for both sections. The concept behind choosing those capacities for the *stationary* energy storage system is to have a capacity that represents an hourly energy storage system solution and one that is significantly bigger. Thus, the 129 kWh for section 25 and 195 kWh for section 23 are chosen since the PV system sizes used at the substations of those sections are 129 kWp and 195 kWp respectively, as described in section 3.2. The bigger

1 MWh capacity is chosen to be used for both sections as an indicative solution of a big size of an energy storage system. This will provide information of how the results are affected by the limitation of the capacity of the energy storage system. A capacity bigger than 1 MWh may not be feasible to be implemented in reality since the amount of space necessary for the chosen technologies of energy storage system increases drastically. This imposes difficulties for their implementation in dense city centers.

Considering the *flywheels*, is chosen to be used an array of them provided by Amber Kinetics. More specifically is chosen to be used the M32 flywheel. The characteristics of this flywheel are presented in table 3.7. As far as the creation of the desired capacities is concerned, multiple flywheels are connected in parallel to create an array. Each *flywheel* can be independently implemented to the grid and multiple of them connected to it are treated as a parallel array. The biggest limitation of these flywheels is their low power of only 8,000 W that are able to handle at any given time. This limitation is more profound the smaller the total capacity of the array is. A solution to this issue would be to be used a different flywheel provided by Beacon Power™. Nevertheless the flywheels provided by this manufacturer have a significantly higher self-discharge of 240% per day. Preliminary results showed extremely poor behaviour by using this brand and type of flywheels for *stationary* energy storage system. Thus, is preferred the one manufactured by Amber Kinetics. The big difference in the self-discharge of those two brands of flywheels lies in the fact that the one from Amber Kinetics utilizes an magnetically elevated bearing while the whole flywheel is in vacuum. This has as a result a significant reduction in losses. In table 3.8 are presented the capacities and array configurations for the *stationary* energy storage system with *flywheels* used in this work while in figure 3.10 is presented a picture of the M32 flywheel from Amber Kinetics.

Table 3.7: Amber Kinetics M32 flywheel characteristics [8].

Variable	**Value**
Capacity (Wh)	32000
Module voltage (V_{DC})	550-750
Round trip efficiency (%)	86
Self-discharge (% per day)	11.625 (coasting) 18 (active)
Maximum accepted and provided electric power when charging and discharging respectively (W)	8,000

Table 3.8: Capacities and array configurations for *stationary* energy storage system with flywheels [8].

Theoretical capacity (kWh)	**Number of modules per string**	**Number of parallel strings**	**Actual capacity (kWh)**	**Maximum accepted and provided power (kW)**
129	1	4	128	32
195	1	6	192	48
1000	1	31	992	248

Like the decisions regarding the simulations for the *on-board* energy storage system, in this is case too is used a usable state of charge (SoC) range from 95% to 20%. This is done for the same reasons as before that mainly have to do with the life-time of the energy storage system. Also, are made the same assumptions regarding the self-discharge and the power electronic converter. Regarding the actual capacities of the created arrays, like for the case of *supercapacitors* (SC), this comes down to the arrangement of the flywheels in arrays.

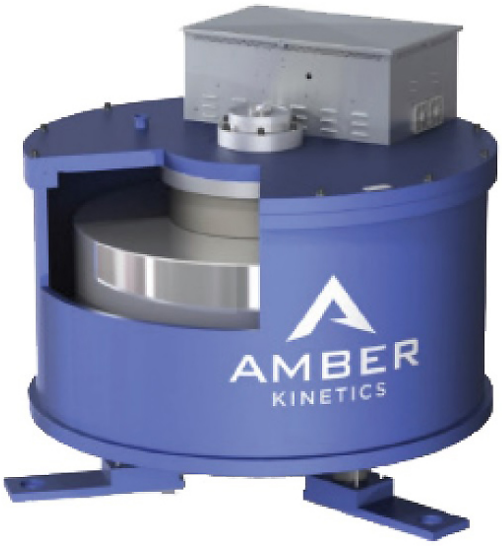

Figure 3.10: Amber Kinetics M32 flywheel [© Amber Kinetics].

For the *lithium-titanate oxide* (LTO) batteries used for the *stationary* energy storage system, those are the same ones as the ones used for the *on-board* energy storage system. Everything that is implied for that case and has already been described, including all the aforementioned assumptions, is implied for this case too. Thus, in table 3.9 are presented the capacities and strings configurations for the *stationary* energy storage system with *lithium-titanate oxide* (LTO) used in this work.

Table 3.9: Capacities and string configurations for *stationary* energy storage system with lithium-titanate oxide (LTO) batteries [7].

Theoretical capacity (kWh)	Number of modules per string	Number of parallel strings	Actual capacity (kWh)	Maximum accepted and provided power (kW)
129	21	4	126	>million
195	21	6	189	>million
1000	21	32	1008	>million

3.4 CONTROL STRATEGY OF THE *ON-BOARD* ENERGY STORAGE SYSTEM

Considering the control strategy of the *on-board* energy storage system used in this work, is rather simple and straightforward. As discussed in section 2.2.2, an *on-board* energy storage system is meant only to accept recuperated power provided by the trolleybus implemented to during regenerative braking and to provide electric power to it after a certain electric power demand value. In other words, it is not meant to be exchanging any electric power with the trolleybus grid directly.

3.4.1 Operational principles of the controller

The basic control strategy that is used for this kind of energy storage system is to get charged when there is recuperating power provided from the trolleybus and to get discharged when the electric power demand of the trolleybus goes above a certain electric power threshold value. This is presented in figure 2.6. It is important to mention that the electric power provided from the *on-board* energy storage sys-

tem is only the one that correlates to the electric power above the set electric power threshold value. In this way, by using a smaller capacity of energy storage system can be satisfied to a great extend all *electric power quality assurance* functionalities.

In figure 3.11 is presented the binary tree chart of the rule-based control strategy used for the *on-board* energy storage system simulated in this work. The control strategy presented is meant to be working for each second, which is the time discretion used for the simulations of this work. When the trolleybus electric power is positive the trolleybus is demanding electric power, while when is negative it is providing electric power via regenerative braking. The output of the controller is a decided, desired value of electric power either to be stored to the *on-board* energy storage system or to be provided by it. This value is the input to the energy system model which is described in section 3.3.

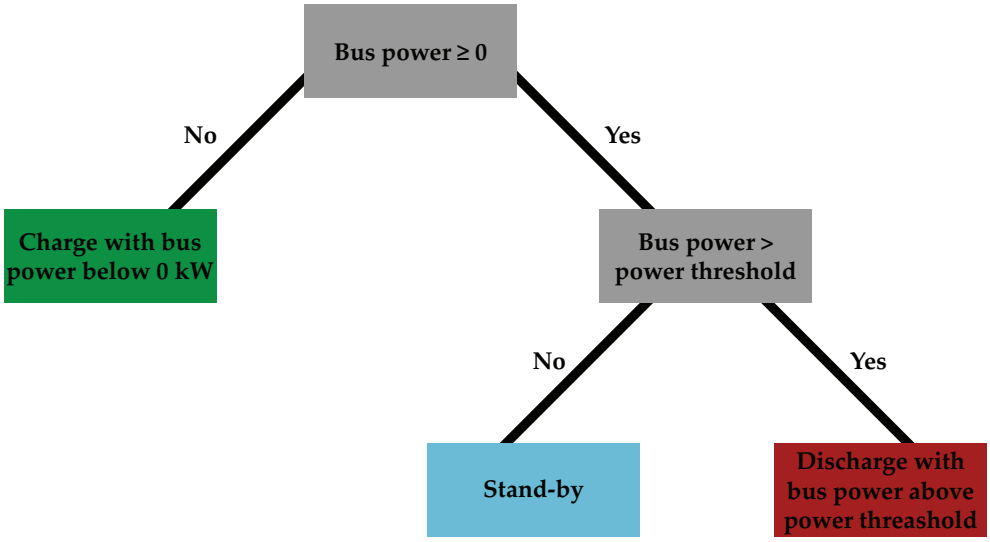

Figure 3.11: Binary tree chart of the rule-based control strategy used for the *on-board* energy storage system.

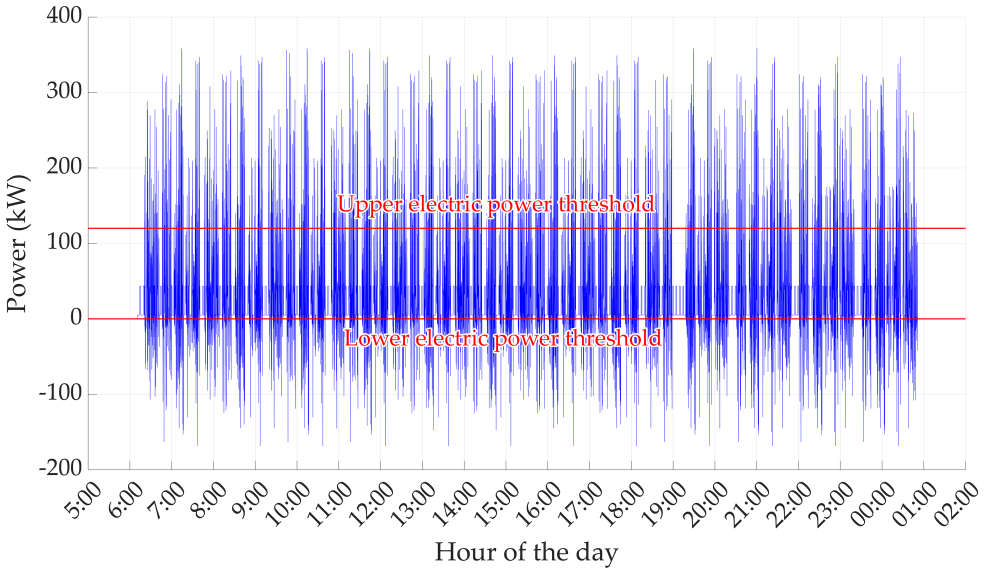

Figure 3.12: Electric power profile of trolleybus No 1 during the first day of the year in Arnhem, with two electric power thresholds of 0 kW and 120 kW for charging and discharging a possible *on-board* energy storage system respectively.

It is interesting to see the the working principles of the controller for the *on-board* energy storage system with the help of an example. In figure 3.12 is presented the electric power profile of trolleybus No 1 during the first day of the year in Arnhem, with two electric power thresholds of 0 kW and 120 kW for charging and discharging a possible *on-board* energy storage system respectively. This figure is similar to figure 2.6 but with the difference that the upper electric power threshold is now set at 120 kW instead of 200 kW.

In figure 3.13 is presented the shaved electric power of trolleybus No 1 during the first day of the year in Arnhem, with two electric power thresholds of 0 kW and 120 kW for charging and discharging a possible *on-board* energy storage system respectively. In other words, is presented only that part of the trolleybus electric power which is above the electric power threshold of 120 kW and below of 0 kW. This figure represents the desired electric power to be charged or to be provided by the *on-board* energy storage system. This has as an effect for the state of charge (SoC) to increase or decrease.

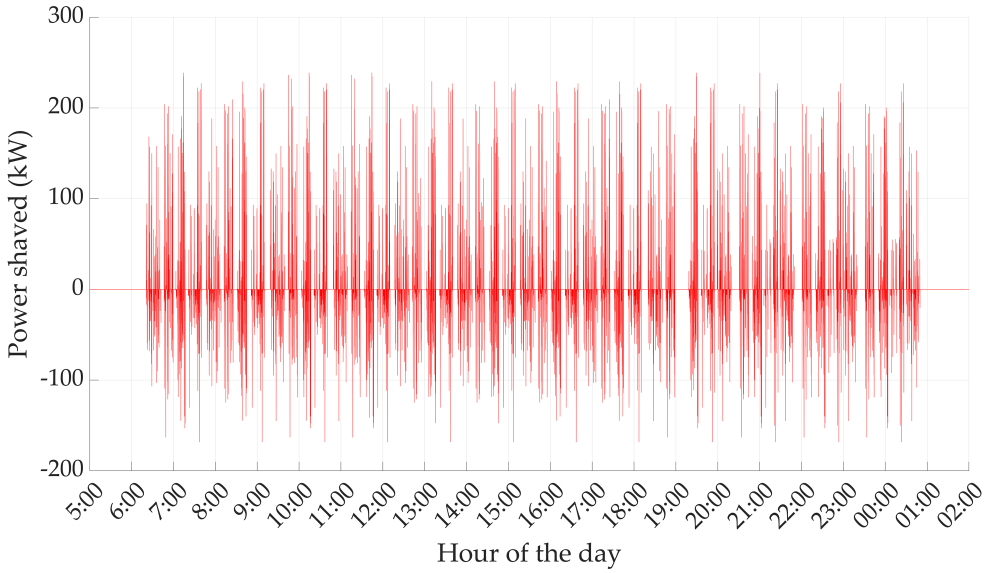

Figure 3.13: Shaved electric power of trolleybus No 1 during the first day of the year in Arnhem, with two electric power thresholds of 0 kW and 120 kW for charging and discharging a possible *on-board* energy storage system respectively.

In figure 3.14 is illustrated the state of charge (SoC) of an *on-board* energy storage system of 3 kWh, with constant charging and discharging efficiencies of 95% and upper and lower limits of 95% and 5% respectively when is handling the shaved electric power of trolleybus No 1 during the first day of the year in Arnhem, with two electric power thresholds of 0 kW and 120 kW for charging and discharging it respectively. For example purposes only, no other parameters are used for this model - i.e. self-discharge, maximum/minimum electric power etc.. Note that a power electronic converter efficiency of 98% is also taken into account.

Finally, is created a new electric power profile for each trolleybus depending on the state of charge (SoC) of the *on-board* energy storage system. If it is full, then the regenerative power is provided back to the trolleybus grid or it gets wasted to the on-board resistors, as it is done without the implementation of an *on-board* energy storage system. If on the other hand the *on-board* energy storage system is empty, the demanded electric power above the upper electric power threshold is provided entirely by the trolleybus grid, again, as it is done without the implementation of an *on-board* energy storage system. In figure 3.15 is depicted the electric power profile of trolleybus No 1 during the first day of the year in Arnhem, with two electric

power thresholds of 0 kW and 120 kW for charging and discharging an *on-board* energy storage system respectively, after the implementation of one of 3 kWh, with constant charging and discharging efficiencies of 95% and upper and lower limits of 95% and 5% respectively. Similarly as before, a power electronic converter efficiency of 98% is also taken into account.

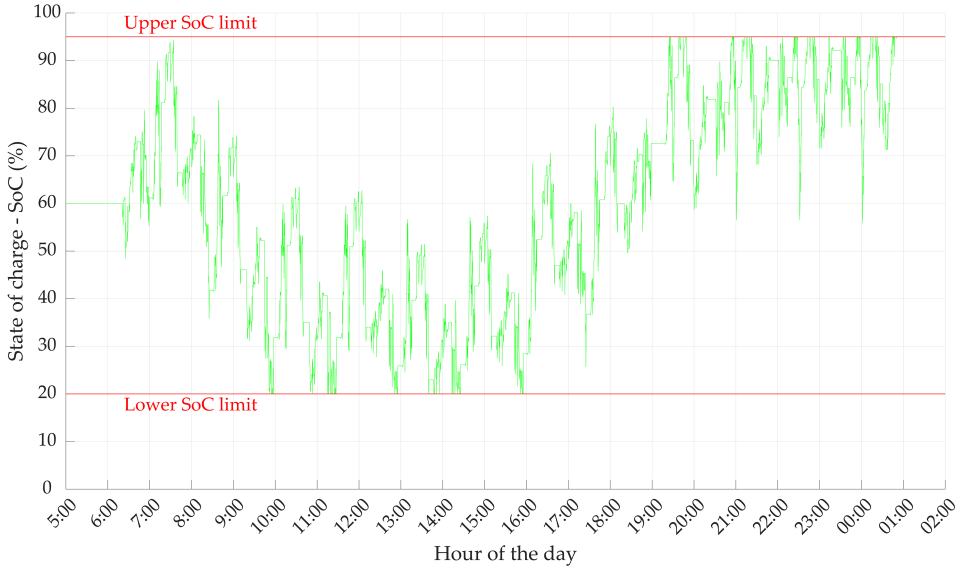

Figure 3.14: State of charge (SoC) of an *on-board* energy storage system of 3 kWh, with constant charging and discharging efficiencies of 95%, upper and lower limits of 95% and 5% respectively, and a power electronic converter efficiency of 98%, when is handling the shaved electric power of trolleybus No 1 during the first day of the year in Arnhem, with two electric power thresholds of 0 kW and 120 kW for charging and discharging it respectively.

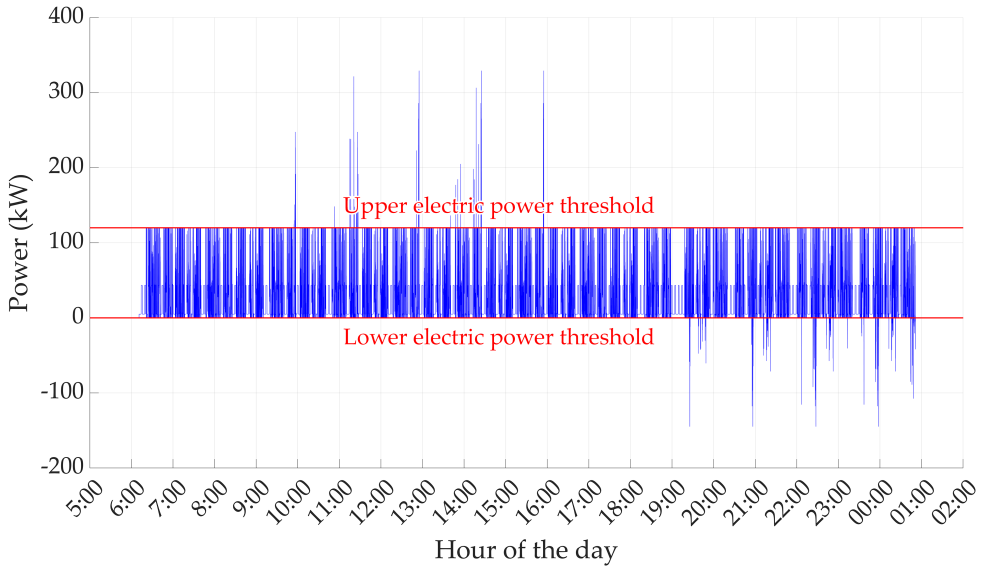

Figure 3.15: Electric power profile of trolleybus No 1 during the first day of the year in Arnhem, with two electric power thresholds of 0 kW and 120 kW for charging and discharging an *on-board* energy storage system respectively, after the implementation of one of 3 kWh, with constant charging and discharging efficiencies of 95%, upper and lower limits of 95% and 5% respectively, and a power electronic converter efficiency of 98%.

3.4.2 Simulation parameters

Regarding the simulation scenarios of this work, are used five (5) different cases of upper electric power threshold values. Those are 60 kW, 80 kW, 100 kW, 120 kW, and 140 kW. Those values are used for all energy storage technologies simulated for the *on-board* energy storage system. A value of 100 kW or 120 kW is found to best balance the energy to get discharged to the energy available for charging in a yearly basis. Thus, threshold values around those values are chosen to best see the impact on the PV system utilization. More specifically, the lower values of 60 kW and 80 kW will lead to more electric power to be discharged than charged. Values of 100 kW to 120 kW create a balance between electric power to be charged and to be discharged while values of 140 kW and above will have as a result for more electric power to be charged than discharged.

3.5 CONTROL STRATEGY OF THE *STATIONARY* ENERGY STORAGE SYSTEM

In contrast to the control strategy of the *on-board* energy storage system described in section 3.4, the control strategy of the *stationary* energy storage system can become significantly more complex depending on the goal that is targeted. Since the main goal of this work is increasing the PV system utilization, the control strategy of the *stationary* energy storage system is built around that. More specifically, its goal is increasing the PV system utilization while targeting to keep the total yearly energy used the same. Considering the effects of it to the voltage drops, this strategy targets to minimize them in a yearly basis but it does not jeopardize decreasing the PV system utilization to compensate for the possible voltage drops. In other words, it tries to achieve the targeted goal as safely as possible, prioritizing the PV system at all times without taking risks that could decrease the PV system utilization. Many and different control strategies can be built for similar applications. Nevertheless, most of them can be categorized into three main categories.

The categories of the control strategies for *stationary* energy storage systems are those:

1. Optimized mainly for increasing the PV system utilization.
2. Optimized mainly for favouring parameters related to the *multifunctionality* of the trolleybus grid (reduction of voltage drops, reduction of transmission losses, increase of recuperation of braking energy etc.).
3. Optimized both for increasing the PV system utilization and favouring parameters regarding the *multifunctionality* of the trolleybus grid - middle ground.

The control strategy used in this work falls mainly into the first category. In general when a control strategy has one goal rather than multiple it tends to be easier to achieve. On the other hand, if a middle ground approach would to be used, to acquire good results then it would be necessary either for the implementation of a more complex system into the trolleybus grid, such a telecommunications systems where the electric powers of each load would be known to the controller of the *stationary* energy storage system, or for a significant amount of resources to be located for research and development for charging methods that do not require the use of advanced measuring devices except of those that measure the voltage at the connection point of the *stationary* energy storage system.

In this work, the controller of the *stationary* energy storage system is able to utilize two pieces of information from two different sources. One is the measured

voltage via a voltage measuring device at its connection point with the trolleybus grid. This is utilized to estimate when a electric power load is present at the section of the trolleybus grid and how big this may be. As already discussed in section 2.1.1, electric power loads create voltage drops depending on their magnitude and their position on the section. Similarly, an increase in voltage may be observed when there is generation of electric power from the regenerative braking of the trolleybuses. As described in section 3.1, the model is based on steady state operation. Thus no measurements of transient phenomena can be taken into consideration for this control strategy. The other piece of information that the controller of the *stationary* energy storage system has access to is a precise estimation of the generated electric power from the PV system. This is easily achieved via a small photoresistor or a small PV panel located at the point of the *stationary* energy storage system. Via this, the controller of the *stationary* energy storage system has knowledge of the electric power generation of the PV system at each instance in time, which is located at the AC side of the grid close to the substation as described in section 3.2. Since the *stationary* energy storage system is located somewhere on the section of the trolleybus grid, the distance from it and the PV system can vary from a few meters up to around 1.5 km in some cases. Thus, the measurements regarding the electric power generation of the PV system taken at the connection point of the *stationary* energy storage system with the trolleybus grid can be used as an accurate indicator, since the distance is short enough for the same meteorological phenomena to occur. Finally, is important to note that the controller of the *stationary* energy storage system has knowledge of other constant parameters too, such as its position on the section, the resistance of the overhead electric power lines, the nominal substation voltage, as well as the time of the day. In figure 3.16 is presented an example of a photoresistor. Its size is a few millimeters in every direction and it incredibly cheap.

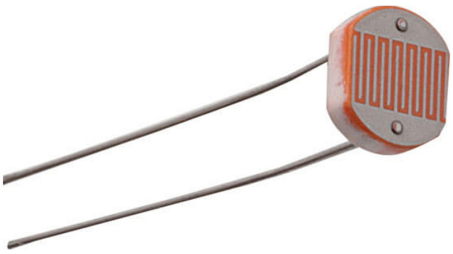

Figure 3.16: GL5516 LDR photosensitive resistor (photoresistor).

3.5.1 Operational principles of the controller

In figure 3.17 is presented the binary tree chart of the rule-based control strategy used for the *stationary* energy storage system simulated in this work. The *stationary* energy storage system may be charged only when there is electric power generation from the PV system and not dense traffic. More analytically, the controller charges it when it observes a voltage equal to that of the substation for a couple seconds or when it observes a constant voltage for a couple seconds that is not the one of the substation.

When voltage is equal to the one of the substation for a couple of seconds, the controller concludes that no other electric power loads are present on the section. Thus, it can charge with electric power equal to the one generated by the PV system. Since the controller can accurately estimate the electric power generation from the PV system and is aware of its position on the section, it can also accurately estimate the transmission losses. Thus, it charges the *stationary* energy storage system with the amount of electric power necessary not to overpass the generated electric power at the location of the PV system. In other words, it reduces the demanded electric

power to account for the transmission losses - i.e. 100 kW demanded at the connection point of the *stationary* energy storage system may be 102 kW at the position of the substation where the PV system is located at. If the controller does not account for the transmission losses, it may demand more electric power than the PV system is generating at each instance. Thus it may charge the *stationary* energy storage system with electric power not provided by the PV system.

Figure 3.17: Binary tree chart of the rule-based control strategy used for the *stationary* energy storage system.

If on the other hand the controller observes the same voltage for a couple seconds but is different than the one of the substation, it concludes that there is traffic idling on the section. As found out from simulations, the traffic idling at the section at each instant is usually only one trolleybus. As described in [2], trolleybuses idling may be using either an electric power of around 5 kW for their auxiliary systems, or of around 45 kW for their auxiliary systems and the HVAC system, either for cooling or heating. In that case, the controller based on the measured voltage, tries to estimate if the electric power load observed in the section is 5 kW or 45 kW. It does that by calculating the theoretical voltage at that point if there was an electric power load of 5 kW or of 45 kW. This is presented by equation 3.8, where $V_{substation}$ is the voltage of the substation, R_{SESS} is the resistance of the electric power lines from the substation to the *stationary* energy storage system connection point with the section including the feeder cable length, and $P_{5kW\_or\_45kW}$ is either the 5 kW or the 45 kW of electric power. Then, it compares that voltage with the measured one and if it is within a range of ±5 V, it chooses the electric power that is best represented by that voltage. This is possible since the electric power load of 45 kW causes a significantly bigger voltage drop at any point of the section compared to the 5 kW one. Thus, the controller is able to differentiate rather accurately which one of those two occasions may occur.

$$V_{indicator} = \frac{V_{substation} + \sqrt{V_{substation}^2 - 4 * R_{SESS} * P_{5kW\_or\_45kW}}}{2} \tag{3.8}$$

To get a better understanding about the voltage drop on the section in regard to the distance for different constant loads, in figure 3.18 is illustrated the voltage drop vs distance for the constant electric power demands of 5 kW (blue) and 45 kW (green), for one trolleybus in section 23 of the trolleybus grid of Arnhem. As observed from table 3.1, section 25 is very similar to section 23 thus it presents a similar voltage drop behaviour. Only if the electric power generation from the PV system is bigger than the electric power load of the idling trolleybuses, the controller charges the *stationary* energy storage with the difference - i.e. if there is 100 kW of electric power generation from the PV system and the controller concludes that there is idling traffic on the section demanding 45 kW, then it charges the *stationary* energy storage system with 100-45 = 55 kW, minus the transmission losses. In case the PV system is able to cover the whole electric power demand, then the controller sets the *stationary* energy storage system to stand-by mode.

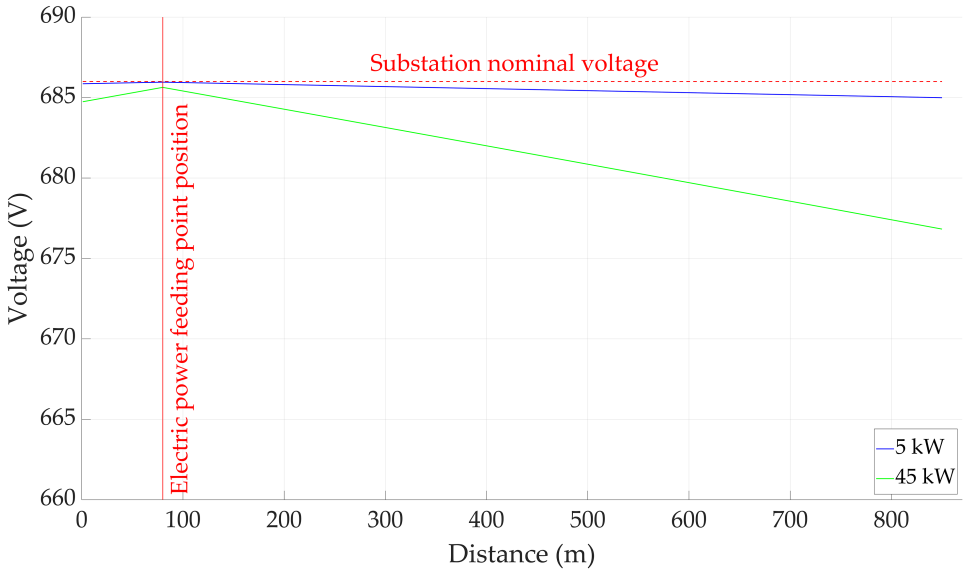

Figure 3.18: Voltage drop vs distance for the constant electric power demands of 5 kW (blue) and 45 kW (green), for one trolleybus in section 23 of the trolleybus grid of Arnhem.

For all charging modes, the charging of the *stationary* energy storage system stops when the controller observes dense traffic in the section. This is done when the controller observes an unexpected big fluctuation of the measured voltage that does not correspond to a possible voltage fluctuation due to fluctuation in the electric power demanded by itself. In other words, when there is a big fluctuation in the voltage, that usually means that an electric power load has entered the section - i.e. a trolleybus. Thus, the controller decides to stop charging and go into stand-by mode, not discharging either. By this, is avoiding to take any risks to further charge or discharge, and possibly increase the energy consumption or decrease the PV system utilization respectively.

Regarding the discharge, if there is no electric power generation from the PV system, the controller of the *stationary* energy storage system discharges with a decided electric power based on a target voltage within a voltage bandwidth zone. If the measured voltage is below the voltage bandwidth zone the controller targets the middle of it, which is the target voltage to reach, and estimates the discharging electric power necessary to reach it. This estimation is done using equation 3.9 where V_{target} is the target voltage, which is the middle of the voltage bandwidth zone,

$V_{measured}$ is the measured voltage at the connection point of the *stationary* energy storage system with the trolleybus grid, and R_{SESS} is the resistance of the electric power lines from the substation to the *stationary* energy storage system connection point with the section including the feeder cable length. It should be noted that this equation is just an estimation for the case that there is one electric power load in the section that causes that voltage drop. Nevertheless, it works adequately and provides adequate voltage support even when used for cases with multiple electric power loads causing the measured voltage drop. If the measured voltage is within the voltage bandwidth zone, then it goes into the same state as it was in the previous instance. In other words, if in the previous instance the *stationary* energy storage system was in stand-by mode, it stays like this. If it was discharging with a specific amount of electric power, then it discharges again with the same amount of electric power. Finally, if the measured voltage is above the voltage bandwidth zone, then the controller sets the *stationary* energy system to stand-by mode. In figure 3.19 is illustrated a discharging scheme example of the *stationary* energy storage system with a target voltage of 650 V and a voltage bandwidth of 20 V.

$$P_{discharge} = \frac{V_{target} * V_{measured} - V_{measured}^2}{R_{SESS}} \tag{3.9}$$

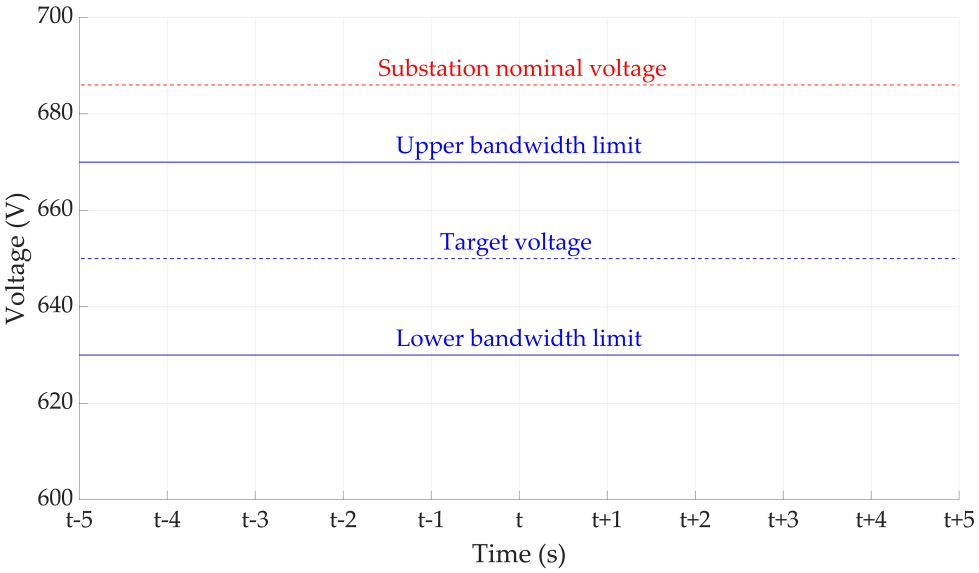

Figure 3.19: *Stationary* energy storage discharging scheme example with a target voltage of 650 V and a voltage bandwidth of 40 V.

In a nutshell, using this control strategy, is prioritized the charge of the *stationary* energy storage system with electric power provided by the PV system while avoiding taking the risk of discharging when there is electric power generation from it. Thus, this control strategy avoids acting in a way that may decrease the PV system utilization in order to try to decrease the voltage drops. Because it is targeted to charge safely only when this is no traffic or when there is idling traffic, it can accurately and safely calculate how much electric power to demand, not to draw more what the PV system provides at that each instance. This comes as an adequate solution to the original problem of the PV system utilization in trolleybus grids which is the intermittency in PV system electric power generation and the trolleybus schedule – i.e. at the gaps where there are no trolleybuses. Since the *stationary* energy storage has to discharge also, this is done by targeting a certain voltage to achieve, thus helping to reduce the severity of voltage drops but only when there is no electric power generation from the PV system. More specifically, the effect of this control strategy of the *stationary* energy storage to the voltage drops is described below.

The magnitude and the density of voltage drops are affected by this control strategy of the *stationary* energy storage in the following ways:

1. With electric power generation by the PV system and no or idle traffic: they get increased from none to whatever the charging electric power cause them to become – around 30 V drop on average in magnitude.
2. With electric power generation by the PV system and dense traffic: they remain the same as without an *stationary* energy storage system.
3. Without electric power generation by the PV system and no traffic: they remain the same as without an *stationary* energy storage system.
4. Without electric power generation by the PV and dense traffic: they are reduced, according to the set target voltage.

This control strategy is a **yearly optimized** control strategy as the intensity of charging changes during the year depending on the intensity of sun during the year and the changes in the traffic schedules. For this work, has been deemed more logical to focus on that since the PV system utilization is something that should be evaluated in a yearly basis. Thus, is clear that if the *stationary* energy system is large enough and if the year ends with the same state of charge (SoC) at the *stationary* energy system as the when it started, the yearly energy used should be the same while the PV system utilization should be increased. That is of course the ideal case scenario. In reality there are loses on the lines, the self-discharge of the energy storage system and the possibility that the control strategy may not be 100% accurate. The latter is explained by charging with electric power higher than the supposed corresponding one of the generated by the PV system. This is something to be taken account when analyzing the results of this work.

3.5.2 Simulation parameters

As described in section 3.1, the sections that are simulated which are equipped with a *stationary* energy storage system are section 25 (substation 9) and section 23 (substation 12). Besides the amount of solar energy provided to the PV system throughout the year, the amount of energy charged in a yearly basis depends also on the schedule and the amount of traffic in the simulated sections. Thus, since the charging scheme remains the same for all simulation scenarios, is clear that the high traffic sections, such as section 25, may provide less opportunities for the *stationary* energy storage to get charged compared to the low traffic ones, such as section 23. Also, the size of the PV system used has a key role on the amount of energy that can be stored as smaller systems provide less energy during the year. This is something to be kept in mind at this work since those differences may change the energy balance of charging-discharging of the *stationary* energy storage system, causing different effects on the behaviour of its state of charge (SoC).

It is important to note that voltage control used for this control strategy means that the *stationary* energy storage system can only estimate the situation on the section that is placed to. Thus, for section 23, which is fed with electric power provided by substation 12, the PV utilization may be increased, but the total energy consumption of the substation will be definitely increased. This is because substation 12 also feeds with electric power section 24. Thus, the *stationary* energy storage system may be getting charged with electric power provided by the PV system that is possibly already being utilized on section 24. This problem could easily be avoided with a simple communication link between the *stationary* energy system and the substation of the simulated section. Via this communication link, the controller could know the total demanded electric power of the other sections which are fed with electric power by the same substation. This is something that is not implemented here.

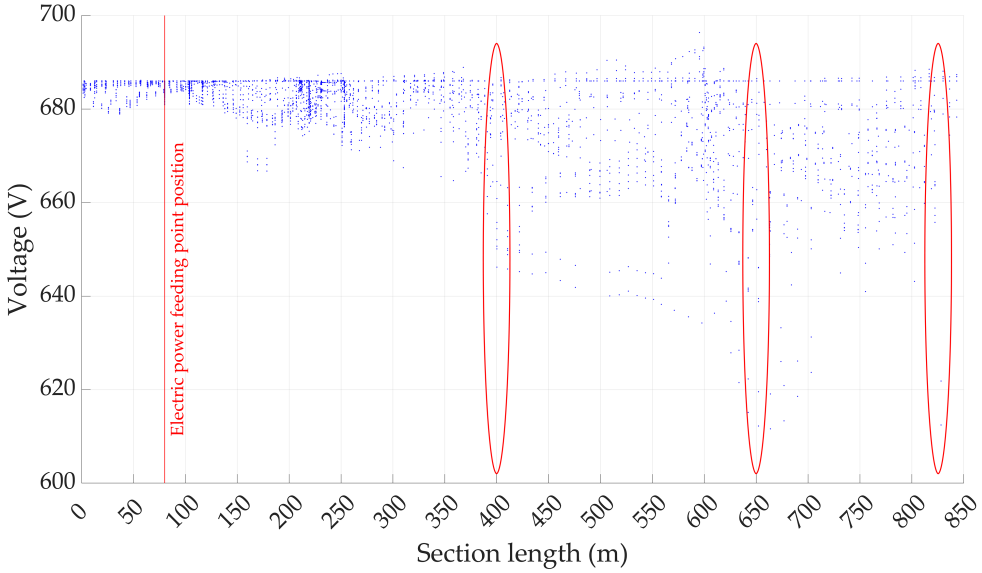

Figure 3.20: Voltage drops vs distance for the whole year for section 23 of the trolleybus grid of Arnhem without the implementation of an *stationary* energy storage system, and the selected positions of placement of one for the simulations of this work (red circles).

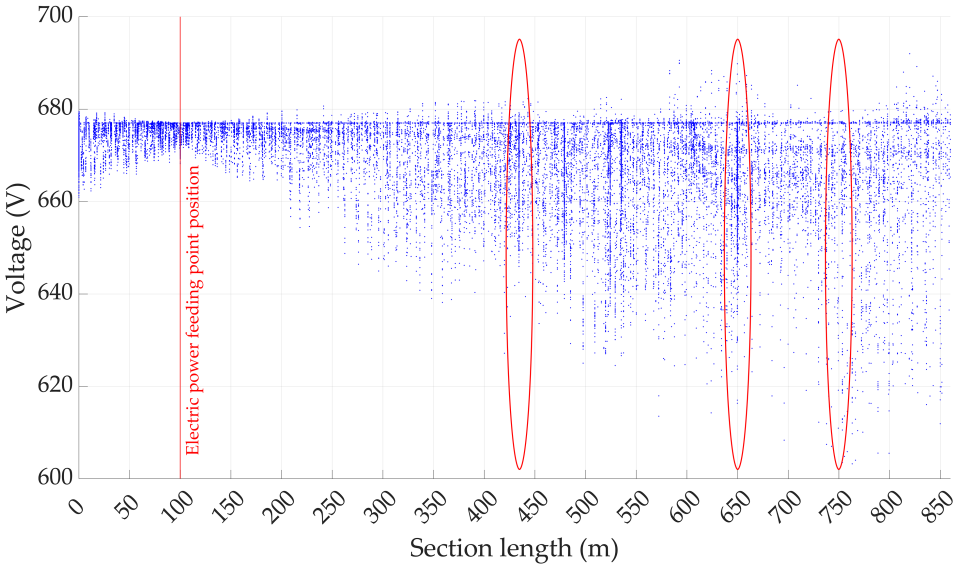

Figure 3.21: Voltage drops vs distance for the whole year for section 25 of the trolleybus grid of Arnhem without the implementation of an *stationary* energy storage system, and the selected positions of placement of one for the simulations of this work (red circles).

Regarding the discharging scheme, for all simulations of this work is utilized a target voltage which is at the middle of a voltage bandwidth zone of 20 V. The voltage bandwidth zone is set in such a way that the upper bandwidth limit is one volt lower than the voltage of the substation that feeds with electric power the simulated section. This one volt reduction is done for safety reasons, accounting for a margin of error to avoid possible overshoots of the voltage above the nominal voltage of the substation, causing *electric power quality assurance* issues. These values are chosen as they are targeted to provide the best case scenario for the reduction of the voltage drops. This also means that the *stationary* energy storage system discharges rather aggressively and this is something that should be kept in mind when looking

over the results of this work. The 20 V bandwidth is chosen as is found to provide an adequate margin for error when estimating the electric power for discharging, preventing overshoots that may cause the measured voltage to jump from values below the lower bandwidth limit to values above the upper one. In equation 3.10 is presented the calculation of the target voltage for the discharging scheme of the control strategy of the *stationary* energy storage system, where $V_{substation}$ is the voltage of the substation and $V_{bandwidth}$ is the bandwidth in volts, which is 20 V for this work.

$$V_{target} = (V_{substation} - 1) - \frac{V_{bandwidth}}{2} \tag{3.10}$$

Regarding the placement of the *stationary* energy storage system, as described in section 2.2.2, in this work is decided to be place on each simulated section of the trolleybus grid of Arnhem. More analytically, multiple locations are used in order to observe the effects of its position in relation to the PV system utilization and the voltage drops. Those locations are decided according to which ones express the most severe voltage drops in a yearly basis, which are usually are the trolleybus stops. Those positions are chosen as those are considered to be needing the most support for reducing the severity of voltage drops. More precisely, for section 23 the selected positions of an *stationary* energy storage system are at 400 m, 650 m, and 825 m while for section 25 are at 435 m, at 650 m, and 750 m. In figure 3.20 and in figure 3.21 are illustrated the voltage drops vs distance for the whole year for section 23 and section 25 respectively of the trolleybus grid of Arnhem without the implementation of an *stationary* energy storage system. With red circles are highlighted the selected positions of placement of a *stationary* energy storage system for the simulations of this work. Is interesting to note that for both cases the electric power feeding point is placed fairly close to the beginning of the section. In cases where it is placed in the middle of the section, then a control of the *stationary* energy storage system using a voltage control based scheme would become rather challenging. This is because, depending on the position of the *stationary* energy storage, the measured voltage will be able to provide information about the traffic on the section only up to the point of the electric power feeding point position. Thus, the controller is able to get an estimation only for part of the section and not for the whole length of it. This is something not analyzed in this work.

3.6 CONCLUSIONS

In this chapter have been presented the models used for the simulations of this work such as the model of Arnhem's trolleybus grid, the model for the PV system, the model of the energy storage system along with the simulation parameters, and the control models of the on-board and the stationary energy storage systems. The creation and the complexity of any model has to do with the specific goal that is targeted. Different goals require models of different complexity. This is especially observed for the case of the control strategy of the *stationary* energy storage system where different strategies can provide significantly different results. In the next chapter (chapter 4) are presented the results regarding the impact of *on-board* and *stationary* energy storage systems on parameters regarding the PV system utilization.

4 RESULTS - IMPACT ON THE PV SYSTEM UTILIZATION

In this chapter are presented the results from the simulations of this work regarding the impact of energy storage systems on the PV system utilization. First, a brief explanation regarding terms important for the interpretation of the results is given, while afterwards, the results regarding the impact of on-board and stationary energy storage systems on the PV system utilization are presented.

4.1 GENERAL NOTES REGARDING THE SIMULATIONS

To get a better understanding of the cases simulated in this work, in table 4.1 and in table 4.2 are presented the simulated scenarios for *on-board* and *stationary* energy storage systems respectively. Is those are summarised all the decisions presented in chapter 3.

Regarding the *on-board* energy storage systems, the various electric powers represent the various upper electric power thresholds while for the *stationary* energy storage systems the various distances represent the various positions in respect to the beginning of the section. It is important to note that for each simulated case there are a set of extra simulations that account for the different PV system sizes. In this work, the PV system size is always presented in percentage (%) in respect to a PV system size for ζ=1 without energy storage. More analytically, regarding the *on-board* energy storage systems, those are eleven (11) per simulation case (10%, 20%, 30%, 40%, 50%, 60%, 70%, 80%, 90%, 100%, 110%). Since the PV system is placed on the AC side of the electric grid, as described in section 3.2, those simulations are conducted after the simulation of each section. They are based on a comparison of the demanded electric power by the substation and the supplied electric power by the PV system to that substation, requiring for each simulation only a few seconds.

For the case of *stationary* energy storage systems, each system is aware of the amount of electric power provided by the PV system at any given time, as described in section 3.5. Thus, for each case multiple simulations must be conducted that account for the different PV system sizes. More specifically, the various PV system sizes are five (5) (10%, 25%, 50%, 75%, 100%). This increases drastically the total simulation time since each simulation that correlates to each PV system size requires around twenty (20) minutes to be conducted. This is why a lower resolution of PV system sizes is used for the *stationary* energy storage systems. Finally, is important to mention that for each simulation case is implemented either an *on-board* or a *stationary* energy storage system for each simulation and not both of them at the same time.

Table 4.1: *On-board* energy storage system simulation scenarios.

Substation 12 - section 23 & section 24

Supercapacitors (SC)			Lithium-Titanate oxide (LTO)		
1.484 kWh	2.968 kWh	4.452 kWh	1.5 kWh	3 kWh	4.5 kWh
↓	↓	↓	↓	↓	↓
60 kW	60 kW	60 kW	60 kW	60 kW	60 kW
80 kW	80 kW	80 kW	80 kW	80 kW	80 kW
100 kW	100 kW	100 kW	100 kW	100 kW	100 kW
120 kW	120 kW	120 kW	120 kW	120 kW	120 kW
140 kW	140 kW	140 kW	140 kW	140 kW	140 kW

Substation 9 - section 25

Supercapacitors (SC)			Lithium-Titanate oxide (LTO)		
1.484 kWh	2.968 kWh	4.452 kWh	1.5 kWh	3 kWh	4.5 kWh
↓	↓	↓	↓	↓	↓
60 kW	60 kW	60 kW	60 kW	60 kW	60 kW
80 kW	80 kW	80 kW	80 kW	80 kW	80 kW
100 kW	100 kW	100 kW	100 kW	100 kW	100 kW
120 kW	120 kW	120 kW	120 kW	120 kW	120 kW
140 kW	140 kW	140 kW	140 kW	140 kW	140 kW

Table 4.2: *Stationary* energy storage system simulation scenarios.

Substation 12 - section 23

Flywheels		Lithium-Titanate oxide (LTO)	
192 kWh	992 kWh	189 kWh	1008 kWh
↓	↓	↓	↓
400 m	400 m	400 m	400 m
650 m	650 m	650 m	650 m
825 m	825 m	825 m	825 m

Substation 9 - section 25

Flywheels		Lithium-Titanate oxide (LTO)	
128 kWh	992 kWh	126 kWh	1008 kWh
↓	↓	↓	↓
435 m	435 m	435 m	435 m
650 m	650 m	650 m	650 m
750 m	750 m	750 m	750 m

4.2 *ON-BOARD* ENERGY STORAGE SYSTEMS

In figure 4.1 until figure 4.12 is illustrated the PV system utilization vs PV system size vs upper electric power threshold for *on-board* energy storage systems equipped with *supercapacitors* (SC) or *lithium-titanate oxide* (LTO) batteries of various capacities for substation 12 and substation 9 in 3D form. The same plots in 2D form are presented in figure 4.13 until figure 4.24 with the case without any energy storage system to be presented with red. The dotted black line indicates the value of PV system size after which the PV system utilization for the case of no storage starts to become greater that the rest of the cases. Note that a different PV system utilization scale is used for the two substations (20% to 60% for substation 12 and 15% to 35% for substation 9) to best represent the range of values observed for each one.

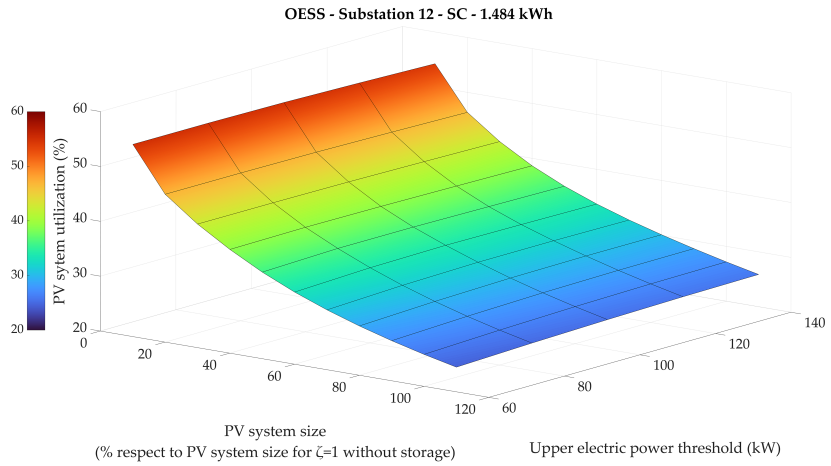

Figure 4.1: Substation 12 PV system utilization vs PV system size vs upper electric power threshold for *on-board* energy storage system equipped with *supercapacitors* (SC) of 1.484 kWh.

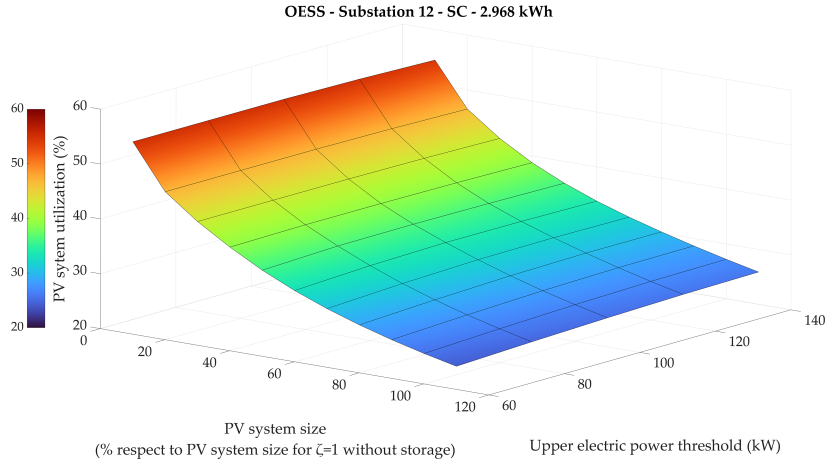

Figure 4.2: Substation 12 PV system utilization vs PV system size vs upper electric power threshold for *on-board* energy storage system equipped with *supercapacitors* (SC) of 2.968 kWh.

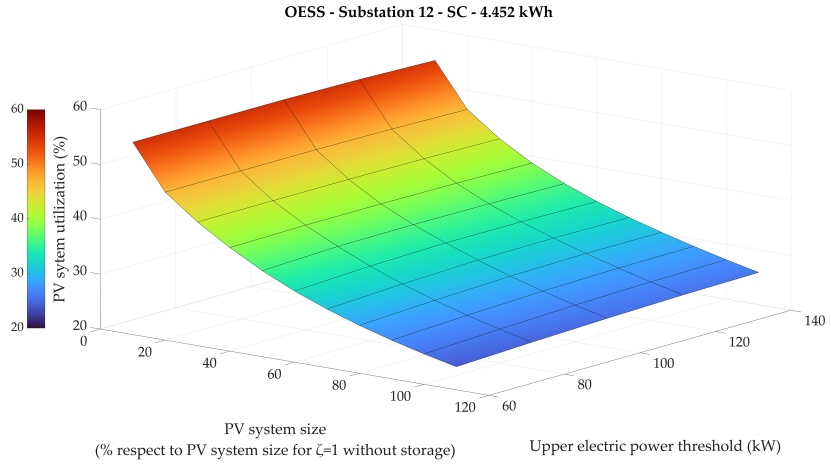

Figure 4.3: Substation 12 PV system utilization vs PV system size vs upper electric power threshold for *on-board* energy storage system equipped with *supercapacitors* (SC) of 4.452 kWh.

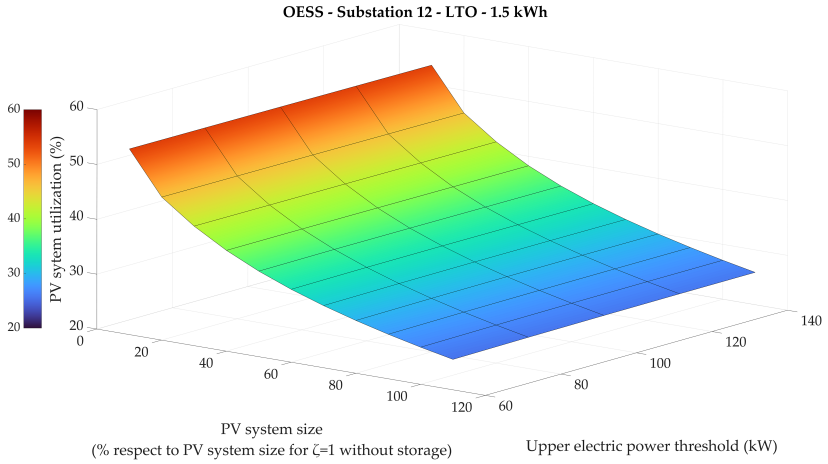

Figure 4.4: Substation 12 PV system utilization vs PV system size vs upper electric power threshold for *on-board* energy storage system equipped with *lithium-titanate oxide* (LTO) batteries of 1.5 kWh.

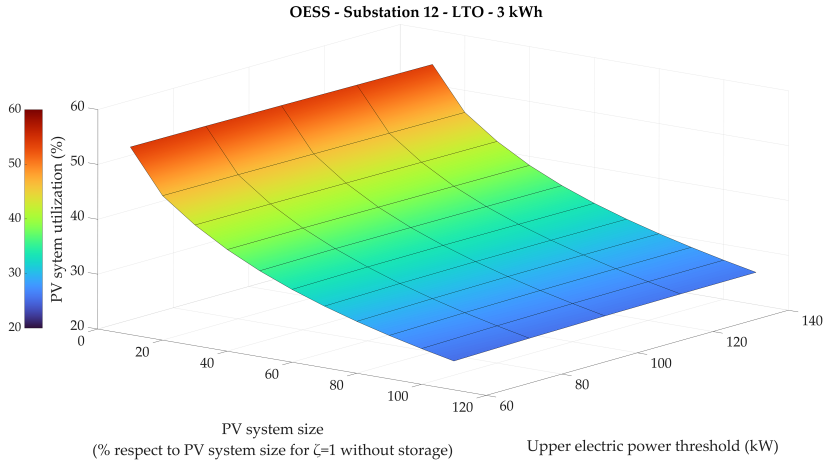

Figure 4.5: Substation 12 PV system utilization vs PV system size vs upper electric power threshold for *on-board* energy storage system equipped with *lithium-titanate oxide* (LTO) batteries of 3 kWh.

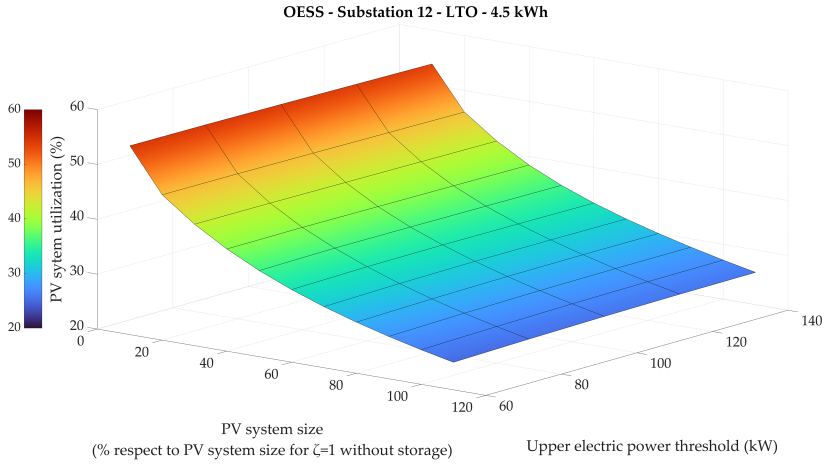

Figure 4.6: Substation 12 PV system utilization vs PV system size vs upper electric power threshold for *on-board* energy storage system equipped with *lithium-titanate oxide* (LTO) batteries of 4.5 kWh.

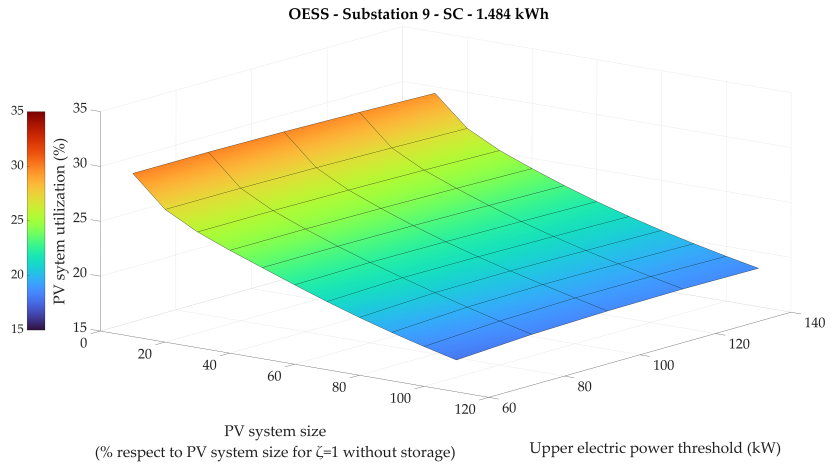

Figure 4.7: Substation 9 PV system utilization vs PV system size vs upper electric power threshold for *on-board* energy storage system equipped with *supercapacitors* (SC) of 1.484 kWh.

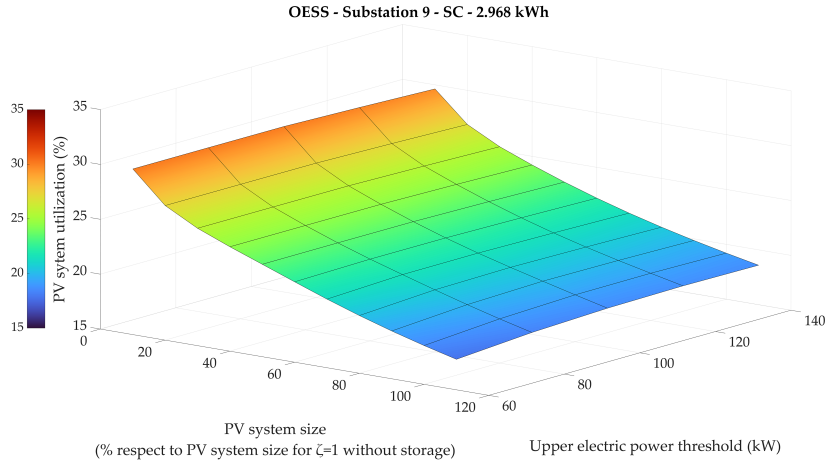

Figure 4.8: Substation 9 PV system utilization vs PV system size vs upper electric power threshold for *on-board* energy storage system equipped with *supercapacitors* (SC) of 2.968 kWh.

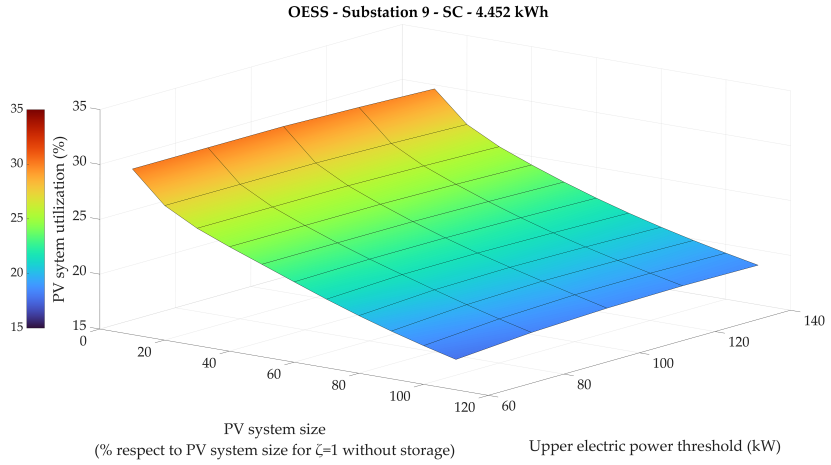

Figure 4.9: Substation 9 PV system utilization vs PV system size vs upper electric power threshold for *on-board* energy storage system equipped with *supercapacitors* (SC) of 4.452 kWh.

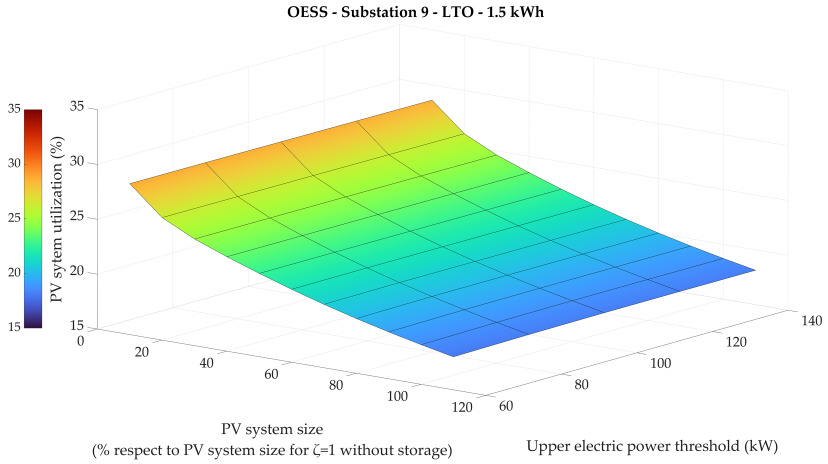

Figure 4.10: Substation 9 PV system utilization vs PV system size vs upper electric power threshold for *on-board* energy storage system equipped with *lithium-titanate oxide* (LTO) batteries of 1.5 kWh.

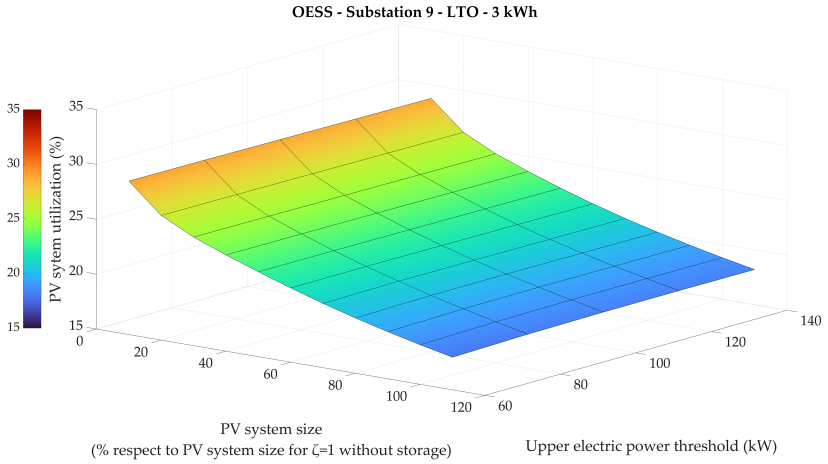

Figure 4.11: Substation 9 PV system utilization vs PV system size vs upper electric power threshold for *on-board* energy storage system equipped with *lithium-titanate oxide* (LTO) batteries of 3 kWh.

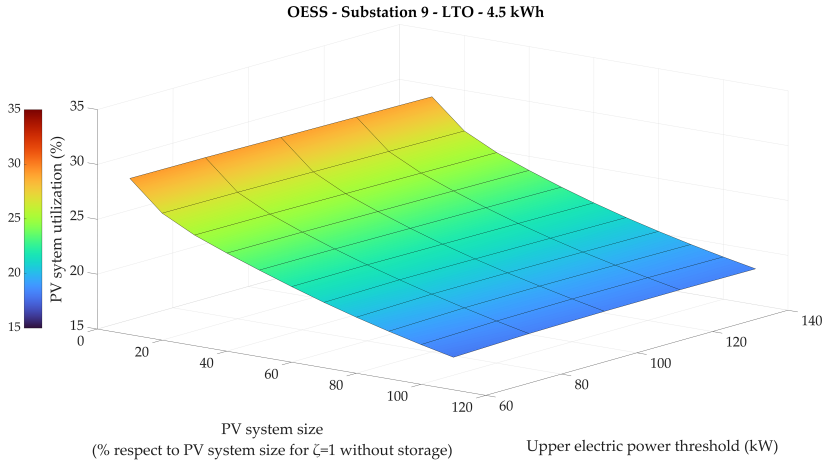

Figure 4.12: Substation 9 PV system utilization vs PV system size vs upper electric power threshold for *on-board* energy storage system equipped with *lithium-titanate oxide* (LTO) batteries of 4.5 kWh.

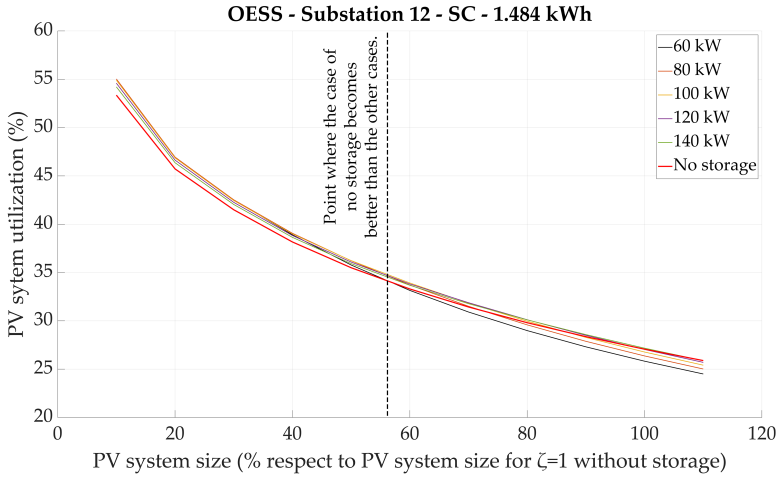

Figure 4.13: Substation 12 PV system utilization vs PV system size for various upper electric power thresholds for *on-board* energy storage system equipped with *supercapacitors* (SC) of 1.484 kWh.

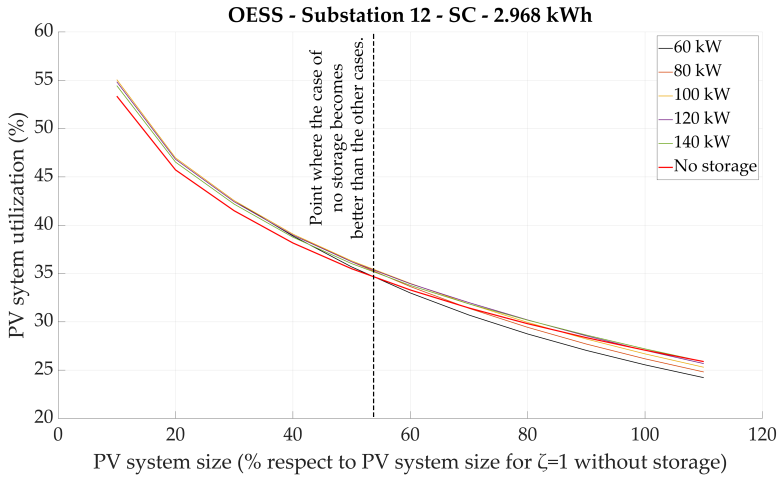

Figure 4.14: Substation 12 PV system utilization vs PV system size for various upper electric power thresholds for *on-board* energy storage system equipped with *supercapacitors* (SC) of 2.968 kWh.

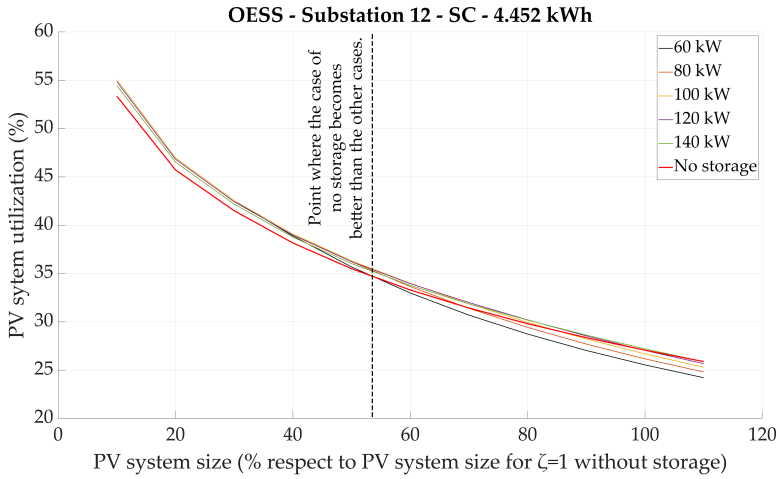

Figure 4.15: Substation 12 PV system utilization vs PV system size for various upper electric power thresholds for *on-board* energy storage system equipped with *supercapacitors* (SC) of 4.452 kWh.

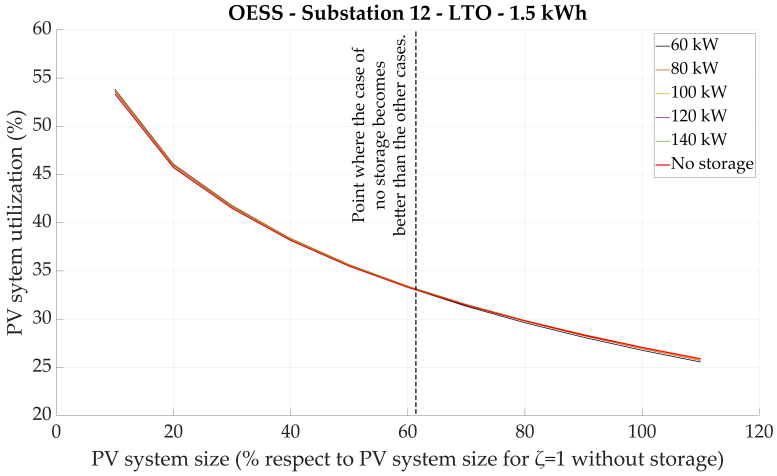

Figure 4.16: Substation 12 PV system utilization vs PV system size for various upper electric power thresholds for *on-board* energy storage system equipped with *lithium-titanate oxide* (LTO) batteries of 1.5 kWh.

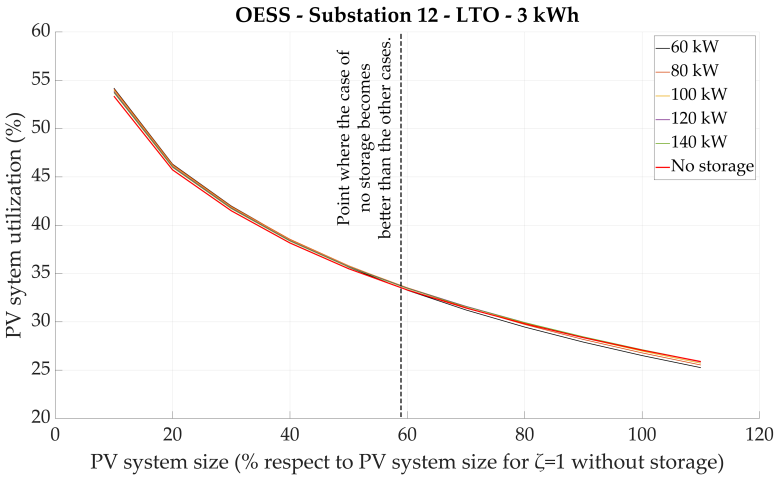

Figure 4.17: Substation 12 PV system utilization vs PV system size for various upper electric power thresholds for *on-board* energy storage system equipped with *lithium-titanate oxide* (LTO) batteries of 3 kWh.

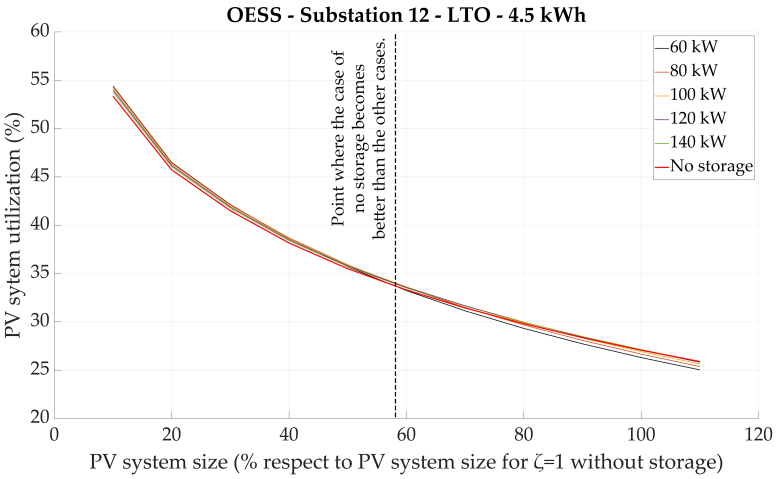

Figure 4.18: Substation 12 PV system utilization vs PV system size for various upper electric power thresholds for *on-board* energy storage system equipped with *lithium-titanate oxide* (LTO) batteries of 4.5 kWh.

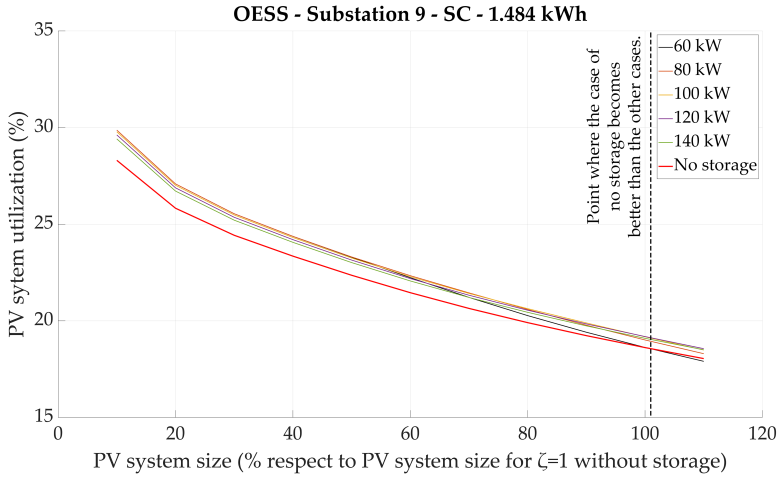

Figure 4.19: Substation 9 PV system utilization vs PV system size for various upper electric power thresholds for *on-board* energy storage system equipped with *supercapacitors* (SC) of 1.484 kWh.

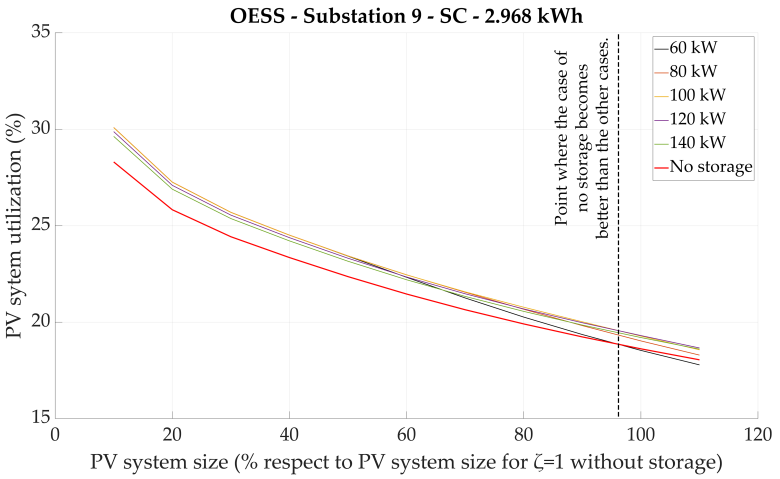

Figure 4.20: Substation 9 PV system utilization vs PV system size for various upper electric power thresholds for *on-board* energy storage system equipped with *supercapacitors* (SC) of 2.968 kWh.

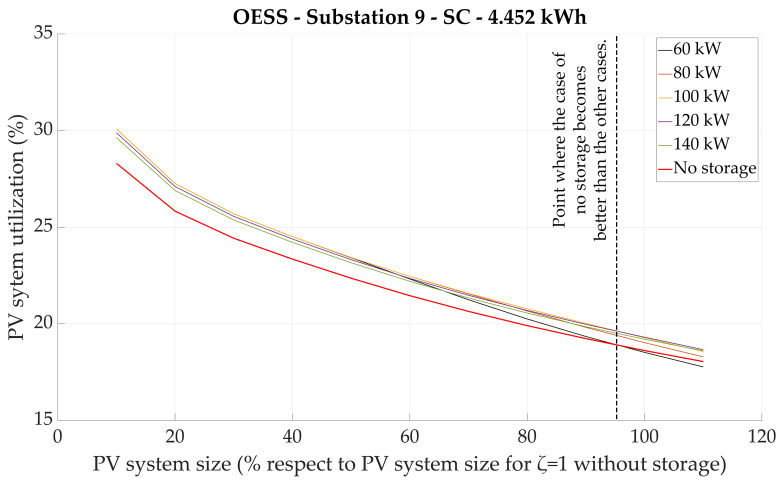

Figure 4.21: Substation 9 PV system utilization vs PV system size for various upper electric power thresholds for *on-board* energy storage system equipped with *supercapacitors* (SC) of 4.452 kWh.

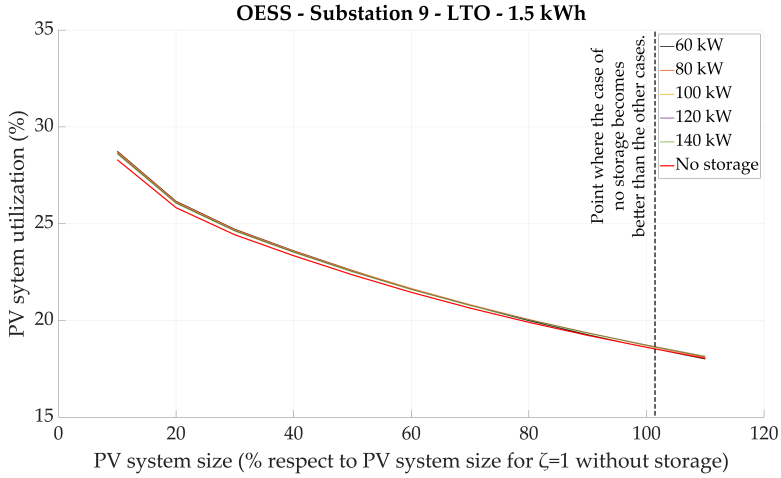

Figure 4.22: Substation 9 PV system utilization vs PV system size for various upper electric power thresholds for *on-board* energy storage system equipped with *lithium-titanate oxide* (LTO) batteries of 1.5 kWh.

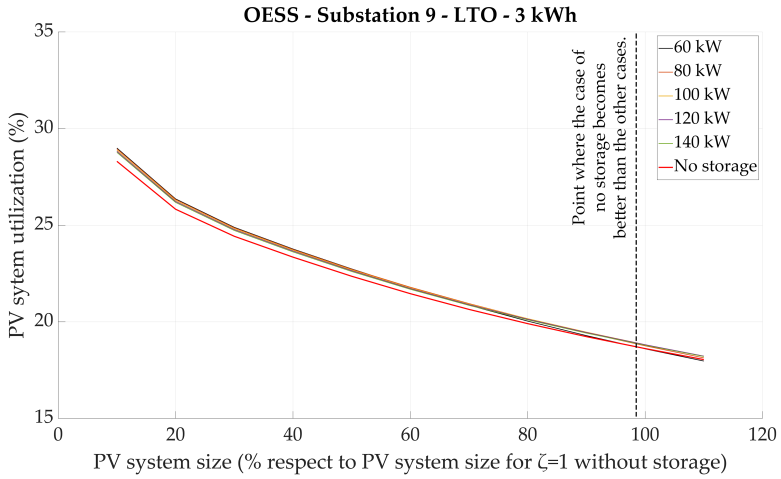

Figure 4.23: Substation 9 PV system utilization vs PV system size for various upper electric power thresholds for *on-board* energy storage system equipped with *lithium-titanate oxide* (LTO) batteries of 3 kWh.

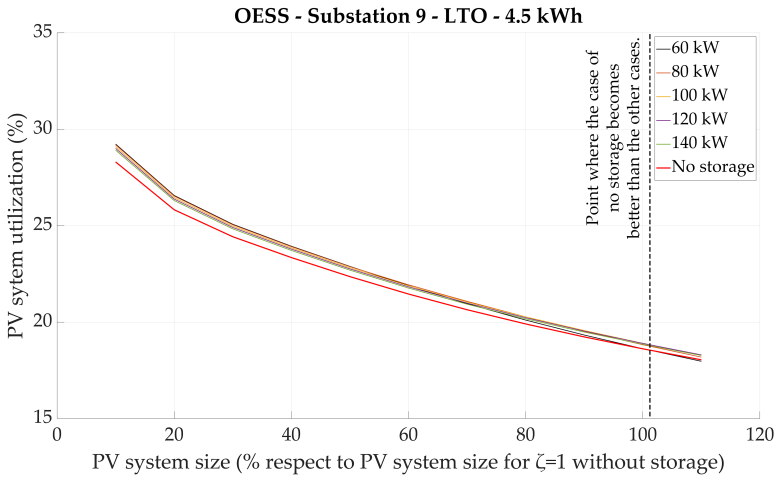

Figure 4.24: Substation 9 PV system utilization vs PV system size for various upper electric power thresholds for *on-board* energy storage system equipped with *lithium-titanate oxide* (LTO) batteries of 4.5 kWh.

OESS - Substation 12 – Comparison of capacities.
For the case of *supercapacitors* (SC), when comparing the various capacities (figure 4.1 to figure 4.3 and figure 4.13 to figure 4.15), is observed a very similar PV system utilization response in regard to the PV system size for the various upper electric power thresholds. This shows that an *on-board* energy storage system equipped with *supercapacitors* (SC) with an energy capacity larger than at least of 1.484 kWh does not provide any significant change in the results for a low traffic substation. Regarding the case of *lithium-titanate oxide* (LTO) batteries (figure 4.4 to figure 4.6 and figure 4.16 to figure 4.18), similar behaviour is observed but with a note. More specifically, although comparing the various capacities is observed that the PV system utilization response in regard to the PV system size for the various upper electric power thresholds is quite similar, is observed that the smaller the energy capacity is, the smaller the spectrum of differences is for the different upper electric power thresholds. In other words, the smaller the energy capacity is, the less impact there is to a change in the PV system utilization compared to the case without any energy storage system implemented. This comes down to the limitations of the *lithium-titanate oxide* (LTO) batteries regarding the amount of electric power that they can accept or provide in small capacities, as described in section 3.3, in Table 3.6. In small capacities, *lithium-titanate oxide* (LTO) batteries are limited to such an extend in accepting or providing electric power that their implementation to *on-board* energy storage systems does not provide any significant benefit. Thus, this proves the initial speculation that *lithium-titanate oxide* (LTO) batteries would not perform adequately enough for increasing PV system utilization when implemented in *on-board* energy storage systems for low traffic substations.

OESS - Substation 12 – Comparison of upper electric power thresholds.
For the case of *supercapacitors* (SC), for all three cases of capacities (figure 4.1 to figure 4.3 and figure 4.13 to figure 4.15), is observed that lower electric power thresholds provide the biggest PV system utilization increase, for PV system sizes smaller than 55% compared to the case without any energy storage system implemented. Nevertheless, for PV system sizes bigger than that, this behaviour gradually changes for increasingly more, different values of upper electric power thresholds, and at 100%, the PV system utilization compared to the case without any energy storage system implemented has either not changed or even decreased up to 0.5 percentage points for the majority of the different electric power thresholds. The same behavior is observed for the case of *lithium-titanate oxide* (LTO) batteries (figure 4.4 to figure 4.6 and figure 4.16 to figure 4.18). Again the differences in PV system utilization for the various upper electric power thresholds are small – i.e, a more similar response between each electric power threshold. For both *supercapacitors* (SC) and *lithium-titanate oxide* (LTO) batteries, this shows that if is utilized a PV system which is sized originally for an energy-neutrality ratio of ζ=1 without energy storage for a substation of low traffic, the implementation of *on-board* energy storage systems may provide a decrease in the PV system utilization or at best not provide any change at all. This phenomenon is interesting and has to do with the properties of the section or sections that are supplied with electric power from the substation. More specifically, this is more evident for sections with low traffic, or for sections which are shorter where trolleybuses are less likely to frequently stop. The fewer times the trolleybuses have to stop the less time there is regenerative braking energy being produced. Thus, fewer times the *on-board* energy storage system is able to store electric energy not letting other trolleybuses to be provided by it, and consequently, force them to be provided with electric power provided by the substation, which in turn may be provided with electric power by the PV system.

OESS - Substation 12 – Comparison of technologies.
As can be understood from the aforementioned results, *lithium-titanate oxide* (LTO) batteries provide a much smaller spectrum of possible results for PV system uti-

lization regarding different capacities and different electric power thresholds, when compared to *supercapacitors* (SC). For smaller PV system sizes and for higher capacities of *lithium-titanate oxide* (LTO) batteries, are observed the best cases for their implementation. Nevertheless, the results show a worse overall behavior compared to *supercapacitors* (SC) when used in *on-board* energy storage systems for substations with low traffic.

OESS - Substation 9 – Comparison of capacities.
For the case of *supercapacitors* (SC), when comparing the various capacities (figure 4.7 to figure 4.9 and figure 4.19 to figure 4.21), is observed the same behavior as with the one for substation 12. More specifically, is once again observed a very similar PV system utilization response in regard to the PV system size for the various upper electric power thresholds. The same behavior as substation 12 is observed for the case of *lithium-titanate oxide* (LTO) batteries too (figure 4.10 to figure 4.12 and figure 4.22 to figure 4.24). More specifically, is observed that the smaller the energy capacity is, the smaller the spectrum of differences is for the different upper electric power thresholds. Thus, for once again, even for substations with higher traffic such as substation 9, *lithium-titanate oxide* (LTO) batteries exhibit a limited benefit when implemented as *on-board* energy storage systems.

OESS - Substation 9 – Comparison of upper electric power thresholds.
For the case of *supercapacitors* (SC), for all three cases of capacities (figure 4.7 to figure 4.9 and figure 4.19 to figure 4.21), is observed that almost all electric power thresholds provide a higher PV system utilization increase, for PV system sizes smaller than 90% compared to the case without any energy storage system implemented. This is quite a different behavior compared to the one observed for a low traffic substation such as substation 12. Even for PV system sizes bigger than 90% this behaviour does not change, except for the case of 60 kW of upper electric power threshold. Especially for the case of 100 kW of upper electric power threshold, the PV system utilization is increased throughout almost the whole PV system size spectrum of around 1.5 percentage points. The same behavior is observed for the case of *lithium-titanate oxide* (LTO) batteries (figure 4.10 to figure 4.12 and figure 4.22 to figure 4.24), but again with smaller differences in PV system utilization for the various upper electric power thresholds – i.e, a more similar response between each electric power threshold, exactly like for the case of substation 12. This shows that if is utilized a PV system which is sized originally for an energy-neutrality ratio of ζ=1 without energy storage for a substation of high traffic, the implementation of *on-board* energy storage systems may provide an increase in the PV system utilization for the majority of upper electric power thresholds. This phenomenon is based on the same logic as described for substation 12. Substation 9 is a high traffic substation, thus providing more time instances when trolleybuses produce electric energy via regenerative braking. Thus, the *on-board* energy storage system is more times able to store this electric energy, not letting other trolleybuses to be provided by it, forcing them to be provided with electric power provided by the substation, which in turn may be provided with electric power by the PV system.

OESS - Substation 9 – Comparison of technologies.
Once again, from the aforementioned results, *lithium-titanate oxide* (LTO) batteries provide a much smaller spectrum of possible results regarding different capacities and different electric power thresholds, when compared to *supercapacitors* (SC). Similarly to the case of substation 12, for smaller PV system sizes and for larger capacities of *lithium-titanate oxide* (LTO) batteries, are observed the best cases, beneficial for their implementation. In general, *lithium-titanate oxide* (LTO) batteries seem to provide a bigger benefit when implemented to a high traffic substation compared to a low one, but still provide worse results compared to *supercapacitors* (SC).

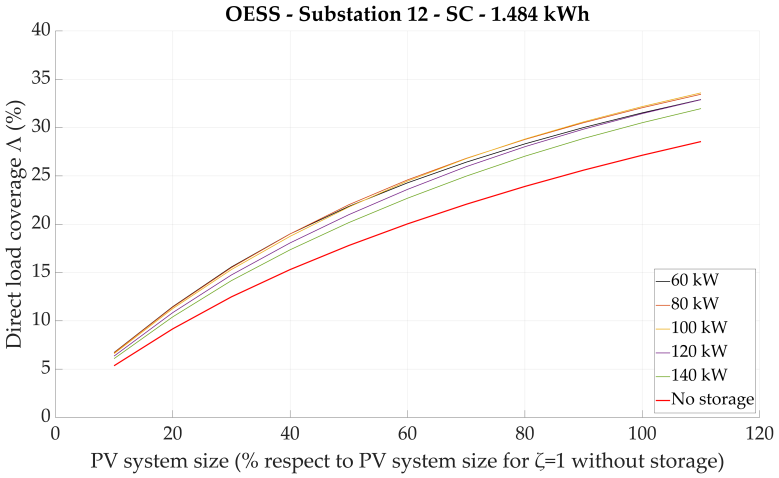

Figure 4.25: Substation 12 PV system utilization vs direct load coverage Λ for various upper electric power thresholds for *on-board* energy storage system equipped with *supercapacitors* (SC) of 1.484 kWh.

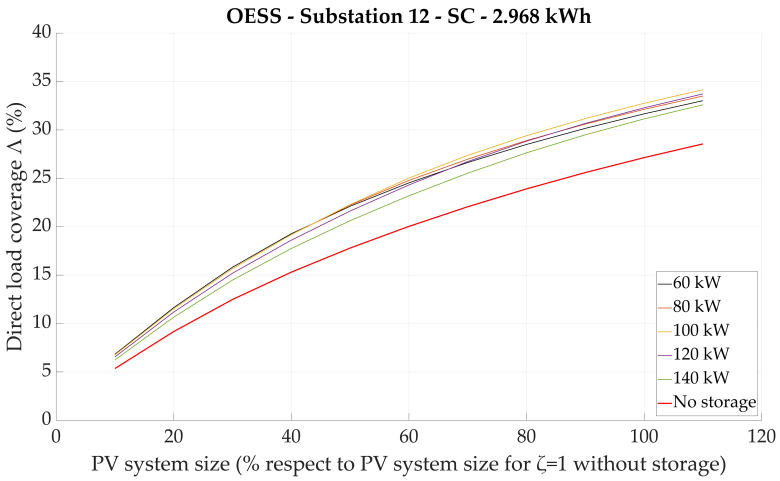

Figure 4.26: Substation 12 PV system utilization vs direct load coverage Λ for various upper electric power thresholds for *on-board* energy storage system equipped with *supercapacitors* (SC) of 2.968 kWh.

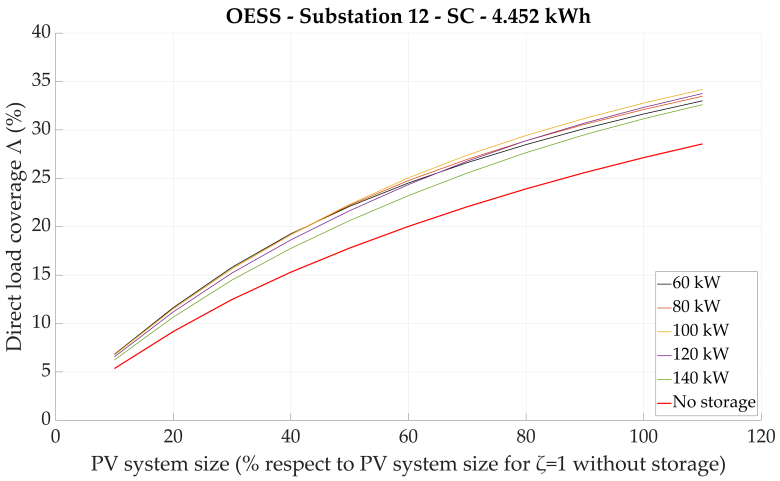

Figure 4.27: Substation 12 PV system utilization vs direct load coverage Λ for various upper electric power thresholds for *on-board* energy storage system equipped with *supercapacitors* (SC) of 4.452 kWh.

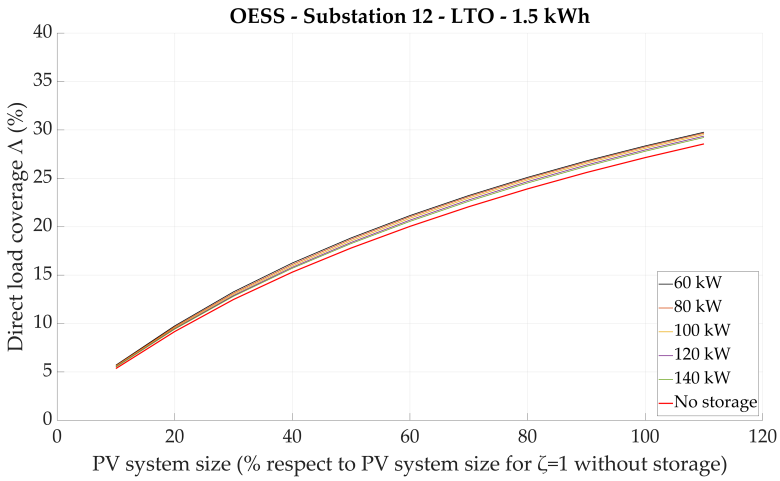

Figure 4.28: Substation 12 PV system utilization vs direct load coverage Λ for various upper electric power thresholds for *on-board* energy storage system equipped with *lithium-titanate oxide* (LTO) batteries of 1.5 kWh.

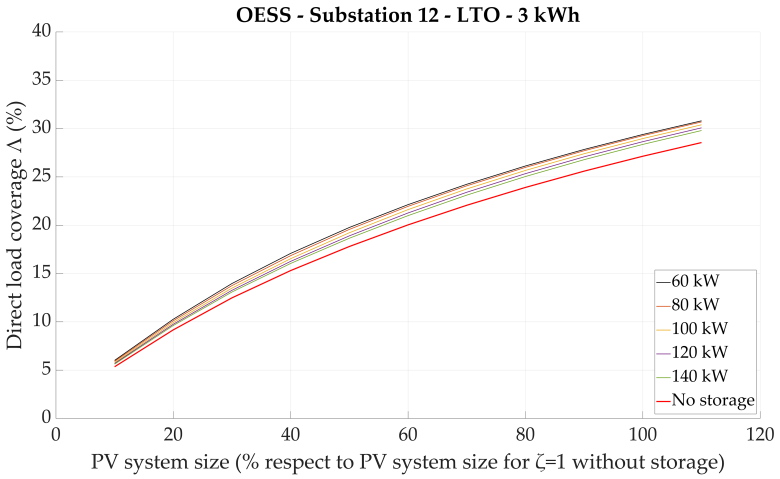

Figure 4.29: Substation 12 PV system utilization vs direct load coverage Λ for various upper electric power thresholds for *on-board* energy storage system equipped with *lithium-titanate oxide* (LTO) batteries of 3 kWh.

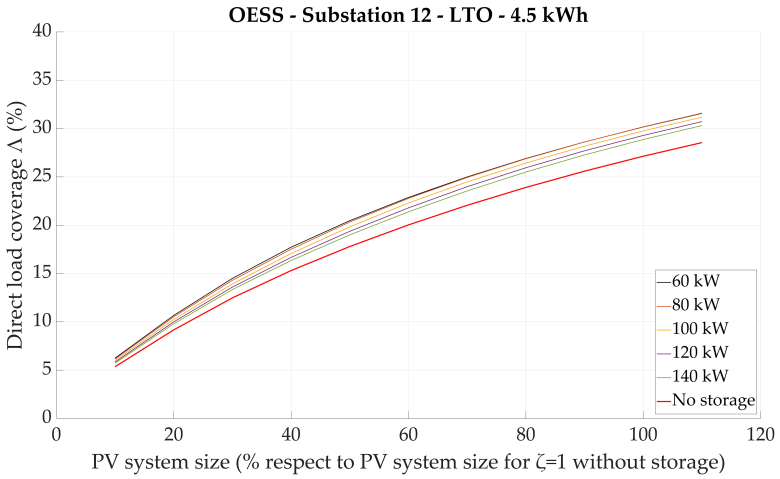

Figure 4.30: Substation 12 PV system utilization vs direct load coverage Λ for various upper electric power thresholds for *on-board* energy storage system equipped with *lithium-titanate oxide* (LTO) batteries of 4.5 kWh.

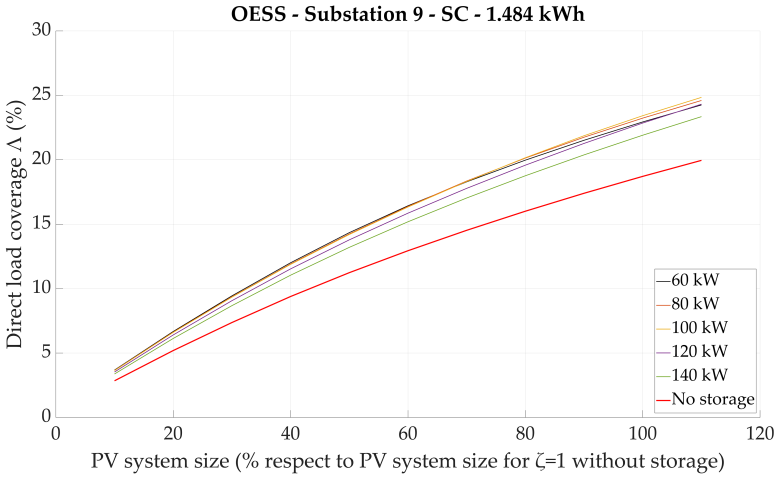

Figure 4.31: Substation 9 PV system utilization vs direct load coverage Λ for various upper electric power thresholds for *on-board* energy storage system equipped with *supercapacitors* (SC) of 1.484 kWh.

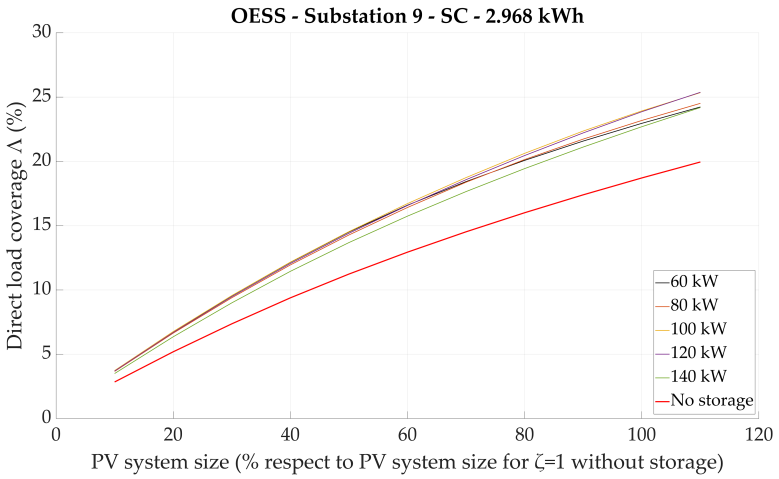

Figure 4.32: Substation 9 PV system utilization vs direct load coverage Λ for various upper electric power thresholds for *on-board* energy storage system equipped with *supercapacitors* (SC) of 2.968 kWh.

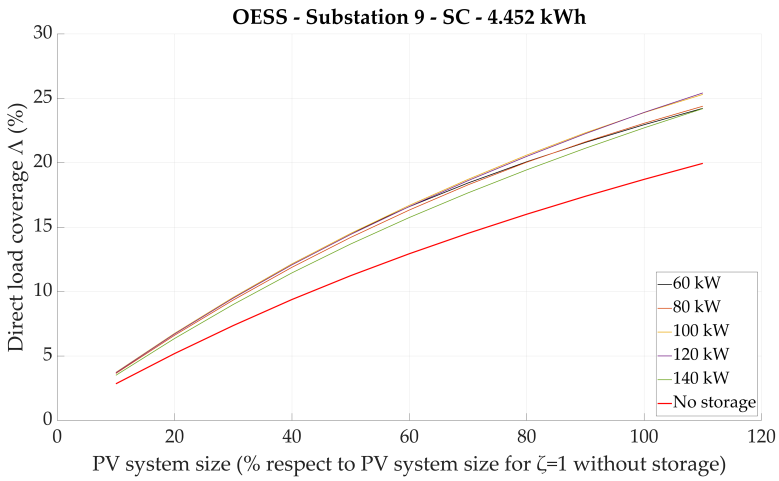

Figure 4.33: Substation 9 PV system utilization vs direct load coverage Λ for various upper electric power thresholds for *on-board* energy storage system equipped with *supercapacitors* (SC) of 4.452 kWh.

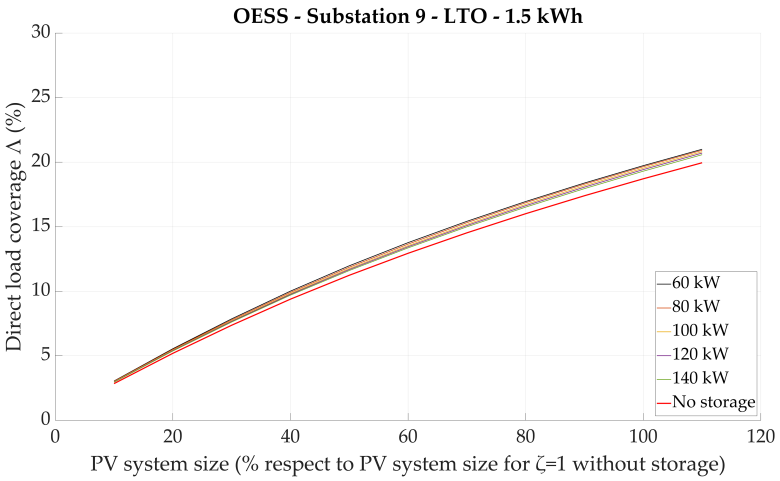

Figure 4.34: Substation 9 PV system utilization vs direct load coverage Λ for various upper electric power thresholds for *on-board* energy storage system equipped with *lithium-titanate oxide* (LTO) batteries of 1.5 kWh.

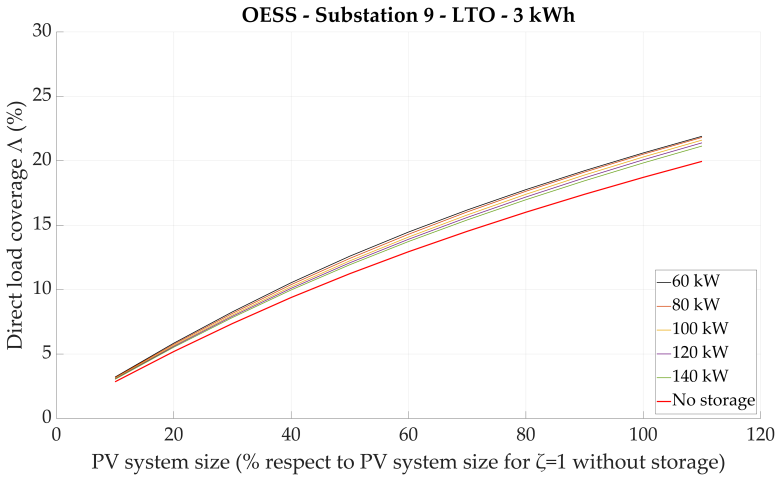

Figure 4.35: Substation 9 PV system utilization vs direct load coverage Λ for various upper electric power thresholds for *on-board* energy storage system equipped with *lithium-titanate oxide* (LTO) batteries of 3 kWh.

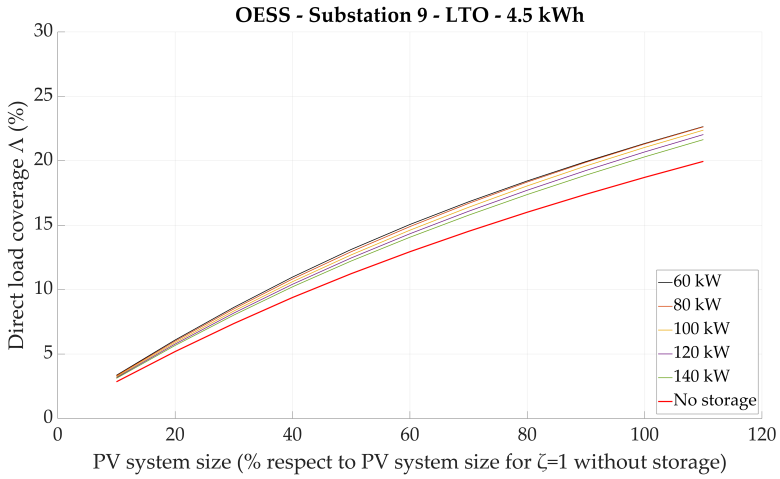

Figure 4.36: Substation 9 PV system utilization vs direct load coverage Λ for various upper electric power thresholds for *on-board* energy storage system equipped with *lithium-titanate oxide* (LTO) batteries of 4.5 kWh.

To get an overall image of the effect of the the *on-board* energy storage systems to the trolleybus grid, is interesting to observed the response of the PV system utilization in regard to the direct load coverage Λ. In figure 4.25 until figure 4.36 is illustrated the PV system utilization vs the direct load coverage Λ for various upper electric power thresholds for *on-board* energy storage systems equipped with *supercapacitors* (SC) or *lithium-titanate oxide* (LTO) batteries of various capacities for substation 12 and substation 9.

For all simulated cases (figure 4.25 to figure 4.36), is evident that the direct load coverage Λ is increased compared to the case without any energy storage system implemented. This is also the case for the *lithium-titanate oxide* (LTO) batteries, even if the increase is smaller compared to the one for the *supercapacitors* (SC). This shows that for all cases the use of *on-board* energy storage systems can help the system achieve the same PV system utilization as the one with a PV system sized for an energy-neutrality ratio ζ=1 without energy storage, while using a smaller PV system size. This phenomenon is observed both for substation 12 and substation 9 and is more profound for the cases of *supercapacitors* (SC) irrespectively of their energy capacity, with an upper electric power threshold of 100 kW. This is because an upper electric power threshold of 100 kW is found to provide the best balance of energy used and stored from the regenerative braking. Similarly, for the cases of *lithium-titanate oxide* (LTO) batteries, this phenomenon is again present, both for substation 12 and substation 9, independently of their energy capacity but with an upper electric power threshold of 60 kW. This is logical due to their limited electric power that they can provide, which translates to a lower total electric energy. A lower upper electric threshold means that the *on-board* energy storage is able to provide more times electric power thus increasing the total provided electric energy, even if the maximum provided electric power is small. As a result, this increases the probability of them getting discharged, thus being more times available to get charged via the energy provided from regenerative braking.

In appendix A are provided extra graphs both for *on-board* energy storage systems. More specifically are provided graphs regarding the the PV system utilization vs energy-neutrality ratio ζ for various upper electric power thresholds for *on-board* energy storage systems equipped with *supercapacitors* (SC) or *lithium-titanate oxide* (LTO) batteries of various capacities for substation 12 and substation 9. Also are provided graphs that illustrate the direct load coverage Λ vs energy-neutrality ratio ζ for various upper electric power thresholds for *on-board* energy storage systems equipped with *supercapacitors* (SC) or *lithium-titanate oxide* (LTO) batteries of various capacities for substation 12 and substation 9.

4.3 *STATIONARY* ENERGY STORAGE SYSTEMS

In figure 4.38 until figure 4.45 is illustrated the PV system utilization vs PV system size vs position for *stationary* energy storage systems equipped with *flywheels* or *lithium-titanate oxide* (LTO) batteries of various capacities for substation 12 and substation 9 in 3D form. The same plots in 2D form are presented in figure 4.46 until figure 4.53 with the case without any energy storage system to be presented with red. Note that a different PV system utilization scale is used for the two substations (20% to 60% for substation 12 and 15% to 35% for substation 9) to best represent the range of values observed for each one. At this point it is crucial to mention that the control strategy implemented for the *stationary* energy storage system is highly affecting the results. Since is a control strategy developed having yearly energy storage charging and discharging schemes in mind, it is not very favorable to be used with *flywheels*. This is because of their very high self-discharge compared to *lithium-titanate oxide* (LTO) batteries.

SESS - Substation 12 – Comparison of capacities.
For the case of *flywheels*, when comparing the various capacities (figure 4.38 to figure 4.39 and figure 4.46 to figure 4.47), is observed quite a different PV system utilization response in regard to the PV system size for the various positions. More specifically, is observed a slightly higher overall increase in PV system utilization for a *stationary* energy storage system equipped with a larger energy capacity of *flywheels* compared to a one with a smaller one, with a response which is almost identical for each position. For the case of a larger capacities of *flywheels*, for all PV system sizes, the state of charge (SoC) was close to zero by the end of the first week of the year. This is an outcome mainly due to the selected control strategy and not a generalizable conclusion that *flywheels* are a bad energy storage technology. This leads for all positions to express the same behavior. In other words, the *stationary* energy storage system was empty, or at least below the lower state of charge (SoC) limit by the end of the first week of the year, which means that all the energy that was provided by the PV system and was stored, was lost as heat due to self-discharge. This is observed in figure 4.37 where is illustrated an example of the state of charge (SoC) of a *stationary* energy storage system equipped with *flywheels* of 992 kWh placed at 650 m on Substation 12 and a PV system size of 100%. This also means that the *stationary* energy storage system was never able to provide any electric power and thus help with the voltage drops. In contrary, for smaller capacities of *flywheels*, there is still a considerable increase in the PV system utilization compared to the case without any energy storage implemented for all positions, but is not the same for all positions for PV system sizes larger than 25%. It is also overall lower compared to the case of a larger capacities of them. This happens because in a low traffic substation where there are more intermittencies, a small energy capacity *stationary* energy storage system is more likely to get full, thus not being able to store more electric energy provided by the PV system, even with the high self-discharge of *flywheels*. For the case of *lithium-titanate oxide* (LTO) batteries, when comparing the various capacities (figure 4.40 to figure 4.41 and figure 4.48 to figure 4.49), is observed a similar PV system utilization response in regard to the PV system size for the various positions. This shows that an *stationary* energy storage system equipped with *lithium-titanate oxide* (LTO) batteries, if placed in a substation with high traffic, needs to be considerably larger since the control strategy used renders it full, not being able to accept any more electric energy by the PV system.

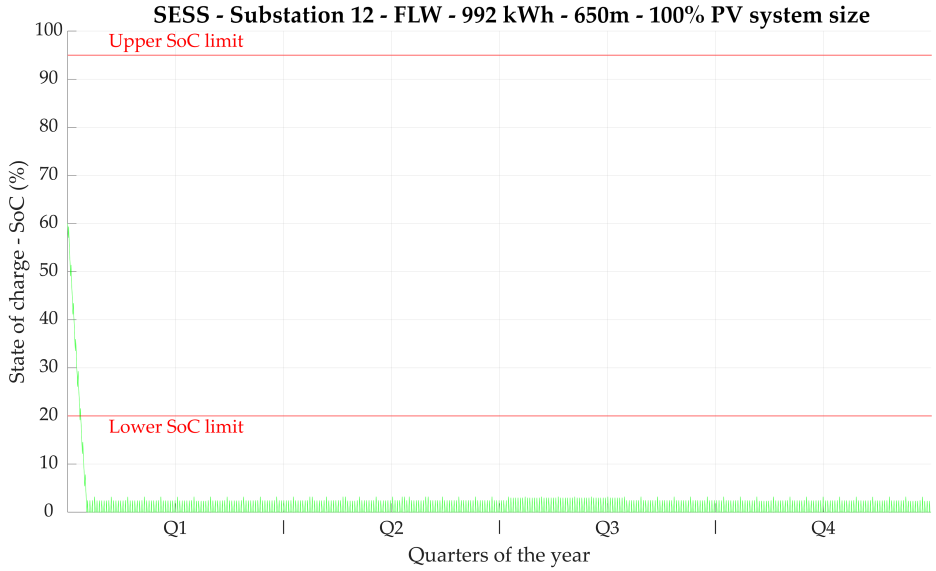

Figure 4.37: State of charge (SoC) of a *stationary* energy storage system equipped with *flywheels* of 992 kWh placed at 650 m on Substation 12 and a PV system size of 100%.

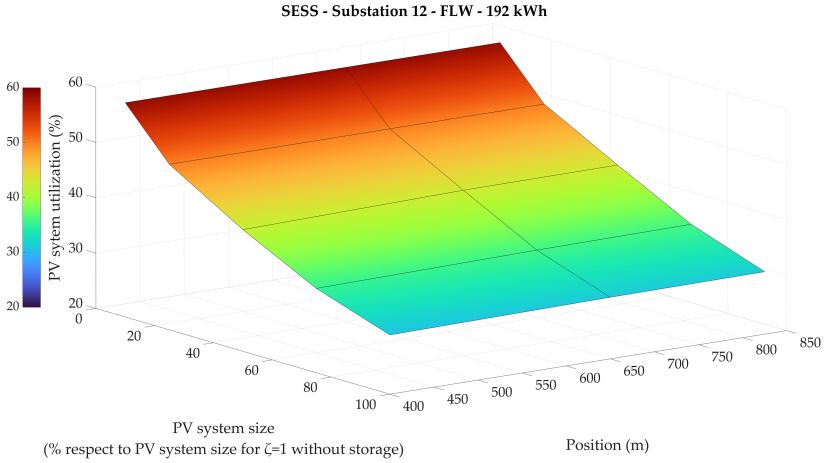

Figure 4.38: Substation 12 PV system utilization vs PV system size vs position for *stationary* energy storage system equipped with *flywheels* of 192 kWh.

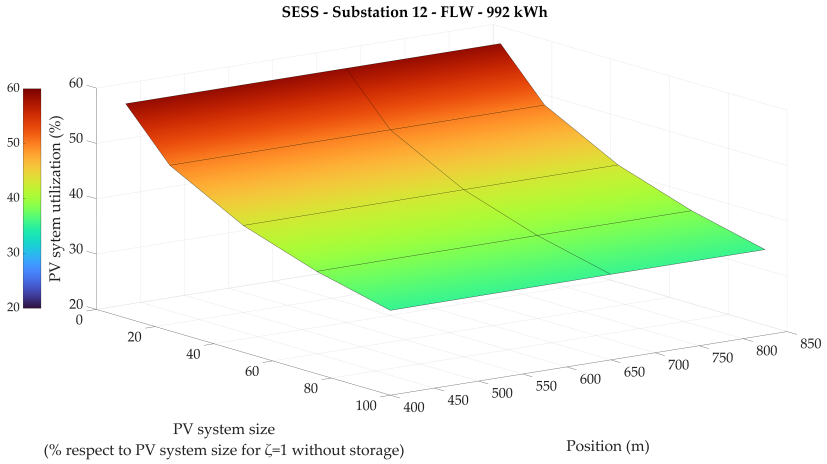

Figure 4.39: Substation 12 PV system utilization vs PV system size vs position for *stationary* energy storage system equipped with *flywheels* of 992 kWh.

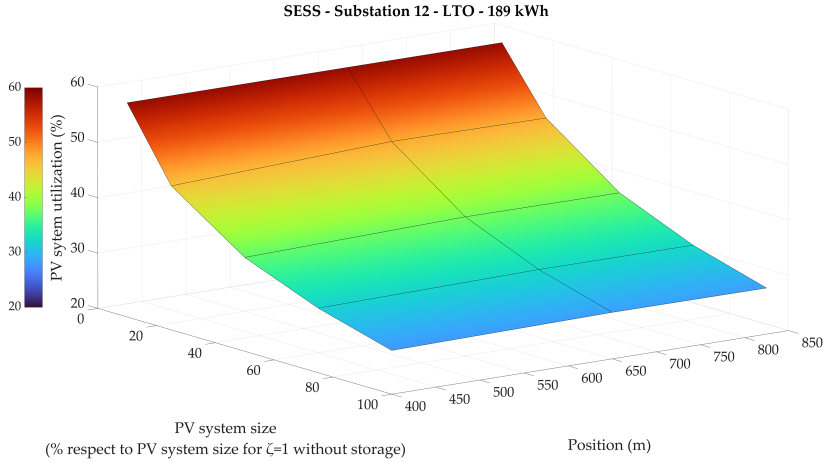

Figure 4.40: Substation 12 PV system utilization vs PV system size vs position for *stationary* energy storage system equipped with lithium-titanate batteries of 189 kWh.

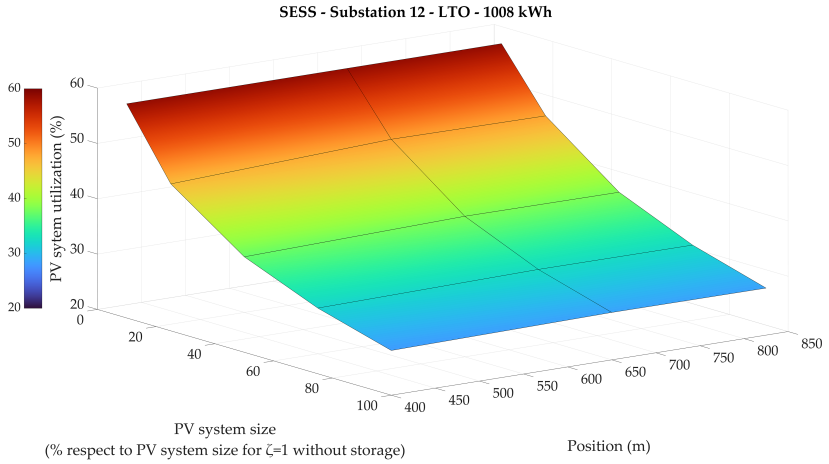

Figure 4.41: Substation 12 PV system utilization vs PV system size vs position for *stationary* energy storage system equipped with lithium-titanate batteries of 1008 kWh.

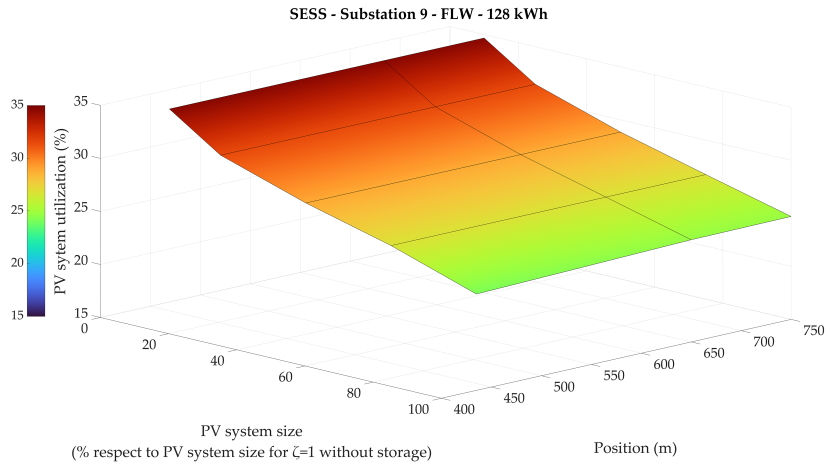

Figure 4.42: Substation 9 PV system utilization vs PV system size vs position for *stationary* energy storage system equipped with *flywheels* of 128 kWh.

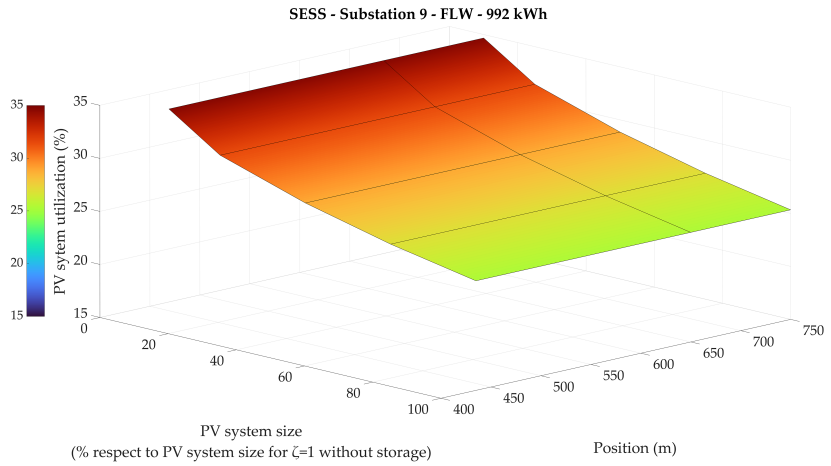

Figure 4.43: Substation 9 PV system utilization vs PV system size vs position for *stationary* energy storage system equipped with *flywheels* of 992 kWh.

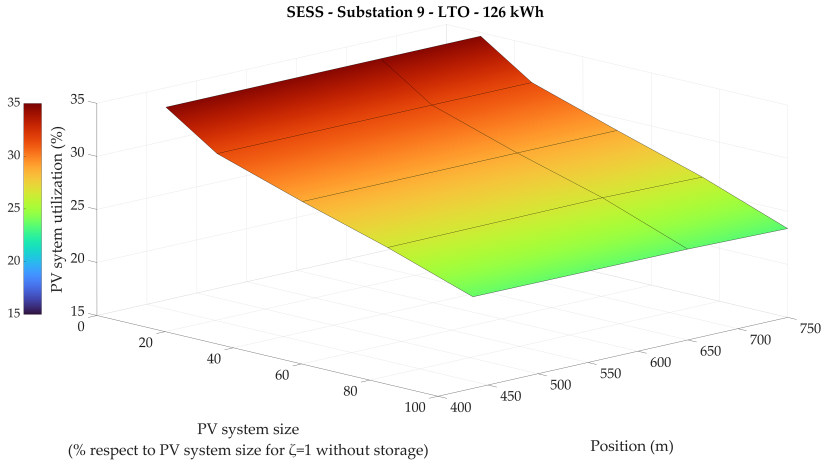

Figure 4.44: Substation 9 PV system utilization vs PV system size vs position for *stationary* energy storage system equipped with *lithium-titanate oxide* (LTO) batteries of 126 kWh.

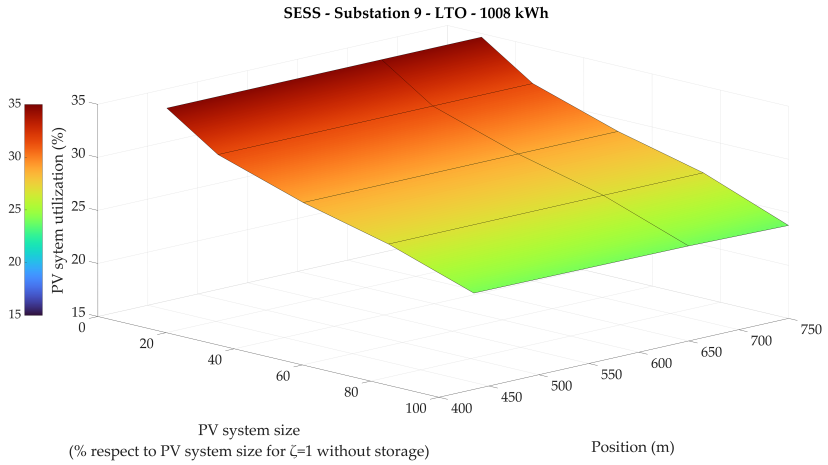

Figure 4.45: Substation 9 PV system utilization vs PV system size vs position for *stationary* energy storage system equipped with *lithium-titanate oxide* (LTO) batteries of 1008 kWh.

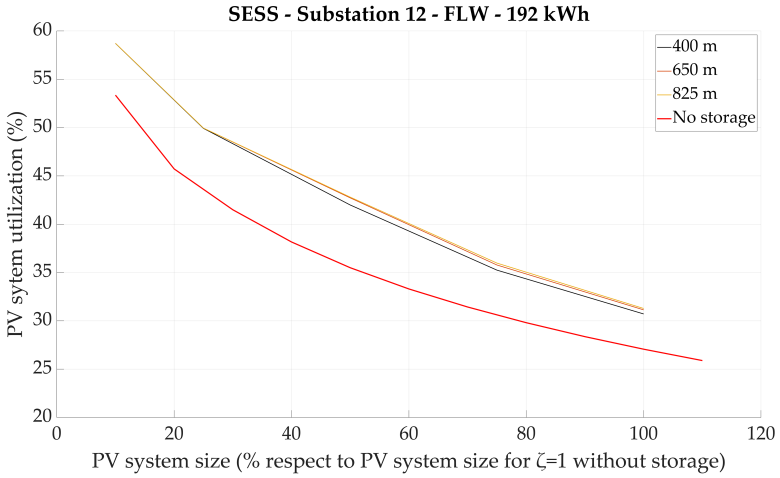

Figure 4.46: Substation 12 PV system utilization vs PV system size for various positions for *stationary* energy storage system equipped with *flywheels* of 192 kWh.

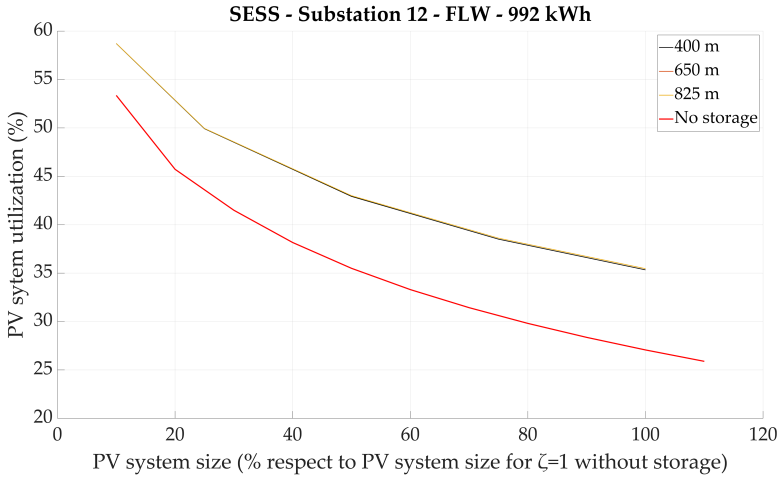

Figure 4.47: Substation 12 PV system utilization vs PV system size for various positions for *stationary* energy storage system equipped with *flywheels* of 992 kWh.

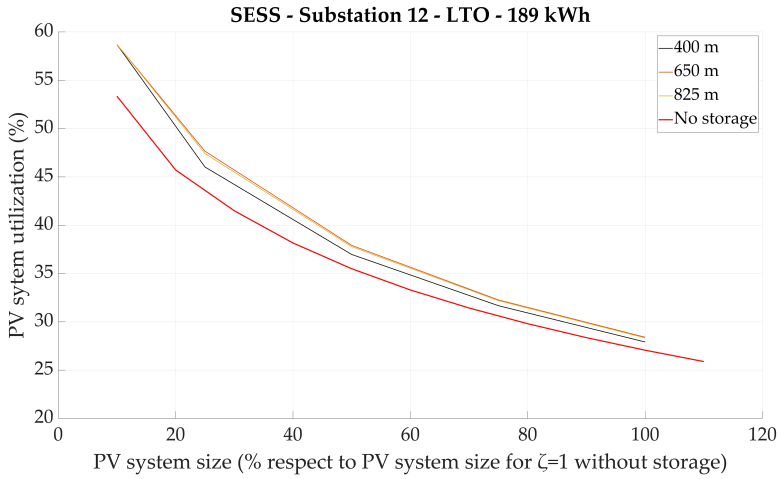

Figure 4.48: Substation 12 PV system utilization vs PV system size for various positions for *stationary* energy storage system equipped with lithium-titanate batteries (LTO) of 189 kWh.

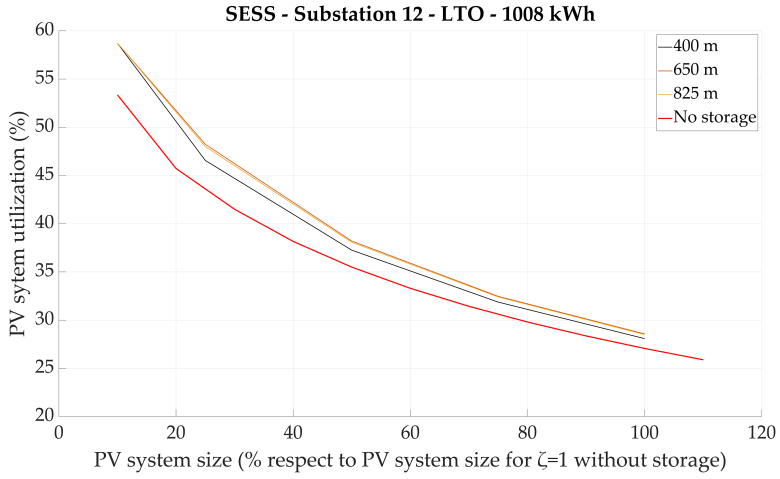

Figure 4.49: Substation 12 PV system utilization vs PV system size for various positions for *stationary* energy storage system equipped with lithium-titanate batteries (LTO) of 1008 kWh.

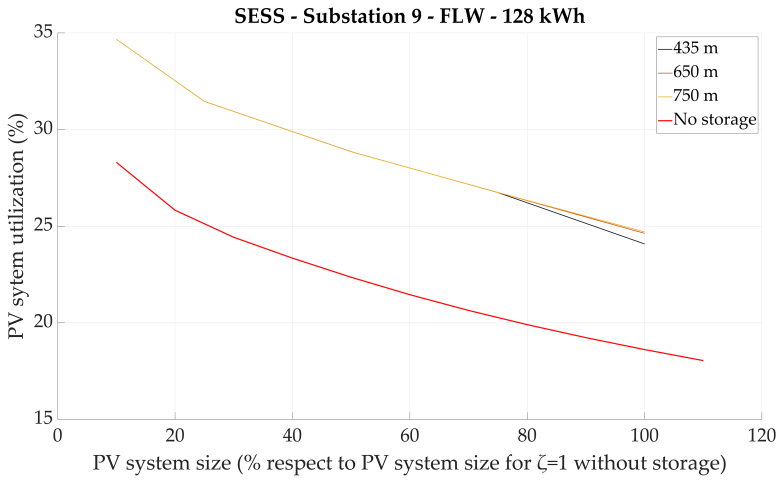

Figure 4.50: Substation 9 PV system utilization vs PV system size for various positions for *stationary* energy storage system equipped with *flywheels* of 128 kWh.

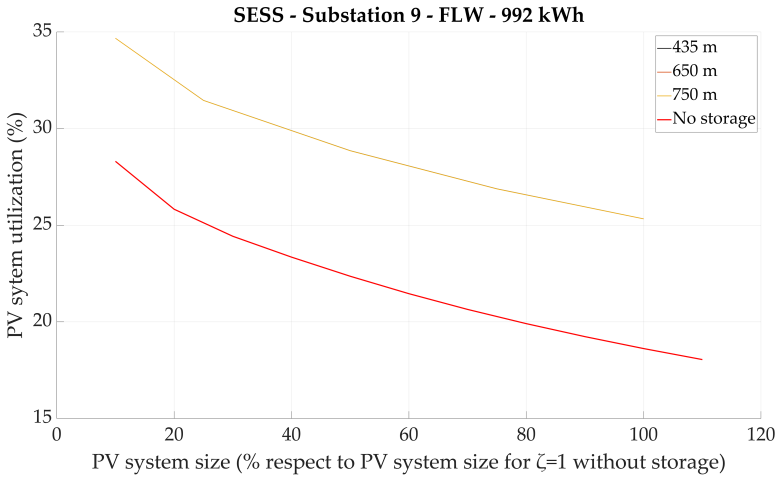

Figure 4.51: Substation 9 PV system utilization vs PV system size for various positions for *stationary* energy storage system equipped with *flywheels* of 992 kWh.

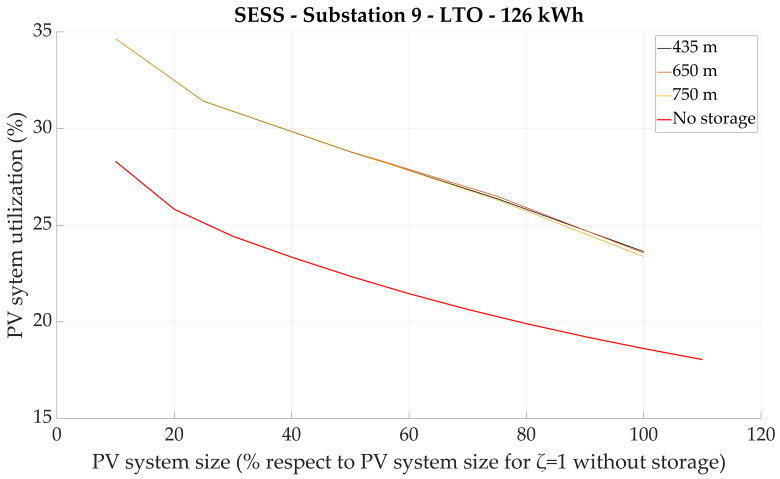

Figure 4.52: Substation 9 PV system utilization vs PV system size for various positions for *stationary* energy storage system equipped with *lithium-titanate oxide* (LTO) batteries of 126 kWh.

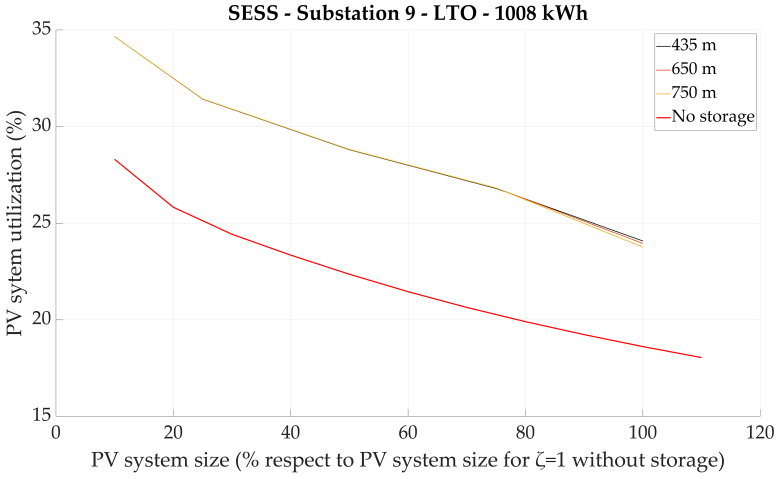

Figure 4.53: Substation 9 PV system utilization vs PV system size for various positions for *stationary* energy storage system equipped with *lithium-titanate oxide* (LTO) batteries of 1008 kWh.

SESS - Substation 12 – Comparison of positions.
For the case of *flywheels*, when comparing the various positions (figure 4.38 to figure 4.39 and figure 4.46 to figure 4.47), is observed that for the case smaller capacities, the further the *stationary* energy storage system is placed from the electric power feeding point, the higher the PV system utilization is. This has to do with the selected positions and the discharging scheme. Since are selected positions with severe voltage drops, the further away the *stationary* energy storage system is placed from the electric power feeding point, the more likely is for these voltage drops to be more severe. Thus, the *stationary* energy storage system can discharge more frequently and have more frequently the availability to get charged again. This increases the PV system utilization since the *stationary* energy storage system control strategy targets to charged with electric energy provided by the PV system. For the case of larger capacities of *flywheels*, as already described, those express the same response for each position since the *stationary* energy storage system is basically empty due to self-discharge. For the case of *lithium-titanate oxide* (LTO) batteries, when comparing the various positions (figure 4.40 to figure 4.41 and figure 4.48 to figure 4.49), is observed that for all capacities, there is a higher PV system utilization the further away the *stationary* energy storage system is placed from the electric power feeding point. This happens due to the same reasons as explained for the case of *flywheels*.

SESS - Substation 12 – Comparison of technologies.
As can be understood from the aforementioned results, *flywheels* perform overall worse compared to *lithium-titanate oxide* (LTO) batteries when it comes to be used in *stationary* energy storage systems in conjunction with the specific control strategy. Their very high self-discharge compared to *lithium-titanate oxide* (LTO) batteries may render them empty rather quickly, thus not being able to provide any electric power to the trolleybus grid. On the other hand, *lithium-titanate oxide* (LTO) batteries provide a much better solution for this kind of applications especially when placed at positions with severe voltage drops. Those positions are are usually further away from the electric power feeding point. The results presented reflect substations with low traffic.

SESS - Substation 9 – Comparison of capacities.
For the case of *flywheels*, when comparing the various capacities (figure 4.42 to figure 4.43 and figure 4.50 to figure 4.51), is observed a similar PV system utilization response in regard to the PV system size for the various positions. There is however an exemption for the case of smaller capacities placed close to the electric power feeding point, when the PV system size becomes bigger than 75%. This happens as the closer the selected position is to the electric power feeding point, the smaller is the severity of the voltage drops. Thus the *stationary* energy storage system is not able to discharge as much using this control strategy. For all the other cases, the PV system utilization increases approximately by the same amount for all positions. This is once again the result of a *stationary* energy storage system which is mainly empty, caused by the high self-discharge of *flywheels*. Both the high self-discharge and the high traffic found in this substation, do not provide ideal conditions for the *stationary* energy storage system to get charged, when using this control strategy. This happens only slightly, for bigger PV system sizes, as there is more electric energy provided by the PV system throughout the year. The same response is observed for the *lithium-titanate oxide* (LTO) batteries too (figure 4.44 to figure 4.45 and figure 4.52 to figure 4.53). Although their self-discharge is much smaller compared to *flywheels*, the high traffic found in this substation simply does not provide enough time gaps where there is no or idling traffic to give the opportunity to the *stationary* energy storage system to get charged. This happens mainly for PV systems larger than 60% and the implemented control strategy has a main role for that.

SESS - Substation 9 – Comparison of positions.
For both cases of *flywheels* and *lithium-titanate oxide* (LTO) batteries, when comparing the various positions (figure 4.42 to figure 4.45 and figure 4.50 to figure 4.53), is observed a very similar PV system utilization response in regard to the PV system size for all positions, especially for smaller PV system sizes. This is the case for all capacities and the reason that this happens is the same one as explained when comparing the capacities; an empty *stationary* energy storage for the most cases due to the lack of enough time gaps where there is no or idling traffic in high traffic substations that provide the opportunity for the *stationary* energy storage system to get charged, using this specific control strategy.

SESS - Substation 9 – Comparison of technologies.
Comparing the two technologies the results are quite different compared to the ones from substation 12. *Flywheels* are still a poor choice when it comes to be used in *stationary* energy storage systems in conjunction with a yearly optimized control strategy for the same reasons as before. Nevertheless, when a *stationary* energy storage is used in a high traffic substation using a yearly optimized control strategy, even *lithium-titanate oxide* (LTO) batteries perform similarly to *flywheels* since there is not enough available time instances throughout the year to get charged to be full. Thus, they end up performing similarly to *flywheels* since they are mainly empty, especially for PV system sizes smaller than 75%.

To get an overall image of the effect of the the *stationary* energy storage systems to the trolleybus grid, is interesting to observed the response of the PV system utilization in regard to the direct load coverage Λ. In figure 4.54 until figure 4.61 is illustrated the PV system utilization vs the direct load coverage Λ for various positions for *stationary* energy storage systems equipped with *flywheels* or *lithium-titanate oxide* (LTO) batteries of various capacities for substation 12 and substation 9.

For all simulated cases (figure 4.54 to figure 4.61), is evident that the direct load coverage Λ is increased compared to the case without any energy storage system implemented. Like for the case of *on-board* energy storage systems, this shows that for all cases, the use of *stationary* energy storage systems can help the system achieve the same PV system utilization as the one with a PV system sized for an energy-neutrality ratio ζ=1 without energy storage, while using a smaller PV system size. This phenomenon is evident both for substation 12 and substation 9 and is more profound for the cases of *flywheels*, irrespectively of their energy capacity, with a position further away from the electric power feeding point. This happens mainly due to the high self-discharge of the *flywheels* which renders them more available to be charged with energy provided by the PV system but in reality, this energy most of the times is wasted in the form of heat. Similarly, for the cases of *lithium-titanate oxide* (LTO) batteries, this behavior is again present for both substation 12 and substation 9, independently of their energy capacity, and similarly is more profound for a position further away from the electric power feeding point.

In appendix A are provided extra graphs *stationary* energy storage systems. More specifically are provided graphs regarding the PV system utilization vs energy-neutrality ratio ζ for various positions for *stationary* energy storage systems equipped with *flywheels* or *lithium-titanate oxide* (LTO) batteries of various capacities for substation 12 and substation 9. Also are provided graphs that illustrate the direct load coverage Λ vs energy-neutrality ratio ζ for various positions for *stationary* energy storage systems equipped with *flywheels* or *lithium-titanate oxide* (LTO) batteries of various capacities for substation 12 and substation 9.

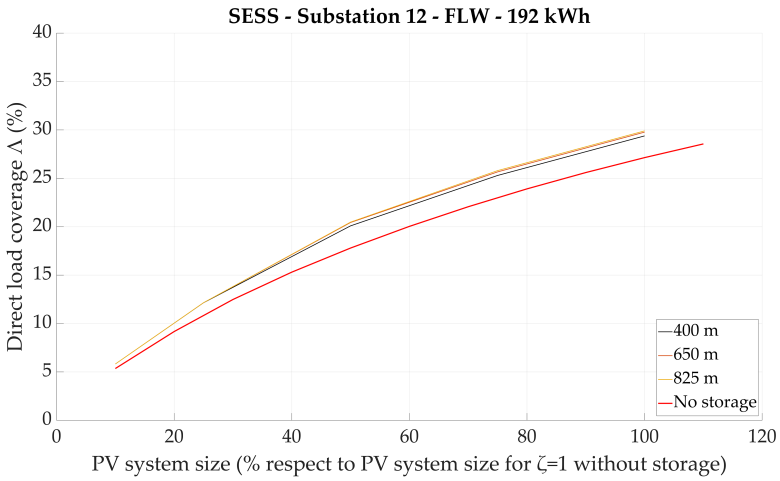

Figure 4.54: Substation 12 PV system utilization vs direct load coverage Λ for various upper electric power thresholds for *stationary* energy storage system equipped with *flywheels* of 192 kWh.

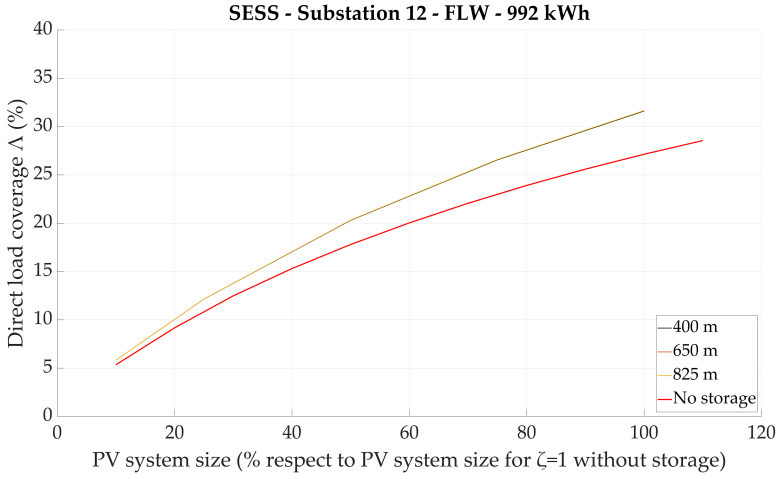

Figure 4.55: Substation 12 PV system utilization vs direct load coverage Λ for various upper electric power thresholds for *stationary* energy storage system equipped with *flywheels* of 992 kWh.

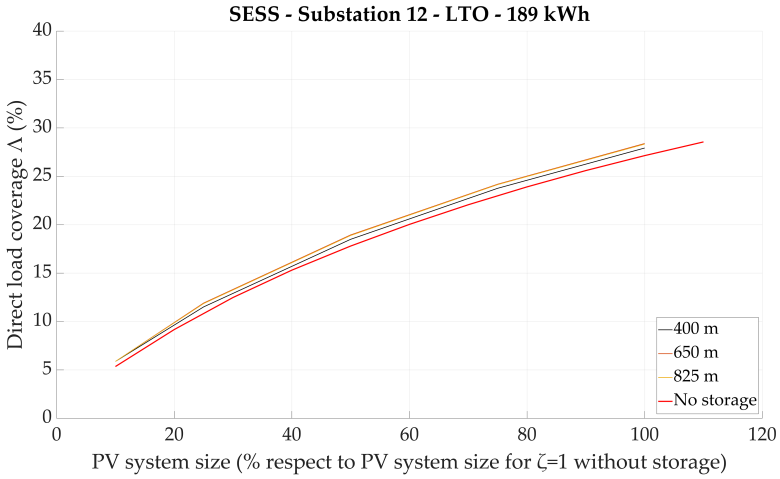

Figure 4.56: Substation 12 PV system utilization vs direct load coverage Λ for various upper electric power thresholds for *stationary* energy storage system equipped with *lithium-titanate oxide* (LTO) batteries of 189 kWh.

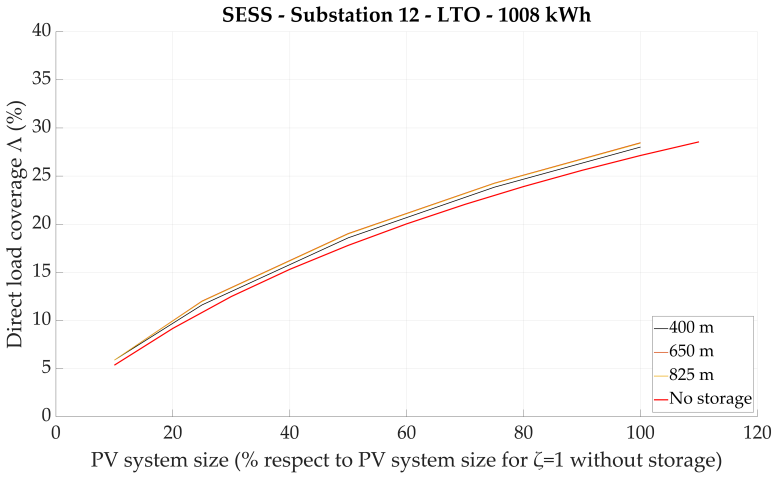

Figure 4.57: Substation 12 PV system utilization vs direct load coverage Λ for various upper electric power thresholds for *stationary* energy storage system equipped with *lithium-titanate oxide* (LTO) batteries of 1008 kWh.

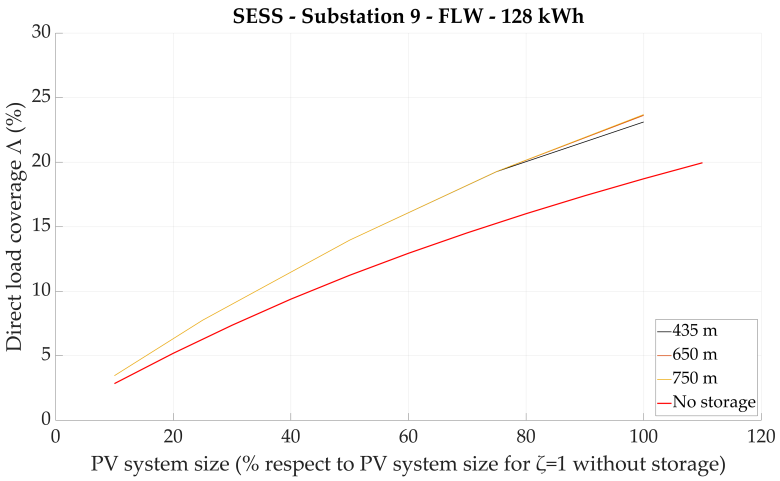

Figure 4.58: Substation 9 PV system utilization vs direct load coverage Λ for various upper electric power thresholds for *stationary* energy storage system equipped with *flywheels* of 128 kWh.

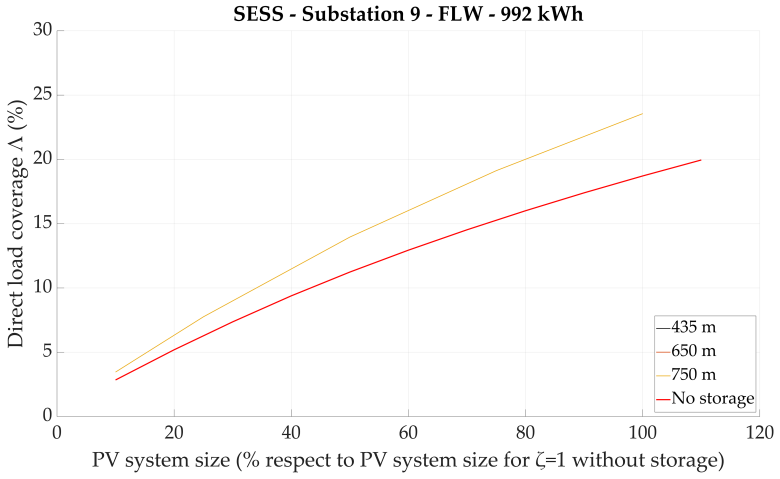

Figure 4.59: Substation 9 PV system utilization vs direct load coverage Λ for various upper electric power thresholds for *stationary* energy storage system equipped with *flywheels* of 992 kWh.

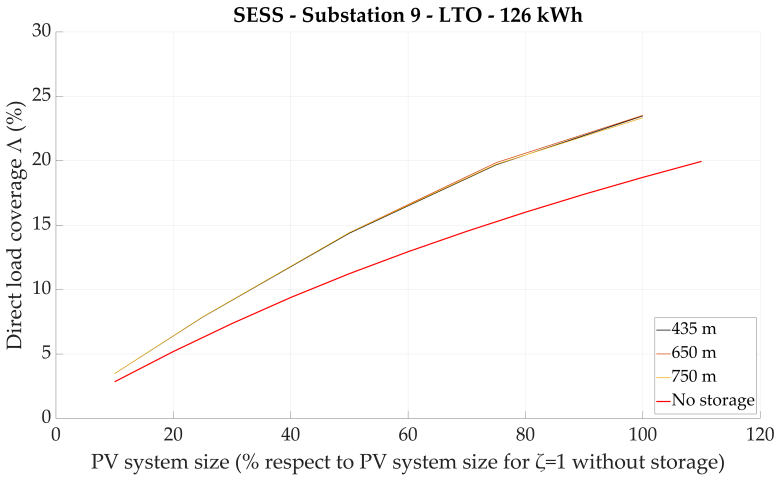

Figure 4.60: Substation 9 PV system utilization vs direct load coverage Λ for various upper electric power thresholds for *stationary* energy storage system equipped with *lithium-titanate oxide* (LTO) batteries of 126 kWh.

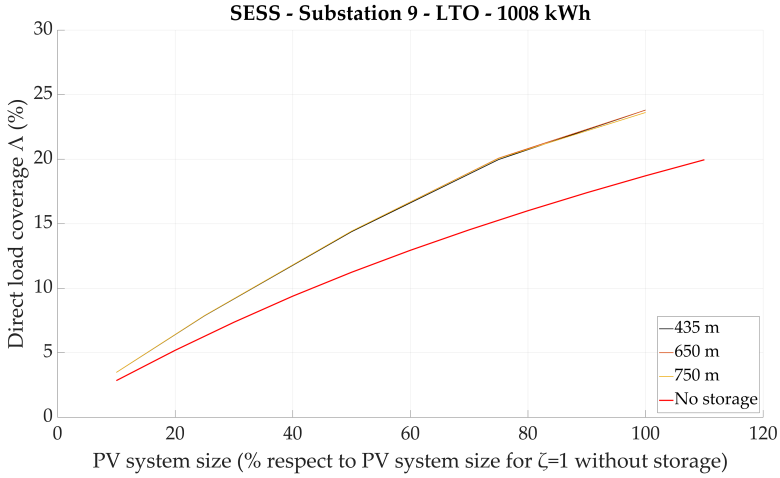

Figure 4.61: Substation 9 PV system utilization vs direct load coverage Λ for various upper electric power thresholds for *stationary* energy storage system equipped with *lithium-titanate oxide* (LTO) batteries of 1008 kWh.

4.4 CONCLUSIONS

In this chapter have been presented the results from the simulations of this work regarding the impact of *on-board* and *stationary* energy storage systems on the PV system utilization. After has been given a brief explanation regarding terms important for the interpretation of the results, there were presented the results regarding the impact of the *on-board* and the *stationary* energy storage systems on the PV system utilization.

On-board energy storage systems are more beneficial to be used when equipped with *supercapacitors* (SC) of small capacities, as there is no additional benefit in using larger ones. It is more beneficial if placed at higher traffic substations with upper electric power thresholds of 80 kW - 100 kW for PV system sizes up to 90%. Nevertheless, even for a PV system size that represents the best-case scenario, which is usually a small one, the expected PV system utilization increase is less than 1.5 percentage points while for a PV system size of 90% it is around 0.5 percentage points. From the simulations, the best overall case scenario is for an *on-board* energy storage system equipped with *supercapacitors* (SC) of small energy capacity, placed at a high traffic substation with a PV system size of 80% and with an upper electric power threshold of 100 kW. This provides an all around best scenario with a PV system utilization increase of around 1 percentage point.

On the other hand, the impact of *stationary* energy storage systems on the PV system utilization and on the trolleybus grid in general is heavily correlated to the control strategy used. As described in section 3.5. For each technology, PV system size, trolleybus grid section, and preferred results (improve the PV system utilization or favour parameters related to the *multifunctionality* of the trolleybus grid) there should be a specific control strategy. Thus, it is safe to conclude that the comparison of *stationary* energy storage systems to other energy storage systems cannot be straightforward. For this control strategy, *stationary* energy storage systems are more beneficial to be used equipped with *lithium-titanate oxide* (LTO) batteries of small or large capacities. For high traffic substations they perform well for small PV system sizes while for low traffic substations they perform well for high PV system sizes. Usually, it is more beneficial if placed to positions further away from the electric power feeding point since the severity of voltage drops is higher there, rendering them more able to discharge. From the simulations, the best overall case scenario is for an *stationary* energy storage system equipped with *lithium-titanate oxide* (LTO) batteries of small energy capacity, placed at a high traffic substation with a PV system size of 75%. This provides a PV system utilization increase of around 6.5 percentage points.

In the next chapter (chapter 5) is analyzed the impact of *on-board* and *stationary* energy storage systems on parameters related to the *multifunctionality* of the trolleybus grid, such as the total yearly electric energy consumption and the voltage drops occurred.

5 RESULTS - IMPACT ON THE MULTIFUNCTIONALITY OF THE TROLLEYBUS GRID

In this chapter are presented the results from the simulations of this work regarding the impact of energy storage systems on the multifunctionality of the trolleybus grid. First, the impact of on-board and stationary energy storage systems on the yearly electric energy consumption of the trolleybus grid is evaluated, and afterwards, the results regarding their impact on the voltage drops occurred in the trolleybus grid are analyzed.

5.1 YEARLY ELECTRIC ENERGY CONSUMPTION

When implementing an energy storage system in a trolleybus grid, either *on-board* or *stationary*, is interesting to observed how it may affect parameters that are correlated to the *multifunctionality* of the trolleybus grid. More specifically, in this section is analyzed the impact of each type of energy storage system on the total electric energy demand from one low traffic and one high traffic substation in a yearly basis.

5.1.1 *On-board* energy storage systems

In figure 5.1 until figure 5.4 are presented the graphs of the yearly electric energy supplied by the substation vs upper electric power threshold for *on-board* energy storage systems equipped with *supercapacitors* (SC) or *lithium-titanate oxide* (LTO) batteries for various capacities for substation 12 and substation 9, with the case without any energy storage system to be presented with a red line.

Regarding *on-board* energy storage systems equipped with *supercapacitors* (SC) (figure 5.1 and figure 5.3), for both substations is observed a similar response for each capacity and for the various upper electric power thresholds. More particularly, is observed that for both technologies and for the majority of cases, the reduction of the yearly electric energy supplied by the substation is around 18%. Even for the smaller capacities this number rarely goes below 16%. The best cases are observed for upper electric power thresholds of 60 kW to 100 kW and for capacities close to 3 kWh, but all the rest cases provide all around good results as well. This behavior is based on the fundamentals of operation of *on-board* energy storage systems as described in section 2.2.2. Since *on-board* energy storage systems are specifically made to be charged with electric energy provided by regenerative braking by the trolleybuses, is logical that they utilize electric energy possibly otherwise wasted on the resistors of the trolleybuses. Of course this electric energy could be utilized for powering other trolleybuses on the section, but the results prove that the intermittencies of trolleybuses providing electric power to the trolleybus grid due to regenerative braking and of the trolleybuses being able to accept this electric power at any given point are many. Thus, *on-board* energy storage systems equipped with *supercapacitors* (SC), even of small capacities, are a great choice to be used for reducing total yearly electric energy consumed in a trolleybus grid, providing a positive impact on the *multifunctionality* of the trolleybus grid, while at the same time increasing for some cases the PV system utilization, as described in section 4.2. This is the case for both low traffic and high traffic substations.

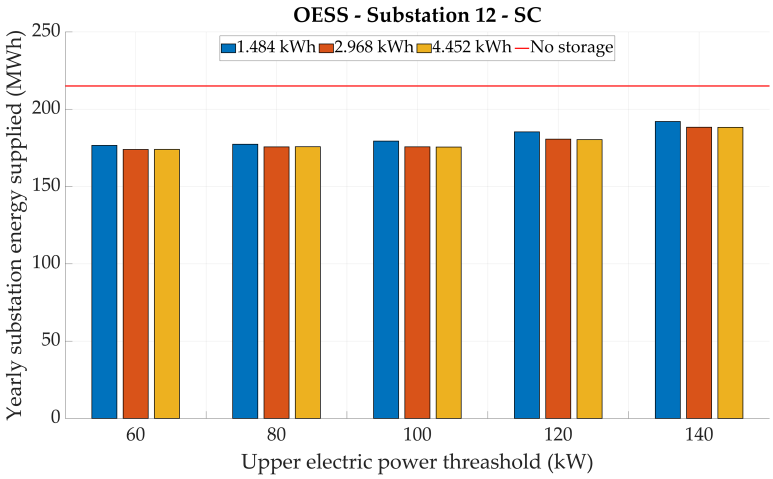

Figure 5.1: Substation 12 yearly energy supplied vs upper electric power threshold for *on-board* energy storage system equipped with *supercapacitors* (SC) for various capacities.

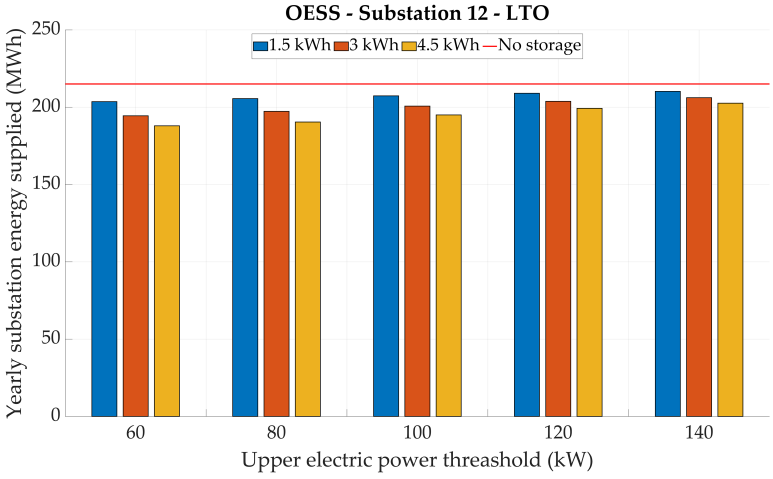

Figure 5.2: Substation 12 yearly energy supplied vs upper electric power threshold for *on-board* energy storage system equipped with *lithium-titanate oxide* (LTO) batteries for various capacities.

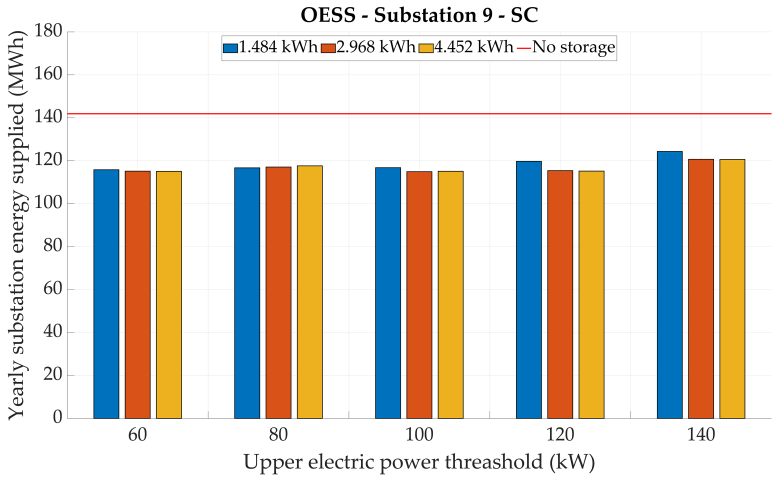

Figure 5.3: Substation 9 yearly energy supplied vs upper electric power threshold for *on-board* energy storage system equipped with *supercapacitors* (SC) for various capacities.

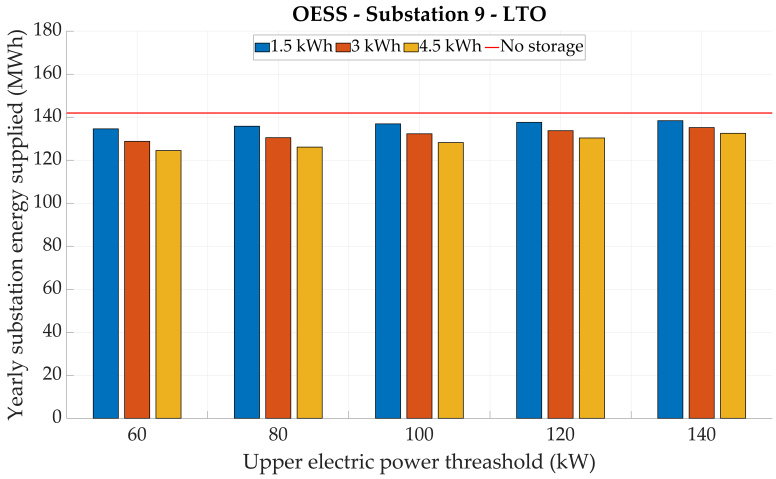

Figure 5.4: Substation 9 yearly energy supplied vs upper electric power threshold for *on-board* energy storage system equipped with *lithium-titanate oxide* (LTO) batteries for various capacities.

On the other hand, regarding *on-board* energy storage systems equipped with *lithium-titanate oxide* (LTO) batteries (figure 5.2 and figure 5.4), for once again is observed for both substations the same response for each capacity and for the various upper electric power thresholds. Although the results are obviously worse compared to the case of *supercapacitors* (SC), in this case too is observed a reduction in the total yearly electric energy supplied by the substation. More specifically, this reduction does not change significantly with the various upper electric power thresholds, but it does change with the various capacities. This is due to the more electric power that the *on-board* energy storage systems can accept or provide when larger capacities of *lithium-titanate oxide* (LTO) batteries are used, as described in section 3.3. Thus, for smaller capacities the yearly electric energy reduction is around 4% while for larger ones is around 9%, for both substations and for the majority of upper electric power thresholds. It is interesting to note that for smaller upper electric power thresholds the reduction in the yearly electric energy consumption is larger compared to larger ones. This happens for the same reason the PV system utilization is higher for smaller values of upper electric power thresholds, as described is section 4.2; the *on-board* energy storage system equipped with *lithium-titanate oxide* (LTO) batteries is more times able to accept electric power for charging, resulting in increasing the electric energy stored in per year basis although the maximum electric power that it can accept at any given instance is small.

5.1.2 *Stationary* energy storage systems

As far *stationary* energy storage systems are concerned, the results are interesting but overall expected. In figure 5.6 until figure 5.17 are presented the graphs of the yearly electric energy supplied by the substation vs PV system size for *stationary* energy storage systems equipped with *flywheels* or *lithium-titanate oxide* (LTO) batteries for various positions for substation 12 and substation 9, with the case without any energy storage system to be presented with a red line. The PV system size is used at the x axis is because is directly correlated to the charging scheme of the *stationary* energy storage system. Thus, for this control strategy, for smaller PV system sizes less electric energy is able to be stored compared to larger ones.

From the graphs regarding the *stationary* energy storage systems equipped with *flywheels* (figure 5.6 to figure 5.8 and figure 5.12 to figure 5.14), is observed a similar trend for each capacity and for each PV system size, correlated to each position. More analytically, is observed that for smaller PV system sizes, the total yearly electric energy supplied by the substation increases slightly, around 1% for both substations, while for larger ones increases around 5% to 12% for substation 12, and 5% to 8% for substation 9, compared to the case without any energy storage implemented. The percentage increase is given as a range (5% to 12% for substation 12 and and 5% to 8% for substation 9) because different capacities have different impact on the PV system utilization. More specifically, for larger capacities of *flywheels* the increase is larger (12% for substation 12 and 8% for substation 9), while for smaller ones is lower (5% for both substations). This happens because *flywheels*, as already described in section 3.3, is a technology with high self-discharge. Thus, most of the times tends to be empty, not being able to provide the stored electric energy back to the trolleybus grid, as already illustrated in an example in figure 4.37. Since is used a yearly optimized control strategy, the *stationary* energy storage system is actively charged by the trolleybus grid only in periods of PV system electric power generation and no or low traffic. Nevertheless, as already explained, the majority of the stored electric energy is lost due to the high self-discharge and as a result, the *stationary* energy storage system in a yearly basis consumes more electric energy than it actually provides back to the grid. Important to note is that the majority of this extra electric energy is considered *green* electric energy which is provided by the PV system. Substations of lower traffic tend to suffer more from this phenomenon since

the time gaps where there is no or idling traffic at the same time with electric power provided by the PV system, are more. Regarding the capacities, for smaller ones, is possible even for *flywheels* to become full using this control strategy, especially for high PV system sizes and substations with low traffic. This is observed in figure 5.5 where is illustrated an example of the state of charge (SoC) of a *stationary* energy storage system equipped with *flywheels* of 192 kWh placed at 650 m on Substation 12 and a PV system size of 100%. This means that for a larger capacity the *stationary* energy storage system is more able to get charged, thus consuming more electric energy. The problem for smaller capacities lies again in the self-discharge. The *stationary* energy storage system may become full for some periods but it quickly looses this energy due to self-discharge. As a result, it is constantly charging to recover the electric energy lost and not providing it back to the trolleybus grid. In general, *stationary* energy storage systems equipped with *flywheels* of any size, using this control strategy, do not provide promising results regarding their impact on the yearly consumed electric energy, mainly due to their high self-discharge.

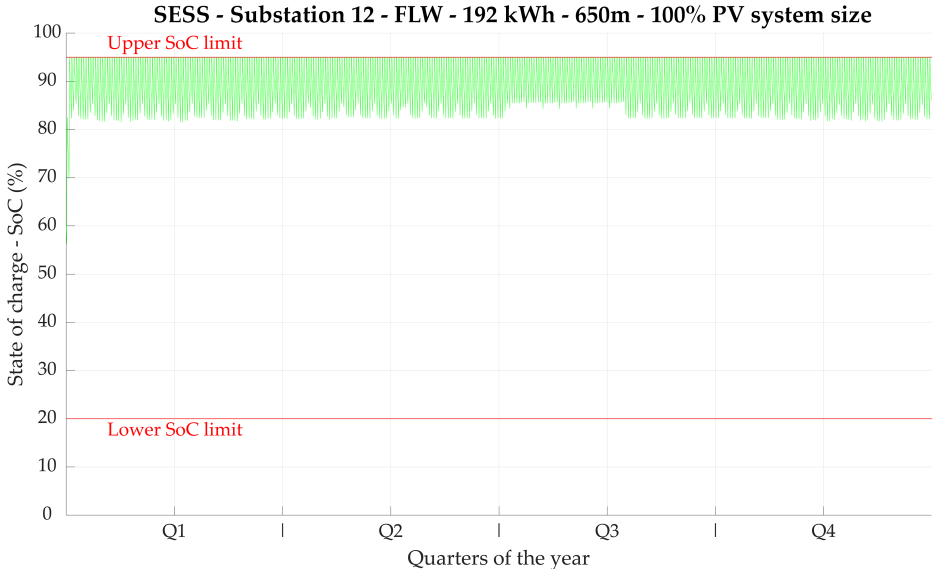

Figure 5.5: State of charge (SoC) of a *stationary* energy storage system equipped with *flywheels* of 192 kWh placed at 650 m on Substation 12.

Regarding *stationary* energy storage systems equipped with *lithium-titanate oxide* (LTO) batteries (figure 5.9 to figure 5.11 and figure 5.15 to figure 5.17), is observed that for all cases and for all substations, the yearly electric energy supplied by the substation has remained the same or increased at most 1.5%. This shows that *lithium-titanate oxide* (LTO) batteries, using this control strategy, are more promising solution compared to *flywheels* regarding their impact on the *multifunctionality* of the trolleybus grid. Consuming the same amount of electric energy while increasing the PV system utilization means that a bigger portion of this electric energy is considered *green*, provided by the PV system. The results confirm the logic behind the control strategy described in section 3.5; since the *stationary* energy storage is only charged with electric power provided by the PV system and provides it back in times when there is no electric power generation by the PV system, the equilibrium of energy used should be the same, assuming that the year ends with the same state of charge (SoC) as when it begun. The small increase in the consumption of yearly electric energy is due to the possibility that the control strategy may not be able to achieve 100% accurately its goal regarding the charging and discharging schemes, and due to transmission losses. In any case, *stationary* energy storage systems equipped with *lithium-titanate oxide* (LTO) batteries of any size, using this control strategy, provide promising results regarding their impact on the yearly consumed electric energy, mainly because of their low self-discharge.

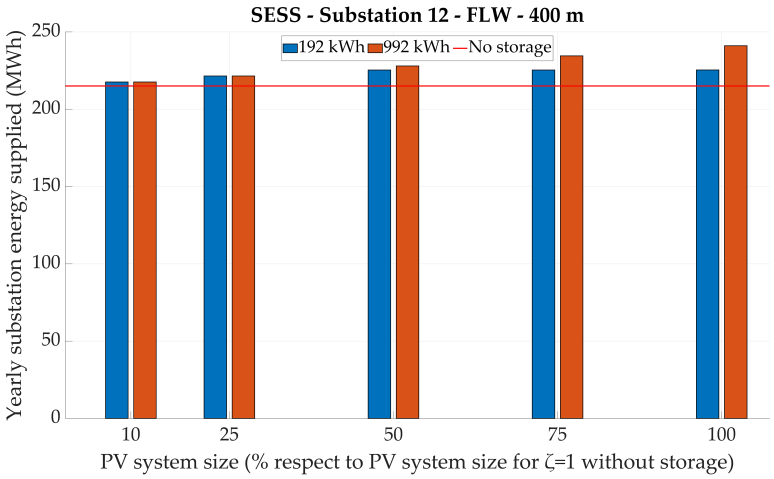

Figure 5.6: Substation 12 yearly energy supplied vs PV system size for *stationary* energy storage system equipped with *flywheels* placed at 400 m.

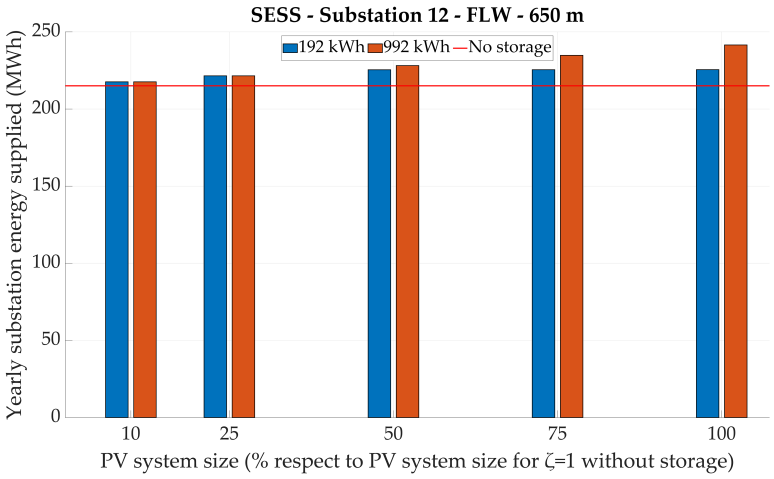

Figure 5.7: Substation 12 yearly energy supplied vs PV system size for *stationary* energy storage system equipped with *flywheels* placed at 650 m.

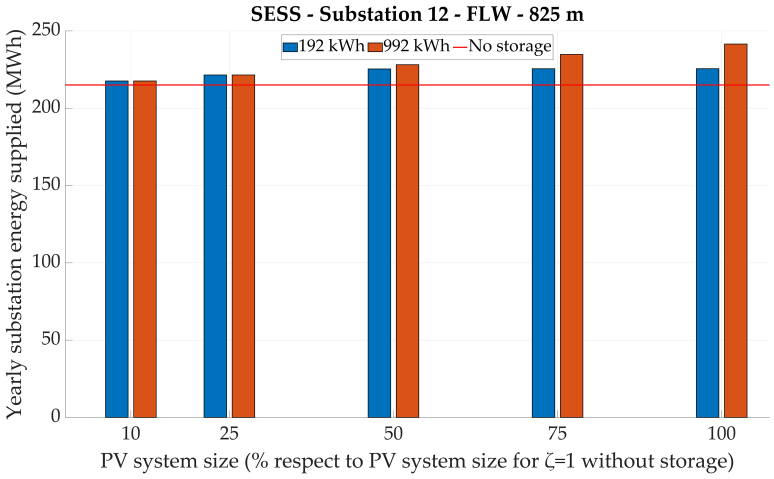

Figure 5.8: Substation 12 yearly energy supplied vs PV system size for *stationary* energy storage system equipped with *flywheels* placed at 825 m.

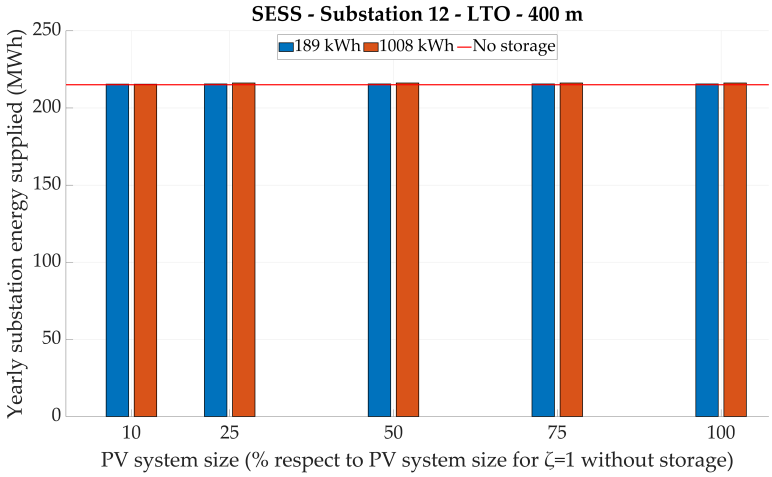

Figure 5.9: Substation 12 yearly energy supplied vs PV system size for *stationary* energy storage system equipped with *lithium-titanate oxide* (LTO) batteries placed at 400 m.

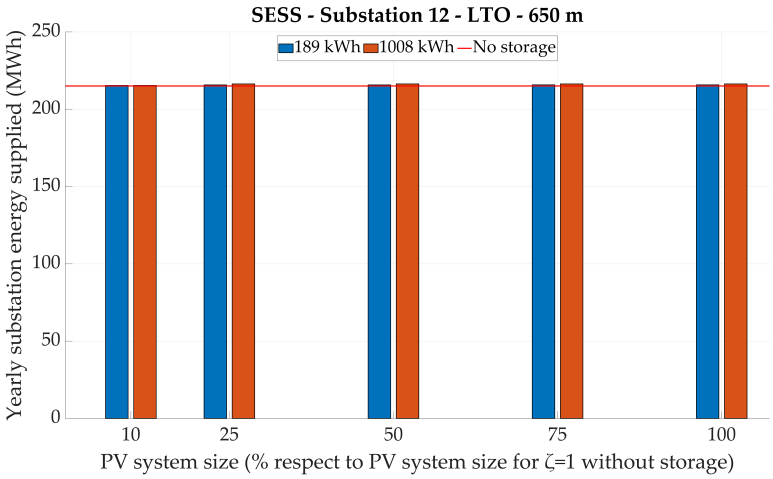

Figure 5.10: Substation 12 yearly energy supplied vs PV system size for *stationary* energy storage system equipped with *lithium-titanate oxide* (LTO) batteries placed at 650 m.

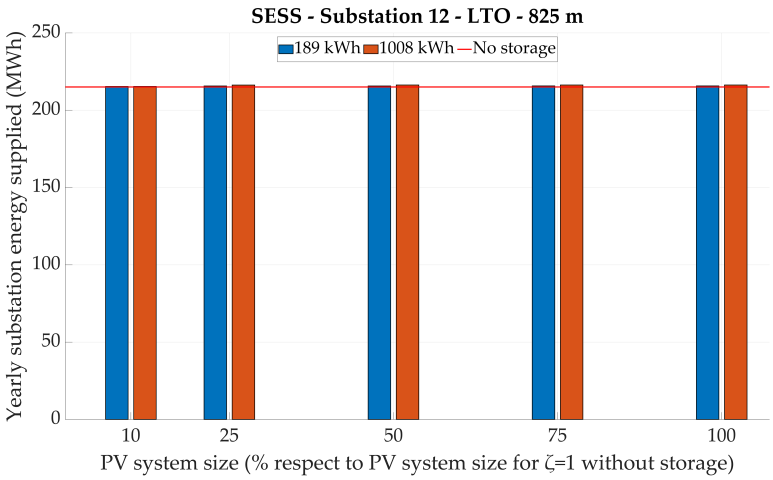

Figure 5.11: Substation 12 yearly energy supplied vs PV system size for *stationary* energy storage system equipped with *lithium-titanate oxide* (LTO) batteries placed at 825 m.

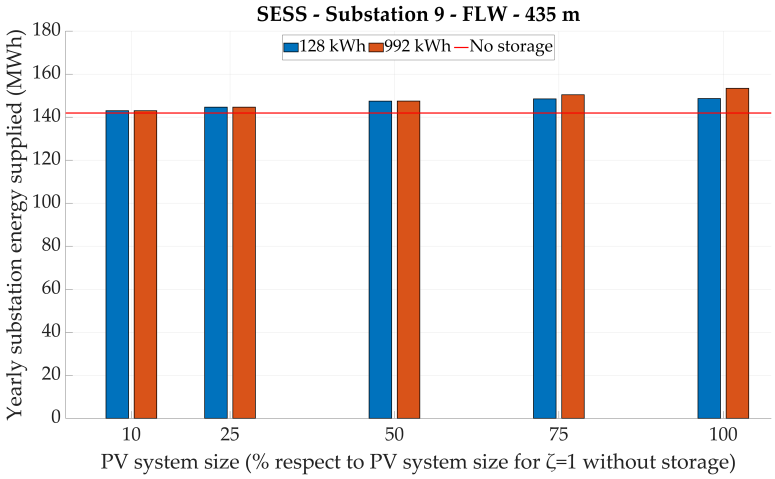

Figure 5.12: Substation 9 yearly energy supplied vs PV system size for *stationary* energy storage system equipped with *flywheels* placed at 435 m.

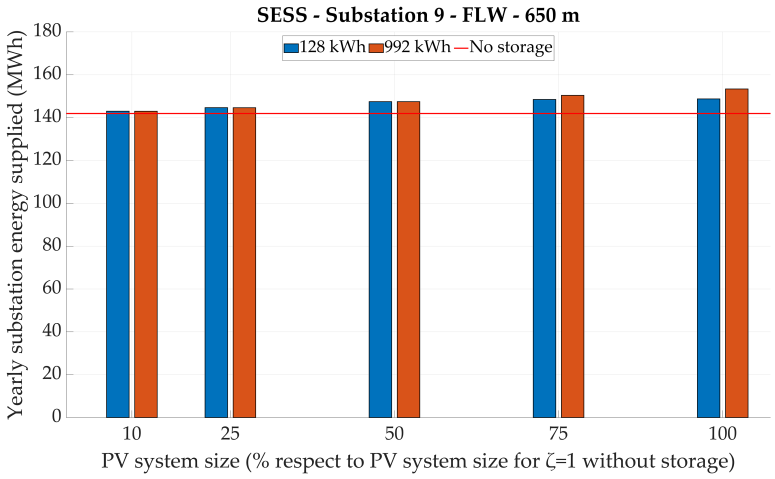

Figure 5.13: Substation 9 yearly energy supplied vs PV system size for *stationary* energy storage system equipped with *flywheels* placed at 650 m.

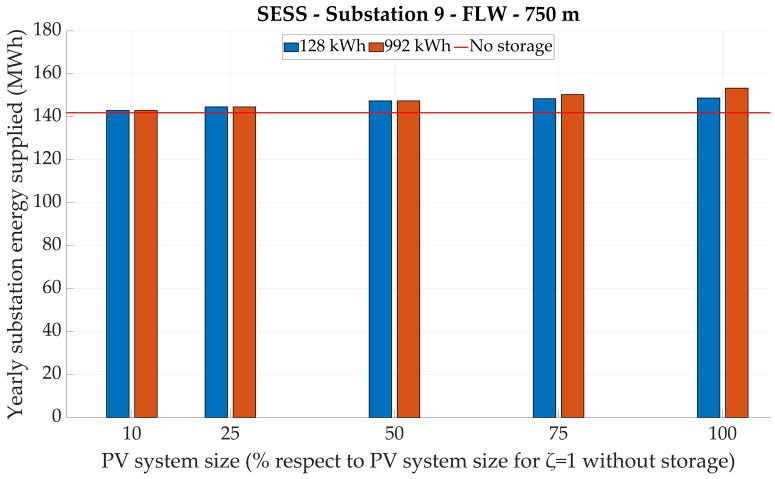

Figure 5.14: Substation 9 yearly energy supplied vs PV system size for *stationary* energy storage system equipped with *flywheels* placed at 750 m.

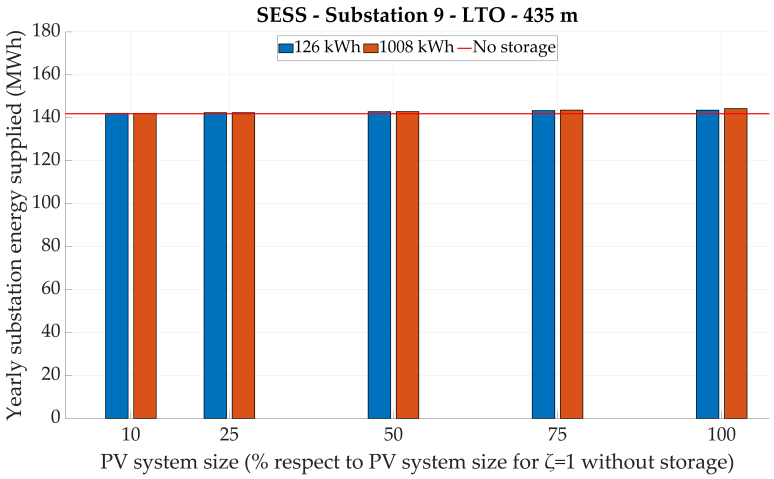

Figure 5.15: Substation 9 yearly energy supplied vs PV system size for *stationary* energy storage system equipped with *lithium-titanate oxide* (LTO) batteries placed at 435 m.

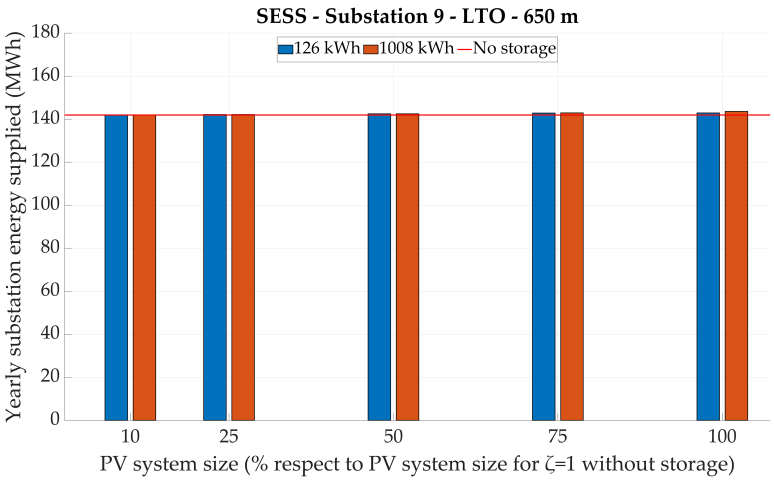

Figure 5.16: Substation 9 yearly energy supplied vs PV system size for *stationary* energy storage system equipped with *lithium-titanate oxide* (LTO) batteries placed at 650 m.

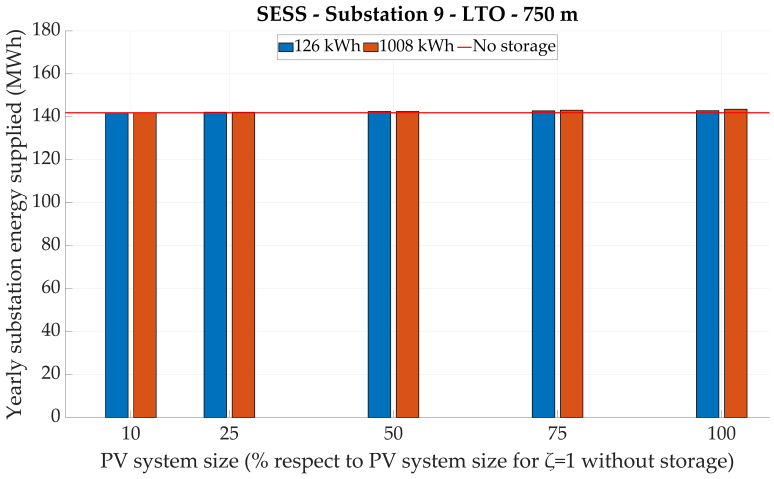

Figure 5.17: Substation 9 yearly energy supplied vs PV system size for *stationary* energy storage system equipped with *lithium-titanate oxide* (LTO) batteries placed at 750 m.

5.2 VOLTAGE DROPS

Besides the impact of the *on-board* and *stationary* storage systems on the yearly electric energy consumption, a key role to the *multifunctionality* of the trolleybus grid has their impact on the voltage drops. Thus, is interesting to observe what is the effect on those, and if it possibly can render the trolleybus grid more ready for a transition to the "*trolleybus grid of the future*". In order to have a reference regarding the voltage drops occurred in the trolleybus grid without the use of any energy storage system, in figure 5.18 and figure 5.19 is illustrated the minimum voltage per simulation instance on section 23 and 25 respectively, for a whole year without the implementation of any energy storage system.

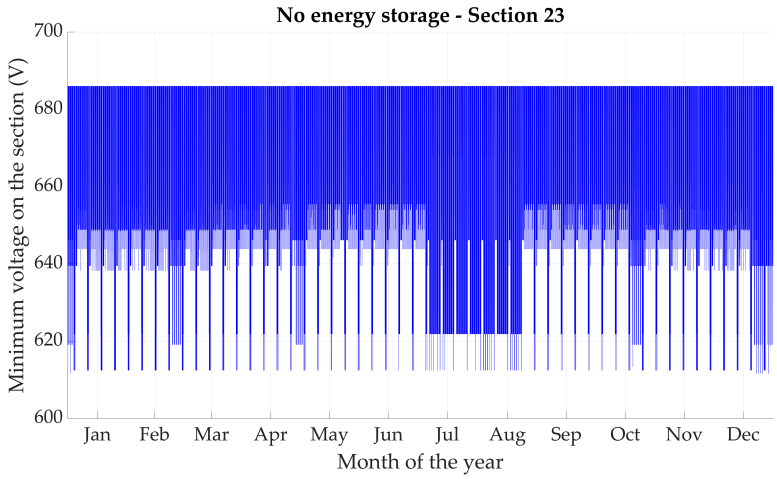

Figure 5.18: Section 23 minimum voltage per simulation instance for a whole year for no energy storage system implemented.

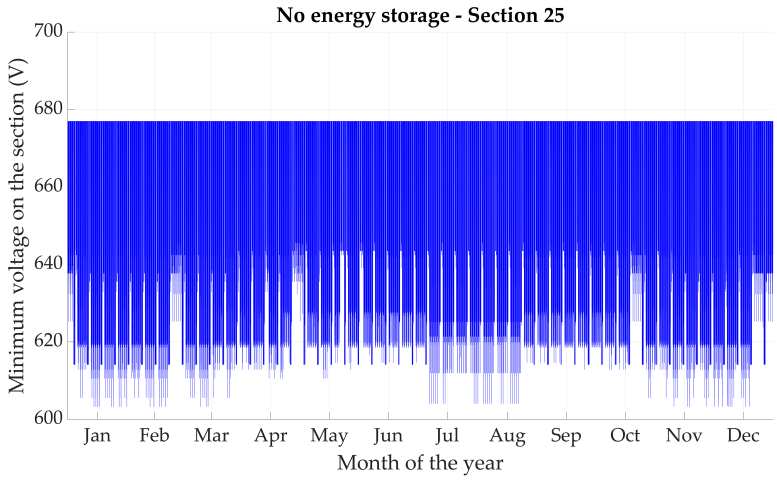

Figure 5.19: Section 25 minimum voltage per simulation instance for a whole year for no energy storage system implemented.

As observed in figure 5.18 and figure 5.19, the two sections which are provided with electric power by substation 12 and substation 9 respectively, express a different behaviour regarding the voltage drops occurred. This is due to the different traffic intensity that they encounter as well as the different physical characteristics found in each one of them. The most important physical characteristics usually are their length and the number of trolleybus stops in them. More specifically, section 23 is considered a low traffic section which generally could be interpreted as an indicator that the voltage drops are not so severe compared to section 25 which is considered

a high traffic section. This is because the lower the traffic is, the less times the trolleybuses are likely to need to stop and start again, thus needing more power that cause the spikes of voltage drops. This is observed in the graphs too, where the overall voltage drops for section 25 (figure 5.19) are more severe compared to the ones for section 23 (figure 5.18).

5.2.1 *On-board* energy storage systems

In figure 5.20 until figure 5.31 are presented the graphs of the minimum voltage on the section per simulation instance for the whole the year for *on-board* energy storage systems equipped with *supercapacitors* (SC) with upper electric power threshold of 80 kW and 100 kW, for various capacities for section 23 and section 25. The reason that are presented the voltage drops for specific scenarios only is because those graphs serve as an indication of the effect of *on-board* energy storage systems to the voltage drops of the trolleybus grid, but only for the cases that seem to be more promising for increasing the PV system utilization. Thus, are selected *on-board* energy storage systems equipped with *supercapacitors* (SC) and only with an upper electric power threshold of 80 kW or 100 kW, as those seem to provide the best balance between the electric energy to be stored and to be used in a yearly basis.

For both sections, and for all capacities (figure 5.20 until figure 5.31), is observed a larger overall reduction in voltage drops for the case of an upper electric power threshold of 100 kW. This is because, as already described many times, an upper electric power threshold of 100 kW is found to provide a better balance between electric energy to be used and electric energy to be stored, which is available via regenerative braking, in a yearly basis. Thus, the *on-board* energy storage system is more likely to never be completely empty or full, and more likely to be able to provide electric energy or to have the capacity to store it respectively. Although an upper electric power threshold of 80 kW also provides a benefit in reducing voltage drops, especially for sections of low traffic, the benefit is not as noticeable compared to an upper electric threshold of 100 kW. Furthermore, when comparing the various capacities, is obvious that *on-board* energy storage systems equipped with *supercapacitors* (SC) of larger capacities tend to provide better reduction in voltage drops. This is because, as before, a larger capacity means that the *on-board* energy storage system is less likely to be completely empty or full, thus being able more times to help with the voltage drops by providing power. Also, it is important to mention that for both sections the voltage without any energy storage implemented never goes below 600 V. This already is a very good start regarding the voltage drops. For all cases and for both sections, an upper electric power threshold of 100 kW in combination with a capacity of *supercapacitors* (SC) of 2.968 kWh is found to be more ideal in reducing the voltage drops. This provides already good results and increasing the capacity to 4.452 kWh does offer a linear scale increase in the benefits of reducing the voltage drops. Thus, for an *on-board* energy storage system equipped with *supercapacitors* SC of a capacity of 2.968 kWh and an upper electric power threshold of 100 kW, the overall reduction in voltage drops is around 20 V to 40 V for section 23 and 10 V to 20 V for section 25. It should be mentioned that this reduction is more profound to some periods of the year than others - i.e. during summer months. This has to do with the state of charge (SoC) trend of each *on-board* energy storage system in each trolleybus and if it has electric energy available to provide at the peaks of electric power demands. It is expected that *on-board* energy storage systems equipped with *lithium-titanate oxide* (LTO) batteries do not provide descent results in regard to reducing the overall voltage drops. This is due to their reduced capabilities in accepting and providing high values of electric power at any given time, as described in section 3.3. For this reason, they are not analyzed in this section of this work.

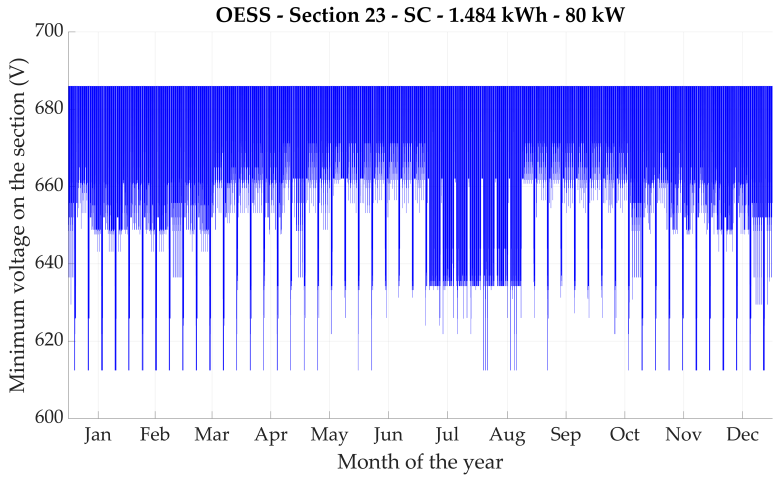

Figure 5.20: Section 23 minimum voltage per simulation instance for a whole year for *on-board* energy storage system equipped with *supercapacitors* (SC) of 1.484 kWh and an upper electric power threshold of 80 kW.

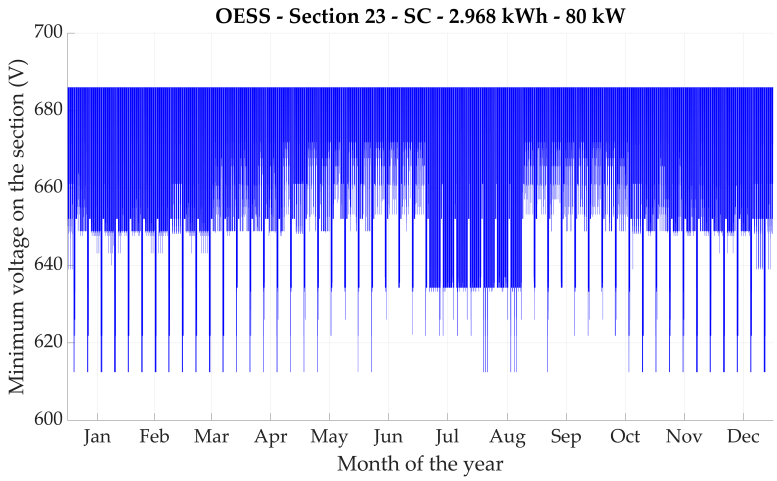

Figure 5.21: Section 23 minimum voltage for per simulation instance a whole year for *on-board* energy storage system equipped with *supercapacitors* (SC) of 2.968 kWh and an upper electric power threshold of 80 kW.

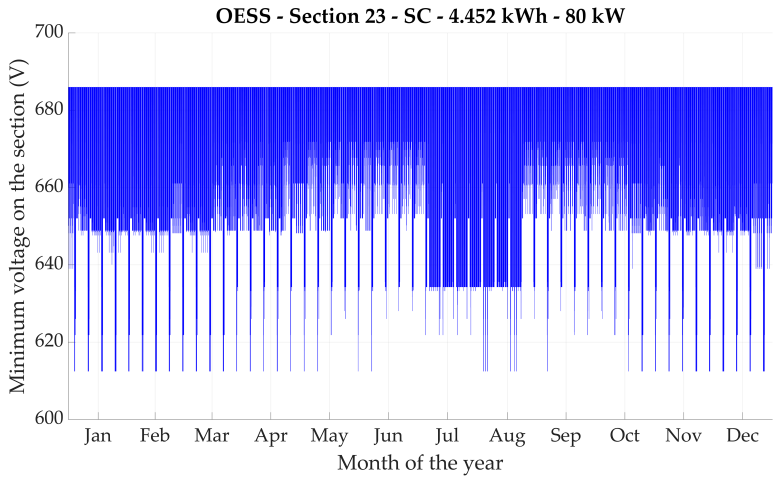

Figure 5.22: Section 23 minimum voltage per simulation instance for a whole year for *on-board* energy storage system equipped with *supercapacitors* (SC) of 4.452 kWh and an upper electric power threshold of 80 kW.

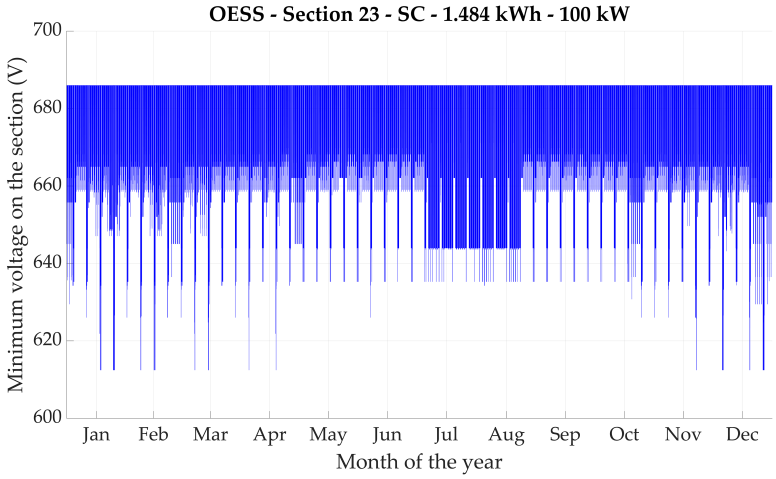

Figure 5.23: Section 23 minimum voltage per simulation instance for a whole year for *on-board* energy storage system equipped with *supercapacitors* (SC) of 1.484 kWh and an upper electric power threshold of 100 kW.

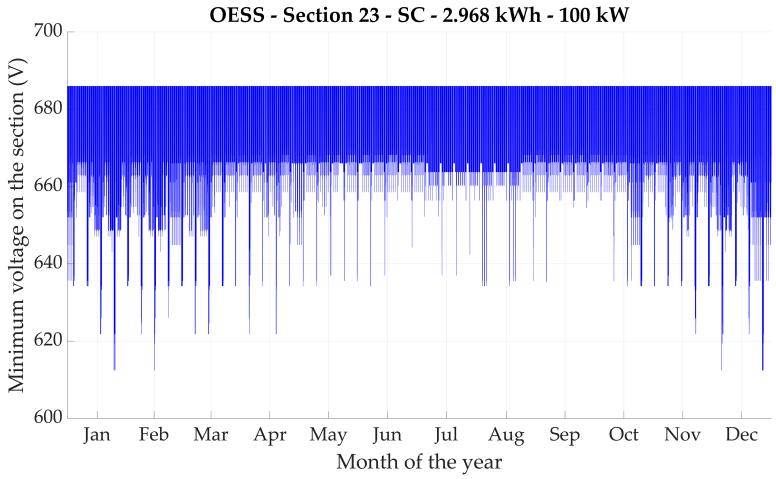

Figure 5.24: Section 23 minimum voltage for a whole year for *on-board* energy storage system equipped with *supercapacitors* (SC) of 2.968 kWh and an upper electric power threshold of 100 kW.

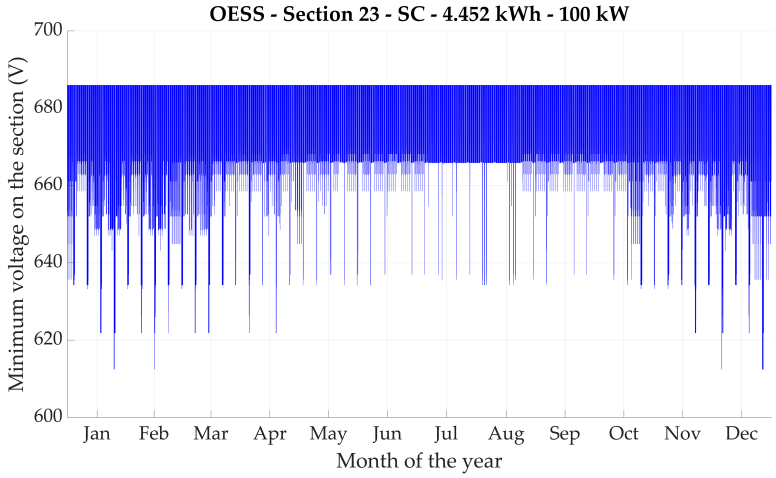

Figure 5.25: Section 23 minimum voltage per simulation instance for a whole year for *on-board* energy storage system equipped with *supercapacitors* (SC) of 4.452 kWh and an upper electric power threshold of 100 kW.

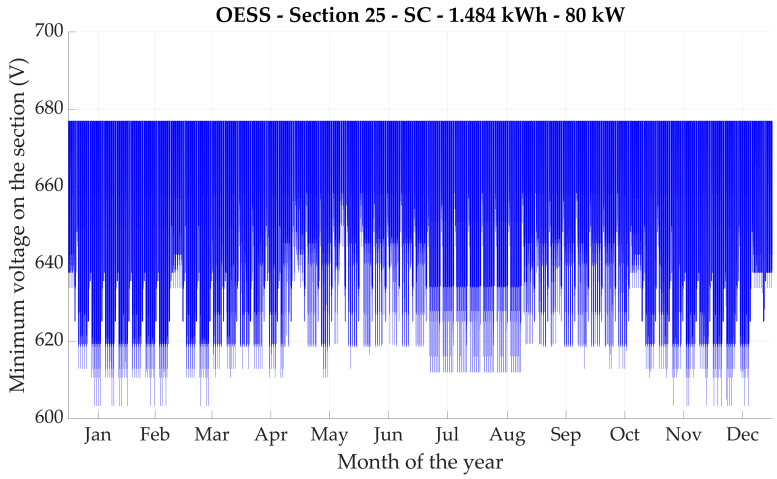

Figure 5.26: Section 25 minimum voltage per simulation instance for a whole year for *on-board* energy storage system equipped with *supercapacitors* (SC) of 1.484 kWh and an upper electric power threshold of 80 kW.

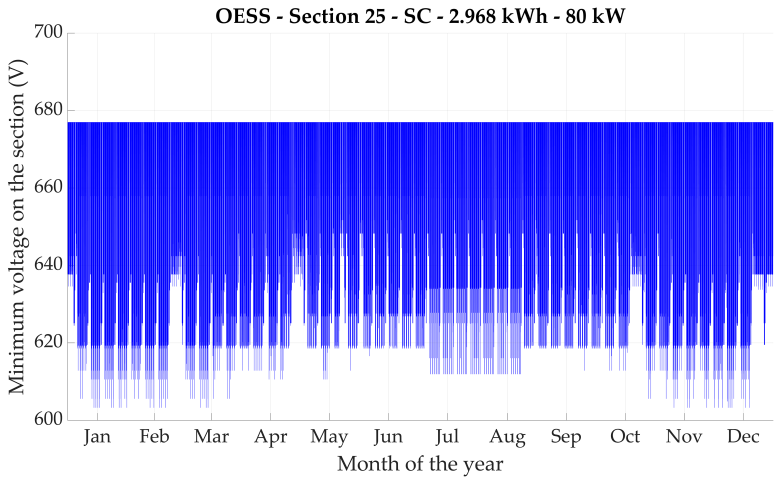

Figure 5.27: Section 25 minimum voltage per simulation instance for a whole year for *on-board* energy storage system equipped with *supercapacitors* (SC) of 2.968 kWh and an upper electric power threshold of 80 kW.

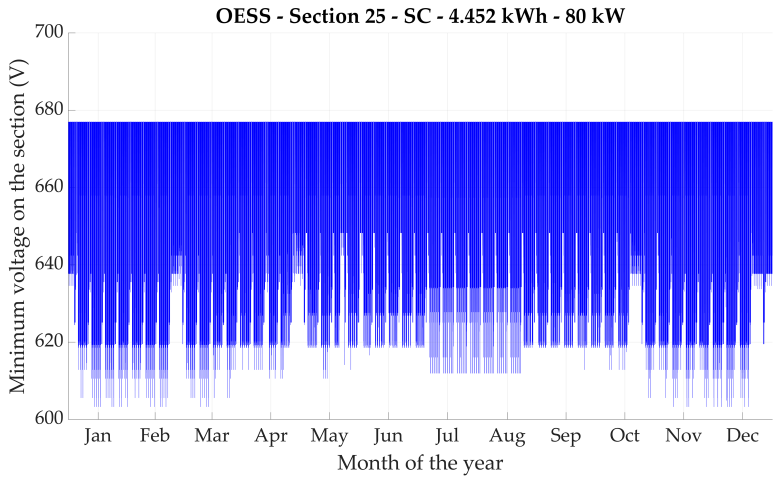

Figure 5.28: Section 25 minimum voltage per simulation instance for a whole year for *on-board* energy storage system equipped with *supercapacitors* (SC) of 4.452 kWh and an upper electric power threshold of 80 kW.

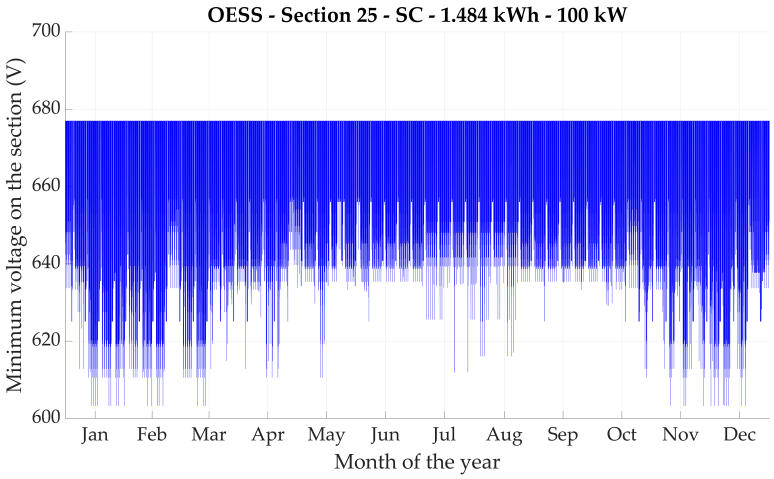

Figure 5.29: Section 25 minimum voltage per simulation instance for a whole year for *on-board* energy storage system equipped with *supercapacitors* (SC) of 1.484 kWh and an upper electric power threshold of 100 kW.

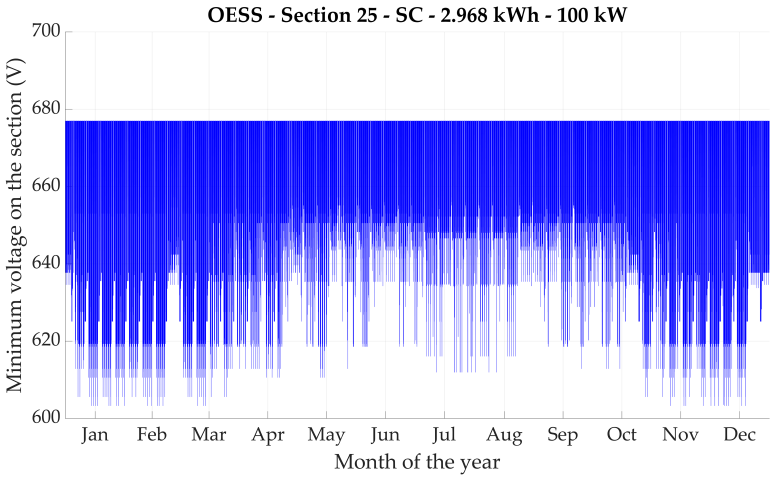

Figure 5.30: Section 25 minimum voltage per simulation instance for a whole year for *on-board* energy storage system equipped with *supercapacitors* (SC) of 2.968 kWh and an upper electric power threshold of 100 kW.

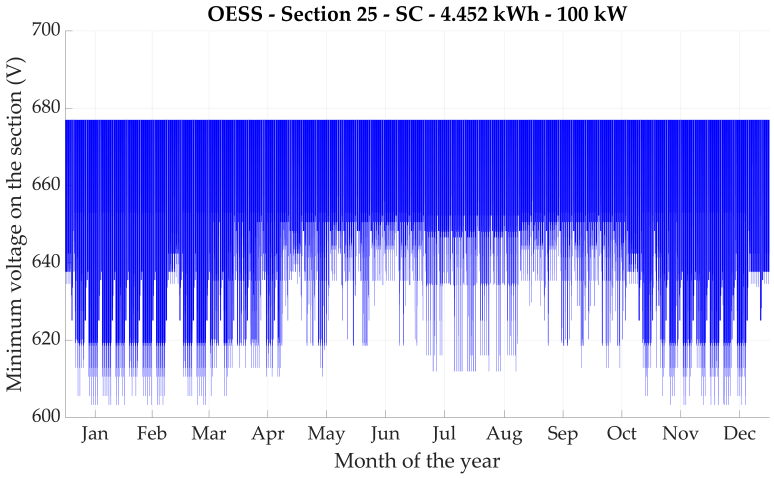

Figure 5.31: Section 25 minimum voltage per simulation instance for a whole year for *on-board* energy storage system equipped with *supercapacitors* (SC) of 4.452 kWh and an upper electric power threshold of 100 kW.

5.2.2 *Stationary* energy storage systems

In figure 5.32 until figure 5.43 are presented the graphs of the minimum voltage on the section per simulation instance for the whole the year for *stationary* energy storage systems equipped with *lithium-titanate oxide* (LTO) batteries for various capacities, for PV system sizes of 50% to 100%, for section 23 and section 25 and placed at 825 m and 750 m respectively. The reason that only these specific scenarios are presented is same as *on-board* energy storage systems; those graphs serve as an indication of the impact of *stationary* energy storage systems to the voltage drops of the trolleybus grid but only for the cases that seem to be more promising for the PV system utilization. Thus, are selected *stationary* energy storage systems equipped with *lithium-titanate oxide* (LTO) batteries, placed at a position further away from the electric power feeding point and only with PV system sizes of 50% to 100%.

Regarding section 23 (figure 5.32 to figure 5.37), which is considered a section with low traffic, is observed the same overall effect on the voltage drops throughout the year for all cases. More specifically, for all cases is observed an overall reduction in the voltage drops of around 10 V but with a note. The reduction of the voltage drops is not observed at the peaks, but in the overall "dense" parts of the graph of the voltage drops. More specifically, the *stationary* energy storage system, with this specific control strategy, provides an increase in the density of the voltage drops while reducing their magnitude. Nevertheless the majority of the peaks are still present. This has to do with the control strategy used and how aggressive the discharging scheme is. As described in section 3.5, the control strategy for the *stationary* energy storage system used in this work does not let it to discharge when there is dense traffic and electric power available from the PV system, in order not to take any risks and possibly decrease the PV system utilization. Thus, although throughout the year there is an overall reduction of the magnitude of the voltage drops, the majority of the peaks still exist. Those are peaks that exist when there is dense traffic on the section while there is also electric power generated by the PV system. Also, is interesting to note that for some cases there are observed some minor increases in the voltage drop peaks. This is more profound for the cases of larger PV system sizes and especially for sections with low traffic. This is because the charging scheme of the control strategy aims to charge the *stationary* energy storage system with as much as possible electric energy provided by the PV system, when there is no traffic or when there is idling traffic. Nevertheless, there may be occasions where the charging scheme may not be 100% accurate when selecting the electric power to charge with. As a result, this leads to occasions where it may demand more electric power or demand electric power in time instances where it should not. This cause the voltage to drop even further for a very short period of time, which is usually a couple of seconds. Nevertheless, these occasions are very rare throughout the year and they usually have a magnitude of 2 V to 3 V.

Regarding section 25 (figure 5.38 to figure 5.43), which is considered a section with high traffic, again is is observed the same overall effect on the voltage drops throughout the year for all cases, as already described for section 23. Nevertheless, in this case the reduction in the voltage drops compared to the case without any energy storage implemented is more profound at the peaks. It is clearly observed that especially for larger PV system sizes the reduction in the voltage drops is around 10 V, which is a considerable decrease of the voltage drops.

For all cases of *stationary* energy storage systems is observed that their impact on the voltage drops can be favorable for reducing them but is highly connected to their control strategy. Thus, it would not be fair to directly compare them with *on-board* energy storage systems without keeping that in mind, and without trying different controls strategies, more optimized for achieving that.

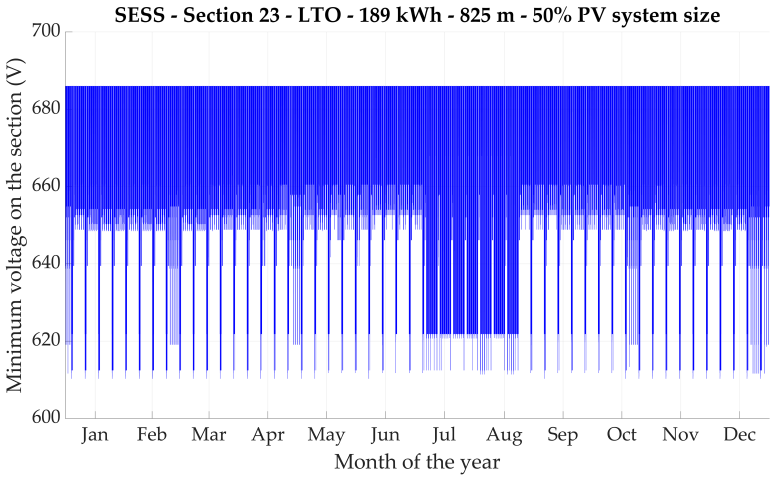

Figure 5.32: Section 23 minimum voltage per simulation instance for a whole year for *stationary* energy storage system equipped with *lithium-titanate oxide* (LTO) batteries of 189 kWh placed at 825 m and an PV system size of 50%.

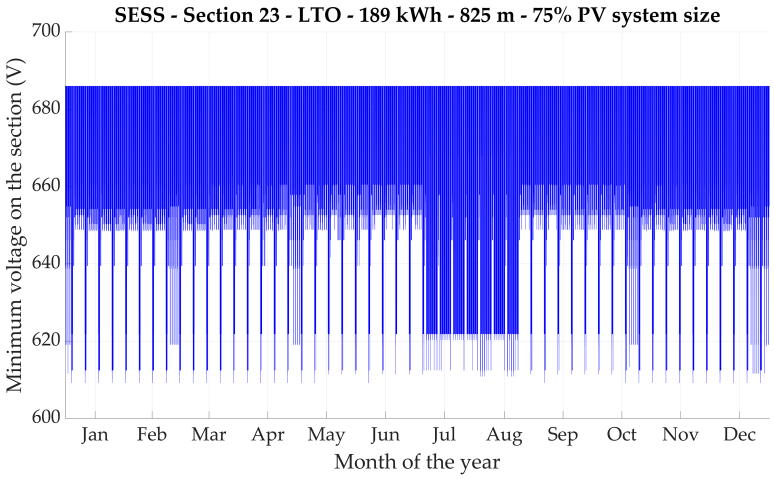

Figure 5.33: Section 23 minimum voltage per simulation instance for a whole year for *stationary* energy storage system equipped with *lithium-titanate oxide* (LTO) batteries of 189 kWh placed at 825 m and an PV system size of 75%.

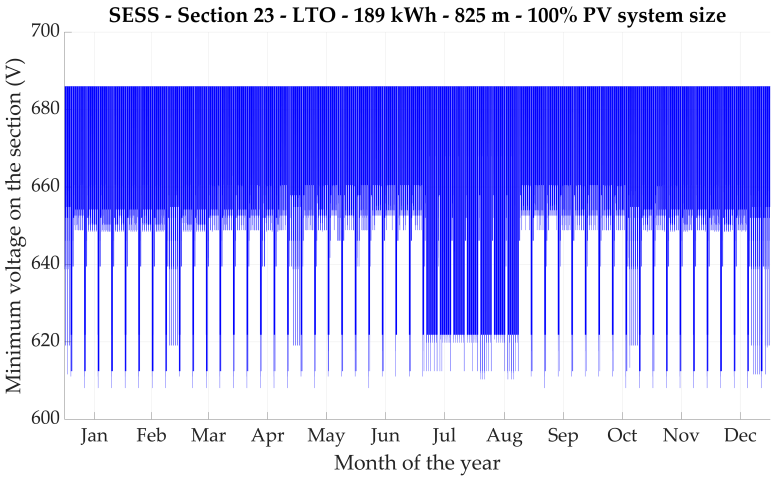

Figure 5.34: Section 23 minimum voltage per simulation instance for a whole year for *stationary* energy storage system equipped with *lithium-titanate oxide* (LTO) batteries of 189 kWh placed at 825 m and an PV system size of 100%.

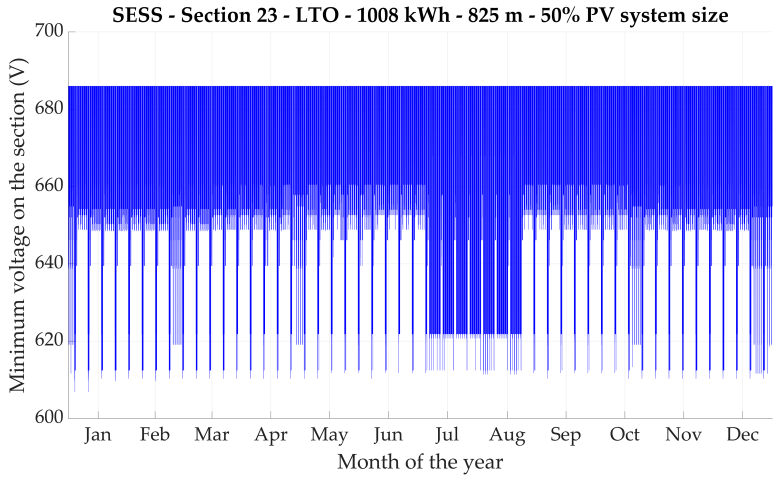

Figure 5.35: Section 23 minimum voltage per simulation instance for a whole year for *stationary* energy storage system equipped with *lithium-titanate oxide* (LTO) batteries of 1008 kWh placed at 825 m and an PV system size of 50%.

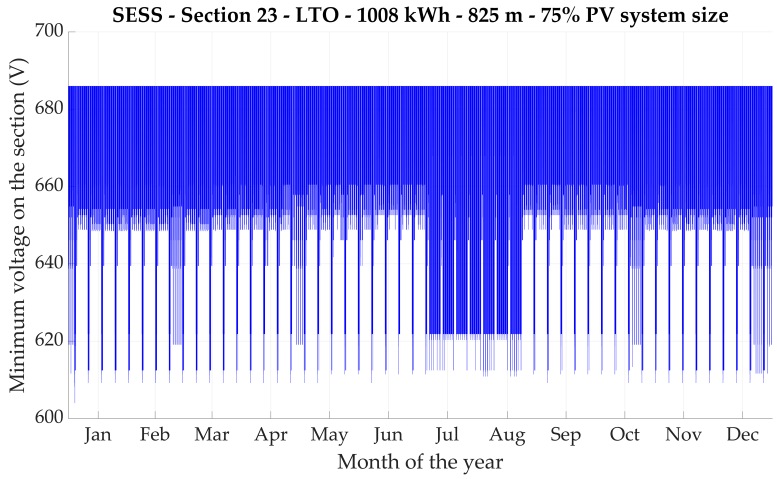

Figure 5.36: Section 23 minimum voltage per simulation instance for a whole year for *stationary* energy storage system equipped with *lithium-titanate oxide* (LTO) batteries of 1008 kWh placed at 825 m and an PV system size of 75%.

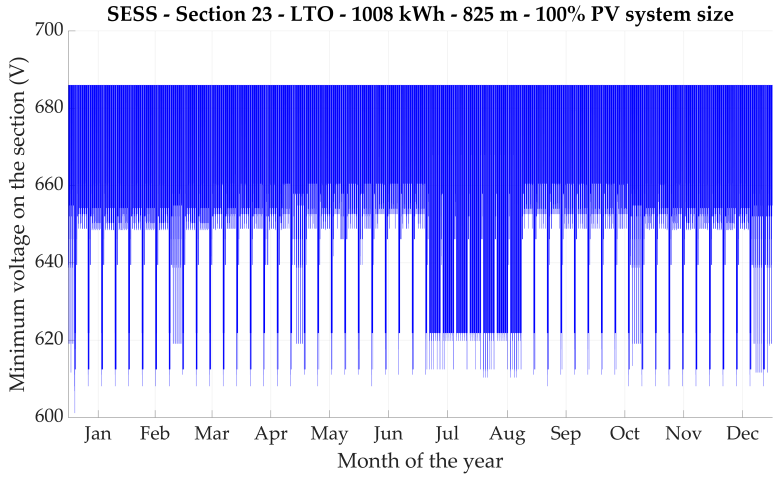

Figure 5.37: Section 23 minimum voltage per simulation instance for a whole year for *stationary* energy storage system equipped with *lithium-titanate oxide* (LTO) batteries of 1008 kWh placed at 825 m and an PV system size of 100%.

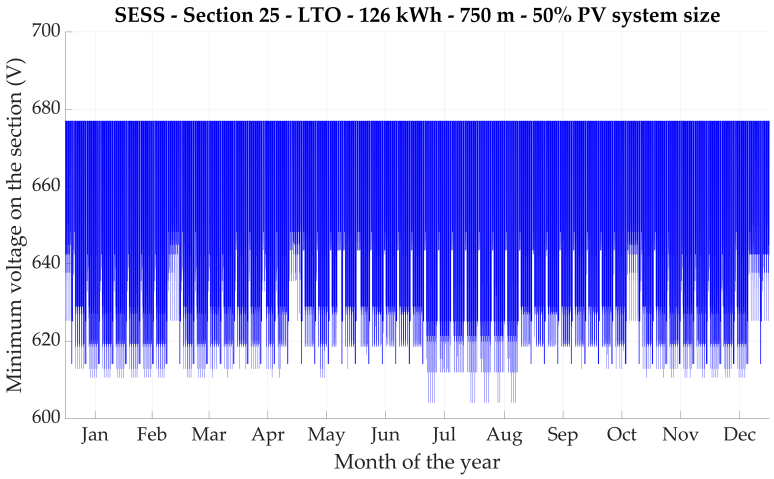

Figure 5.38: Section 25 minimum voltage per simulation instance for a whole year for *stationary* energy storage system equipped with *lithium-titanate oxide* (LTO) batteries of 126 kWh placed at 750 m and an PV system size of 50%.

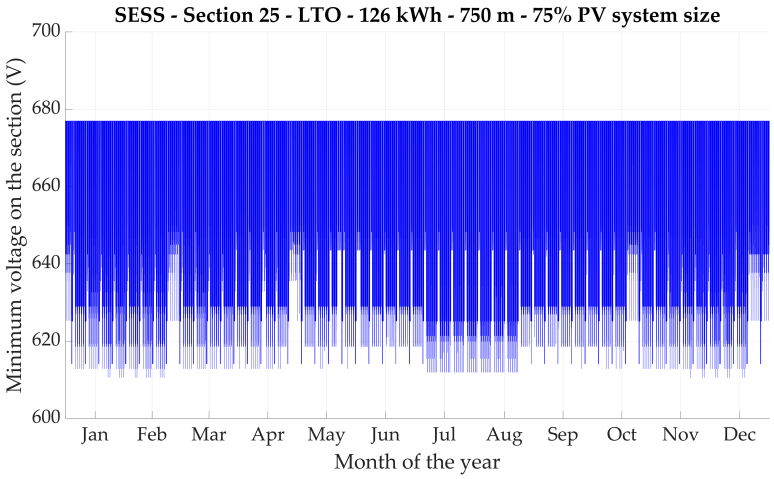

Figure 5.39: Section 25 minimum voltage per simulation instance for a whole year for *stationary* energy storage system equipped with *lithium-titanate oxide* (LTO) batteries of 126 kWh placed at 750 m and an PV system size of 75%.

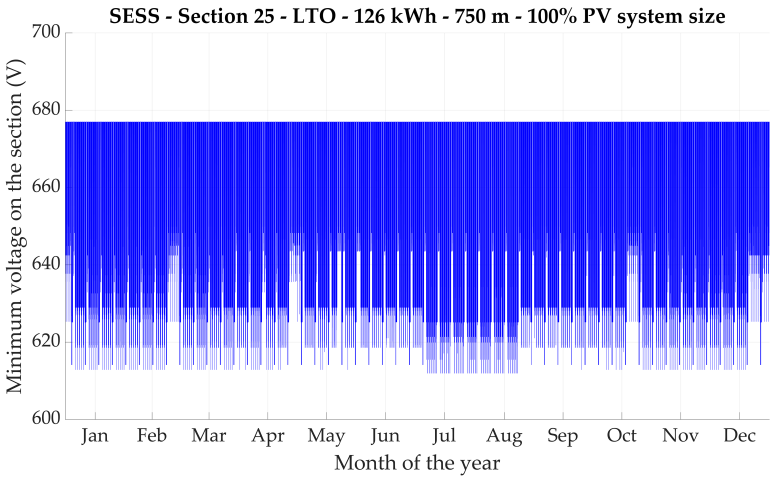

Figure 5.40: Section 25 minimum voltage per simulation instance for a whole year for *stationary* energy storage system equipped with *lithium-titanate oxide* (LTO) batteries of 126 kWh placed at 750 m and an PV system size of 100%.

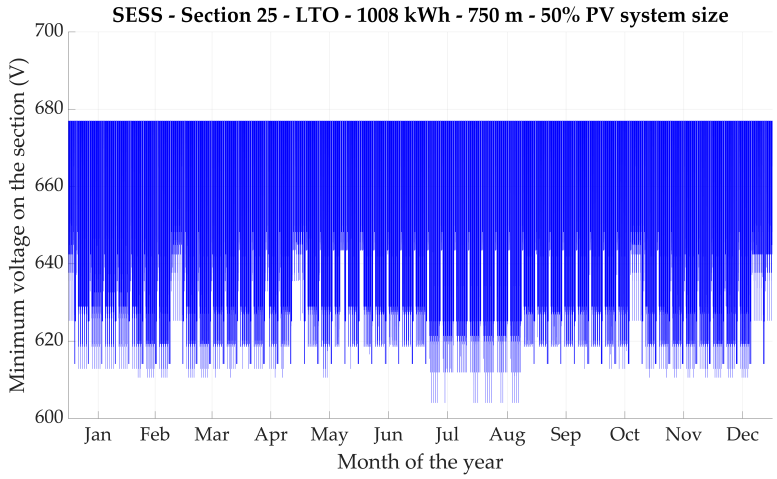

Figure 5.41: Section 25 minimum voltage per simulation instance for a whole year for *stationary* energy storage system equipped with *lithium-titanate oxide* (LTO) batteries of 1008 kWh placed at 750 m and an PV system size of 50%.

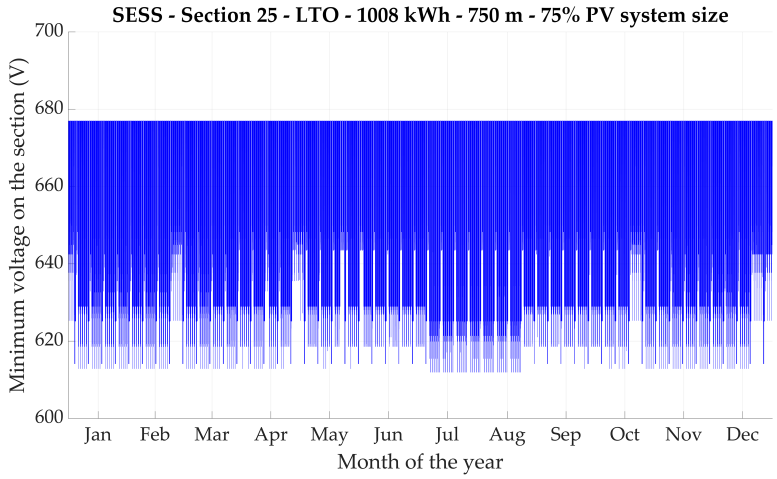

Figure 5.42: Section 25 minimum voltage per simulation instance for a whole year for *stationary* energy storage system equipped with *lithium-titanate oxide* (LTO) batteries of 1008 kWh placed at 750 m and an PV system size of 75%.

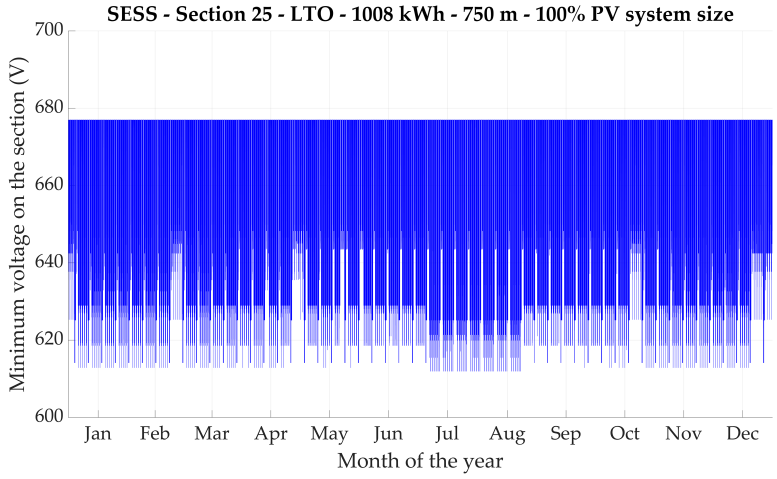

Figure 5.43: Section 25 minimum voltage per simulation instance for a whole year for *stationary* energy storage system equipped with *lithium-titanate oxide* (LTO) batteries of 1008 kWh placed at 750 m and an PV system size of 100%.

5.3 CONCLUSIONS

In this chapter have been presented the results from the simulations of this work regarding the impact of *on-board* and *stationary* energy storage systems on the *multifunctionality* of the trolleybus grid. First were presented the results regarding the impact of the *on-board* and the *stationary* energy storage systems on the yearly electric energy consumption of the trolleybus grid, and after that were analyzed the results regarding their impact on the voltage drops occurred in the trolleybus grid.

On-board energy storage systems equipped with *supercapacitors* (SC), even of small capacities, are a great choice to be used for reducing the total yearly electric energy consumed in a trolleybus grid, providing a positive impact its *multifunctionality* while at the same time increasing, even briefly, for some cases the PV system utilization. On the other hand, *on-board* energy storage systems equipped with *lithium-titanate oxide* (LTO) batteries, although they provide also a reduction in the yearly electric energy consumed, they perform overall worse compared to the ones equipped with *supercapacitors* (SC). Regarding their impact on the voltage drops, *on-board* energy storage systems equipped with *supercapacitors* (SC) are considered to provide much more benefit in mitigating the voltage drops in the trolleybus grid compared to the ones equipped with *lithium-titanate oxide* (LTO) batteries, for both low and high traffic substations. From the simulations, for an *on-board* energy storage system equipped with *supercapacitors* SC of a capacity of 2.968 kWh and an upper electric power threshold of 100 kW, the overall magnitude reduction in voltage drops is around 20 V to 40 V for section 23 and 10 V to 20 V for section 25, compared to the case without any energy storage system implemented. Capacities larger than that do not provide a linear increasing in benefit of mitigating voltage drops.

On the other hand, *stationary* energy storage systems equipped with *flywheels* of any size produce overall worse results regarding the yearly electric energy consumed in the trolleybus grid, compared to ones equipped with *lithium-titanate oxide* (LTO). Although the increased yearly electric energy consumed is mainly considered to be *green*, provided by the PV system, their high self-discharge means that this stored electric energy is lost in the form of heat. The same is not observed for the case of *stationary* energy storage systems equipped with *lithium-titanate oxide* (LTO) batteries, where the total yearly electric energy consumed remains almost the same with the case of no energy storage implemented. Regarding their impact on the voltage drops, *stationary* energy storage systems equipped with *lithium-titanate oxide* (LTO) batteries are considered to provide much more benefit in reducing voltage drops in the trolleybus grid compared to the ones equipped with *flywheels*. From the simulations is concluded that the impact of *stationary* energy storage systems, on any parameter of the trolleybus grid, is deeply interconnected with their control strategy. Thus, for the specific one used in this work, regarding the reduction of voltage drops, is found in general to be more beneficial to be used on sections of high traffic, and PV system sizes of 75% to 100%.

In the next chapter (chapter 6) are presented the conclusions from this work regarding both *on-board* and *stationary* energy storage systems. Also, are presented recommendations for improvements and further research, that could possibly help provide better results for the scope of this work.

6 CONCLUSIONS AND RECOMMENDATIONS

In this chapter are presented the conclusions of this work regarding the impact of on-board and stationary energy storage systems on the PV system utilization and the multifunctionality of the trolleybus grid. Also, recommendations for improvements and further research are presented, that could possibly help provide better results for the scope of this work.

6.1 CONCLUSIONS

The conclusions from the results of this work are divided into three subsections. First are presented the conclusions regarding *on-board* energy storage systems, then are presented the conclusions regarding *stationary* energy storage systems, and afterwards are presented general conclusions regarding both types of energy storage systems. Before proceeding to the conclusions, it is rather important to remember the research questions that this work is based on. The research questions were presented in section 1.3, in table 1.1.

The research questions are:

1. Which energy storage systems (*on-board* or *stationary*) are most favorable for a PV-powered multifunctional trolleybus grid for increasing the PV system utilization and improving its multifunctionality?
2. Which energy storage systems technology in terms of their characteristics (capacity, self-discharge etc.) is preferable for a PV-powered multifunctional trolleybus grid?
3. What effect do these energy storage systems have on the PV system utilization, the yearly electric energy consumption, and the voltage drops on the trolleybus grid?
4. Which of energy storage systems' variables (capacity, placement position etc.) have a greater effect on each trolleybus grid parameter (PV system utilization, yearly electric energy consumption, voltage drops)?

6.1.1 *On-board* energy storage systems

The following conclusions provide answers to research questions 2, 3, and 4.

• Larger **capacities** of *on-board* energy storage systems equipped with *supercapacitors* (SC) do not provide a significant change in results between each other, both for high traffic and low traffic substations. They provide slightly better results for *lithium-titanate oxide* (LTO) batteries mainly due to the higher amount of electric power that they can accept and provide.

• An **upper electric power threshold** of 80 kW - 100 kW provides the best results for PV system utilization for *on-board* energy storage systems equipped with *supercapacitors* (SC) for PV system sizes up to 55% - 65% for low traffic substations and up to 90% for high traffic substations.

• Regarding the **technologies**, *on-board* energy storage systems equipped with *lithium-titanate oxide* (LTO) batteries, especially of small capacities, do not provide adequate results for PV system utilization compared to the ones equipped with *supercapacitors* (SC) for any upper electric power threshold, both low traffic and high traffic substations.

• **Direct load coverage** Λ is increased for all cases with best overall scenarios for *on-board* energy storage systems equipped with *supercapacitors* (SC) with upper electric power threshold of 100 kW, and *on-board* energy storage systems equipped with *lithium-titanate oxide* (LTO) batteries with an upper electric power threshold of 60 kW, independently of the traffic of the substation. A higher direct load coverage Λ means it can be achieved the same PV system utilization with the case with no energy storage implemented while having a smaller PV system.

• The intermittencies of trolleybuses providing electric power to the trolleybus grid due to regenerative braking and of the trolleybuses being able to accept this electric power at any given point are many. Thus, *on-board* energy storage systems equipped with *supercapacitors* (SC) provide a great choice for reducing the overall **yearly electric energy** consumption of the trolleybus grid. The ones equipped with *lithium-titanate oxide* (LTO) batteries still provide a reduction in the total yearly electric energy consumed but not as high as the ones equipped with *supercapacitors* (SC).

• *On-board* energy storage systems equipped with *supercapacitors* (SC) are considered to be more favorable in reducing **voltage drops** in the trolleybus grid compared to the ones equipped with *lithium-titanate oxide* (LTO) batteries. Capacities above 3 kWh do not provide a linear decrease of voltage drops while a more suitable upper electric power threshold is the one of 100 kW.

6.1.2 *Stationary* energy storage systems

The following conclusions provide answers to research questions 2, 3, and 4.

• Larger **capacities** of *stationary* energy storage systems equipped with *flywheels*, using this control strategy, provide a better PV system utilization for substations with high traffic but this is due to their large self-discharge which renders them more times empty and able to accept further electric energy provided by the PV system. Smaller capacities of *stationary* energy storage systems equipped with *flywheels* and *lithium-titanate oxide* (LTO) batteries as well as larger capacities of the latter technology, can get full using this control strategy, thus reaching a plateau in increasing the PV system utilization.

• For most cases and substations and using this control strategy, the further away the **position** of the *stationary* energy storage system is, the higher the PV system utilization may be, as in those positions the severity of the voltage drops is higher thus rendering the *stationary* energy storage system more times empty and available to store electric energy provided by the PV system.

• Regarding the **technologies**, *stationary* energy storage systems equipped with *flywheels*, no matter of the capacity, do not provide preferable results regarding the PV system utilization compared to the ones equipped with *lithium-titanate oxide* (LTO) batteries, using this control strategy. Although it seems that the PV system utilization is increased for all the cases for this technology, in reality all the electric energy is lost in the form of heat due to self-discharge.

• **Direct load coverage** Λ is increased for all cases with best overall scenarios for *sta-*

tionary energy storage systems equipped with *lithium-titanate oxide* (LTO) batteries, irrespectively of their size and positions placed on a high traffic substation, using this control strategy. A higher direct load coverage Λ means it can be achieved the same PV system utilization with the case with no energy storage implemented while having a smaller PV system.

• *Stationary* energy storage systems equipped with *flywheels* of any size, using this control strategy, do not provide promising results regarding their impact on the yearly consumed electric energy mainly due to their high self-discharge. Although the increased **yearly electric energy** consumed is considered to be mainly *green* electric energy provided by the PV system, this is lost in the form of heat due to self-discharge and not given back to the trolleybus grid. On the other hands, the ones equipped with *lithium-titanate oxide* (LTO) batteries manage to keep the yearly electric energy consumption almost the same with the case without any energy storage implemented. This is due to their low self-discharge and their more optimal operation with the specific control strategy.

• *Stationary* energy storage systems equipped with *lithium-titanate oxide* (LTO) batteries are considered to be more favorable in reducing **voltage drops** in the trolleybus grid compared to *stationary* energy storage systems equipped with *flywheels*. It is important to note that it has been concluded that the impact of *stationary* energy storage systems on any parameter on the trolleybus grid is deeply interconnected with the control strategy used. Thus, for the specific control strategy used in this work, is found to provide more benefit regarding the reduction of voltage drops for sections of high traffic and PV system sizes of 75% to 100%.

6.1.3 General

Before proceeding to the general conclusions, it is important to remember that the impact of *stationary* energy storage systems on the PV system utilization and on parameters regarding the trolleybus grid in general is heavily correlated to the control strategy used. As described in section 3.5, for each technology, PV system size, trolleybus grid section, and targeted outcome (improve the PV system utilization or favour parameters related to the *multifunctionality* of the trolleybus grid) there should be a specific control strategy. **Thus, it is safe to conclude that the comparison of *stationary* energy storage systems to other energy storage systems cannot be straightforward**.

The following conclusions provide answers to research question 1.

• Generally, *on-board* energy storage systems can perform better on parameters regarding the *multifunctionality* of the trolleybus grid such as the total yearly electric energy consumption and the mitigation of the severity of the voltage drops. On the other hand *stationary* energy storage systems can perform well on a wide range of parameters according to their control strategy. For the one used in this work, they perform better on parameters regarding the PV system utilization, managing to have a positive impact on those. For all cases, not matter the technologies and the various parameters, is observed that the direct load coverage Λ is increased.

6.2 RECOMMENDATIONS FOR FURTHER RESEARCH

Getting close to the end of this thesis work, after overviewing all the results, it is interesting to propose recommendations for improvements and for further research. Those have as an main target to possibly provide higher quality of results and an

extension of this work to a larger set of possible solutions. More specifically, the recommendations are divided into two basic categories; those related to *on-board* energy storage systems, and those related to *stationary* energy storage systems.

• Recommendations regarding *on-board* energy storage systems
It would be interesting to see the effect of hybrid energy storage systems using two different technologies, such as *lithium-ion* (Li-ion) batteries with *supercapacitors* (SC) or *flywheels* with *supercapacitors*. This could provide interesting results by using the benefits of two different energy storage technologies. Also, it would be engrossing to observe the behavior of such systems when used with an energy system model that has response times (ramp-up and ramp-down times) implemented in it. This could provide more realistic results and provide information of how important the use of such parameters really is.

• Recommendations regarding *stationary* energy storage systems
As already mentioned multiple times in this work, the control strategy of the *stationary* energy storage system has a key role to its behavior and thus its impact to either the PV system utilization or the *multifunctionality* of the trolleybus grid. It would be intriguing to observe the behavior of such energy storage systems when used with different controls strategies Those could be ones more focused on mitigating the voltage drops, or ones achieving the best of both worlds, by increasing the PV system utilization and reducing the voltage drops. In conjunction to that, it would be interesting to observe how a control strategy that uses a telemetry technology, wired or wireless, impacts on those parameters and if it is actually beneficial to be used instead of a control strategy based on voltage control. Finally, in this case too like *on-board* energy storage systems, it would be interesting to see how hybrid energy storage systems would behave, as well as if response times (ramp-up and ramp-down times) could have a measurable impact on the results.

BIBLIOGRAPHY

[1] J. Olivier and J. Peters, "Trends in global co2 and total greenhouse gas emissions," *PBL Netherlands Environmental Assessment Agency: The Hague, The Netherlands*, 2020.

[2] I. Diab, A. Saffirio, G. R. C. Mouli, A. S. Tomar, and P. Bauer, "A complete dc trolleybus grid model with bilateral connections, feeder cables, and bus auxiliaries," *IEEE Transactions on Intelligent Transportation Systems*, 2022.

[3] I. Diab, B. Scheurwater, A. Saffirio, G. R. Chandra-Mouli, and P. Bauer, "Placement and sizing of solar pv and wind systems in trolleybus grids," *Journal of Cleaner Production*, vol. 352, p. 131533, 2022.

[4] "Maxwell® technologies: New 48v module (cob)," https://maxwell.com/wp-content/uploads/2022/02/3001491-EN.7_48V-165F-CoB-Datasheet_20220216.pdf, accessed: 2022-05-23.

[5] "Maxwell® technologies: Ultracapacitors bus application brief," https://maxwell.com/wp-content/uploads/2021/08/Bus_Application_3000620_EN_1.pdf, accessed: 2022-05-23.

[6] "Maxwell® technologies: Ultracapacitors energy storage application brief," https://maxwell.com/wp-content/uploads/2021/08/Energy_Storage_Application_Brief_3001003-EN_1.pdf, accessed: 2022-05-23.

[7] "Altair® nanotechnologies: 24v 70ah battery module," https://altairnano.com/products/battery-module/, accessed: 2022-05-25.

[8] "Amber kinetics: M32 flywheel," https://amberkinetics.com/wp-content/uploads/2020/05/Amber-Kinetics-DataSheet.pdf, accessed: 2022-05-29.

[9] M. Wołek, M. Wolański, M. Bartłomiejczyk, O. Wyszomirski, K. Grzelec, and K. Hebel, "Ensuring sustainable development of urban public transport: A case study of the trolleybus system in gdynia and sopot (poland)," *Journal of Cleaner Production*, vol. 279, p. 123807, 2021.

[10] L. Brunton, "The trolleybus story," *IEE Review*, vol. 38, no. 2, pp. 57–61, 1992.

[11] J. Kubín and A. Richter, "Efficiency of mechanical energy recovery from a tram by different input conditions," in *2012 15th International Power Electronics and Motion Control Conference (EPE/PEMC)*. IEEE, 2012, pp. DS1c–6.

[12] M. R. Raupach, G. Marland, P. Ciais, C. Le Quéré, J. G. Canadell, G. Klepper, and C. B. Field, "Global and regional drivers of accelerating co2 emissions," *Proceedings of the National Academy of Sciences*, vol. 104, no. 24, pp. 10 288–10 293, 2007.

[13] G. Krajačić, N. Duić, Z. Zmijarević, B. V. Mathiesen, A. A. Vučinić, and M. da Graça Carvalho, "Planning for a 100% independent energy system based on smart energy storage for integration of renewables and co2 emissions reduction," *Applied thermal engineering*, vol. 31, no. 13, pp. 2073–2083, 2011.

[14] A. Namboodiripad and C. Nimal, "Predicting the timeline for earth achieving kardashev scale type 1 status," *J. Sci. Technol*, vol. 6, pp. 2456–5660, 2021.

[15] M. Salih, D. Baumeister, M. Wazifehdust, P. Steinbusch, M. Zdrallek, S. Mour, P. Deskovic, T. Küll, and C. Troullier, "Impact assessment of integrating novel battery-trolleybuses, pv units and ev charging stations in a dc trolleybus network," in *2nd E-Mobility Power System Integration Symposium*, 2018.

[16] M. Bartłmiejczyk and L. Jarzebowicz, "Utility analysis and rating of energy storages in trolleybus power supply system," in *2020 Zooming Innovation in Consumer Technologies Conference (ZINC)*. IEEE, 2020, pp. 237–241.

[17] M. Ogasa, "Application of energy storage technologies for electric railway vehicles—examples with hybrid electric railway vehicles," *IEEJ Transactions on Electrical and Electronic Engineering*, vol. 5, no. 3, pp. 304–311, 2010.

[18] F. Ciccarelli, D. Iannuzzi, K. Kondo, and L. Fratelli, "Line-voltage control based on wayside energy storage systems for tramway networks," *IEEE Transactions on power electronics*, vol. 31, no. 1, pp. 884–899, 2015.

[19] C. Sankaran, *Power quality*. CRC press, 2017.

[20] Y. Takeuchi, T. Ogawa, K. Sato, H. Morimoto, and T. Saito, "Power control optimization of an energy storage system in dc electric railways," *IEEJ Journal of Industry Applications*, vol. 8, no. 5, pp. 827–834, 2019.

[21] S. Aatif, X. Yang, H. Hu, Z. He *et al.*, "Integration of pv and battery storage for catenary voltage regulation and stray current mitigation in mvdc railways," *Journal of Modern Power Systems and Clean Energy*, vol. 9, no. 3, pp. 585–594, 2020.

[22] M. Gussow, *Basic electricity*. McGraw-Hill, 2007.

[23] G. Parise, L. Parise, A. Malerba, F. M. Pepe, A. Honorati, and P. B. Chavdarian, "Comprehensive peak-shaving solutions for port cranes," *IEEE Transactions on Industry Applications*, vol. 53, no. 3, pp. 1799–1806, 2016.

[24] R. Ko, H.-C. Jo, and S.-K. Joo, "Energy storage system capacity sizing method for peak-demand reduction in urban railway system with photovoltaic generation," *Journal of Electrical Engineering & Technology*, vol. 14, no. 4, pp. 1771–1775, 2019.

[25] M. Steiner, M. Klohr, and S. Pagiela, "Energy storage system with ultracaps on board of railway vehicles," in *2007 European conference on power electronics and applications*. IEEE, 2007, pp. 1–10.

[26] A. E. Díez and M. Restrepo, "A planning method for partially grid-connected bus rapid transit systems operating with in-motion charging batteries," *Energies*, vol. 14, no. 9, p. 2550, 2021.

[27] J. P. Torreglosa, P. García, L. M. Fernández, and F. Jurado, "Predictive control for the energy management of a fuel-cell–battery–supercapacitor tramway," *IEEE Transactions on Industrial Informatics*, vol. 10, no. 1, pp. 276–285, 2013.

[28] Y. Han, Q. Li, T. Wang, W. Chen, and L. Ma, "Multisource coordination energy management strategy based on soc consensus for a pemfc–battery–supercapacitor hybrid tramway," *IEEE Transactions on Vehicular Technology*, vol. 67, no. 1, pp. 296–305, 2017.

[29] S. Wei, N. Murgovski, J. Jiang, X. Hu, W. Zhang, and C. Zhang, "Stochastic optimization of a stationary energy storage system for a catenary-free tramline," *Applied Energy*, vol. 280, p. 115711, 2020.

[30] V. Brazis, L. Latkovskis, and L. Grigans, "Simulation of trolleybus traction induction drive with supercapacitor energy storage system," *Latvian Journal of Physics and Technical Sciences*, vol. 47, no. 5, p. 33, 2010.

[31] V. Gelman, "Braking energy recuperation," *IEEE Vehicular Technology Magazine*, vol. 4, no. 3, pp. 82–89, 2009.

[32] C. Feng, Z. Gao, Y. Sun, and P. Chen, "Electric railway smart microgrid system with integration of multiple energy systems and power-quality improvement," *Electric Power Systems Research*, vol. 199, p. 107459, 2021.

[33] L. P. Di Noia and R. Rizzo, "Analysis of integration of pv power plant in railway power systems," in *2019 8th International Conference on Modern Power Systems (MPS)*. IEEE, 2019, pp. 1–5.

[34] F. Ning, L. Ji, J. Ma, L. Jia, and Z. Yu, "Research and analysis of a flexible integrated development model of railway system and photovoltaic in china," *Renewable Energy*, vol. 175, pp. 853–867, 2021.

[35] X. Shen, H. Wei, and L. Wei, "Study of trackside photovoltaic power integration into the traction power system of suburban elevated urban rail transit line," *Applied Energy*, vol. 260, p. 114177, 2020.

[36] S. Park and S. R. Salkuti, "Optimal energy management of railroad electrical systems with renewable energy and energy storage systems," *Sustainability*, vol. 11, no. 22, p. 6293, 2019.

[37] S. A. Meshram, S. A. Kapade, A. D. Choudhari, R. S. Kakade, A. V. Mhala, and K. B. Nagane, "Solar pv system for electric traction application with battery backup," 2019.

[38] İ. Şengör, H. C. Kılıçkıran, H. Akdemir, B. Kekezoğlu, O. Erdinc, and J. P. Catalao, "Energy management of a smart railway station considering regenerative braking and stochastic behaviour of ess and pv generation," *IEEE Transactions on Sustainable Energy*, vol. 9, no. 3, pp. 1041–1050, 2017.

[39] M. Ahmadi, H. Jafari Kaleybar, M. Brenna, F. Castelli-Dezza, and M. S. Carmeli, "Integration of distributed energy resources and ev fast-charging infrastructure in high-speed railway systems," *Electronics*, vol. 10, no. 20, p. 2555, 2021.

[40] F. Ciccarelli, L. P. Di Noia, and R. Rizzo, "Integration of photovoltaic plants and supercapacitors in tramway power systems," *Energies*, vol. 11, no. 2, p. 410, 2018.

[41] A. Okui, S. Hase, H. Shigeeda, T. Konishi, and T. Yoshi, "Application of energy storage system for railway transportation in japan," in *The 2010 International Power Electronics Conference-ECCE ASIA-*. IEEE, 2010, pp. 3117–3123.

[42] X. Luo, J. Wang, M. Dooner, and J. Clarke, "Overview of current development in electrical energy storage technologies and the application potential in power system operation," *Applied energy*, vol. 137, pp. 511–536, 2015.

[43] A. K. Rohit, K. P. Devi, and S. Rangnekar, "An overview of energy storage and its importance in indian renewable energy sector: Part i–technologies and comparison," *Journal of Energy Storage*, vol. 13, pp. 10–23, 2017.

[44] M. Beaudin, H. Zareipour, A. Schellenberglabe, and W. Rosehart, "Energy storage for mitigating the variability of renewable electricity sources: An updated review," *Energy for sustainable development*, vol. 14, no. 4, pp. 302–314, 2010.

[45] I. Hadjipaschalis, A. Poullikkas, and V. Efthimiou, "Overview of current and future energy storage technologies for electric power applications," *Renewable and sustainable energy reviews*, vol. 13, no. 6-7, pp. 1513–1522, 2009.

[46] P. Jandura, A. Richter, and Ž. Ferková, "Flywheel energy storage system for city railway," in *2016 International Symposium on Power Electronics, Electrical Drives, Automation and Motion (SPEEDAM)*. IEEE, 2016, pp. 1155–1159.

[47] L. Zhang, Y. Yang, M. Sun, and H. Liu, "Energy management strategy based on dynamic programming for dual source trolleybus," *Teh. Vjesn. Tech. Gaz*, vol. 24, pp. 1439–1447, 2017.

[48] H. Chen, T. N. Cong, W. Yang, C. Tan, Y. Li, and Y. Ding, "Progress in electrical energy storage system: A critical review," *Progress in natural science*, vol. 19, no. 3, pp. 291–312, 2009.

[49] I. E. Commission, "Electrical energy storage," 2011.

[50] A. Du Pasquier, I. Plitz, S. Menocal, and G. Amatucci, "A comparative study of li-ion battery, supercapacitor and nonaqueous asymmetric hybrid devices for automotive applications," *Journal of power sources*, vol. 115, no. 1, pp. 171–178, 2003.

[51] F. A. Farret and M. G. Simoes, *Integration of alternative sources of energy*. John Wiley & Sons, 2006.

[52] S. M. Schoenung, "Characteristics and technologies for long-vs. short-term energy storage," *United States Department of Energy*, 2001.

[53] D. Rastler, "A white paper primer on applications costs and benefits," *Electric Power Research Institute, Tech. Rep.*, 2010.

[54] P. Nikolaidis and A. Poullikkas, "Cost metrics of electrical energy storage technologies in potential power system operations," *Sustainable Energy Technologies and Assessments*, vol. 25, pp. 43–59, 2018.

[55] C. J. Rydh and B. A. Sandén, "Energy analysis of batteries in photovoltaic systems. part ii: Energy return factors and overall battery efficiencies," *Energy conversion and management*, vol. 46, no. 11-12, pp. 1980–2000, 2005.

[56] T. Nemeth, P. J. Kollmeyer, A. Emadi, and D. U. Sauer, "Optimized operation of a hybrid energy storage system with lto batteries for high power electrified vehicles," in *2019 IEEE Transportation Electrification Conference and Expo (ITEC)*. IEEE, 2019, pp. 1–6.

[57] A. Burke and M. Miller, "Life cycle testing of lithium batteries for fast charging and second-use applications," in *2013 World Electric Vehicle Symposium and Exhibition (EVS27)*. IEEE, 2013, pp. 1–10.

[58] A. Harris, D. Soban, B. M. Smyth, and R. Best, "Assessing life cycle impacts and the risk and uncertainty of alternative bus technologies," *Renewable and Sustainable Energy Reviews*, vol. 97, pp. 569–579, 2018.

[59] X. Liu, K. Li, and X. Li, "The electrochemical performance and applications of several popular lithium-ion batteries for electric vehicles-a review," *Advances in Green Energy Systems and Smart Grid*, pp. 201–213, 2018.

[60] X. Hu, C. Zou, C. Zhang, and Y. Li, "Technological developments in batteries: a survey of principal roles, types, and management needs," *IEEE Power and Energy Magazine*, vol. 15, no. 5, pp. 20–31, 2017.

[61] M. Baumann, J. Peters, M. Weil, and A. Grunwald, "Co2 footprint and life-cycle costs of electrochemical energy storage for stationary grid applications," *Energy Technology*, vol. 5, no. 7, pp. 1071–1083, 2017.

[62] L. Wang, Z. Wang, Q. Ju, W. Wang, and Z. Wang, "Characteristic analysis of lithium titanate battery," *Energy Procedia*, vol. 105, pp. 4444–4449, 2017.

[63] D. I. Stroe, A.-I. Stan, R. Teodorescu, D. Sauer *et al.*, "Selection and performance-degradation modeling of limo 2/li 4 ti 5 o 12 and lifepo 4/c battery cells as suitable energy storage systems for grid integration with wind power plants: An example for the primary frequency regulation service," *IEEE Transactions on Sustainable Energy*, vol. 5, no. 1, pp. 90–101, 2014.

[64] A. Chatzivasileiadi, E. Ampatzi, and I. Knight, "Characteristics of electrical energy storage technologies and their applications in buildings," *Renewable and Sustainable Energy Reviews*, vol. 25, pp. 814–830, 2013.

[65] T. Yamamura, X. Wu, S. Ohta, K. Shirasaki, H. Sakuraba, I. Satoh, and T. Shikama, "Vanadium solid-salt battery: solid state with two redox couples," *Journal of Power Sources*, vol. 196, no. 8, pp. 4003–4011, 2011.

[66] A. Taniguchi, N. Fujioka, M. Ikoma, and A. Ohta, "Development of nickel/metal-hydride batteries for evs and hevs," *Journal of power sources*, vol. 100, no. 1-2, pp. 117–124, 2001.

[67] G. Pistoia, *Electric and hybrid vehicles: Power sources, models, sustainability, infrastructure and the market*. Elsevier, 2010.

[68] P. Li, "Energy storage is the core of renewable technologies," *IEEE Nanotechnology Magazine*, vol. 2, no. 4, pp. 13–18, 2008.

[69] C. J. Rydh and B. A. Sandén, "Energy analysis of batteries in photovoltaic systems. part i: Performance and energy requirements," *Energy conversion and management*, vol. 46, no. 11-12, pp. 1957–1979, 2005.

[70] J. Baker, "New technology and possible advances in energy storage," *Energy Policy*, vol. 36, no. 12, pp. 4368–4373, 2008.

[71] F. Díaz-González, A. Sumper, O. Gomis-Bellmunt, and R. Villafáfila-Robles, "A review of energy storage technologies for wind power applications," *Renewable and sustainable energy reviews*, vol. 16, no. 4, pp. 2154–2171, 2012.

[72] J. San Martín, I. Zamora, J. San Martín, V. Aperribay, and P. Eguia, "Energy storage technologies for electric applications," in *International Conference on Renewable Energies and Power Quality*, no. 2, 2011.

[73] J. Kaldellis and D. Zafirakis, "Optimum energy storage techniques for the improvement of renewable energy sources-based electricity generation economic efficiency," *Energy*, vol. 32, no. 12, pp. 2295–2305, 2007.

[74] J. Kondoh, I. Ishii, H. Yamaguchi, A. Murata, K. Otani, K. Sakuta, N. Higuchi, S. Sekine, and M. Kamimoto, "Electrical energy storage systems for energy networks," *Energy conversion and management*, vol. 41, no. 17, pp. 1863–1874, 2000.

[75] S. Schoenung, "Energy storage systems cost update a study for the doe energy storage systems program (report sand2011-2730)," *New Mexico and California, Sandia National Laboratories*, 2011.

[76] N. Author, "Review of electrical energy storage technologies and systems and of their potential for the uk," *EA Technology*, vol. 1, p. 34, 2004.

[77] Z. Wen, J. Cao, Z. Gu, X. Xu, F. Zhang, and Z. Lin, "Research on sodium sulfur battery for energy storage," *Solid State Ionics*, vol. 179, no. 27-32, pp. 1697–1701, 2008.

[78] S. J. Kazempour, M. P. Moghaddam, M. Haghifam, and G. Yousefi, "Electric energy storage systems in a market-based economy: Comparison of emerging and traditional technologies," *Renewable energy*, vol. 34, no. 12, pp. 2630–2639, 2009.

[79] A. Bito, "Overview of the sodium-sulfur battery for the ieee stationary battery committee," in *IEEE Power Engineering Society General Meeting, 2005*. IEEE, 2005, pp. 1232–1235.

[80] M. Kamibayashi, D. K. Nichols, and T. Oshima, "Development update of the nas battery," in *IEEE/PES Transmission and Distribution Conference and Exhibition*, vol. 3. IEEE, 2002, pp. 1664–1668.

[81] A. Barin, L. N. Canha, K. Magnago, and A. da Rosa Abaide, "Fuzzy multisets and multi-rules: analysis of hybrid systems concerning renewable sources with conventional and flow batteries," in *2009 15th International Conference on Intelligent System Applications to Power Systems*. IEEE, 2009, pp. 1–6.

[82] A. Z. Weber, M. M. Mench, J. P. Meyers, P. N. Ross, J. T. Gostick, and Q. Liu, "Redox flow batteries: a review," *Journal of applied electrochemistry*, vol. 41, no. 10, pp. 1137–1164, 2011.

[83] L. Barote, R. Weissbach, R. Teodorescu, C. Marinescu, and M. Cirstea, "Standalone wind system with vanadium redox battery energy storage," in *2008 11th International Conference on Optimization of Electrical and Electronic Equipment*. IEEE, 2008, pp. 407–412.

[84] N. Tokuda, T. Kumamoto, T. Shigematsu, H. Deguchi, T. Ito, N. Yoshikawa, and T. Hara, "Development of a redox flow battery system," *SUMITOMO ELECTRIC TECHNICAL REVIEW-ENGLISH EDITION-*, pp. 88–94, 1998.

[85] C. P. De Leon, A. Frías-Ferrer, J. González-García, D. Szánto, and F. C. Walsh, "Redox flow cells for energy conversion," *Journal of power sources*, vol. 160, no. 1, pp. 716–732, 2006.

[86] M. G. Molina, "Dynamic modelling and control design of advanced energy storage for power system applications," *Dynamic Modelling*, vol. 300, 2010.

[87] P. Gevorkian, *Large-scale solar power systems: Construction and economics*. Cambridge University Press, 2012.

[88] Z. Yang, J. Zhang, M. C. Kintner-Meyer, X. Lu, D. Choi, J. P. Lemmon, and J. Liu, "Electrochemical energy storage for green grid," *Chemical reviews*, vol. 111, no. 5, pp. 3577–3613, 2011.

[89] P. Boer and J. Raadschelders, "Briefing paper: Flow batteries," *KEMA, Netherlands. Retrieved on*, vol. 18, 2013.

[90] W. Tong, *Wind power generation and wind turbine design*. WIT press, 2010.

[91] M. Winter and R. J. Brodd, "What are batteries, fuel cells, and supercapacitors?" *Chemical reviews*, vol. 104, no. 10, pp. 4245–4270, 2004.

[92] E. N. Power, "Capacitors age and capacitors have an end of life," *White paper*, 2008.

[93] S. C. Smith, P. Sen, and B. Kroposki, "Advancement of energy storage devices and applications in electrical power system," in *2008 IEEE Power and Energy Society General Meeting-Conversion and Delivery of Electrical Energy in the 21st Century*. IEEE, 2008, pp. 1–8.

[94] P. Taylor, R. Bolton, D. Stone, X.-P. Zhang, C. Martin, and P. Upham, "Pathways for energy storage in the uk," *Report for the centre for low carbon futures, York*, 2012.

[95] A. Vecchi, Y. liang Li, Y. Ding, P. Mancarella, and A. Sciacovelli, "Liquid air energy storage (laes): a review on technology state-of-the-art, integration pathways and future perspectives," *Advances in Applied Energy*, p. 100047, 2021.

[96] H. Power, "Highview power storage, secure, clean power."

[97] M. Akhurst, I. Arbon, M. Ayres, N. Brandon, R. Bruges, S. Cooper, Y. Ding, T. Evison, N. Goode, P. Grünewald, A. Heyes, Y. Li, C. Markides, R. Morgan, R. Morris, S. Nelmes, N. Owen, T. Peters, A. Price, J. Raquet, D. Sanders, S. Saunders, A. Schlotmann, D. Wen, and M. Wilks, "Liquid air in the energy and transport systems: opportunities for industry and innovation in the uk," Center for Low Carbon Futures, WorkingPaper, May 2013.

[98] G. Ries and H.-W. Neumueller, "Comparison of energy storage in flywheels and smes," *Physica C: Superconductivity*, vol. 357, pp. 1306–1310, 2001.

[99] H. L. Ferreira, R. Garde, G. Fulli, W. Kling, and J. P. Lopes, "Characterisation of electrical energy storage technologies," *Energy*, vol. 53, pp. 288–298, 2013.

[100] M. Falvo, R. Lamedica, and A. Ruvio, "Energy storage application in trolleybuses lines for a sustainable urban mobility," in *2012 Electrical Systems for Aircraft, Railway and Ship Propulsion*. IEEE, 2012, pp. 1–6.

[101] A. Rufer, "Energy storage for railway systems, energy recovery and vehicle autonomy in europe," in *The 2010 International Power Electronics Conference-ECCE ASIA-*. IEEE, 2010, pp. 3124–3127.

[102] Y. Liu, M. Chen, S. Lu, Y. Chen, and Q. Li, "Optimized sizing and scheduling of hybrid energy storage systems for high-speed railway traction substations," *Energies*, vol. 11, no. 9, p. 2199, 2018.

[103] H. Hayashiya, H. Itagaki, Y. Morita, Y. Mitoma, T. Furukawa, T. Kuraoka, Y. Fukasawa, and T. Oikawa, "Potentials, peculiarities and prospects of solar power generation on the railway premises," in *2012 International Conference on Renewable Energy Research and Applications (ICRERA)*. IEEE, 2012, pp. 1–6.

[104] C. P. Nazir, "Solar energy for traction of high speed rail transportation: a techno-economic analysis," *Civil Engineering Journal*, vol. 5, no. 7, pp. 1566–1576, 2019.

[105] J. P. Trovão, P. G. Pereirinha, H. M. Jorge, and C. H. Antunes, "A multi-level energy management system for multi-source electric vehicles–an integrated rule-based meta-heuristic approach," *Applied Energy*, vol. 105, pp. 304–318, 2013.

[106] M. Bartłomiejczyk and S. Mirchevski, "Reducing of energy consumption in public transport—results of experimental exploitation of super capacitor energy bank in gdynia trolleybus system," in *2014 16th International Power Electronics and Motion Control Conference and Exposition*. IEEE, 2014, pp. 94–101.

[107] M. Wei, W. Wei, H. Ruonan, and W. Ziyi, "Auxiliary power supply system of passenger train based on photovoltaic and energy storage," in *2016 IEEE 11th Conference on Industrial Electronics and Applications (ICIEA)*. IEEE, 2016, pp. 784–788.

[108] A. Awasthi, A. Sinha, A. K. Singh, and R. Veeraganesan, "Solar pv fed grid integration with energy storage system for electric traction application," in *2016 10th International Conference on Intelligent Systems and Control (ISCO)*. IEEE, 2016, pp. 1–5.

[109] M. Yan, M. Li, H. He, J. Peng, and C. Sun, "Rule-based energy management for dual-source electric buses extracted by wavelet transform," *Journal of Cleaner Production*, vol. 189, pp. 116–127, 2018.

[110] V. A. Kleftakis and N. D. Hatziargyriou, "Optimal control of reversible substations and wayside storage devices for voltage stabilization and energy savings in metro railway networks," *IEEE Transactions on Transportation Electrification*, vol. 5, no. 2, pp. 515–523, 2019.

[111] M. Bartłomiejczyk, L. Jarzebowicz, and J. Kohout, "Compensation of voltage drops in trolleybus supply system using battery-based buffer station," *Energies*, vol. 15, no. 5, p. 1629, 2022.

[112] U. Bodenhofer, M. De Cock, and E. E. Kerre, "Openings and closures of fuzzy preorderings: theoretical basics and applications to fuzzy rule-based systems," *International Journal of General Systems*, vol. 32, no. 4, pp. 343–360, 2003.

[113] Z. Wang, F. Chen, and J. Li, "Implementing transformer nodal admittance matrices into backward/forward sweep-based power flow analysis for unbalanced radial distribution systems," *IEEE Transactions on Power Systems*, vol. 19, no. 4, pp. 1831–1836, 2004.

[114] L. Alfieri, A. Bracale, P. Caramia, D. Iannuzzi, and M. Pagano, "Optimal battery sizing procedure for hybrid trolley-bus: A real case study," *Electric Power Systems Research*, vol. 175, p. 105930, 2019.

[115] M. Bartłomiejczyk, R. Hrbáč, V. Stỳskala, and M. Połom, "Trolleybus with traction batteries for autonomous running," in *The 7th International Scientific Symposium ELEKTROENERGETIKA*. Technical University of Košice, 2013.

[116] M. Bartłomiejczyk, "Super capacitor energy bank medcom ucer-01 in gdynia trolleybus system," in *IECON 2016-42nd Annual Conference of the IEEE Industrial Electronics Society*. IEEE, 2016, pp. 2124–2128.

A APPENDIX

Extra plots for *on-board* energy storage systems
In figure A.1 until figure A.6 are illustrated the PV system utilization vs energy-neutrality ratio ζ for various upper electric power thresholds for *on-board* energy storage systems equipped with *supercapacitors* (SC) or *lithium-titanate oxide* (LTO) batteries of various capacities for substation 12.

In figure A.7 until figure A.12 are illustrated the direct load coverage Λ vs energy-neutrality ratio ζ for various upper electric power thresholds for *on-board* energy storage systems equipped with *supercapacitors* (SC) or *lithium-titanate oxide* (LTO) batteries of various capacities for substation 12.

In figure A.13 until figure A.18 are illustrated the PV system utilization vs energy-neutrality ratio ζ for various upper electric power thresholds for *on-board* energy storage systems equipped with *supercapacitors* (SC) or *lithium-titanate oxide* (LTO) batteries of various capacities for substation 9.

In figure A.19 until figure A.24 are illustrated the direct load coverage Λ vs energy-neutrality ratio ζ for various upper electric power thresholds for *on-board* energy storage systems equipped with *supercapacitors* (SC) or *lithium-titanate oxide* (LTO) batteries of various capacities for substation 9.

Extra plots for *stationary* energy storage systems

In figure A.25 until figure A.28 are illustrated the PV system utilization vs energy-neutrality ratio ζ for various positions for *stationary* energy storage systems equipped with *flywheels* or *lithium-titanate oxide* (LTO) batteries of various capacities for substation 12.

In figure A.29 until figure A.32 are illustrated the direct load coverage Λ vs energy-neutrality ratio ζ for various positions for *stationary* energy storage systems equipped with *flywheels* or *lithium-titanate oxide* (LTO) batteries of various capacities for substation 12.

In figure A.33 until figure A.36 are illustrated the PV system utilization vs energy-neutrality ratio ζ for various positions for *stationary* energy storage systems equipped with *flywheels* or *lithium-titanate oxide* (LTO) batteries of various capacities for substation 9.

In figure A.37 until figure A.40 are illustrated the direct load coverage Λ vs energy-neutrality ratio ζ for various positions for *stationary* energy storage systems equipped with *flywheels* or *lithium-titanate oxide* (LTO) batteries of various capacities for substation 9.

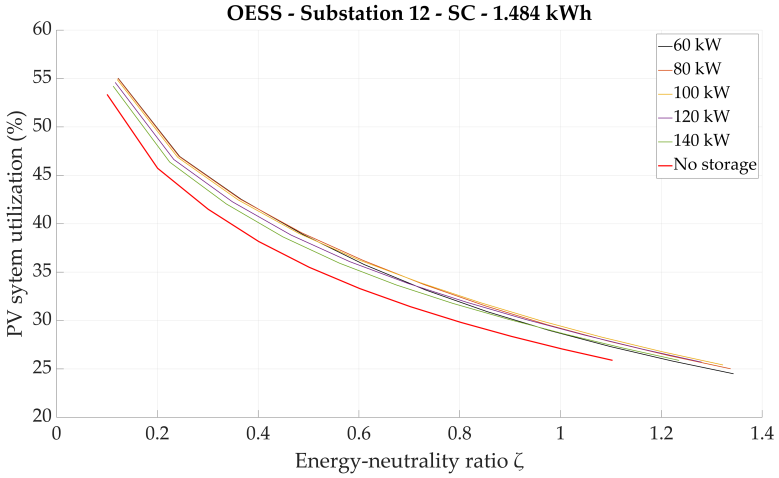

Figure A.1: Substation 12 PV system utilization vs energy-neutrality ratio ζ for various upper electric power thresholds for *on-board* energy storage system equipped with *supercapacitors* (SC) of 1.484 kWh.

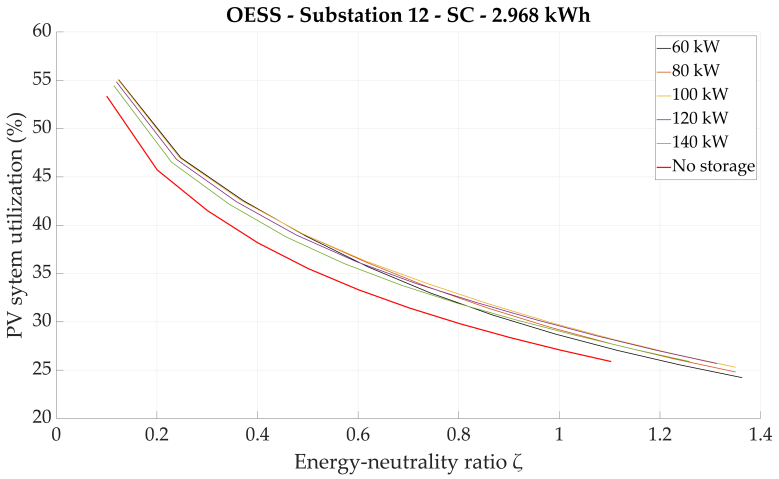

Figure A.2: Substation 12 PV system utilization vs energy-neutrality ratio ζ for various upper electric power thresholds for *on-board* energy storage system equipped with *supercapacitors* (SC) of 2.968 kWh.

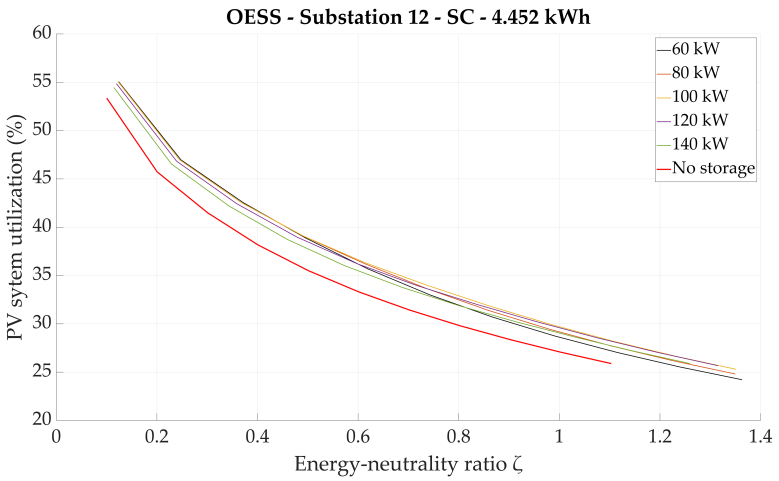

Figure A.3: Substation 12 PV system utilization vs energy-neutrality ratio ζ for various upper electric power thresholds for *on-board* energy storage system equipped with *supercapacitors* (SC) of 4.452 kWh.

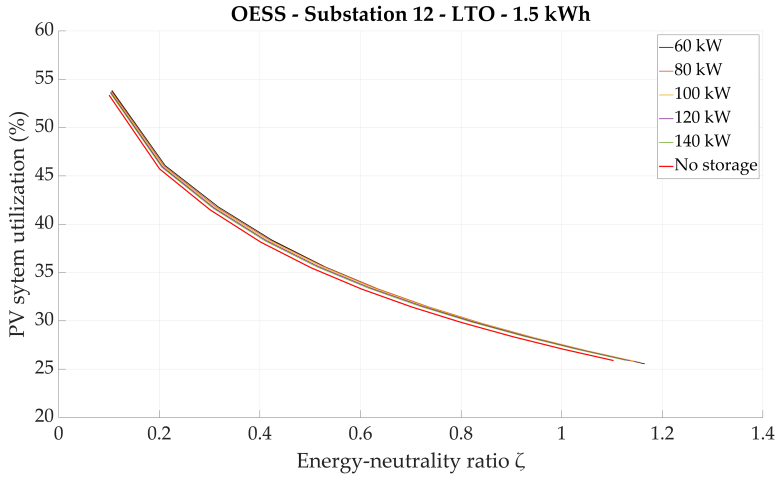

Figure A.4: Substation 12 PV system utilization vs energy-neutrality ratio ζ for various upper electric power thresholds for *on-board* energy storage system equipped with *lithium-titanate oxide* (LTO) batteries of 1.5 kWh.

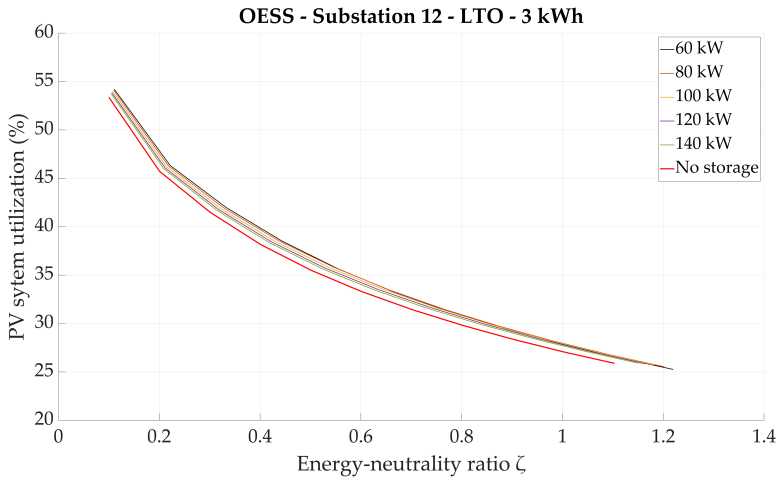

Figure A.5: Substation 12 PV system utilization vs energy-neutrality ratio ζ for various upper electric power thresholds for *on-board* energy storage system equipped with *lithium-titanate oxide* (LTO) batteries of 3 kWh.

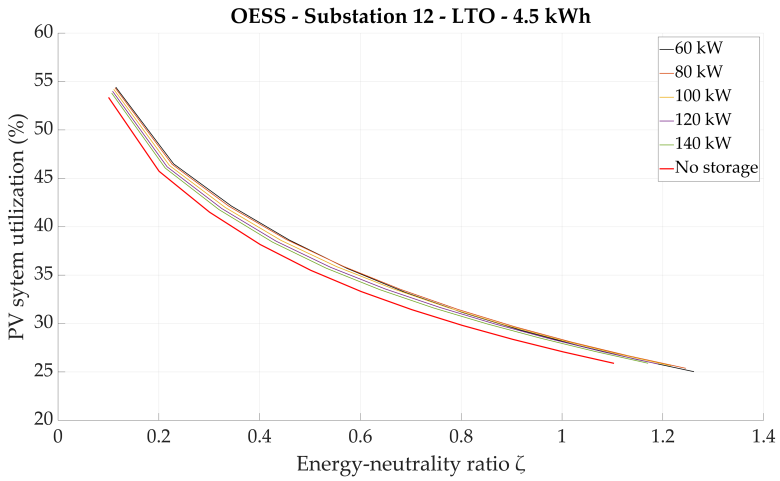

Figure A.6: Substation 12 PV system utilization vs energy-neutrality ratio ζ for various upper electric power thresholds for *on-board* energy storage system equipped with *lithium-titanate oxide* (LTO) batteries of 4.5 kWh.

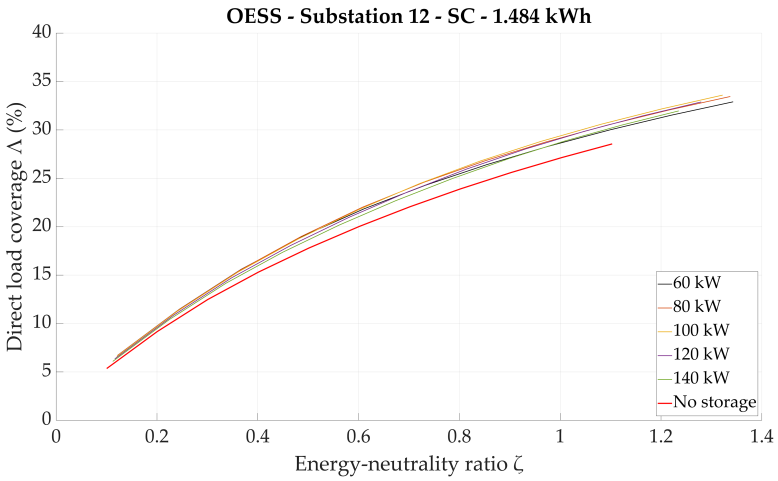

Figure A.7: Substation 12 direct load coverage Λ vs energy-neutrality ratio ζ for various upper electric power thresholds for *on-board* energy storage system equipped with *supercapacitors* (SC) of 1.484 kWh.

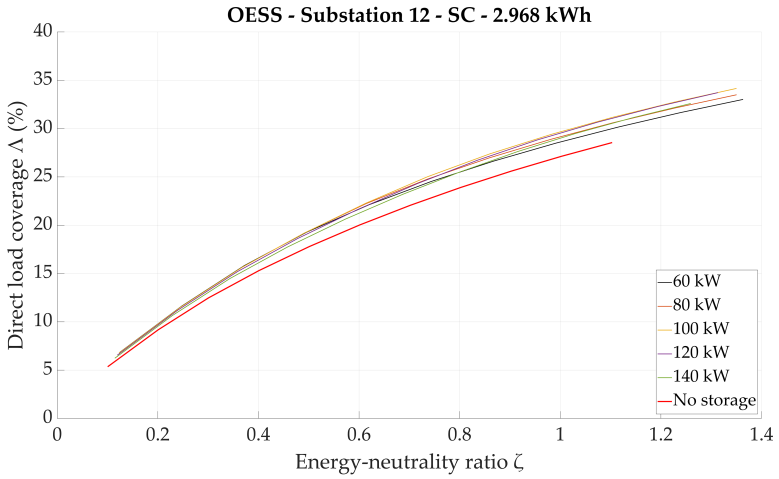

Figure A.8: Substation 12 direct load coverage Λ vs energy-neutrality ratio ζ for various upper electric power thresholds for *on-board* energy storage system equipped with *supercapacitors* (SC) of 2.968 kWh.

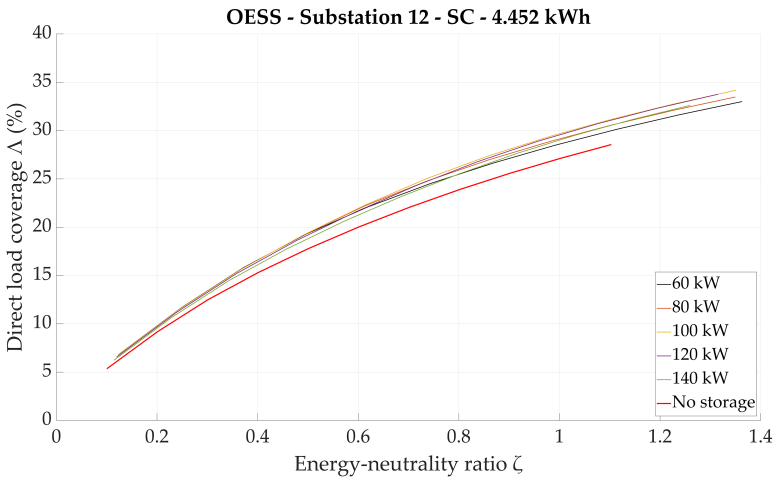

Figure A.9: Substation 12 direct load coverage Λ vs energy-neutrality ratio ζ for various upper electric power thresholds for *on-board* energy storage system equipped with *supercapacitors* (SC) of 4.452 kWh.

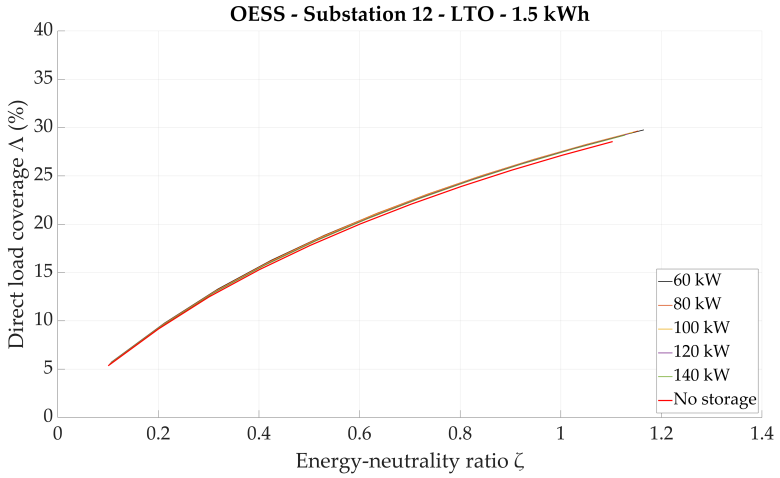

Figure A.10: Substation 12 direct load coverage Λ vs energy-neutrality ratio ζ for various upper electric power thresholds for *on-board* energy storage system equipped with *lithium-titanate oxide* (LTO) batteries of 1.5 kWh.

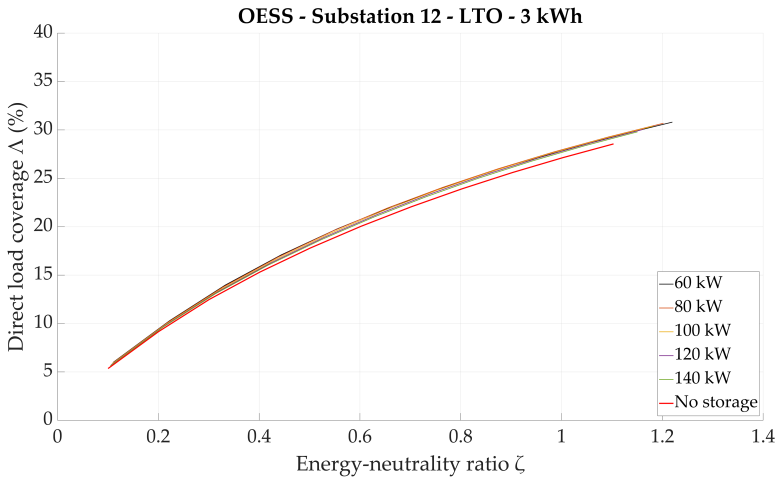

Figure A.11: Substation 12 direct load coverage Λ vs energy-neutrality ratio ζ for various upper electric power thresholds for *on-board* energy storage system equipped with *lithium-titanate oxide* (LTO) batteries of 3 kWh.

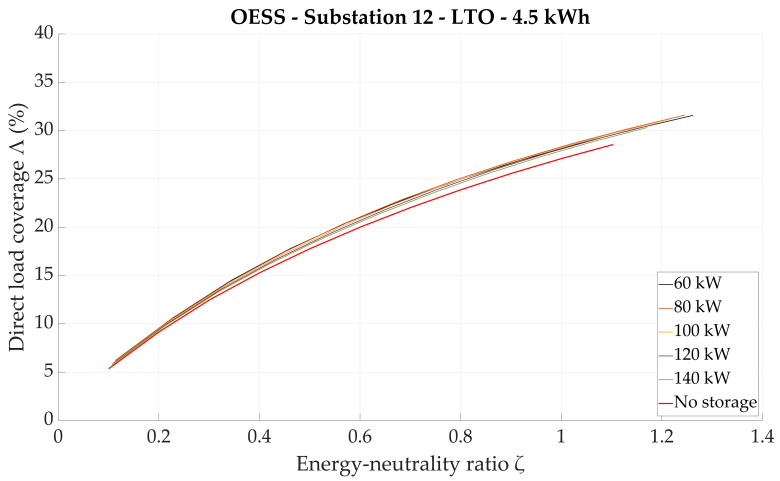

Figure A.12: Substation 12 direct load coverage Λ vs energy-neutrality ratio ζ for various upper electric power thresholds for *on-board* energy storage system equipped with *lithium-titanate oxide* (LTO) batteries of 4.5 kWh.

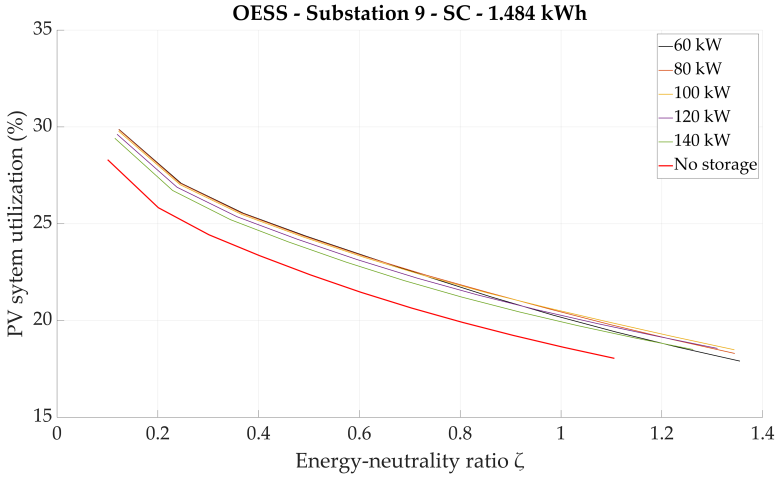

Figure A.13: Substation 9 PV system utilization vs energy-neutrality ratio ζ for various upper electric power thresholds for *on-board* energy storage system equipped with *supercapacitors* (SC) of 1.484 kWh.

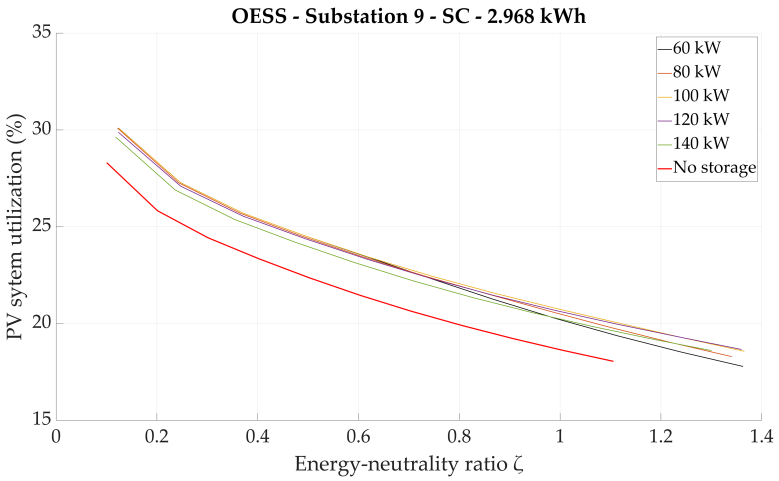

Figure A.14: Substation 9 PV system utilization vs energy-neutrality ratio ζ for various upper electric power thresholds for *on-board* energy storage system equipped with *supercapacitors* (SC) of 2.968 kWh.

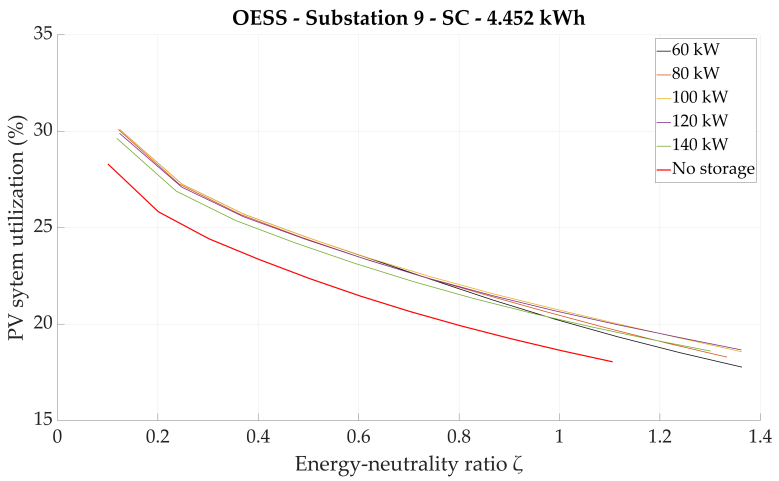

Figure A.15: Substation 9 PV system utilization vs energy-neutrality ratio ζ for various upper electric power thresholds for *on-board* energy storage system equipped with *supercapacitors* (SC) of 4.452 kWh.

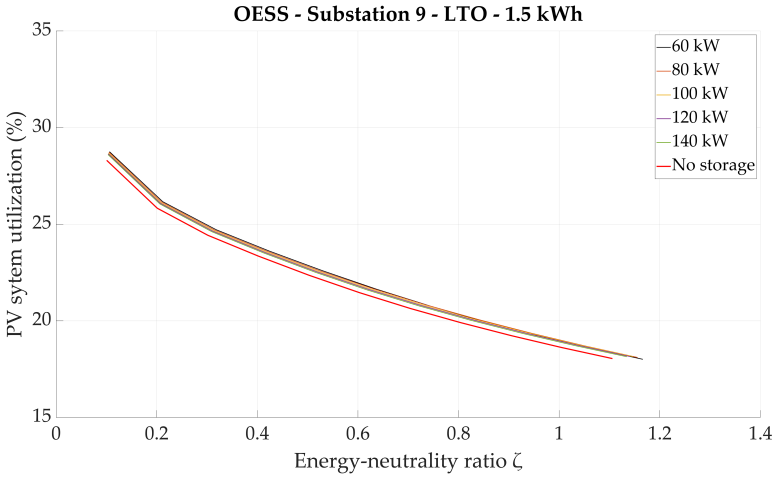

Figure A.16: Substation 9 PV system utilization vs energy-neutrality ratio ζ for various upper electric power thresholds for *on-board* energy storage system equipped with *lithium-titanate oxide* (LTO) batteries of 1.5 kWh.

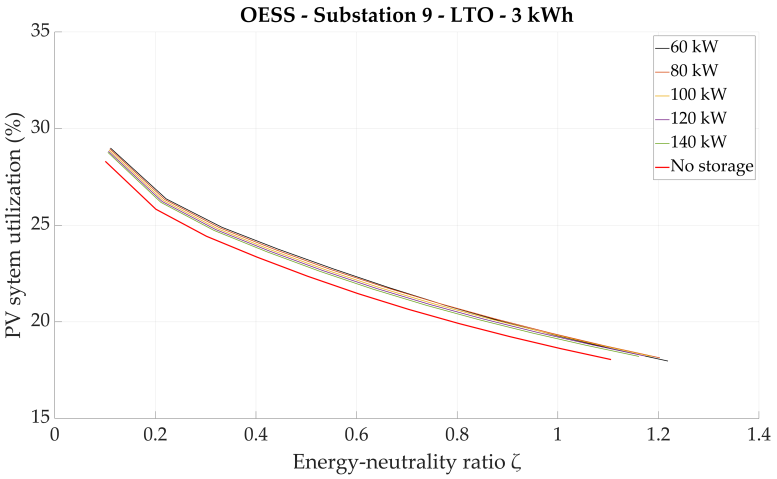

Figure A.17: Substation 9 PV system utilization vs energy-neutrality ratio ζ for various upper electric power thresholds for *on-board* energy storage system equipped with *lithium-titanate oxide* (LTO) batteries of 3 kWh.

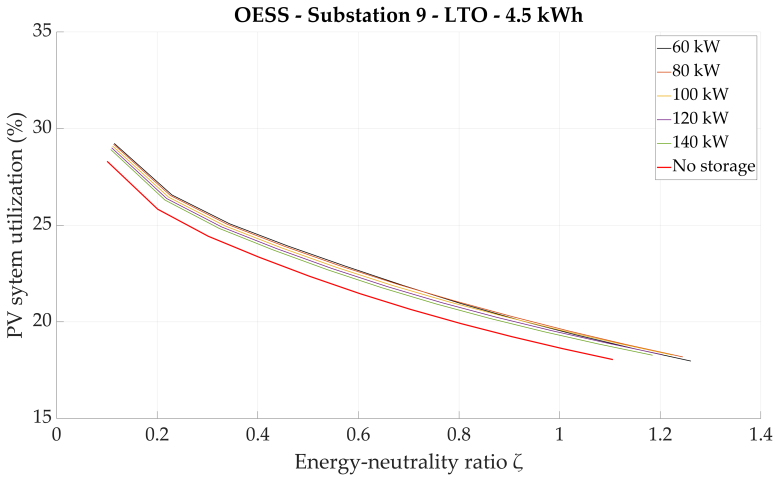

Figure A.18: Substation 9 PV system utilization vs energy-neutrality ratio ζ for various upper electric power thresholds for *on-board* energy storage system equipped with *lithium-titanate oxide* (LTO) batteries of 4.5 kWh.

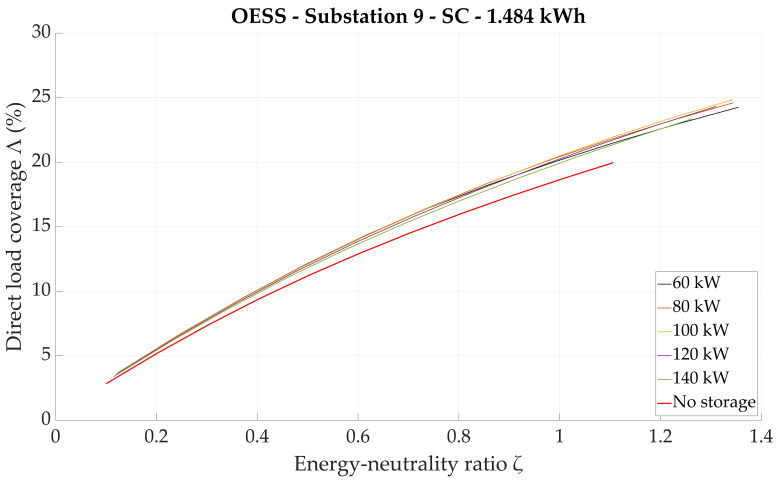

Figure A.19: Substation 9 direct load coverage Λ vs energy-neutrality ratio ζ for various upper electric power thresholds for *on-board* energy storage system equipped with *supercapacitors* (SC) of 1.484 kWh.

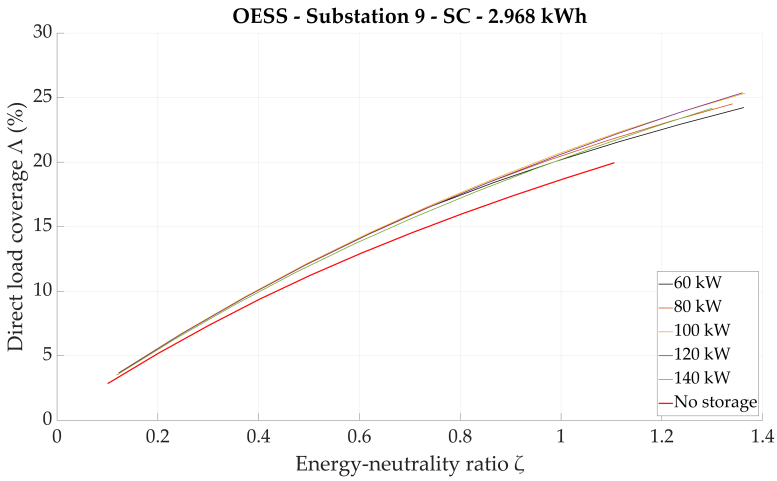

Figure A.20: Substation 9 direct load coverage Λ vs energy-neutrality ratio ζ for various upper electric power thresholds for *on-board* energy storage system equipped with *supercapacitors* (SC) of 2.968 kWh.

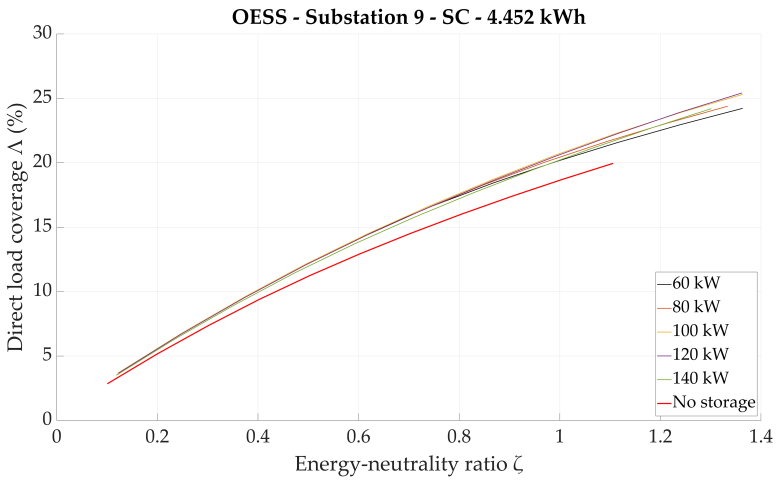

Figure A.21: Substation 9 direct load coverage Λ vs energy-neutrality ratio ζ for various upper electric power thresholds for *on-board* energy storage system equipped with *supercapacitors* (SC) of 4.452 kWh.

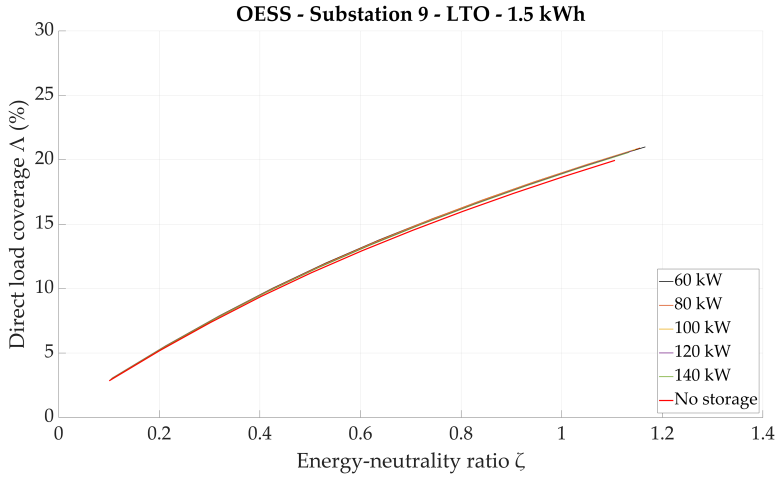

Figure A.22: Substation 9 direct load coverage Λ vs energy-neutrality ratio ζ for various upper electric power thresholds for *on-board* energy storage system equipped with *lithium-titanate oxide* (LTO) batteries of 1.5 kWh.

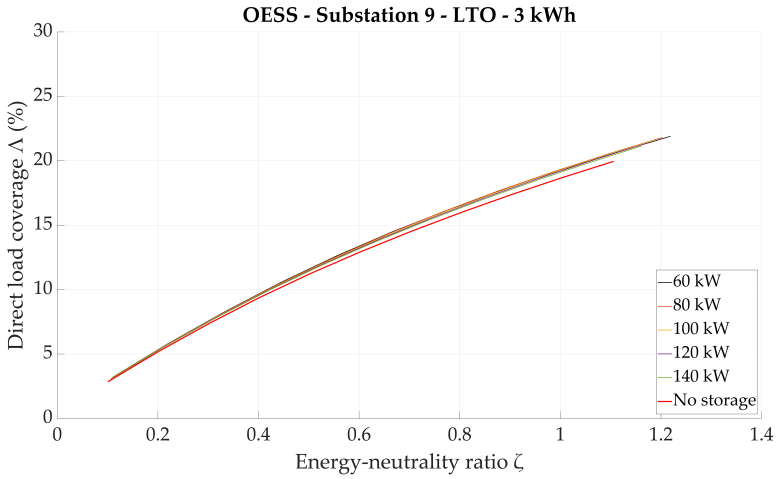

Figure A.23: Substation 9 direct load coverage Λ vs energy-neutrality ratio ζ for various upper electric power thresholds for *on-board* energy storage system equipped with *lithium-titanate oxide* (LTO) batteries of 3 kWh.

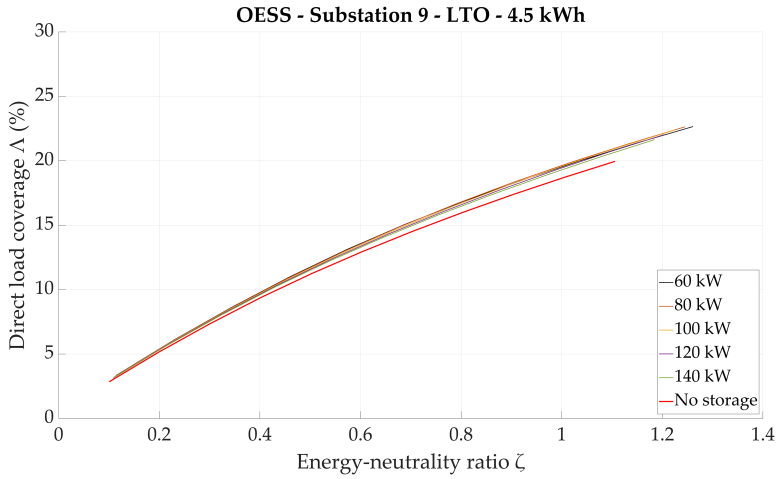

Figure A.24: Substation 9 direct load coverage Λ vs energy-neutrality ratio ζ for various upper electric power thresholds for *on-board* energy storage system equipped with *lithium-titanate oxide* (LTO) batteries of 4.5 kWh.

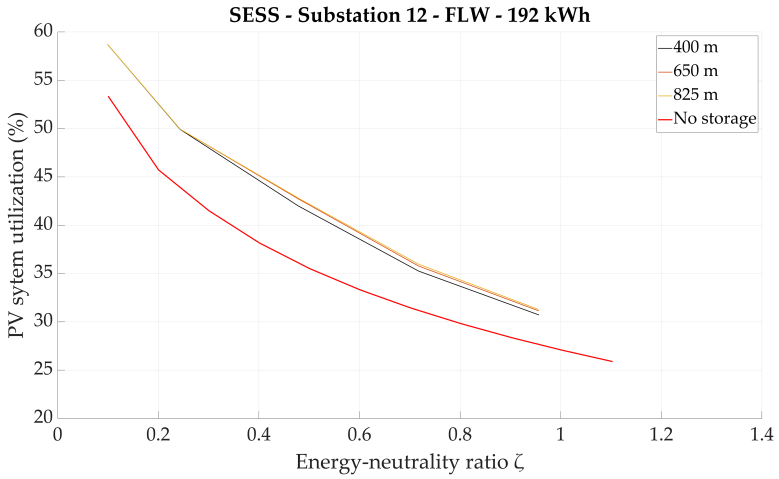

Figure A.25: Substation 12 PV system utilization vs energy-neutrality ratio ζ for various positions for *stationary* energy storage system equipped with *flywheels* of 192 kWh.

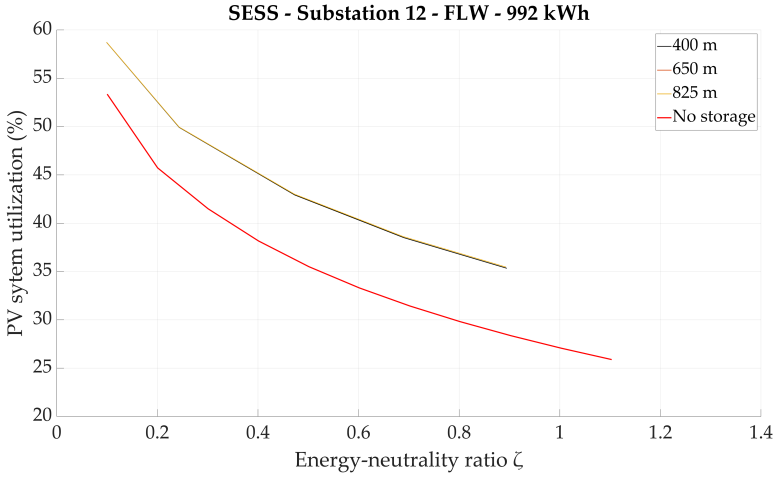

Figure A.26: Substation 12 PV system utilization vs energy-neutrality ratio ζ for various positions for *stationary* energy storage system equipped with *flywheels* of 992 kWh.

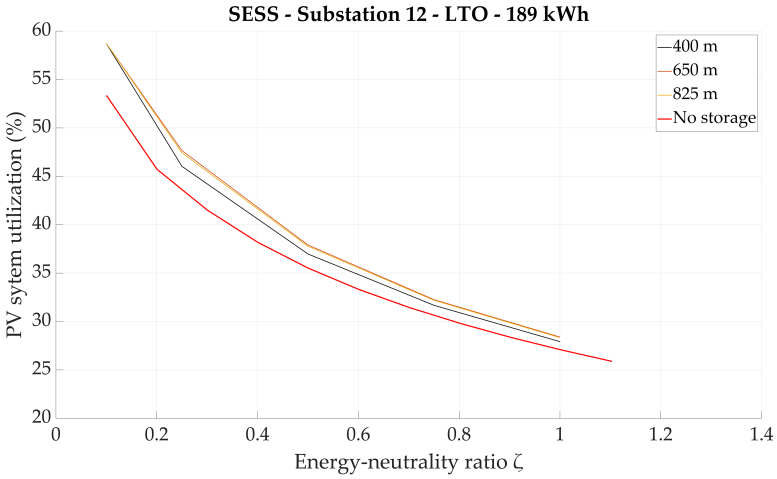

Figure A.27: Substation 12 PV system utilization vs energy-neutrality ratio ζ for various positions for *stationary* energy storage system equipped with lithium-titanate oxide batteries of 189 kWh.

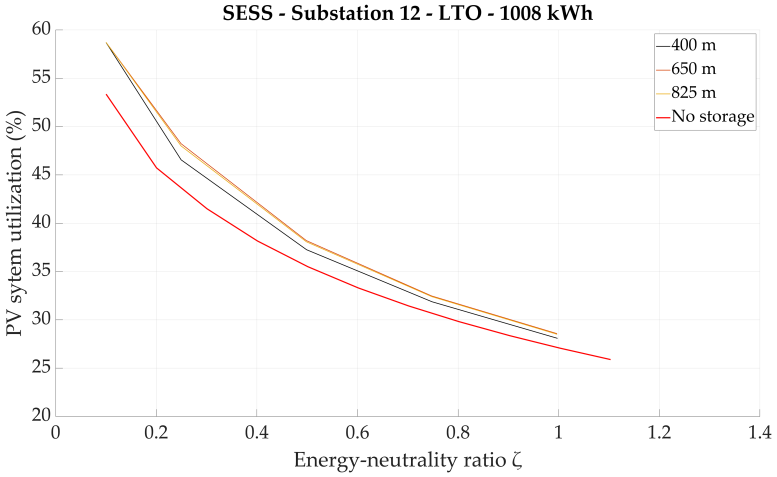

Figure A.28: Substation 12 PV system utilization vs energy-neutrality ratio ζ for various positions for *stationary* energy storage system equipped with lithium-titanate oxide batteries of 1008 kWh.

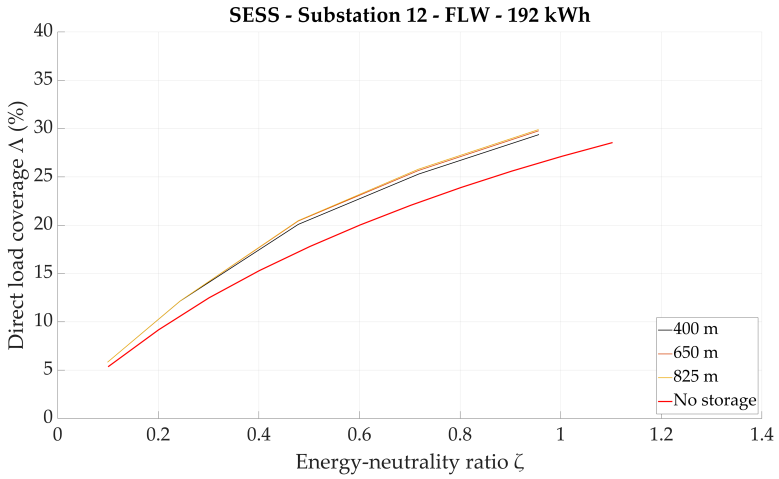

Figure A.29: Substation 12 direct load coverage Λ vs energy-neutrality ratio ζ for various positions for *stationary* energy storage system equipped with *flywheels* of 192 kWh.

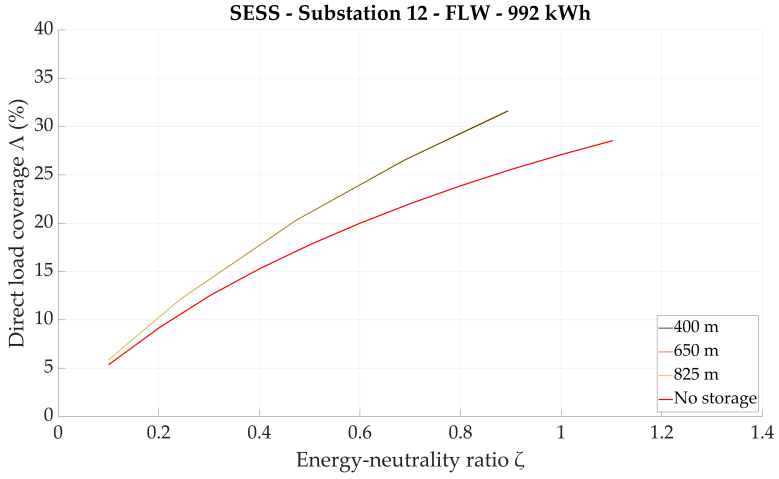

Figure A.30: Substation 12 direct load coverage Λ vs energy-neutrality ratio ζ for various positions for *stationary* energy storage system equipped with *flywheels* of 992 kWh.

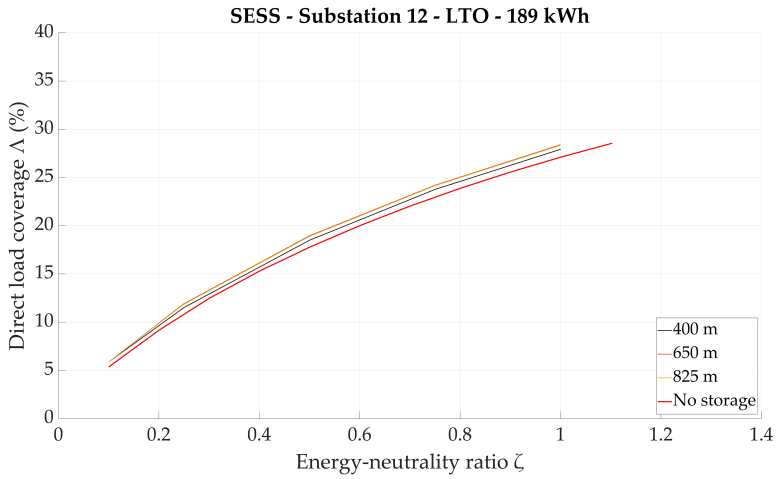

Figure A.31: Substation 12 direct load coverage Λ vs energy-neutrality ratio ζ for various positions for *stationary* energy storage system equipped with lithium-titanate oxide batteries of 189 kWh.

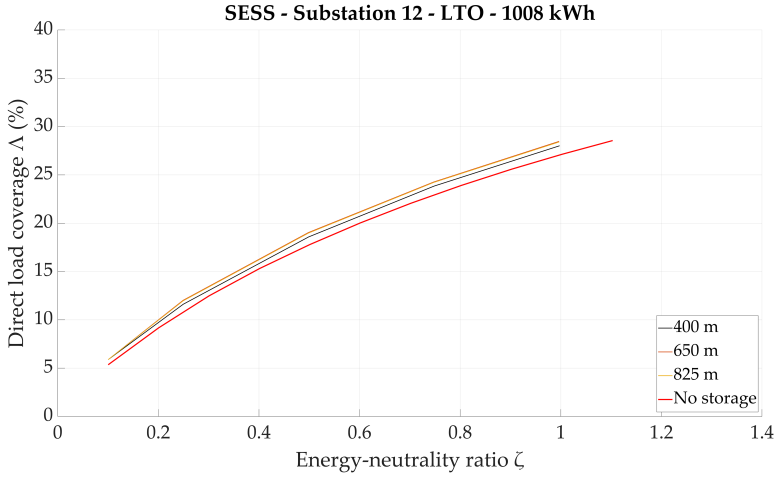

Figure A.32: Substation 12 direct load coverage Λ vs energy-neutrality ratio ζ for various positions for *stationary* energy storage system equipped with lithium-titanate oxide batteries of 1008 kWh.

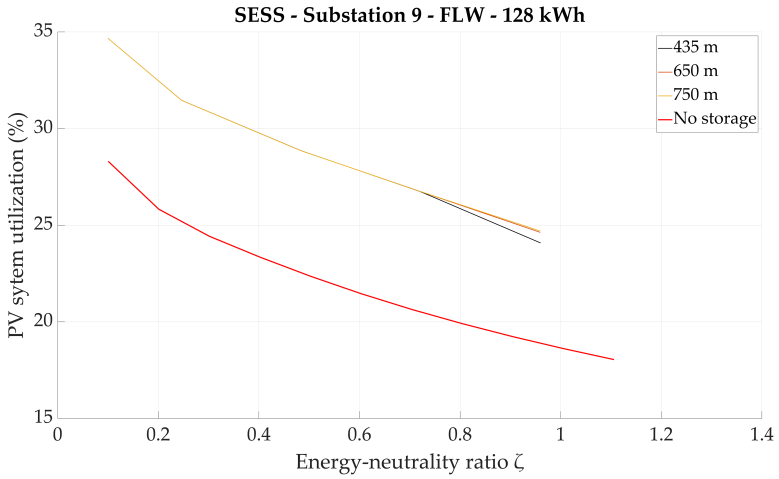

Figure A.33: Substation 9 PV system utilization vs energy-neutrality ratio ζ for various positions for *stationary* energy storage system equipped with *flywheels* of 128 kWh.

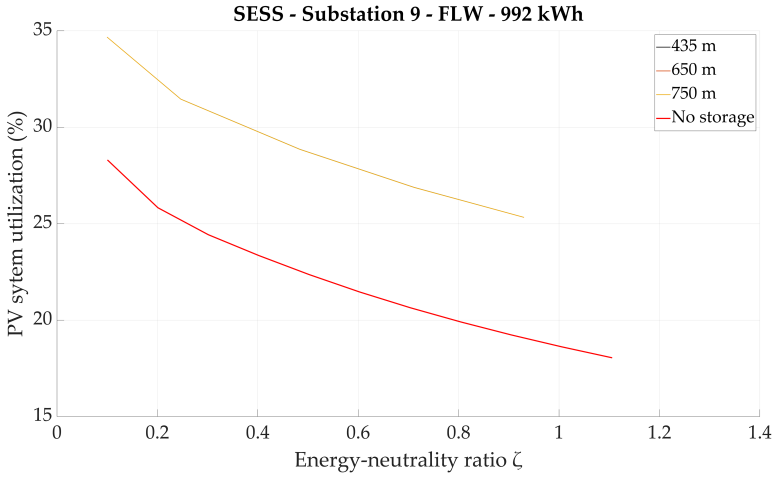

Figure A.34: Substation 9 PV system utilization vs energy-neutrality ratio ζ for various positions for *stationary* energy storage system equipped with *flywheels* of 992 kWh.

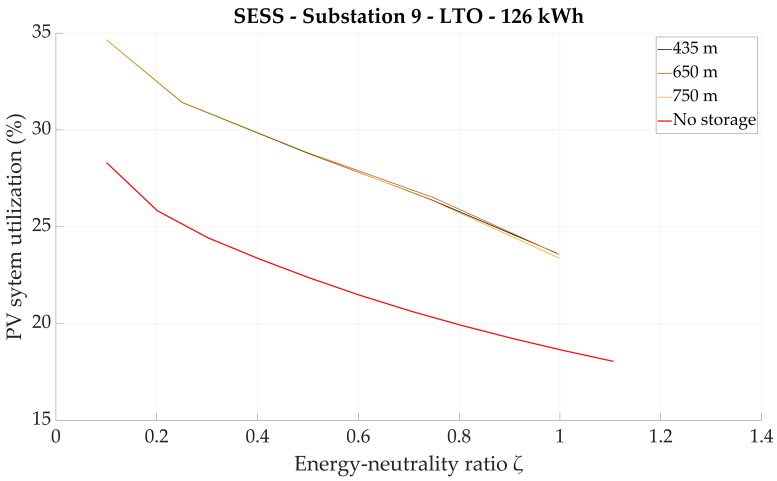

Figure A.35: Substation 9 PV system utilization vs energy-neutrality ratio ζ for various positions for *stationary* energy storage system equipped with lithium-titanate oxide batteries of 126 kWh.

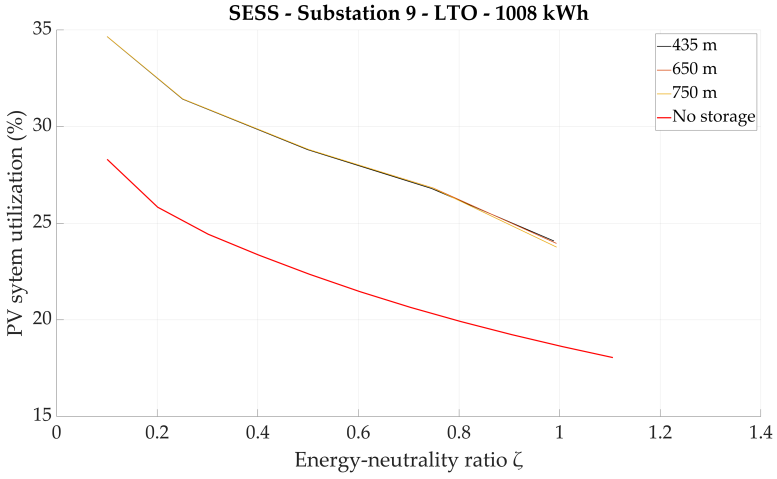

Figure A.36: Substation 9 PV system utilization vs energy-neutrality ratio ζ for various positions for *stationary* energy storage system equipped with lithium-titanate oxide batteries of 1008 kWh.

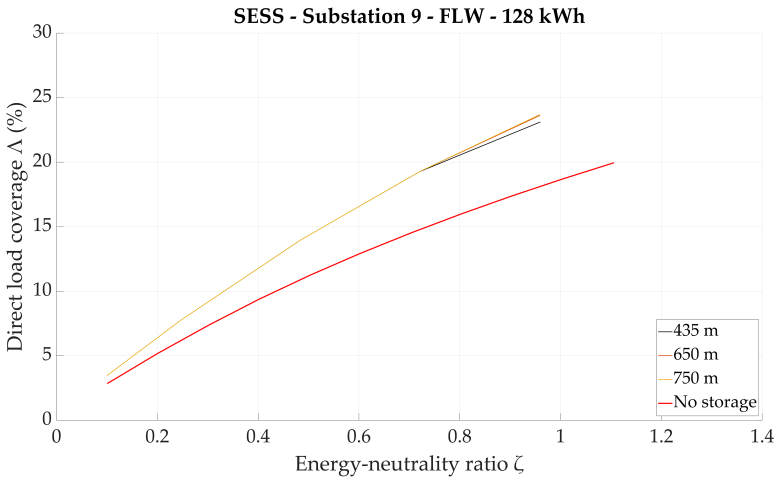

Figure A.37: Substation 9 direct load coverage Λ vs energy-neutrality ratio ζ for various positions for *stationary* energy storage system equipped with *flywheels* of 128 kWh.

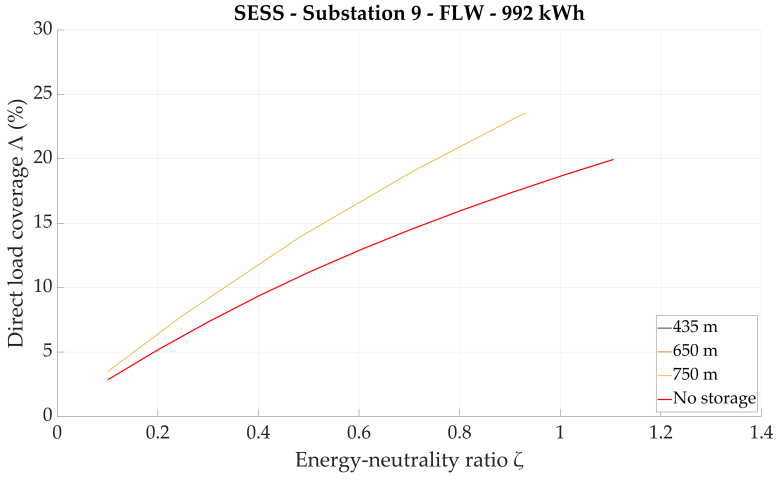

Figure A.38: Substation 9 direct load coverage Λ vs energy-neutrality ratio ζ for various positions for *stationary* energy storage system equipped with *flywheels* of 992 kWh.

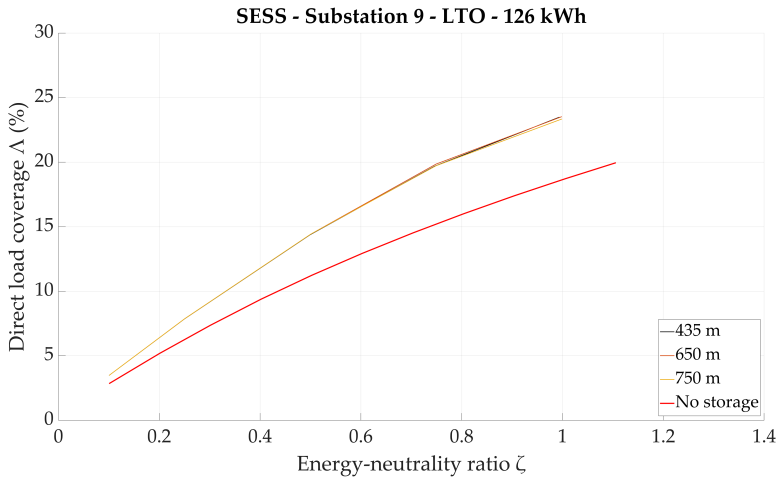

Figure A.39: Substation 9 direct load coverage Λ vs energy-neutrality ratio ζ for various positions for *stationary* energy storage system equipped with lithium-titanate oxide batteries of 126 kWh.

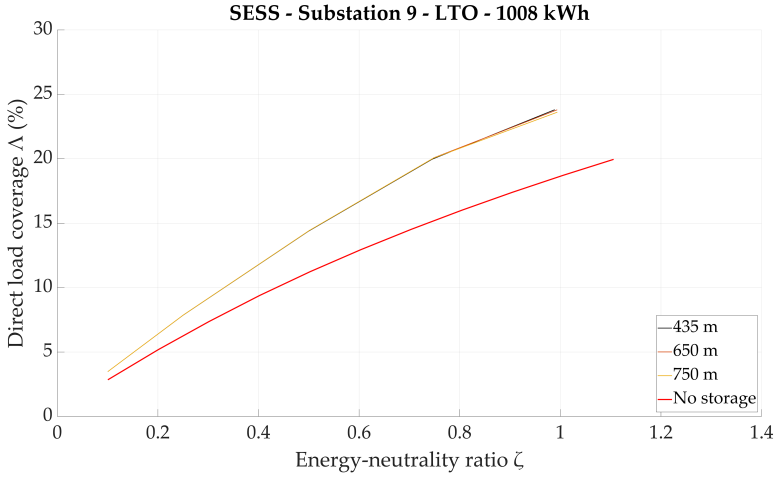

Figure A.40: Substation 9 direct load coverage Λ vs energy-neutrality ratio ζ for various positions for *stationary* energy storage system equipped with lithium-titanate oxide batteries of 1008 kWh.

COLOPHON

This document was typeset using LaTeX. The document layout was generated using the arsclassica package by Lorenzo Pantieri, which is an adaption of the original classicthesis package from André Miede.

The figures and diagrams were mostly drawn using MATLAB®.

TU Delft